



UNIVERSIDADE
ESTADUAL DE LONDRINA

AMANDA LOPES HASUDA

**AVALIAÇÃO DA TOXICIDADE DE DESOXINIVALENOL E
MICOTOXINAS EMERGENTES EM SUÍNOS**

Londrina
2023

AMANDA LOPES HASUDA

**AVALIAÇÃO DA TOXICIDADE DE DESOXINIVALENOL E
MICOTOXINAS EMERGENTES EM SUÍNOS**

Tese apresentada ao Programa de Pós-graduação em Ciência Animal (Área de concentração em Sanidade Animal) da Universidade Estadual de Londrina - UEL, como requisito parcial para a obtenção do título de Doutor.

Orientadora: Prof^a. Dr^a. Ana Paula Frederico Rodrigues Loureiro Bracarense

Londrina
2023

Ficha de identificação da obra elaborada pelo autor, através do Programa de Geração Automática do Sistema de Bibliotecas da UEL

H358a Hasuda, Amanda Lopes.
Avaliação da toxicidade de desoxinivalenol e micotoxinas emergentes em suínos / Amanda Lopes Hasuda. - Londrina, 2023.
158 f. : il.

Orientador: Ana Paula Frederico Rodrigues Loureiro Bracarense.
Tese (Doutorado em Ciência Animal) - Universidade Estadual de Londrina, Centro de Ciências Agrárias, Programa de Pós-Graduação em Ciência Animal, 2023.
Inclui bibliografia.

1. Micotoxinas emergentes - Tese. 2. Tricotecenos - Tese. 3. Fígado - Tese. 4. Jejuno - Tese. I. Bracarense, Ana Paula Frederico Rodrigues Loureiro. II. Universidade Estadual de Londrina. Centro de Ciências Agrárias. Programa de Pós-Graduação em Ciência Animal. III. Título.

CDU 619

AMANDA LOPES HASUDA

AVALIAÇÃO DA TOXICIDADE DE DESOXINIVALENOL E MICOTOXINAS EMERGENTES EM SUÍNOS

Tese apresentada ao Programa de Pós-graduação em Ciência Animal (Área de concentração em Sanidade Animal) da Universidade Estadual de Londrina - UEL, como requisito parcial para a obtenção do título de Doutor.

BANCA EXAMINADORA

Prof. Orientador: Prof^a. Dr^a. Ana Paula
Frederico Rodrigues Loureiro Bracarense
Universidade Estadual de Londrina - UEL

Prof^a. Dr^a. Giovana Wingeter Di Santis
Universidade Estadual de Londrina - UEL

Prof^a. Dr^a. Daniele Sartori
Universidade Estadual de Londrina – UEL

Prof^a. Dr^a. Kelly Moura Keller
Universidade Federal de Minas Gerais – UFMG

Prof. Dr. Carlos Augusto Fernandes de Oliveira
Universidade de São Paulo – USP

Londrina, 02 de março de 2023.

AGRADECIMENTOS

À Prof^a Ana Paula, minha orientadora, que sempre compartilhou seu conhecimento e experiência, que me fez dar o meu melhor para o trabalho durante o doutorado. Que abriu novas possibilidades e me mostrou um pouquinho do mundo da patologia. Que me deu a oportunidade de trabalhar em outro país e conhecer outra cultura e novas pessoas durante o doutorado-sanduíche.

Aos professores da banca, Prof^a Giovana, Prof^a Daniele, Prof^a Kelly e Prof Carlos que aceitaram o convite de participar da banca e por compartilharem seu conhecimento para ajudar a melhorar esse trabalho.

Às amigadas que a patologia me deu, Camila Ribeiro, Andressa Rorato, Mariellen de Souza, Ana Xavier, Bárbara “Lilo”, Juliana Rubira e Ricardo Matos. Por toda amizade e ajuda dentro e fora do laboratório. Pelas conversas *online* quando, no início da pandemia, eu estava sozinha em outro país e pelos momentos de alegria e diversão durante esses anos.

Às novas amigadas em solo francês, Carine Ayoubi, Alix Pierron, Ophélie Rocher, Chrys Zetina e Nadia Tahtah. Que trouxeram alegria e compartilharam bons momentos durante minha passagem por lá.

À Isabelle Oswald, Sylvie Puel e Philippe Pinton, que me receberam muito bem no laboratório do Inrae, compartilharam seu conhecimento e experiência e me ensinaram muitas coisas novas durante o doutorado-sanduíche.

E finalmente à minha família, que sempre me apoiou em todas as decisões na vida acadêmica e fora dela. Meu marido e melhor parceiro de vida, que mesmo sabendo que ficaríamos separados por vários meses continuou incentivando a conquistar esse sonho. Minha mãe e irmã incríveis, que sempre me apoiaram na vida, que conversavam comigo quando a ansiedade era maior que a confiança.

Meu muito obrigada a todos que fizeram parte dessa etapa da vida. Sem vocês a caminhada seria mais difícil e solitária.

“Existem muitas hipóteses em ciência que estão erradas. Isso é perfeitamente aceitável, elas são a abertura para achar as que estão certas.” (Carl Sagan)

HASUDA, Amanda Lopes. **Avaliação da toxicidade de desoxinivalenol e micotoxinas emergentes em suínos**. 2023. 158f. Tese (Doutorado em Ciência Animal) – Universidade Estadual de Londrina, Londrina, 2023.

RESUMO

O desoxinivalenol (DON) é uma micotoxina que causa danos intestinais por meio do estresse ribotóxico e oxidativo. Algumas micotoxinas detectadas recentemente são chamadas de micotoxinas emergentes, entre elas a beauvericina (BEA) e as eniatinas (ENNs). No entanto, dada a falta de estudos *in vivo*, o risco de BEA e ENNs para a saúde animal e humana não pode ser confirmado. Portanto, o objetivo desse trabalho foi verificar os efeitos tóxicos de DON, BEA e ENNs em suínos. Para isso, foram realizados três experimentos. O primeiro avaliou o efeito da ingestão de DON (2,5 mg/kg) sozinho (grupo DON), uma mistura de BEA (2,5 mg/kg) e ENN B + ENN B1 (1,35 mg/kg) (grupo EB) e uma associação entre todas as micotoxinas (2, 3,5 e 1,8 mg/kg, respectivamente) (grupo EB + DON) em 32 leitões por 14 dias. O sangue dos animais foi colhido 7 e 14 dias após o início dos tratamentos para obtenção do plasma para avaliações hepáticas (atividade de enzimas e metabolismo hepático) e intestinais (i-FABP, ZON e IGF-1). Os animais foram eutanasiados para obter amostras de jejuno, cólon, fígado e linfonodos. Todos os fragmentos de órgãos foram processados para análise histológica e a expressão de genes no jejuno e fígado. As fezes foram colhidas ao final do experimento para análise do microbioma. A ingestão de EB + DON diminuiu o ganho de peso dos animais. As atividades das enzimas hepáticas diminuíram após 14 dias em leitões recebendo dieta EB + DON em comparação com leitões recebendo dieta controle. Todas as dietas contaminadas com as micotoxinas levaram a alterações histológicas moderadas a graves no jejuno, fígado e linfonodos. A análise metagenômica revelou que a ingestão de EB diminuiu a diversidade da microbiota intestinal. O segundo e o terceiro experimentos utilizaram uma associação do modelo *in vitro* (células HepG2) e o modelo *ex vivo*, com uma técnica de corte de precisão (PCLS) do fígado. Foram avaliados a viabilidade celular, os biomarcadores hepáticos, a morfologia hepática e a expressão de diversos genes. Para avaliar a citotoxicidade, as células foram incubadas em concentrações crescentes (0-100 µM). Para as demais análises, os dois modelos foram expostos ao DON (10 µM) ou às micotoxinas emergentes (BEA, ENN A1/B/B1, emodina - EMO, apicidina - API e aurofusarina - AFN) (10 µM). No segundo experimento, o DON diminuiu a viabilidade celular, induziu alterações teciduais, apoptose e modificou a expressão de genes inflamatórios e de fatores de transcrição de forma semelhante em ambos os modelos. Os biomarcadores hepáticos não mostraram alteração, e a expressão dos genes apoptóticos e do estresse oxidativo alterou-se apenas *in vitro*. Os resultados demonstram que o fígado é um alvo relevante para observar a resposta inflamatória devido à superexpressão de fatores de transcrição em ambos os modelos. Os parâmetros avaliados *in vitro* e *ex vivo* mostraram perfis semelhantes, apesar de algumas diferenças na intensidade da expressão gênica. No terceiro experimento, a maioria das micotoxinas foram citotóxicas e alteraram os níveis de genes relacionados à inflamação, fator de transcrição e metabolismo hepático *in vitro*. Nos explantes, apenas ENN B1 foi capaz de causar alteração morfológica significativa, mas sem mudanças nos níveis plasmáticos dos bioquímicos hepáticos. A ENN B1 também alterou poucos genes relacionados à inflamação, estresse oxidativo e proteínas de junção. No geral, nossos resultados fornecem novos *insights* sobre o impacto das micotoxinas emergentes sozinhas ou com DON no desempenho, saúde intestinal e parâmetros imunológicos

em suínos. Também fornecem dados adicionais sobre os efeitos tóxicos do DON e das micotoxinas emergentes no fígado e mostram que explantes de fígado são uma ferramenta relevante para avaliar a toxicologia de contaminantes alimentares.

Palavras-chave: Fígado. Jejuno. Micotoxinas não regulamentadas. Tricotecenos. *Ex vivo*. RT-qPCR.

HASUDA, Amanda Lopes. **Evaluation of deoxynivalenol and emerging mycotoxins toxicity in pigs**. 2023. 158pp. Thesis (Doctorate degree in Animal Science) – Universidade Estadual de Londrina, Londrina, 2023.

ABSTRACT

The deoxynivalenol (DON) is a mycotoxin that cause intestinal damage through ribotoxic and oxidative stress. Some recently detected mycotoxins are called emerging mycotoxins, among them beauvericin (BEA) and enniatins (ENNs). However, given the lack of *in vivo* studies, the risk of BEA and ENNs to animal and human health cannot be confirmed. Therefore, this work aimed to verify the toxic effects of DON, BEA, and ENNs in swine. For this, three experiments were carried out. The first evaluated the effect of the ingestion of DON (2.5 mg/kg) alone (DON group), a mixture of BEA (2.5 mg/k) and ENN B + ENN B1 (1.35 mg/kg) (EB group) and an association between all mycotoxins (2, 3.5 and 1.8 mg/kg, respectively) (EB + DON group) in 32 piglets for 14 days. The animals' blood was collected 7 and 14 days after the start of the treatments to obtain plasma for liver (enzyme activity and liver metabolism) and intestinal (i-FABP, ZON and IGF-1) evaluations. Animals were euthanized to obtain jejunum, colon, liver, and lymph node samples. All the organ fragments were processed for histological analysis and gene expression in the jejunum and liver. Feces were collected at the end of the experiment for microbiome analysis. The ingestion of EB + DON decreased the animals' weight gain. Liver enzyme activities decreased after 14 days in piglets receiving the EB + DON diet compared to piglets receiving the control diet. All diets contaminated with mycotoxins led to moderate to severe histological changes in the jejunum, liver, and lymph nodes. The metagenomic analysis revealed that EB ingestion decreased the intestinal microbiota diversity. The second and third experiments used an association of the *in vitro* model (HepG2 cells) and the *ex vivo* model, with a precision-cut technique (PCLS) of the liver. Cell viability, liver biomarkers, liver morphology, and the expression of several genes were evaluated. To assess cytotoxicity, cells were incubated at increasing concentrations (0-100 μ M). For the other analyses, both models were exposed to DON (10 μ M) or to emerging mycotoxins (BEA, ENN A1/B/B1, emodin - EMO, apicidin – API, and aurofusarin - AFN) (10 μ M). In the second experiment, DON decreased cell viability, induced tissue alterations, apoptosis and similarly modified the expression of genes related to inflammation and transcription factor in both models. Liver biomarkers did not show changes, and the expression of apoptotic genes and oxidative stress changed only *in vitro*. The results demonstrate that the liver is a relevant target to observe the inflammatory response due to the overexpression of transcription factors in both models. The parameters evaluated *in vitro* and *ex vivo* showed similar profiles, despite some differences in the intensity of gene expression. In the third experiment, most of the mycotoxins were cytotoxic and changed the levels of genes related to inflammation, transcription factor and hepatic metabolism *in vitro*. In explants, only ENN B1 was able to cause significant morphological change, but without changes in plasmatic levels of liver biochemicals. ENN B1 also altered few genes related to inflammation, oxidative stress and junction proteins. Overall, our results provide new insights into the impact of emerging mycotoxins alone or with DON on animal performance, gut health, and immune parameters in pigs. They also provide additional data on the effects of DON or the emerging mycotoxins in the liver and show that liver explants are a relevant tool to assess the toxicology of food contaminants.

Keywords: Liver. Jejunum. Non-regulated mycotoxins. Trichothecenes. *Ex vivo*. RT-qPCR.

LISTA DE FIGURAS

- Figura 1** – Mecanismos de defesa na barreira intestinal. A – superfície epitelial do intestino delgado. C – Aumento de um enterócito. Receptores de reconhecimento padrão (PRR) detectam a presença de microrganismos na superfície epitelial e no citoplasma, estimulando uma resposta celular transcricional como a produção de citocinas.....23
- Figura 2** – Estrutura química do desoxinivalenol. Molécula com três radicais hidroxila (–OH) livres30
- Figura 3** – Interação entre o local de ligação da subunidade 60S do ribossomo e DON. A – vista frontal, B – vista ortogonal direita, C – vista ortogonal esquerda. Sítios P (roxo) e A (amarelo) da subunidade 60S. Radicais hidroxila (vermelho) de DON (azul). Átomo de magnésio dentro do bolso do sítio A (verde).....31
- Figura 4** – Mecanismo de ação do estresse oxidativo mediado por DON na mitocôndria. Produção de espécies reativas de oxigênio (ROS) que levam à danos oxidativos e perda do potencial de membrana mitocondrial, com liberação de citocromo C (CytC) no citoplasma e ativação das caspases 9 e 3.33
- Figura 5** – Mecanismo de ação da toxicidade de DON na mitocôndria de células intestinais. A – Intestino com saúde normal, B – Intestino após a ingestão de alimentos contaminados com DON.....34
- Figura 6** – Estrutura química da beauvericina e eniatinas (A, A1, B e B1). Beauvericina, R1 = R2 = R3: fenilmetil; Eniatina A, R1 = R2 = R3: –CH(CH₃)CH₂CH₃; Eniatina A1, R1 = R2: –CH(CH₃)CH₂CH₃, R3: –CH(CH₃)₂; Eniatina B, R1 = R2 = R3: –CH(CH₃)₂; Eniatina B1, R1 = R2: –CH(CH₃)₂, R3 = –CH(CH₃)CH₂CH₃43
- Figura 7** – Mecanismo de ação de BEA e ENNs nas junções intercelulares. Transporte de cátions através de poros formados na membrana celular.43

ARTIGO A

- Figura 1** – Boxplot of the body weight gain of piglets (**A**; n = 8) and feed consumption of two piglets per cage (**B**; n = 4) during a time period

of D0-14	084
Figura 2 – Intestinal-fatty acid binding protein (pg/mL) measured in heparin plasma samples from D7 (A) and D14 (B); n = 8; Significant differences are indicated with * $p \leq 0.05$	088
Figura 3 – IGF-1 concentration (ng/mL) measured in heparin plasma samples from D7 (A) and D14 (B); n = 8	088
Figura 4 – Zonulin concentration (ng/mL) measured in heparin plasma samples from D7 (A) and D14 (B); n = 8	088
Figura 5 – mRNA expression of selected genes in the jejunum of animals fed a control or contaminated diet. Mean values of gene expression levels for the control group are set to 1	089
Figura 6 – mRNA expression of selected genes in the liver of animals fed a control or contaminated diet. Mean values of gene expression levels for the control group are set to 1	089
Figura 7 – Lesion score of jejunum tissue (A , n = 8) and histological images of experimental groups. Control (B) showing a normal aspect of villi; DON (C) with villi atrophy and edema of lamina propria; EB (D) showing enterocyte flattening; EB+DON showing edema of lamina propria (E) and villi atrophy (F). Alcian blue staining. Scale bar 100 μm (B, C, E, F), 10 μm (D). Significant differences are indicated with * $p \leq 0.05$	091
Figura 8 – Number of goblet cells per field (A) and villi height (B) in the jejunum (n = 8). Significant differences are indicated with * $p \leq 0.05$	091
Figura 9 – Lesion score of colon tissue (A). Control: Normal aspect of colon (B). DON: Edema of the lamina propria, focal necrosis of enterocytes (arrow) (C). EB: Edema of lamina propria, flattening of enterocytes. Insert: Flattening of enterocytes (D). EB+DON: Multifocal flattening of enterocytes and necrosis (arrows) (E). Alcian blue staining. Scale bar 50 μm	092
Figura 10 – Lesion score of liver tissue (A) and histological images of control (B) showing a normal aspect of liver; DON (C) showing diffuse and severe vacuolar degeneration of hepatocytes; EB (D) showing moderate vacuolar degeneration of hepatocytes; EB+DON showing moderate vacuolar degeneration of hepatocytes (E) and	

megalocytosis (F). Hematoxylin and Eosin (H&E) staining. Scale bar 100 µm (B-E), 20 µm (F). Significant differences are indicated with * p ≤ 0.05	093
Figura 11 – Lesion score of lymph nodes tissue (A) and histological images of control (B) showing a normal aspect of lymph node; DON showing lymphoid depletion (C) and lymphocyte apoptosis (D); EB (E) showing lymphoid hyperplasia; EB+DON (F) showing severe lymphoid depletion. Hematoxylin and Eosin (H&E) staining. Scale bar 100 µm (B, C, E and F), 20 µm (D). Significant differences are indicated with * p ≤ 0.05	094
Figura 12 – Relative abundance of 10 most abundant microbial phyla (A) and microbial species (B) found in the fecal microbiome of pigs fed with the different diets.....	095
Figura 13 – Alpha diversity analysis of the taxa in pig fecal microbiome (A: Shannon index, B: observed index); n = 8; *p ≤ 0.05, **p ≤ 0.01, ***p ≤ 0.001	096

ARTIGO B

Figura 1 – Toxicity of DON in HepG2 cells evaluated by measurement of the reducing potential of cells (RealTime-Glo™ MT Cell Viability Assay) after 4, 24, and 48 h. Cell viability is expressed as % of control cells. Data are presented as mean ± SEM of six replicates, *p ≤ 0.05.	118
Figura 2 – Apoptosis, inflammatory, transcription factors, and oxidative stress mRNA levels measured by RT-PCR in HepG2 cells exposed or not to 10 µM DON for 4 h. Data are presented as mean ± SEM of six replicates, *p ≤ 0.05, **p ≤ 0.01, ***p ≤ 0.001, and ****p ≤ 0.0001.....	119
Figura 3 – Effects of 4 h DON exposure on PCLS. A- Lesion score (A.U. – arbitrary units). Data are presented as mean ± SEM of five different animals, ***p ≤ 0.001. B- control group. Mild disorganization of hepatocytes trabeculae and cytoplasmic vacuolation (arrows). HE. Scale bar 20 µm. C – DON group. Moderate cytoplasmic vacuolation of hepatocytes (arrows) and apoptosis (arrowhead). HE. Scale bar 20 µm. D- DON group. Cytoplasmic vacuolation (arrowheads) and nuclear vacuolation (arrows) of hepatocytes. HE. Scale bar 10 µm.	120

- Figura 4** – Analysis of apoptosis in PCLS. A- Mean number of immunoreactive cells for CASP3 in PCLS/field. Data are presented as mean \pm SEM of five different animals), **p \leq 0.01. B–C- Immunoperoxidase staining. B- control group. Mild positive CASP3 staining (arrowhead). Scale bar 20 μ m. C- DON group. Moderate CASP3 positive staining in hepatocytes and Kupffer cells (arrows). Scale bar 20 μ m. 121
- Figura 5** – Inflammatory and transcription factors mRNA levels measured by RT-PCR in PCLS exposed or not to DON for 4 h. Data are mean \pm SEM from 9 different animals. *p \leq 0.05, **p \leq 0.01, and ***p \leq 0.001 122

ARTIGO C

- Figura 1** – Toxicity of DON in HepG2 cells by CellTiter-Glo® Assay after 24h. Cell viability was evaluated by measurement of ATP and was expressed as % of control cells. Data are expressed as mean \pm SEM of six replicates. *p \leq 0.05, **p \leq 0.01, ***p \leq 0.001, and ****p \leq 0.0001 141
- Figura 2** – Inflammatory, transcription factors, and liver metabolism mRNA levels measured by RT-qPCR in HepG2 cells exposed or not to 10 μ M emerging mycotoxins for 4 h. Data are presented as mean \pm SEM of six replicates, **p \leq 0.01, ***p \leq 0.001 and ****p \leq 0.0001 . 142
- Figura 3** – Effects of emerging mycotoxins exposure on liver PCLS. A) Lesion score (A.U. – arbitrary units), data are presented as mean \pm SEM, n=6. B) Control, mild disorganization of hepatic cords, HE, 50 μ m bar. C) ENN B1, megalocytosis, HE, 10 μ m bar. D) ENN B1, nuclear vacuolation of hepatocytes, HE, 10 μ m bar..... 143
- Figura 4** – Significant changes in mRNA levels measured by RT-qPCR in PCLS exposed or not to 10 μ M of ENN B1 and AFN for 4 h. Data are presented as mean \pm SEM (SOD2 and Ecad) or median \pm interquartile (CCL20), n=6, **p \leq 0.01 and ***p \leq 0.001 144
- Figura 5** – Cytokines mRNA levels measured by RT-qPCR in PCLS exposed or not to 10 μ M of ENN B1 and AFN for 4 h. Data are presented as mean \pm SEM, n=6..... 145

LISTA DE TABELAS

Tabela 1 – Efeitos das micotoxinas BEA e ENNs em estudos realizados diferentes tipos celulares	48
---	----

ARTIGO A

Tabela 1 – Mycotoxin concentration in the respective diet.....	79
Tabela 2 – Primer sequences of genes used for qRT-PCR analysis of the jejunum (J) and liver (L)	82
Tabela 3 – Plasma biochemical analysis at D7 (left side) and D14 (right side).....	86

ARTIGO B

Tabela 1 – Histological criteria for liver lesion score establishment	114
Tabela 2 – Table of human primer sequences used for RT-qPCR analysis (F: Forward; R: Reverse)	116
Tabela 3 – Table of pig primer sequences used for RT-qPCR analysis (F: Forward; R: Reverse).....	117

ARTIGO C

Tabela 1 – Histological criteria for liver lesion score establishment	137
Tabela 2 – Table of human primer sequences used for RT-qPCR analysis (F: Forward; R: Reverse)	138
Tabela 3 – Table of pig primer sequences used for RT-qPCR analysis (F: Forward; R: Reverse).....	139

LISTA DE ABREVIATURAS E SIGLAS

3ADON	3-acetil-DON
15ADON	15-acetil-DON
ABTS	ácido 2,2'-azino-bis-3-etilbenzotiazolina-6-sulfônico
AOH	alternariol
ASC	ascladiol
BEA	beauvericina
Ca ²⁺	íon cálcio
Caco-2	linhagem celular contínua de células de heterogêneas de adenocarcinoma colorretal epitelial humano
CAT	catalase
CCF-STTG1	linhagem celular de astrocitoma humano estabelecido a partir de um astrocitoma grau IV
CCL20	ligante quimiocina 20
CCRF-CEM	linhagem celular de leucemia linfoblástica aguda humana
CHO-K1	linhagem celular de ovário de hamster chinês
COX2	ciclo-oxigenase 2
CT-26	linhagem celular de adenocarcinoma de cólon de camundongo
CTAO	capacidade total antioxidante
D3G	3-O-glicosídeo-DON
D3GA	DON-3-glicuronídeo
D15GA	DON-15-glicuronídeo
DE ₅₀	dose efetiva
DOM-1	de-epóxi-DON
DON	desoxinivalenol
EFSA	Autoridade Europeia para a Segurança dos Alimentos
ENNs	eniatinas
ENN A	eniatina A
ENN A1	eniatina A1
ENN B	eniatina B
ENN B1	eniatina B1
ERN	espécies reativas de nitrogênio
ERO	espécies reativas de oxigênio
FB	fumonisina
FB1	fumonisina B1

FRAP	capacidade plasmática de redução do ferro
FUS	fusaproliferina
FX	fusarenona X
GCLM	subunidade reguladora da glutamato-cisteína ligase
GPx	glutaciona peroxidase
GR	glutaciona redutase
GSH	glutaciona
H295R	linhagem celular de adenocarcinoma humano
H4IIE	linhagem celular de hepatoma de rato
HBMEC	linhagem celular de células endoteliais microvasculares de cérebro humano
HDP	peptídeos de defesa do hospedeiro
HepG2	linhagem celular de câncer de fígado humano
HIF-1 α	fator 1-alfa induzível por hipóxia
HL-60	linhagem celular de humano com leucemia promielocítica aguda
HMOX	heme-oxigenase 1
IC ₅₀	concentração inibitória
IDT	ingestão diária tolerável
IFN- γ	interferon gama
Ig	imunoglobulina
IgA	imunoglobulina A
IL	interleucina
IL1 α	interleucina 1 alfa
IL1 β	interleucina 1 beta
IL6	interleucina 6
IL8	Interleucina 8
IL10	interleucina 10
IPEC-J2	linhagem celular de epitélio intestinal de suíno
KB-3-1	linhagem celular de carcinoma primário do colo do útero de uma mulher negra de 31 anos
Keap1	proteína 1 associada à ECH do tipo Kelch
MAPKs	proteínas quinases ativadas por mitógeno
MDA	malondialdeído
MON	moniliformina
N ₂	nitrogênio
NAC	N-acetilcisteína
NF- κ B	fator de transcrição nuclear kappa B

NIV	nivalenol
NQO1	NAD(P)H desidrogenase quinona 1
Nrf2	fator nuclear 2 relacionado ao eritroide 2
NSCLC A549	linhagem celular de carcinoma pulmonar humano de células não pequenas
O ₂	oxigênio
ORAC	capacidade de absorbância de radicais de oxigênio
OTA	ocratoxina A
PAT	patulina
PBCEC	linhagem celular de células endoteliais capilares de cérebro de suíno
PC	peso corporal
PK15	linhagem celular de rim de suíno
PLHC-1	linhagem celular de carcinoma hepatocelular de peixe <i>Poeciliopsis lucida</i>
RAW 265.7	linhagem celular de células murinas de macrófagos
RTH-149	linhagem celular de hepatoma de truta arco-íris
SCF	Comitê Científico para Alimentos da Comissão Europeia
SOD	superóxido dismutase
STE	esterigmatocistina
TEAC	capacidade antioxidante equivalente ao trolox
TEER	resistência elétrica transepitelial
TNF α	fator de necrose tumoral alfa
TRAP	potencial antioxidante reativo total
TFF3	fator trifólio 3
U-937	linhagem celular de leucemia mieloide pró-monocítica humana
V79	linhagem celular do pulmão de um hamster chinês normal
ZEA	zearalenona

SUMÁRIO

1	INTRODUÇÃO	21
2	REFERENCIAL TEÓRICO	23
2.1	MORFOLOGIA DO INTESTINO DELGADO	23
2.2	MORFOLOGIA DO FÍGADO	25
2.3	MODELO <i>EX VIVO</i>	26
2.4	MICOTOXINAS	28
2.4.1	Desoxinivalenol	30
2.4.1.1	Toxicocinética	35
2.4.1.2	Estudos <i>in vitro</i>	36
2.4.1.3	Estudos <i>in vivo</i> e <i>ex vivo</i>	38
2.4.2	Micotoxinas Emergentes	42
2.4.2.1	Toxicocinética	44
2.4.2.2	Estudos <i>in vitro</i>	46
2.4.2.3	Estudos <i>in vivo</i>	56
3	REFERÊNCIAS	58
4	HIPÓTESE	73
5	OBJETIVOS	74
5.1	OBJETIVO GERAL	74
5.2	OBJETIVOS ESPECÍFICOS	74
6	ARTIGO A – EFFECTS OF FUSARIUM METABOLITES BEAUVERICIN AND ENNIATINS ALONE OR IN MIXTURE WITH DEOXYNIVALENOL ON WEANING PIGLETS	75
7	ARTIGO B – DEOXYNIVALENOL INDUCES APOPTOSIS AND INFLAMMATION IN THE LIVER: ANALYSIS USING PRECISION-CUT LIVER SLICES	110
8	ARTIGO C – EMERGING MYCOTOXINS INDUCE EX VIVO AND IN VITRO HEPATOTOXICITY IN PIGS PRECISION-CUT LIVER SLICES AND HEPG2 CELLS	133
9	CONSIDERAÇÕES FINAIS	155
	APÊNDICES	156

APÊNDICE A – Tabela complementar ao artigo B “Deoxynivalenol induces apoptosis and inflammation in the liver: Analysis using precision-cut liver slices”.....157

APÊNDICE B – Tabela complementar ao artigo C “Emerging mycotoxins induce ex vivo and in vitro hepatotoxicity in pigs precision-cut liver slices and HepG2 cells”158

1 1 INTRODUÇÃO

2 Vários fungos podem produzir micotoxinas, principalmente os gêneros
3 *Aspergillus*, *Penicilium*, *Alternaria*, *Fusarium* e *Claviceps*. Em torno de 300 a 400
4 metabólitos dos fungos se enquadram como micotoxinas. Eles contaminam vários
5 tipos de grãos, como trigo, cevada, centeio, aveia, milho e arroz. Por isso, em animais
6 alimentados à base de grãos, esses metabólitos podem afetar o organismo, levando
7 à manifestação clínica de lesões nos diversos tecidos (BRYDEN, 2012).

8 O desoxinivalenol (DON) é uma micotoxina do grupo dos tricotecenos,
9 produzida por fungos do gênero *Fusarium*, principalmente *F. graminearum*. O DON
10 permanece estável em temperaturas muito altas (170 a 350°C) e está presente em
11 grande parte das amostras de alimentos à base de grãos. Em torno de 90% das
12 amostras de grãos estão contaminadas com DON e ele também é um potencial
13 marcador da ocorrência de outras micotoxinas (GROVE, 1993; SOBROVA *et al.*,
14 2010). A toxicidade do DON está associada à sua capacidade de inibir a síntese
15 proteica ao se ligar na subunidade 60s do ribossomo. Além do estresse ribotóxico, o
16 DON também é capaz de causar estresse oxidativo e disfunção mitocondrial nas
17 células intestinais, levando a alterações morfológicas e de função em diversos órgãos
18 (PESTKA; SMOLINSKI, 2005; WANG *et al.*, 2021).

19 A beauvericina (BEA) é encontrada em cereais como trigo, aveia,
20 cevada e centeio, em uma prevalência de contaminação que pode variar de 12 a
21 100%, mas geralmente a concentração não ultrapassa 100 µg/kg. Porém, em outros
22 cereais como arroz, o nível de contaminação pode chegar a 26.300 µg/kg
23 (FRAEYMAN *et al.*, 2017; MALLEBRERA *et al.*, 2018). As eniatinas (ENNs) também
24 contaminam cereais como trigo, aveia, cevada e centeio, mas com alta frequência de
25 ocorrência (96 a 100%). Os níveis de contaminação geralmente variam entre 41–569
26 µg/kg, mas ocasionalmente podem ultrapassar 1000 µg/kg (FRAEYMAN *et al.*, 2017;
27 PROSPERINI *et al.*, 2017). Ambos os metabólitos são considerados micotoxinas
28 emergentes, que por definição são micotoxinas que não são rotineiramente avaliadas,
29 nem possuem uma regulamentação, mas tem alta frequência de ocorrência (JESTOI,
30 2008).

31 O intestino é considerado um órgão-alvo para a ação das micotoxinas,

32 pois, como é a primeira barreira de defesa contra agentes patogênicos e substâncias
33 tóxicas, ele é exposto à altas concentrações das micotoxinas presentes nos alimentos
34 (BOUHET; OSWALD, 2005; PINTON; OSWALD, 2014). Além do intestino, o fígado
35 também pode ser considerado um órgão de interesse para a ação das micotoxinas,
36 pois é o principal órgão de detoxificação do organismo (TENNANT; CENTER, 2008;
37 TOLOSA *et al.*, 2021).

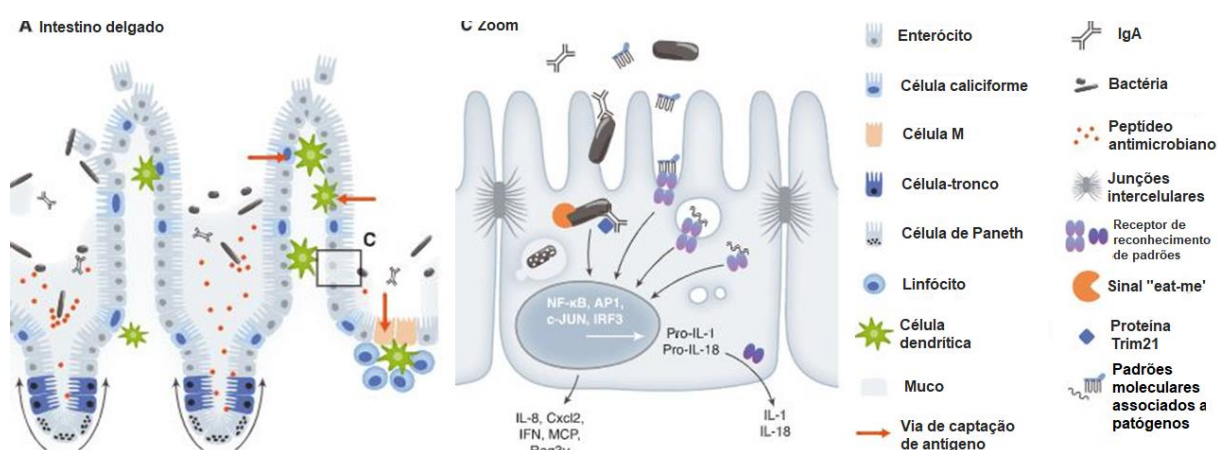
38 A Autoridade Europeia para a Segurança dos Alimentos (EFSA)
39 expressou preocupação com a saúde humana e animal em relação à ingestão crônica
40 dessas micotoxinas emergentes (EFSA, 2014). Como esses cereais estão presentes
41 em concentrações elevadas na alimentação animal e humana, há grande interesse
42 com possíveis consequências à ingestão aguda ou crônica de alimentos
43 contaminados com micotoxinas. Algumas, como o DON, já têm seus efeitos bem
44 conhecidos em órgãos como o intestino, mas para as micotoxinas ditas emergentes é
45 limitado o conhecimento do impacto delas na saúde humana e animal, por isso há
46 necessidade de mais estudos *in vivo* e *ex vivo* para determinar se a ingestão de BEA
47 e ENNs é nociva para a saúde.

48 2 REFERENCIAL TEÓRICO

49 2.1. MORFOLOGIA DO INTESTINO DELGADO

50 O intestino delgado é dividido em três partes: duodeno, jejuno e íleo. É
 51 responsável pela absorção de nutrientes, absorção e secreção de eletrólitos e água,
 52 secreção de imunoglobulinas (Ig) e mucina, além de ser uma barreira de proteção
 53 contra possíveis patógenos (Figura 1) (HORNBUCKLE; SIMPSON; TENNANT, 2008;
 54 LALLÈS *et al.*, 2004).

55 **Figura 1** – Mecanismos de defesa na barreira intestinal. A – superfície epitelial do
 56 intestino delgado. C – Aumento de um enterócito. Receptores de reconhecimento
 57 padrão (PRR) detectam a presença de microrganismos na superfície epitelial e no
 58 citoplasma, estimulando uma resposta celular transcricional como a produção de
 59 citocinas.



60
 61 Fonte: Adaptado de Zhang, Hornef, Dupont et al. (2015)

62 É composto por várias estruturas como as vilosidades intestinais, que
 63 são projeções da mucosa contendo uma camada de epitélio colunar e lâmina própria
 64 (composta de tecido conjuntivo frouxo), medindo cerca de 0,5 a 1,5mm de altura.
 65 Nesse epitélio pode-se encontrar dois tipos celulares: os enterócitos e células
 66 caliciformes. O primeiro tipo são células colunares altas com uma borda em escova
 67 no seu ápice, formando assim as microvilosidades, que aumentam a superfície de
 68 absorção. A célula M é um tipo especializado de enterócito presente no epitélio
 69 associado aos folículos linfoides que recobrem a região das placas de Peyer, tendo a
 70 função de facilitar a apresentação de antígenos no lúmen intestinal para o tecido
 71 linfóide adjacente. Já as células caliciformes estão presentes entre os enterócitos e

72 em menor quantidade no duodeno do que no jejuno e íleo, sua principal função é a
73 produção de mucina (JUNQUEIRA; CARNEIRO, 2008; ZACHARY; MCGAVIN, 2013).

74 Entre as vilosidades, na região de lâmina própria, existem pequenas
75 glândulas tubulares simples que são chamadas de criptas de Lieberkühn, ou somente
76 criptas, que secretam enzimas e hormônios. As criptas são formadas por enterócitos
77 e células caliciformes (ambas na parte superior da cripta), células de Paneth e células-
78 tronco. As células de Paneth são células exócrinas localizadas na parte basal das
79 criptas e produzem lisozimas e defesinas, duas enzimas de defesa contra patógenos,
80 mas não se sabe com certeza se esse tipo celular está presente nos suínos. Além
81 disso, outros mecanismos de defesa do intestino delgado são a presença de linfócitos
82 intraepiteliais e das junções intercelulares oclusivas (JUNQUEIRA; CARNEIRO, 2008;
83 ZACHARY; MCGAVIN, 2013; ZHANG; HORNEF; DUPONT, 2015).

84 A mucina secretada pelas células caliciformes forma uma camada de
85 muco que impede que as bactérias se aproximem do epitélio intestinal e essa camada
86 também é enriquecida com peptídeos antimicrobianos e proteínas produzidos nas
87 células de Paneth, conferindo atividade antibacteriana local. As células nas
88 vilosidades apresentam junções intercelulares, principalmente, ocludinas e claudinas,
89 junções aderentes (E-caderinas) e desmossomos. Essa forte adesão intercelular cria
90 uma barreira na mucosa intestinal. No entanto, patógenos e as micotoxinas podem
91 alterar a integridade dessas junções bem como mediadores inflamatórios podem
92 influenciar essa permeabilidade (PINTON *et al.*, 2009; ZHANG; HORNEF; DUPONT,
93 2015).

94 Além da barreira física, os enterócitos expressam receptores de
95 reconhecimento de padrões (PRR) que reconhecem padrões moleculares associados
96 a patógenos (PAMP), além de produzir diversas citocinas (IL-1 β , IL6, IL8, IFN- γ e
97 TNF α) que vão recrutar e ativar células do sistema imune (STADNYK, 2002). Porém,
98 resultados demonstraram que as micotoxinas, em especial o desoxinivalenol, são
99 capazes de modular essa resposta imune tanto no intestino quanto de maneira
100 sistêmica (ALASSANE-KPEMBI *et al.*, 2017b; BOUHET; OSWALD, 2005; GAUTHIER
101 *et al.*, 2013; OSWALD *et al.*, 2005; PINTON *et al.*, 2008).

102 2.2. MORFOLOGIA DO FÍGADO

103 O fígado é revestido por uma fina cápsula de tecido conjuntivo, sua
104 unidade funcional é o lóbulo hepático e em suínos eles são separados entre si por
105 uma camada de tecido conjuntivo (EKATAKSIN; WAKE, 1991). Essa unidade
106 funcional é composta por hepatócitos, células epiteliais cuboides, ligados por junções
107 intercelulares, organizadas em cordões ou trabéculas. Esses cordões estão
108 arrançados em uma distribuição radial ao redor da veia central. O espaço entre esses
109 cordões contém canalículos biliares, capilares chamados de sinusoides hepáticos,
110 que são compostos de uma camada descontínua de células endoteliais fenestradas,
111 e macrófagos ou células de Kupffer (representando aproximadamente 15-35% das
112 células do fígado). Na periferia dos lóbulos hepáticos encontram-se vasos
113 sanguíneos, vasos linfáticos e ductos biliares (EKATAKSIN; WAKE, 1991; GISSEN;
114 ARIAS, 2015; JUNQUEIRA; CARNEIRO, 2008).

115 Ao contrário de outros órgãos, o fígado recebe sangue de duas fontes
116 distintas, a artéria hepática (30-40%) e a veia portal hepática (60-70%), que drena o
117 sangue do intestino delgado para o fígado. Danos no epitélio intestinal podem resultar
118 na translocação de patógenos do intestino para o sangue portal. A ausência de
119 infecção sistêmica quando essa translocação ocorre é uma prova da função
120 imunológica desempenhada pelo fígado (KUBES; JENNE, 2018). Os canalículos
121 biliares coletam a bile secretada pelos hepatócitos e a drenam para os ductos biliares,
122 que se juntam para formar o ducto hepático, que junto com os ductos pancreático e
123 cístico desembocam no duodeno para secretar a bile no intestino delgado (ZACHARY;
124 MCGAVIN, 2013; STEADMAN; BRAUNFELD; PARK, 2019).

125 O fígado desempenha várias funções e é essencial para o
126 metabolismo de nutrientes, detoxificação e excreção de substâncias tóxicas, síntese
127 de proteínas e o processo de absorção e digestão de lipídios e vitaminas lipossolúveis.
128 Além disso, o fígado possui capacidade regenerativa, por conta disso, manifestações
129 de falência hepática, como concentração diminuída especificamente de albumina e
130 ácidos biliares e aumento de amônia, só são observadas quando 70% ou mais do
131 parênquima está comprometido (TENNANT; CENTER, 2008). As enzimas hepáticas
132 são excelentes marcadores de lesão hepatocelular e colestase. As enzimas aspartato
133 aminotransferase (AST), alanina aminotransferase (ALT), sorbitol desidrogenase

134 (SDH) e lactato desidrogenase (LDH) estão presentes no citoplasma dos hepatócitos
135 e seu extravasamento está associado à ruptura da membrana dos hepatócitos ou
136 quando há alteração de permeabilidade por lesão subletal. Quando ocorre o dano às
137 membranas, elas são imediatamente extravasadas e caem na circulação sanguínea.
138 A fosfatase alcalina (FA) e a γ -glutamiltanspeptidase (GGT) são enzimas produzidas
139 na membrana das células epiteliais biliares e em menor extensão nos hepatócitos
140 associados aos sinusoides e canálculos biliares. A presença de alguma obstrução do
141 fluxo biliar estimula a produção dessas enzimas, que pode demorar algumas horas
142 após o início do estímulo (PAVENTI; PIZZUTO; PASSARELLA, 2017; TENNANT;
143 CENTER, 2008; THRALL *et al.*, 2015).

144 Além do intestino, o fígado é um dos primeiros órgãos a entrar em
145 contato com potenciais patógenos e contaminantes de alimentos, como as
146 micotoxinas (KUBES; JENNE, 2018). Estudos já demonstraram que o desoxinivalenol
147 é capaz de alterar a morfologia hepática, causar apoptose e modular a expressão de
148 vários genes no fígado de animais (BRACARENSE *et al.*, 2017; MIKAMI *et al.*, 2010;
149 REDDY *et al.*, 2018; SKIEPKO *et al.*, 2020). Também afeta a viabilidade dos
150 hepatócitos, promove a expressão de fatores de transcrição e induz o estresse
151 oxidativo e a apoptose em culturas celulares hepáticas (NIELSEN *et al.*, 2009; SUN,
152 LV-HUI *et al.*, 2015; YANG, JUN *et al.*, 2019; DARWISH *et al.*, 2020).

153 2.3. MODELO *EX VIVO*

154 Um modelo que tem sido bastante utilizado no estudo do efeito das
155 micotoxinas é o modelo *ex vivo*, que consiste na cultura de um fragmento de tecido
156 (explante) em meio propício. No intestino, essa técnica foi descrita pela primeira vez
157 em 1969 por Browning e Trier em um modelo de cultivo do intestino humano
158 (COOPER; WILSON; FEIGHERY, 2015; RUSSO *et al.*, 2016). Além disso, o uso de
159 um modelo animal, como o suíno, apresenta bons resultados para extrapolação em
160 humanos (HELKE; SWINDLE, 2013).

161 Uma vantagem dessa técnica em relação ao modelo *in vitro* é que o
162 cultivo celular não consegue reproduzir a morfologia da mucosa intestinal presente no
163 modelo *in vivo* e nem a interação complexa dos mecanismos inflamatórios. O modelo

164 de cultivo de explantes tem uma resposta bem específica e é preferível porque
165 preserva a interação entre diferentes tipos e compartimentos celulares e utiliza menos
166 animais no experimento (RUSSO *et al.*, 2016). Ele é utilizado como uma ferramenta
167 intermediária entre animais e humanos para estudar a homeostase do órgão-alvo e
168 seu comportamento em condições fisiológicas e patológicas (MARESCA *et al.*, 2018).

169 Os explantes de intestino de animais são os modelos mais próximos
170 do intestino humano do que os modelos *in vitro*, pois contém todos os tipos de células
171 epiteliais normalmente presentes na mucosa. Além das células epiteliais intestinais,
172 os explantes contêm células do sistema imunológico, fibroblastos e células nervosas
173 entéricas que também desempenham papéis importantes na fisiologia intestinal
174 (MARESCA *et al.*, 2018). Eles são preparados a partir de segmentos intestinais, que
175 são cortados com o auxílio de *punch* cirúrgico e os fragmentos teciduais mantidos em
176 meio de cultura. A manutenção deles pode ser por diferentes abordagens: cultura na
177 interface ar-líquido, cultura de imersão em poços ou em uma câmara de Ussing, que
178 é um dispositivo que permite acesso específico aos compartimentos apical/luminal ou
179 aos compartimentos basolaterais/serosais do tecido (RANDALL; TURTON; FOSTER,
180 2011).

181 Já para estudos de fisiologia, patologia, metabolismo e toxicidade de
182 drogas no fígado, a técnica de cultivo de hepatócitos isolados de ratos é a mais
183 utilizada. No entanto, em 1980, Krumdieck, Santos e Ho descreveram um novo
184 instrumento para preparar fatias finas de fígado cortadas com precisão e de maneira
185 reproduzível. A espessura dessas fatias de fígado é fina o suficiente para permitir o
186 suprimento de oxigênio e nutrientes para as camadas celulares internas. Os
187 hepatócitos dessas fatias retêm sua membrana e polarização intracelular, ao contrário
188 dos hepatócitos isolados. A técnica de fatias de corte de precisão promove o uso mais
189 eficiente do tecido e não depende do uso de enzimas proteolíticas que potencialmente
190 danificam as células, como é o caso do isolamento dos hepatócitos. Porém, há a
191 necessidade de adquirir equipamentos específicos, como um fatiador Krumdieck ou
192 fatiador Brendel-Vitron, que aumentam o seu custo (DE GRAAF *et al.*, 2010).

193 A técnica *ex vivo* possui algumas limitações. Alguns tecidos, como o
194 intestino, não podem ser incubados por um longo período (> 4-6 horas), pois têm sua

195 integridade tecidual comprometida (COOPER; WILSON; FEIGHERY, 2015; KOLF-
196 CLAUW *et al.*, 2009). Mas para outros tecidos, como o ovariano, esse período de
197 incubação pode ser mais longo, até 48 horas (GEREZ; DESTO; BRACARENSE,
198 2017). Também não é viável a utilização desse modelo em estudos de triagem de
199 larga escala (MARESCA *et al.*, 2018). Mas, mesmo com essas limitações, o cultivo de
200 explantes ainda é preferível porque tem menor custo menor do que estudos *in vivo* e
201 apresenta resultados que podem ser extrapolados para o organismo vivo (RUSSO *et*
202 *al.*, 2016).

203 Devido a necessidade de se utilizar cada vez menos animais em
204 experimentos, pelos aspectos éticos e de bem-estar, essa técnica está cada vez mais
205 em evidência, mostrando-se eficaz nos estudos sobre os efeitos das micotoxinas no
206 organismo (KOLF-CLAUW *et al.*, 2009). Diversos estudos com explantes intestinais,
207 avaliando os efeitos das micotoxinas, já foram relatados (ALASSANE-KPEMBI *et al.*,
208 2017a; GEREZ *et al.*, 2021; LUCIOLI *et al.*, 2013; MAIDANA *et al.*, 2016; PIERRON
209 *et al.*, 2016; SILVA *et al.*, 2014, 2019). No entanto, estudos sobre os efeitos das
210 micotoxinas nos explantes hepáticos são escassos (AJANDOUZ *et al.*, 2016).

211 O modelo *ex vivo*, apesar de ter se mostrado altamente relevante para
212 estudos de fisiologia, toxicidade e metabolismo de drogas e xenobióticos em animais
213 e humanos, foi subutilizado nas últimas décadas e ganhou destaque apenas
214 recentemente. Seu uso é interessante também quando em conjunto com outros
215 modelos *in vitro* para a avaliação de risco de contaminantes tóxicos em alimentos
216 humanos (MARESCA *et al.*, 2018).

217 2.4. MICOTOXINAS

218 Micotoxinas são metabólitos secundários produzidos por fungos
219 encontrados em alimentos consumidos por animais e humanos, que podem causar
220 doenças ao alterar a imunidade dos indivíduos (OSWALD *ET AL.*, 2005). As principais
221 vias de contaminação são por ingestão, inalação e contato na pele. A metabolização
222 das micotoxinas no organismo pode levar ao seu acúmulo em diferentes tecidos e,
223 consequentemente, podem entrar na cadeia alimentar por meio de produtos de origem

224 animal, como carne, leite ou ovos contaminados (MARIN *ET AL.*, 2013).

225 Os principais gêneros de fungos que produzem micotoxinas são:
226 *Alternaria*, *Claviceps*, *Aspergillus*, *Fusarium* e *Penicilium*. Sendo os três últimos de
227 maior importância, pois a maioria das micotoxinas pode ser produzida por esses três
228 gêneros (BRYDEN, 2012). As principais micotoxinas são: aflatoxinas, ocratoxina A
229 (OTA), tricotecenos (tipo A: toxina T-2 e tipo B: desoxinivalenol), zearalenona (ZEA),
230 fumonisinas (B1 e B2), alcaloides do ergot, alternariol (AOH) e as micotoxinas
231 emergentes (MARIN *et al.*, 2013).

232 Algumas micotoxinas emergentes como beauvericina (BEA),
233 eniatinas (ENNs), fusaproliferina (FUS) e moniliformina (MON) também são
234 produzidas por fungos do gênero *Fusarium* (JESTOI, 2008). Elas são consideradas
235 emergentes, pois são micotoxinas com alta frequência de ocorrência e com o avanço
236 de técnicas de detecção é possível identificar metabólitos que antes não eram
237 identificados e não são regulamentadas (FRAEYMAN *et al.*, 2017). Como ainda foram
238 pouco estudadas e os estudos de toxicidade *in vivo* sobre essas micotoxinas são
239 escassos, não há nenhum tipo de regulamentação quanto aos limites máximos
240 toleráveis que essas micotoxinas podem apresentar nos alimentos.

241 Estimativas demonstraram que 60–80% dos grãos de cereais no
242 mundo estão contaminados com algum tipo de micotoxina (ESKOLA *et al.*, 2020). Em
243 2021, a Pesquisa Mundial de Micotoxinas da BIOMIN, empresa de saúde e nutrição
244 animal, demonstrou que das 16.164 amostras de alimentos para animais colhidos em
245 74 países, 64% das amostras estavam contaminadas com mais de uma micotoxina.
246 Na América do Sul e Europa, as duas micotoxinas mais frequentes são as fumonisinas
247 (FB) e o desoxinivalenol (DON). Em 618 amostras originárias de 68 países, 10 em
248 cada 10 amostras de rações acabadas e matérias-primas estavam contaminadas com
249 toxinas do gênero *Fusarium* e dessas amostras, 96% delas estavam contaminadas
250 com 10 ou mais metabólitos (BIOMIN, 2021).

251 Sabe-se que algumas micotoxinas são capazes de alterar a barreira
252 intestinal (BOUHET; OSWALD, 2005). Os tricotecenos, entre eles o DON, são as
253 principais micotoxinas a causar danos na integridade da barreira intestinal, com

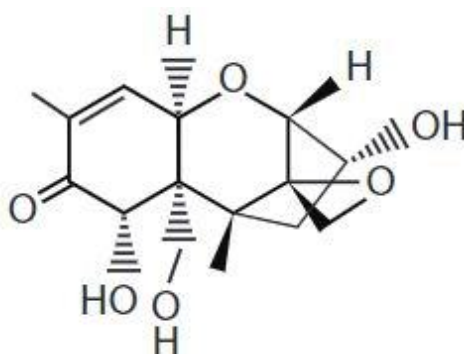
254 comprometimento das células de revestimento epitelial e das proteínas de junção
255 intercelular, enquanto a patulina (PAT) afeta diretamente a monocamada das células
256 epiteliais no intestino (AKBARI *et al.*, 2017). Isso pode levar ao aumento da
257 permeabilidade, por conta da diminuição da resistência elétrica transepitelial (TEER),
258 que pode ter como consequência a translocação de patógenos ou outras substâncias
259 (AKBARI *et al.*, 2017; BOUHET; OSWALD, 2005; LUO *et al.*, 2019; PINTON;
260 OSWALD, 2014).

261 Porém, os efeitos tóxicos das micotoxinas emergentes ainda não
262 foram bem estudados. A maioria dos estudos na literatura envolvem micotoxinas já
263 regulamentadas, como o DON e outros tricotecenos, fumonisinas, ocratoxina A,
264 zearalenona e patulina, principalmente em intestino e órgãos linfoides (ALASSANE-
265 KPEMBI *et al.*, 2017a, 2017b; BRACARENSE *et al.*, 2017; GEREZ *et al.*, 2015;
266 LEWCZUK *et al.*, 2016a; LUO *et al.*, 2019; MAIDANA *et al.*, 2016; PIERRON *et al.*,
267 2018; PINTON; OSWALD, 2014; SILVA *et al.*, 2014, 2019).

268 2.4.1. Desoxinivalenol

269 O desoxinivalenol (DON) é o principal representante da família dos
270 tricotecenos tipo B. O DON foi isolado pela primeira vez em cevada contaminada por
271 fungos do gênero *Fusarium* no Japão (MOROOKA *et al.*, 1972). O DON é um
272 composto orgânico polar e seu nome químico é 12,13-epoxi3 α ,7 α ,15-trihidroxitricotec-
273 9-en-8-one e contém em sua molécula três radicais hidroxila (-OH) livres (Figura 2),
274 que estão associados com sua toxicidade (SOBROVA *et al.*, 2010).

275 **Figura 2** – Estrutura química do desoxinivalenol. Molécula com três radicais hidroxila
276 (-OH) livres.

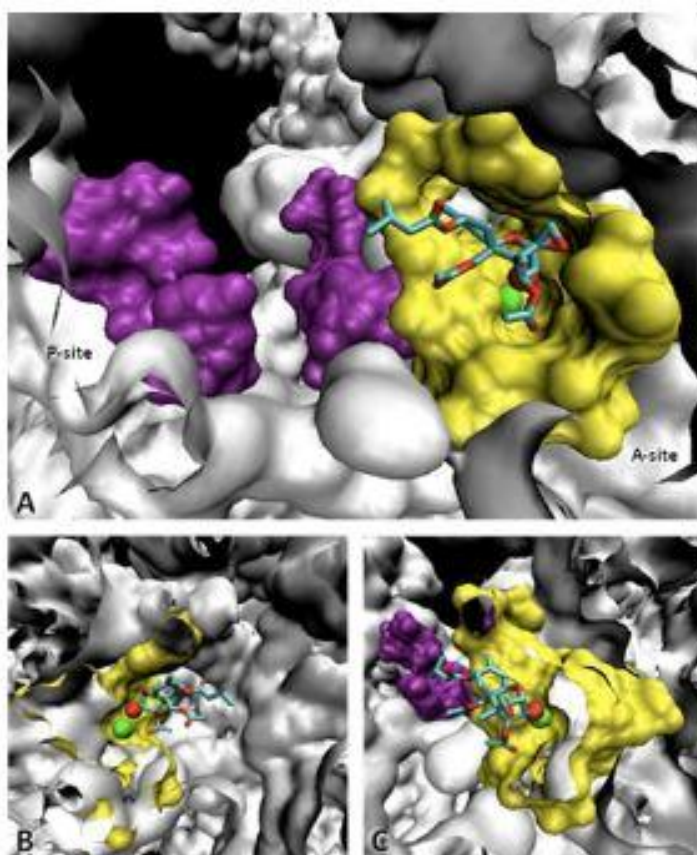


277
278

Fonte: Sobrova *et al.* (2010)

279 O DON inibe a síntese proteica ao se ligar no sítio A do centro da
280 proteína peptidil-transferase da subunidade 60S do ribossomo (Figura 3) e interfere
281 na tradução de proteínas (PESTKA, 2010b). O DON se encaixa no bolso do sítio A da
282 subunidade 60S do ribossomo, e seu terceiro radical –OH está associado a um átomo
283 de magnésio e estabilizado por outros nucleotídeos (PIERRON *et al.*, 2016). A ligação
284 de DON no ribossomo vai gerar uma resposta de estresse ribotóxico, resultando na
285 ativação de proteínas quinases ativadas por mitógeno (MAPKs) (PESTKA, 2010a). A
286 via de sinalização das MAPKs regula diversos processos biológicos, entre eles a
287 apoptose e a imunidade (PESTKA; SMOLINSKI, 2005). A ativação das MAPKs pelo
288 DON leva à ativação de fatores de transcrição (NIELSEN *et al.*, 2009; SUN *et al.*, 2014;
289 YUAN *et al.*, 2018) que vão levar à produção e secreção de citocinas, expressão de
290 ciclo-oxigenase 2 (COX2) e apoptose (KINSER *et al.*, 2005; MOON, 2002).

291 **Figura 3** – Interação entre o local de ligação da subunidade 60S do ribossomo e DON.
292 A – vista frontal, B – vista ortogonal direita, C – vista ortogonal esquerda. Sítios P
293 (roxo) e A (amarelo) da subunidade 60S. Radicais hidroxila (vermelho) de DON (azul).
294 Átomo de magnésio dentro do bolso do sítio A (verde).



295
296

Fonte: Pierron et al. (2016)

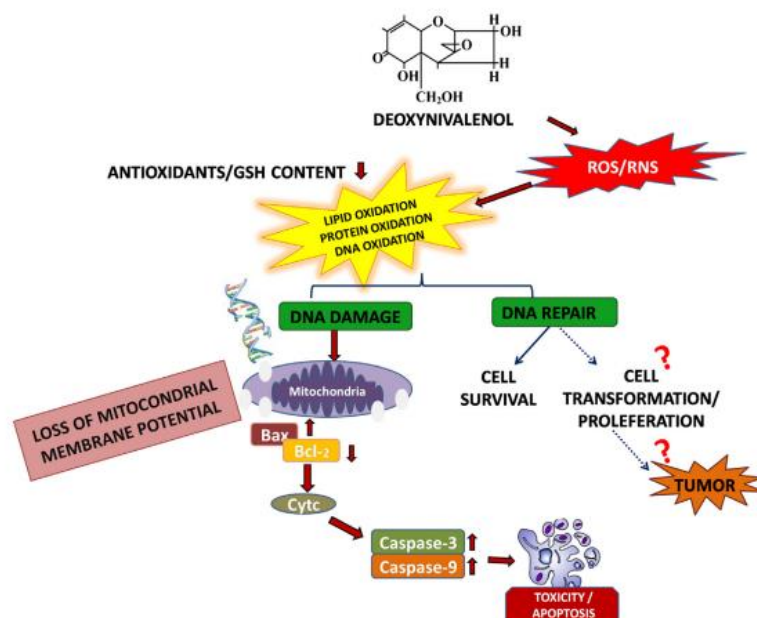
297

A disfunção mitocondrial também desenvolve um papel fundamental

298 na toxicidade induzida por DON, principalmente no intestino (WANG *et al.*, 2021). Essa
299 disfunção ocorre por causa do estresse oxidativo na organela. A oxidação é um
300 processo que ocorre em todos os organismos aeróbios durante processos fisiológicos.
301 Nesse processo, há formação de uma pequena quantidade de substâncias químicas
302 altamente reativas que são chamadas de radicais livres. Esses radicais livres são
303 moléculas que contém um ou mais elétrons desemparelhados na camada orbital
304 externa de átomos de oxigênio (O₂) ou nitrogênio (N₂) e podem ser denominadas
305 como espécies reativas de oxigênio (ERO ou ROS) e espécies reativas de nitrogênio
306 (ERN ou RNS) (BARREIROS; DAVID, 2006; MCMICHAEL, 2007; PAVELESCU, 2015;
307 RUSSO; BRACARENSE, 2016).

308 O estresse oxidativo ocorre quando o equilíbrio está prejudicado e a
309 quantidade de ERO ultrapassa a quantidade de antioxidantes, levando a danos
310 celulares com consequentes lesões teciduais, sendo comum em órgãos com alta
311 demanda e metabolismo energéticos. Isso ocorre por conta de mudanças oxidativas
312 em macromoléculas celulares, morte celular por apoptose ou necrose que geram
313 danos estruturais nos tecidos (BARREIROS; DAVID, 2006; BIRBEN *et al.*, 2012;
314 LYKKESFELDT; SVENDSEN, 2007; PUPPEL; KAPUSTA; KUCZYNSKA, 2014). No
315 proposto mecanismo de ação de estresse oxidativo mediado pelo DON (Figura 4) há
316 um aumento na produção de ERO e ERN e uma diminuição nos compostos
317 antioxidantes (SOD, CAT, GSH, HMOX1), levando à oxidação de lipídios, proteínas e
318 do DNA. Em seguida, a via intrínseca da apoptose será ativada, porque o excesso de
319 ERO leva à perda do potencial de membrana mitocondrial e, conseqüentemente, à
320 liberação do citocromo C, desencadeando a ativação das caspases 9 e 3 que
321 promovem a apoptose (MISHRA *et al.*, 2014; WANG *et al.*, 2021).

322 **Figura 4** – Mecanismo de ação do estresse oxidativo mediado por DON na
 323 mitocôndria. Produção de espécies reativas de oxigênio (ROS) que levam à danos
 324 oxidativos e perda do potencial de membrana mitocondrial, com liberação de
 325 citocromo C (Cytc) no citoplasma e ativação das caspases 9 e 3.



326
327

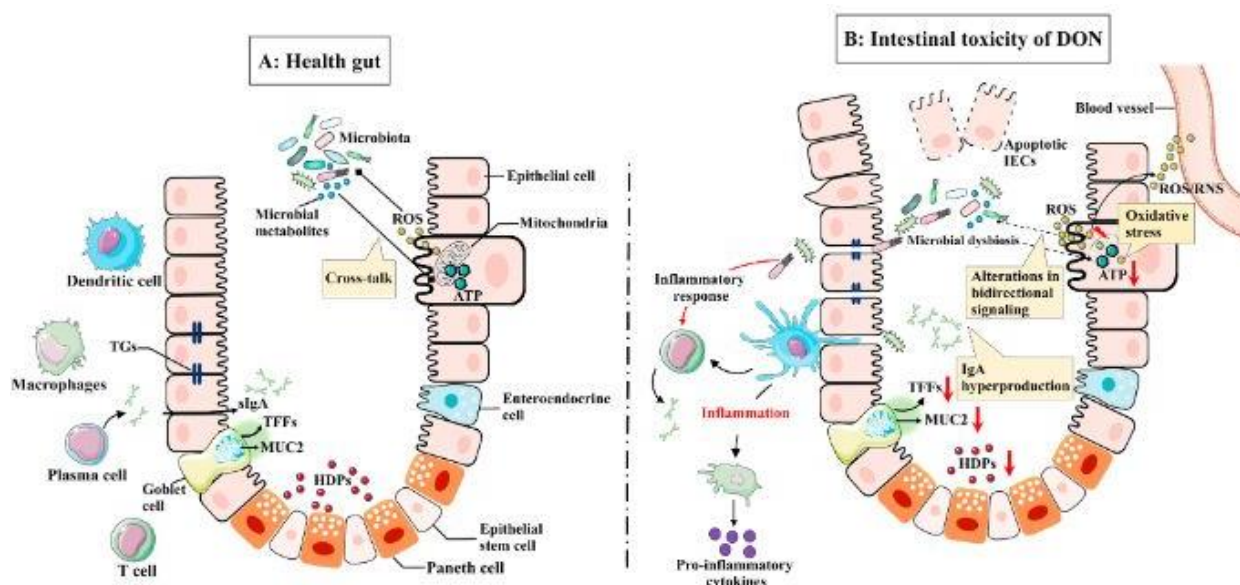
Fonte: Mishra et al. (2014)

328 Os mecanismos gerais de defesa intestinal para eliminar bactérias da
 329 superfície epitelial contam com a liberação de mucinas e fator trifólio 3 (TFF3) pelas
 330 células caliciformes, secreção de peptídeos de defesa do hospedeiro (HDP) pelas
 331 células de Paneth e de Imunoglobulina A (IgA) pelos plasmócitos (WANG *et al.*, 2021).

332 Além disso, como a renovação do epitélio intestinal e a manutenção
 333 da integridade das junções intercelulares são dependentes de energia, a mitocôndria
 334 é cada vez mais reconhecida como essencial na manutenção da saúde intestinal
 335 (NOVAK; MOLLEN, 2015). A disfunção mitocondrial caracterizada pela perda das
 336 capacidades respiratórias, geração reduzida de ATP e superprodução de ERRO, foi
 337 demonstrada em células intestinais expostas ao DON (FAVERO *et al.*, 2018; GUO *et*
 338 *al.*, 2019; KALAISELVI *et al.*, 2013; KANG *et al.*, 2019). O excesso de ERO leva ao
 339 início precoce da apoptose e ao fornecimento insuficiente de ATP. A apoptose
 340 substancial das células epiteliais intestinais comprometem a integridade das junções
 341 intercelulares, e conseqüentemente da barreira intestinal, levando à translocação de
 342 bactérias e antígenos luminiais (Figura 5). Assim, há inflamação, com aumento na
 343 produção de IgA. Já a secreção de mucinas, TFF3 e HDP é inibida pela exposição ao
 344 DON e há uma diminuição de células caliciformes (GEREZ *et al.*, 2015; WANG *et al.*,

345 2021).

346 **Figura 5** – Mecanismo de ação da toxicidade de DON na mitocôndria de células
 347 intestinais. A – Intestino com saúde normal, B – Intestino após a ingestão de alimentos
 348 contaminados com DON.



349
 350

Fonte: Wang et al. (2021)

351 Na União Europeia, as diretrizes regulatórias estabeleceram limites
 352 máximos de DON para a alimentação completa de leitões em 0,9 mg/kg, e em
 353 matérias-primas, como cereais e produtos de milho, em 8 e 12 mg/kg, respectivamente
 354 (EUROPEAN COMMISSION, 2006). Ainda, na Europa, em 2002 foi estabelecida a
 355 ingestão diária tolerável (IDT) provisória para humanos para DON de 1 µg/kg de peso
 356 corporal (PC)/dia pelo Comitê Científico para Alimentos (SCF). No Brasil, não há
 357 legislação para níveis de contaminação por micotoxinas em rações animais. Já para
 358 humanos, a legislação prevê limites máximos toleráveis (LMT) de 200 µg/kg para
 359 alimentos infantis e 750 a 2.000 µg/kg, variando de acordo com o tipo de grão e
 360 beneficiamento utilizado (BRASIL, 2021). Em 2017, a EFSA estabeleceu o risco para
 361 a presença de DON e seus compostos acetilados em alimentos e rações na saúde
 362 humana e animal. Para humanos, o risco não é considerado um problema grave de
 363 saúde. E para suínos, o risco de efeitos agudos para a saúde é baixo com base nas
 364 concentrações dietéticas estimadas (EFSA *et al.*, 2017).

365 Em 2021, na América do Sul e na Europa as duas micotoxinas mais
 366 frequentes foram o desoxinivalenol (46% e 59%, respectivamente) e as fumonisinas
 367 (66% e 49%, respectivamente) (BIOMIN, 2021). Estudos demonstraram que DON está

368 entre as 10 micotoxinas mais frequentes na ração para suínos, com prevalência de
369 77–88% sob uma concentração mediana de 193 µg/kg, e que DON é um potencial
370 marcador da presença de outras micotoxinas, pois a co-ocorrência de DON com
371 outras micotoxinas é muito comum, especialmente com ZEA (97%), BEA (89%) e
372 ENNs (89–93%) (KHOSHAL *et al.*, 2019; NOVAK *et al.*, 2019; SOBROVA *et al.*, 2010).

373 Além disso, uma crescente preocupação está surgindo por conta das
374 mudanças climáticas. Observou-se que o perfil das espécies de *Fusarium* que
375 produzem micotoxinas está mudando no continente europeu (MORETTI; PASCALE;
376 LOGRIECO, 2019). Na Espanha, uma meta-análise em amostras de trigo descreveu
377 uma alta exposição ao DON, especialmente em bebês e crianças abaixo de 3 anos
378 de idade, que tiveram uma ingestão de 175% e 119% da IDT, respectivamente. Pão
379 e produtos derivados foram os principais contribuintes para exposição ao DON em
380 todas as faixas etárias, com valores de IDT variando de 12% a 34% (NARVÁEZ *et al.*,
381 2022).

382 2.4.1.1 Toxicocinética

383 Todas as espécies estudadas possuem algum grau de sensibilidade
384 ao DON, e as espécies mais estudadas estão classificadas em ordem decrescente de
385 sensibilidade: suínos > camundongos > ratos > aves ≈ ruminantes (PRELUSKY *et al.*,
386 1994).

387 A diferença entre elas se deve principalmente ao diferente tipo de
388 metabolização a que o DON é submetido em cada espécie, pois aves e ruminantes
389 possuem bactérias comensais que são capazes de transformar rapidamente o DON
390 em um derivado de-epóxido (DOM-1) não-tóxico antes de chegar ao intestino delgado
391 e ser absorvido (MARESCA, 2013). Outros derivados do DON também podem ser
392 formados por fungos (derivados acetilados: 3ADON e 15ADON) e plantas (D3G), ou
393 por animais (D3GA e D15GA) pelo processo de glicuronidação hepática (MARESCA,
394 2013). O D3GA também não apresenta toxicidade, já que sua molécula não consegue
395 se ligar no sítio A da subunidade 60S ribossomal (PIERRON *et al.*, 2016).

396 Não se sabe exatamente como o DON entra nas células, mas é
397 provavelmente através de um mecanismo de difusão passivo (SERGENT *et al.*, 2006).
398 Ainda não existem estudos identificando a entrada dos derivados de DON nas células,

399 e supõe-se que os derivados que passaram pela metabolização hepática têm menor
400 capacidade de entrar nas células, por terem maior polaridade e massa molecular que
401 o DON (MARESCA, 2013).

402 Em suínos, o DON é rapidamente absorvido no intestino delgado e
403 atinge o pico de concentração plasmática em 15–30 minutos, sendo que em torno de
404 82% de todo DON ingerido é absorvido pelos intestinos (PESTKA; SMOLINSKI, 2005).
405 Porém, a concentração máxima no plasma não excede 25% da dose ingerida e o DON
406 possui uma meia-vida plasmática de 4 horas (ERIKSEN; PETTERSSON; LINDBERG,
407 2003). Quanto à sua excreção, a maior parte parece ser eliminada na forma de D3GA,
408 D15GA, DON, glicuronídeo-DOM1 e DOM-1. Em suínos, 68% do total de DON
409 ingerido é eliminado na urina como DON ou D3GA/D15GA, o restante é eliminado nas
410 fezes na forma de DOM-1 e DON (80% e 20%, respectivamente) (MARESCA, 2013).

411 2.4.1.2 Estudos *in vitro*

412 Estudos *in vitro* têm sido amplamente realizados para estudar os
413 efeitos das micotoxinas em diversos tipos celulares (DARWISH *et al.*, 2020; KATIKA
414 *et al.*, 2012; MAYER *et al.*, 2017; NOVAK *et al.*, 2018; WENTZEL *et al.*, 2017). Um
415 dos principais parâmetros avaliados nesse modelo de estudo é a viabilidade celular.
416 Os resultados encontrados na literatura já demonstraram que o DON diminui a
417 viabilidade celular em vários tipos celulares. O DON apresentou citotoxicidade para
418 células hepáticas de carcinoma humano (HepG2) após 24 horas em concentrações
419 variando de 1-10 μM (DARWISH *et al.*, 2020; FERNÁNDEZ-BLANCO *et al.*, 2018;
420 MAYER *et al.*, 2017). Uma concentração inibitória (IC_{50}) de 41,4 μM foi encontrada em
421 HepG2, mas em hepatócitos primários de humanos e hepatócitos de ratos (BRL 3A)
422 tiveram uma IC_{50} de 6 e 13 μM , respectivamente. Esses resultados mostram que
423 células saudáveis são mais sensíveis ao DON (KÖNIGS *et al.*, 2008; SUN *et al.*, 2015).
424 A partir de doses intermediárias (4-16 μM), o DON também causou citotoxicidade nos
425 hepatócitos de suínos e em co-culturas de hepatócitos + células de Kupffer (DÖLL *et*
426 *al.*, 2009).

427 Levando em consideração a sensibilidade do tipo celular, as células
428 intestinais aparentam ser mais sensíveis ao DON do que as células hepáticas. Após
429 24 horas, a viabilidade celular estava diminuída com doses baixas de DON (0,5 e 0,9

430 μM) em células intestinais de suínos IPEC-J2 e IPEC-1 (YANG *et al.*, 2019). E após
431 48 horas houve uma inibição na viabilidade de 50% das células com 1 e 3 μM em
432 células intestinais humanas (Caco-2) e em IPEC-1 (KHOSHAL *et al.*, 2019; PIERRON
433 *et al.*, 2016).

434 O DON é capaz de alterar a imunidade no órgão em que se encontra
435 (PAYROS *et al.*, 2016). Os leucócitos são importantes alvos da ação
436 imunomoduladora de DON. Em linfócitos do baço de suínos e linfócitos circulantes de
437 humanos houve citotoxicidade de maneira dose-dependente ao DON em
438 concentrações que variaram de 0,02 – 25 μM por 24 horas; nos linfócitos do baço a
439 IC_{50} foi de 5 μM após 48 horas e nos linfócitos circulantes a IC_{50} foi de 0,3 μM após 24
440 horas (REN *et al.*, 2017; YANG *et al.*, 2014). O DON também inibiu a proliferação de
441 linfócitos circulantes de humanos e suínos, e a IC_{50} foi de 0,4 e 0,5 μM ,
442 respectivamente (TARANU *et al.*, 2010). Portanto, linfócitos circulantes parecem ser
443 mais sensíveis ao DON do que linfócitos do baço. Já em neutrófilos de suínos,
444 concentrações de 0,5–10 μM por até 24 horas diminuíram a secreção de interleucina
445 8 (IL8), a quimiotaxia e a capacidade de fagocitose dessas células. A ação do DON
446 nos neutrófilos foi mediada pela fosforilação da MAPK p38 nos primeiros 30 minutos
447 de exposição (GAUTHIER *et al.*, 2013). O contrário foi encontrado em macrófagos
448 expostos ao DON, em que houve aumento na secreção de interleucina 8 (IL8) e fator
449 de necrose tumoral alfa (TNF- α) (SUGITA-KONISHI; PESTKA, 2001).

450 No intestino, o DON aumenta a resposta inflamatória. Em células
451 IPEC-1 expostas à 10 μM por 24 horas, houve aumento na expressão de várias
452 citocinas (IL8, IL1 α , IL1 β e TNF- α) (CANO *et al.*, 2013). E em células Caco-2 expostas
453 por 24 horas à 2,5-100 μM , o aumento na secreção de interleucinas (IL) foi diretamente
454 afetada pelo DON, que também potencializou o efeito de interleucina 1 β (IL1 β) na
455 secreção de IL8, diminuiu a resistência elétrica transepitelial (TEER) e permitiu o
456 aumento na translocação de bactérias intestinais (MARESCA *et al.*, 2008). No mesmo
457 tipo celular, o DON (30 μM) também aumentou a atividade do fator nuclear κB (NF-
458 κB) e a secreção de IL8 e esse efeito foi acentuado com a presença de uma
459 estimulação inflamatória (VAN DE WALLE *et al.*, 2008).

460 O estresse oxidativo induzido por DON causa danos em proteínas,
461 lipídios e DNA, sendo um dos seus mecanismos de toxicidade (MISHRA *et al.*, 2014).

462 Em linfócitos de humanos (0,2-1,7 μM de DON por 24h) houve danos ao DNA,
463 aumento na expressão de ERO e na peroxidação lipídica e diminuição na expressão
464 de um gene antioxidante (HMOX1) (YANG *et al.*, 2014). Em células HepG2, a
465 exposição à 2,5-60 μM por até 24 horas aumentou a geração de ERO, os danos ao
466 DNA e os níveis de enzimas antioxidantes (CAT, SOD e GPx), além de diminuir os
467 níveis do antioxidante glutathiona (GSH) (BODEA *et al.*, 2009; ZHANG *et al.*, 2009).
468 Efeitos semelhantes foram relatados em HepG2 expostas à 0,1-5 μM por 24 horas,
469 em que o DON também causou uma regulação negativa nas enzimas antioxidantes
470 reguladas pela via Keap1-Nrf2 (DARWISH *et al.*, 2020). A apoptose mediada pelo
471 estresse oxidativo que o DON promove nas células, foi verificada pelo aumento de
472 atividade de caspase-3, também esteve presente em HepG2 e hepatócitos primários
473 de humanos expostos à 0,1-100 μM de DON por até 48 horas (KÖNIGS *et al.*, 2008).
474 Em hepatócitos de ratos BRL 3, o DON, em concentrações de 1-4 μM por 24 horas,
475 diminuiu a expressão do gene anti-apoptótico Bcl-2 e aumentou a expressão dos
476 genes caspase-3 e Bax e a produção de proteínas (p53) envolvida na apoptose (SUN
477 *et al.*, 2015).

478 Em células intestinais HT-69, após 24 horas de exposição à 0,8-1,7
479 μM de DON, houve aumento na geração de ERO e ERN, alteração do estado
480 antioxidante e indução de COX2 e NF- κ B que levam à apoptose (KALAISELVI *et al.*,
481 2013; KRISHNASWAMY; DEVARAJ; PADMA, 2010). O DON, em concentrações de
482 0,9-13,5 μM por 24 horas, também foi capaz de regular negativamente a via Keap1-
483 Nrf2 em células IPEC-J2, além de aumentar o número de células apoptóticas (YANG
484 *et al.*, 2019). E nesse mesmo tipo celular, a exposição de 0,7-20 μM de DON por 24
485 horas diminuiu os níveis de enzimas antioxidantes (CAT e GPx), aumentou a geração
486 de ERO e a expressão de genes inflamatórios (IL1 β , IL6 e TNF- α) e apoptóticos
487 (caspase-3/8/9) (KANG *et al.*, 2019).

488 2.4.1.3 Estudos *in vivo* e *ex vivo*

489 A morfologia tecidual é um importante parâmetro para verificar os
490 efeitos tóxicos das substâncias e é uma das vantagens dos modelos *in vivo* e *ex vivo*
491 em relação ao modelo *in vitro*. Em baixas doses, DON (12 $\mu\text{g}/\text{kg}$ de PC) e/ou ZEA (40
492 $\mu\text{g}/\text{kg}$ de PC), fornecidos na ração por seis semanas, não afetou a morfologia do
493 duodeno de suínos. A espessura da mucosa e o comprimento das vilosidades

494 permaneceram inalterados, porém o número de linfócitos presentes no epitélio das
495 vilosidades foi significativamente maior do que no grupo controle (LEWCZUK *et al.*,
496 2016b). Em leitões recém-nascidos (mães consumiram 9,5 mg/kg DON por cinco
497 semanas) e suínos adultos (4,6 mg/kg por quatro semanas), não houve alteração da
498 morfologia hepática (RENNER *et al.*, 2017; TIEMANN *et al.*, 2008).

499 Já a ingestão dessas mesmas micotoxinas, em doses realistas de
500 DON (1,5 ou 3 mg/kg), além do nivalenol (NIV) em associação ou sozinhas por quatro
501 semanas, induziu alterações histológicas sistêmicas, afetando o fígado, intestinos
502 (jejuno e íleo) e órgão linfoides de suínos. No fígado as principais alterações foram
503 desorganização dos cordões de hepatócitos, vacuolização citoplasmática e
504 megalocitose. No intestino houve atrofia e fusão de vilosidades e edema de lâmina
505 própria multifocalmente, assim como houve diminuição de células caliciformes em
506 ambas as regiões do intestino. Em linfonodos mesentéricos e em baço as alterações
507 foram leves e consistiram principalmente em depleção folicular e apoptose de
508 linfócitos (GEREZ *et al.*, 2015).

509 Alterações compatíveis também foram observadas no fígado de
510 leitões alimentados com DON (3 mg/kg) e/ou FB (6 mg/kg) na dieta por cinco semanas
511 apresentou desorganização dos cordões de hepatócitos, megalocitose e vacuolização
512 citoplasmática (GRENIER *et al.*, 2011). Da mesma forma, em ratos, a ingestão de
513 DON (1,75 ou 11,4 mg/kg) por quatro semanas causou desorganização dos cordões
514 hepáticos, vacuolização citoplasmática moderada, presença de infiltrado inflamatório
515 e megalocitose (BRACARENSE *et al.*, 2017). Nos dois estudos a proliferação de
516 hepatócitos estava aumentada nos animais que receberam micotoxinas em baixas
517 doses, reforçando a hipótese de que uma baixa concentração de DON ativa a via das
518 MAPKs para aumentar a sobrevivência celular (BRACARENSE *et al.*, 2017; GRENIER
519 *et al.*, 2011). A associação de DON a um metal traço, o cádmio, na ração de ratos por
520 quatro semanas também provocou atrofia e fusão das vilosidades, edema intersticial,
521 achatamento dos enterócitos apicais e redução de profundidade de cripta, porém não
522 causou alteração no comprimento de vilosidade (LUO *et al.*, 2019).

523 Em aves, a ingestão por três semanas (7,5 mg/kg) diminuiu a altura
524 de vilosidades e a profundidade de criptas tanto no duodeno, como no jejuno
525 (OSSELAERE *et al.*, 2013). A morfologia intestinal de aves alimentadas com 19,3

526 mg/kg por uma semana também causou atrofia de vilosidades, edema e vacuolização
527 de enterócitos, edema intersticial, infiltrado inflamatório e aderência de bactérias às
528 vilosidades. Aumentou a profundidade de cripta e o número de células caliciformes e
529 linfócitos intraepiteliais. No fígado, também aumentou o escore lesional, com
530 desorganização trabecular, infiltrado inflamatório, congestão, vacuolização
531 citoplasmática dos hepatócitos, megalocitose e necrose (SOUZA *et al.*, 2020). No
532 entanto, a ingestão por seis semanas de uma dieta contaminada com DON (10 mg/kg)
533 promoveu poucas alterações, com diminuição da altura e espessura de vilosidades
534 em duodeno e jejuno (AWAD *et al.*, 2006).

535 A exposição de explantes de jejuno de suínos ao DON e/ou
536 fumonisina B1 (FB1) também levou a alterações histológicas como atrofia e fusão das
537 vilosidades de maneira multifocal a difusa, perda do epitélio apical das vilosidades,
538 vacuolização celular, achatamento dos enterócitos, diminuição do comprimento de
539 vilosidade e no número de células caliciformes nas vilosidades e em região de cripta.
540 Mas quando associadas a um antioxidante, o ácido fítico, o escore dessas lesões
541 diminuiu, indicando que o ácido fítico tem um efeito protetor contra essas micotoxinas
542 (SILVA *et al.*, 2014, 2019). Também se observou que os efeitos de fusarenona X (FX)
543 foram mais prejudiciais para a estrutura jejunal do que o DON, embora ambas as
544 micotoxinas causaram lesão nas células intestinais. A principal alteração observada
545 foi a fusão de vilosidades, mas também foram visualizadas alterações como: células
546 epiteliais cuboides, edema de lâmina própria, atrofia das vilosidades e desnudamento
547 apical com perda de enterócitos (ALASSANE-KPEMBI *et al.*, 2017b)

548 Em relação à imunidade dos animais, o DON é capaz de alterar a
549 resposta imune do organismo, promovendo aumento de imunoglobulinas e citocinas
550 (OSWALD *et al.*, 2005). O aumento desses mediadores inflamatórios induzido por
551 DON já foi descrito em vários órgãos como intestino, baço, linfonodos, fígado, rins e
552 pulmões (PESTKA, 2010a). O aumento na expressão de citocinas (IL1 α , IL1 β , IL6,
553 IL8, IL10, TNF α , NF- κ B e CCL20) foi observado no jejuno, fígado e baço de leitões
554 alimentados por 1 semana com 3 mg/kg (BRACARENSE *et al.*, 2020) e no jejuno de
555 leitões alimentados com 0,5 nmol/kg PC por três semanas ou 1 nmol/kg PC por duas
556 semanas (PIERRON *et al.*, 2018) e 3 mg/kg por 5 semanas (BRACARENSE *et al.*,
557 2012), no fígado de suínos alimentados com 1 mg/kg por seis semanas (CHEN *et al.*,
558 2008) e nos explantes intestinais de suínos expostos à 0,05-40 μ M por 4-5 horas

559 (ALASSANE-KPEMBI *et al.*, 2017b; PIERRON *et al.*, 2016).

560 Assim como nas células, estudos já comprovaram que DON é capaz
561 de alterar o estado redox do organismo de animais *in vivo*. A ingestão de 4 mg/kg por
562 duas semanas em leitões levou ao aumento de danos ao DNA de linfócitos e à
563 diminuição da capacidade total antioxidante (CTAO) plasmática (FRANKIČ; SALOBIR;
564 REZAR, 2008), e quando consumido por três semanas, também diminuiu a CTAO e
565 outros antioxidantes (GSH, GPx e SOD) e aumentou os níveis de ERO e a
566 peroxidação lipídica (MDA) (TANG; YUAN; LIAO, 2021). Em camundongos
567 alimentados com 2,4 mg/kg de PC por quatro semanas, houve diminuição de
568 antioxidantes (CAT e GPx) e aumento na expressão de genes que participam da
569 proteção ao estresse oxidativo (Keap1, Nrf2, HMOX1, NQO1 e GCLM) e são ativados
570 em baixos níveis de estresse oxidativo (BAI *et al.*, 2021).

571 Mesmo as aves, sendo animais mais resistentes ao DON, tiveram
572 alterações no estado redox após o consumo de concentrações altas de DON. Quando
573 ingerida uma concentração de 7,5 mg/kg por três semanas, o DON diminuiu a
574 expressão de genes antioxidantes (HMOX e HIF-1 α) no fígado e aumentou a
575 expressão de um gene de oxidação tardio (XOR) no jejuno e fígado (OSSELAERE *et*
576 *al.*, 2013). A ingestão de 10 mg/kg por cinco semanas também levou ao aumento da
577 peroxidação lipídica (TBARS) e danos ao DNA de linfócitos (AWAD *et al.*, 2014;
578 OSSELAERE *et al.*, 2013). Nos animais alimentados com 19,3 mg/kg por duas
579 semanas, houve redução da capacidade antioxidante (GSH, FRAP e ABTS) e
580 aumento do estresse oxidativo (TBARS e NBT) no intestino e fígado (SOUZA *et al.*,
581 2020).

582 A apoptose *in vivo* induzida por DON foi confirmada pela imuno-
583 histoquímica de caspase-3 no fígado de leitões injetados com 1 mg/kg de PC (MIKAMI
584 *et al.*, 2010) e de camundongos alimentados com 5 mg/kg por duas semanas (SUN *et*
585 *al.*, 2014), nos linfonodos de leitões alimentados com 1,5 mg/kg por quatro semanas
586 (GEREZ *et al.*, 2015) e de ratos alimentados com 1,75 ou 11,4 mg/kg por até quatro
587 semanas (BRACARENSE *et al.*, 2017) e em explantes intestinais de suínos expostos
588 à 10 μ M por 4 horas (SILVA *et al.*, 2014). No entanto, em explantes ovarianos de
589 suínos expostos à 10 μ M de DON por 48 horas, não se observou apoptose (GEREZ
590 *et al.*, 2021).

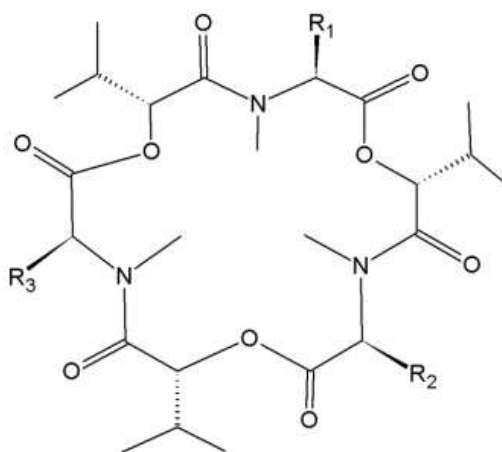
591 2.4.2 Micotoxinas Emergentes

592 Micotoxinas emergentes são micotoxinas que não são determinadas
593 rotineiramente e nem possuem uma regulamentação. Porém, sua incidência está
594 aumentando rapidamente (VACLAVIKOVA *et al.*, 2013). Podem contaminar uma
595 grande variedade de alimentos e são consideradas emergentes, pois, com o
596 desenvolvimento de técnicas avançadas, como cromatografia líquida associada à
597 espectrometria de massa, foi possível identificar diferentes tipos de micotoxinas que
598 não eram detectadas antes da existência desses métodos (FRAEYMAN *et al.*, 2017).

599 A beauvericina (BEA) e as eniatinas (ENNs) são exemplos dessas
600 micotoxinas emergentes. Elas são hexadepsipeptídeos que contém três N-metil
601 aminoácidos e três grupos de hidroxiácido em sua estrutura (Figura 6) (URBANIAK;
602 WAŚKIEWICZ; STEPIEŃ, 2020). A BEA foi isolada pela primeira vez em 1969 a partir
603 do fungo *Beauveria bassiana* (HAMILL *et al.*, 1969) e as ENNs foram descobertas a
604 partir de culturas de *Fusarium oxysporum* (GÄUMANN; ROTH; ETTLINGER, 1947),
605 mas tanto a BEA quanto as ENNs também são produzidas a partir de várias espécies
606 de *Fusarium*, como *F. acuminatum*, *F. avenaceum*, *F. oxysporum*, *F. poae*, *F.*
607 *sporotrichioides*, *F. sambucinum* and *F. tricinctum*.

608 No total, existem 27 tipos de ENNs já descritas, mas os tipos mais
609 frequentes são ENN A, ENN A1, ENN B e ENN B1. A ENN A possui três radicais
610 isoleucina e a ENN B tem três radicais valina, enquanto a ENN A1 tem um radical
611 valina e dois isoleucina e a ENN B1 possui dois radicais valina e um radical isoleucina
612 (FRAEYMAN *et al.*, 2017; JESTOI, 2008).

613 **Figura 6** – Estrutura química da beauvericina e eniatinas (A, A1, B e B1).
 614 Beauvericina, R1 = R2 = R3: fenilmetil; Eniatina A, R1 = R2 = R3: $-\text{CH}(\text{CH}_3)\text{CH}_2\text{CH}_3$;
 615 Eniatina A1, R1 = R2: $-\text{CH}(\text{CH}_3)\text{CH}_2\text{CH}_3$, R3: $-\text{CH}(\text{CH}_3)_2$; Eniatina B, R1 = R2 = R3:
 616 $-\text{CH}(\text{CH}_3)_2$; Eniatina B1, R1 = R2: $-\text{CH}(\text{CH}_3)_2$, R3 = $-\text{CH}(\text{CH}_3)\text{CH}_2\text{CH}_3$;

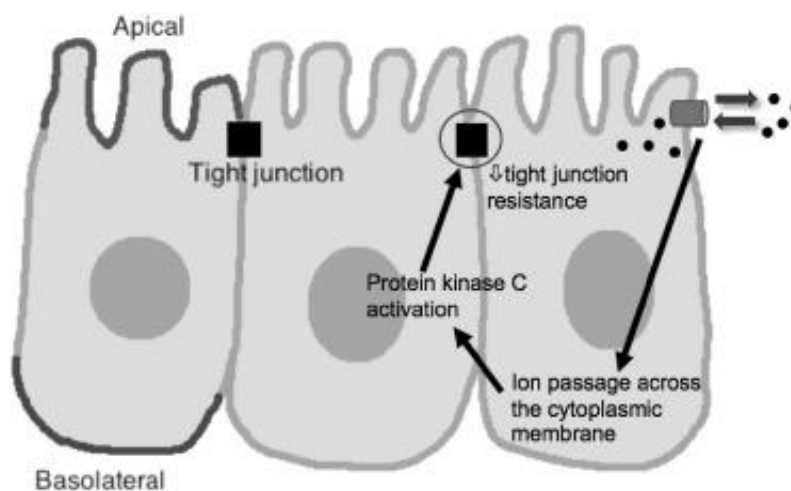


617
618

Fonte: Fraeyman et al. (2017)

619 Sabe-se que sua toxicidade está relacionada às suas propriedades
 620 ionóforas, pois tanto BEA quanto as ENNs são capazes de transportar cátions
 621 monovalentes (K^+) e divalentes (Ca^{2+}) através da membrana celular, levando a
 622 alterações tóxicas por causar uma desproporção intracelular nos íons transportados,
 623 afetando a homeostase celular e provavelmente diminuindo a resistência entre as
 624 junções intercelulares no intestino (Figura 7) (BERTERO; SPICER; CALONI, 2018;
 625 FRAEYMAN *et al.*, 2017; JESTOI, 2008; MALLEBRERA *et al.*, 2018; PROSPERINI *et*
 626 *al.*, 2017).

627 **Figura 7** – Mecanismo de ação de BEA e ENNs nas junções intercelulares de
 628 enterócitos. Transporte de cátions através de poros formados na membrana celular.



629
630

Fonte: Bertero et al. (2018)

631 As ENNs têm alta seletividade por íons potássio (K^+) e em
632 mitocôndrias de ratos, promovem um aumento no influxo de K^+ para a matriz
633 mitocondrial, causando edema da organela. O aumento de cálcio (Ca^{2+}) intracelular
634 também pode ocorrer porque a capacidade de retenção de cálcio na matriz
635 mitocondrial está diminuída na presença de BEA e ENNs. Esse aumento de Ca^{2+} pode
636 induzir a apoptose, pois esse íon é responsável por ativar a via das caspases (JOW
637 *et al.*, 2004; TONSHIN *et al.*, 2010).

638 BEA e ENNs já foram detectados em uma variedade de alimentos ou
639 rações originários de vários países (URBANIÁK; WAŚKIEWICZ; STEPIEŃ, 2020). A
640 BEA é encontrada em cereais como trigo, aveia, cevada e centeio, com prevalência
641 que pode variar de 12 a 100%, mas geralmente a concentração não ultrapassa 100
642 $\mu\text{g}/\text{kg}$. Porém, em outros cereais, como arroz, os níveis de contaminação podem
643 chegar a 26.300 $\mu\text{g}/\text{kg}$ (FRAEYMAN *et al.*, 2017; MALLEBRERA *et al.*, 2018). As
644 ENNs também contaminam cereais como trigo, aveia, cevada e centeio, com
645 prevalência de 96 a 100%. Os níveis de contaminação geralmente variam entre 41-
646 569 $\mu\text{g}/\text{kg}$, mas ocasionalmente podem ultrapassar 1.000 $\mu\text{g}/\text{kg}$ (FRAEYMAN *et al.*,
647 2017; PROSPERINI *et al.*, 2017).

648 Estudos com muitas amostras e análises de várias micotoxinas
649 revelaram uma alta prevalência de micotoxinas emergentes (GRUBER-DORNINGER
650 *et al.*, 2017; KHOSHAL *et al.*, 2019; NOVAK *et al.*, 2019). No entanto, existem poucos
651 estudos, a maioria *in vitro*, sobre os efeitos dessas micotoxinas na saúde animal e
652 humana e nenhuma legislação ou recomendação foi desenvolvida até o momento. O
653 que existe na literatura é uma opinião científica para avaliação de riscos para BEA e
654 ENNs e a conclusão é de que essa avaliação não pode ser realizada devido à falta de
655 dados sobre a toxicidade *in vivo* dessas micotoxinas (EFSA, 2014).

656 2.4.2.1 Toxicocinética

657 Não existem muitos estudos de toxicocinética para BEA
658 (MALLEBRERA *et al.*, 2018) e com os resultados encontrados na literatura não foi
659 possível delinear um perfil tempo-concentração em suínos após administração oral,
660 pois apenas em 2 momentos a concentração plasmática de BEA ultrapassou limite de
661 quantificação (DEVREESE *et al.*, 2013).

662 Com a administração crônica (4 semanas) de ENN A em ratos, foi
663 possível detectar aumento nos níveis dessa micotoxina no soro a partir da segunda
664 semana de tratamento, mas ela não foi detectada nas fezes ou urina em nenhum
665 momento. A hipótese apontada seria que a ENN A sofre bioacumulação em alguns
666 órgãos e, por consequência, é encontrada no soro (JUAN *et al.*, 2014). Outro estudo
667 com fases *in vitro* e *in vivo* sobre a toxicocinética de ENN A em ratos também foi
668 conduzido. Os autores verificaram que a ENN A teve alta ligação às proteínas
669 plasmáticas (99%), alta depuração hepática, sofreu metabolização principalmente
670 pela via da CYP3A4 e a administração oral de 5 mg/kg de ENN A obteve uma
671 biodisponibilidade oral absoluta de 47% (BHATERIA *et al.*, 2022).

672 Após a administração intraperitoneal de BEA e ENN B, por três e dois
673 dias, respectivamente, ficou demonstrado que BEA estava presente em vários tecidos
674 (músculo, intestinos, gordura, cérebro, rim e fígado) e no soro na forma não
675 metabolizada e em concentrações baixas. Também foi verificado que a BEA sofre
676 bioacumulação no fígado desses animais, com sua concentração sendo 18 vezes
677 maior que a de ENN B nesse tecido (RODRÍGUEZ-CARRASCO *et al.*, 2016).

678 Pela via oral, a biodisponibilidade varia de acordo com a espécie
679 (FRAEYMAN *et al.*, 2017; MALLEBRERA *et al.*, 2018; PROSPERINI *et al.*, 2017). A
680 ENN B1 em suínos tem biodisponibilidade de aproximadamente 91%, mas em frangos
681 a ENN B e B1 não são muito absorvidas, com biodisponibilidade de 11% e 5%,
682 respectivamente (DEVREESE *et al.*, 2014; FRAEYMAN *et al.*, 2016).

683 Essas diferenças entre as espécies podem ser explicadas pela
684 biotransformação que essas micotoxinas sofrem no organismo dos animais, esse
685 processo gera metabólitos hidroxilados e carboxilados. Em suínos, após
686 administração oral, foi encontrada maior razão metabólito/ENN B1 do que após
687 administração intravenosa, indicando que há um metabolismo pré-sistêmico atuando
688 nessa espécie (IVANOVA *et al.*, 2017). Em frangos não foram encontradas evidências
689 de que esse metabolismo pré-sistêmico atue de forma diferente do metabolismo
690 sistêmico, já que há baixa concentração plasmática dos metabólitos após
691 administração oral (FRAEYMAN *et al.*, 2017).

692 2.4.2.2 Estudos *in vitro*

693 Muitos dos estudos descritos na literatura com micotoxinas
694 emergentes foram realizado com experimentos *in vitro*. A tabela 1 traz as informações
695 a respeito dos principais efeitos dessas micotoxinas em diferentes tipos celulares.

696 Os efeitos citotóxicos para BEA e ENNs já foram demonstrados em
697 vários estudos *in vitro* em diversos tipos celulares (FRAEYMAN *et al.*, 2017, 2018b;
698 JUAN-GARCÍA *et al.*, 2019; MALLEBRERA *et al.*, 2018; PROSPERINI *et al.*, 2013a,
699 2013b, 2017).

700 Em células Caco-2 tratadas com BEA, a IC₅₀ foi equivalente à 24,6 e
701 12,7 µM após 24 e 48 horas de exposição, respectivamente. E em células HT-29 a
702 IC₅₀ correspondeu a 15 e 9,7 µM após 24 e 48 horas, respectivamente (PROSPERINI
703 *et al.*, 2013a). Ainda nas células Caco-2, outras micotoxinas também foram testadas.
704 A exposição combinada à ENN B, DON e alternariol (AOH) comprovou que a
705 viabilidade celular diminuiu na seguinte ordem: (DON + AOH + ENN B) > (DON +
706 AOH) > (ENN B + AOH) > (DON + ENN B) (FERNÁNDEZ-BLANCO; FONT; RUIZ,
707 2016).

708 Em três tipos celulares diferentes, células Caco-2, HT-29 e HepG2, a
709 citotoxicidade das ENNs (A, A1, B, B1, B4 e J3) (0-30 µM) foi testada por 24 e 48
710 horas, e entre todas, a ENN A1 foi a mais citotóxica (IC₅₀ 9,1-12,3 µM e 1,4-2,7 após
711 24 e 48 horas, respectivamente) e as ENNs A, B1 e B4 foram as menos citotóxicas
712 entre todas (MECA; FONT; RUIZ, 2011). Em outro estudo com células HepG2 e Balb
713 3T3, a menor dose efetiva (DE₅₀), em que 50% das foram afetadas, foi equivalente à
714 0,50 µM de ENN B em HepG2, indicando que esse tipo celular é mais sensível à ENN
715 B (JONSSON *et al.*, 2016).

716 Nesse mesmo tipo celular, verificou-se que a exposição tanto de BEA
717 e ocratoxina A (OTA) isoladamente quanto em conjunto foi citotóxica para essas
718 células, com BEA sendo mais tóxica que OTA quando comparadas isoladamente e
719 quando misturadas a toxicidade ocorreu de maneira dose-dependente (JUAN-
720 GARCÍA *et al.*, 2019). Já em células de hepatoma de rato (H4IIE) e células hepáticas
721 de peixes (RTH-149 e PLHC-1), em que foram analisadas a citotoxicidade de BEA,
722 DON e OTA, a micotoxina com menor toxicidade foi OTA, enquanto BEA e DON

723 mostraram toxicidade similar nessas células (GARCÍA-HERRANZ *et al.*, 2019).

724 Um tratamento com ENN B e outras micotoxinas em células
725 pulmonares (V79) demonstrou que a ENN B produziu citotoxicidade e a IC₅₀
726 encontrada foi de 4 µM, sendo inferior apenas à IC₅₀ de DON, que foi equivalente à
727 0,8 µM (FÖLLMANN; BEHM; DEGEN, 2009).

728 A citotoxicidade também foi verificada em células ovarianas CHO-K1,
729 as micotoxinas BEA (2,2-10,7 µM), patulina (PAT) (2,9 µM) e esterigmatocistina (STE)
730 (12,5-25 µM) foram testadas isoladamente e em combinação. Após 24-72 horas, as
731 combinações de 2 ou 3 micotoxinas tiveram efeito citotóxico dose-dependente, agindo
732 de maneira sinérgica (ZOUAOU *et al.*, 2016). Já nas células de origem mieloide de
733 humanos, HL-60 e U-937, o tratamento com BEA (0,1-300 µM) por 4 ou 24 horas
734 causou diminuição da viabilidade celular dose e tempo dependente (CALÒ *et al.*,
735 2004).

736 Tabela 1. Efeitos das micotoxinas BEA e ENNs em estudos realizados em diferentes tipos celulares.

Linagem celular	Micotoxina	Dose	Tempo de exposição	Principais efeitos	Referência
A549	BEA	1-30 μ M	24 h	BEA induziu a apoptose de maneira concentração e tempo dependentes, perda do potencial de membrana mitocondrial e aumentou a liberação de citocromo C mitocondrial e a ativação da caspase 3.	(LIN <i>et al.</i> , 2005)
Blastocistos de camundongos	ENN B1	1-10 μ M	24 h	Diminuição da viabilidade celular, induziu estresse oxidativo intracelular e aumentou a apoptose.	(HUANG <i>et al.</i> , 2019)
Caco-2	BEA	3,125-25 μ M	24-72 h	Diminuição da viabilidade celular, aumento da geração de ERO, indução de apoptose, perda do potencial de membrana mitocondrial e parada do ciclo celular em fase G2/M.	(PROSPERINI <i>et al.</i> , 2013a)
Caco-2	ENN (A, A1, B e B1)	0.5-15 μ M	24-72 h	Diminuição da viabilidade celular na seguinte ordem: ENN A = ENN A1 > ENN B1 > ENN B. Aumento da geração de ERO e peroxidação lipídica. Induziu apoptose, danos ao DNA, perda do potencial de membrana mitocondrial e parada do ciclo celular nas fases G2/M (24h) e S (72h).	(PROSPERINI <i>et al.</i> , 2013b)
Caco-2	ENN B	1-25 μ M	24 h	Perda de funcionalidade lisossômica, parada do ciclo celular na fase G2/M e aumento da produção intracelular de ERO.	(IVANOVA <i>et al.</i> , 2012)
Caco-2	ENN B, DON e AOH	0,312-10 μ M (ENN B e DON) e 1,85-90 μ M (AOH).	24-72 h	Diminuição da viabilidade celular de maneira dose-dependente. Combinações terciárias produziram uma diminuição menor em comparação com combinações binárias.	(FERNÁNDEZ-BLANCO <i>et al.</i> , 2016)
Caco-2 e HT-29	BEA e FUS	0,6-30 μ M	24-48 h	Apenas BEA foi citotóxica para essas linhagens celulares. A biodisponibilidade de BEA foi de 50,1-54,3%, enquanto a biodisponibilidade de FUS foi de 80,2-83,2%.	(PROSPERINI <i>et al.</i> , 2012)
Caco-2, HL-60, A549, GLC-4, SW-1573, KB-3-1, KBC-1, MDA-MB-231 e A549	BEA e ENN	0,5-10 μ M	24-72 h	Houve citotoxicidade por ENN e BEA e ambas as micotoxinas interagiram de forma potente com as funções de transporte ABCB1 e ABCG2.	(DORNETSHUBER <i>et al.</i> , 2009b)
Caco-2, HT-29 e HepG2	ENN (A, A1, B, B1, B4 e J3)	0-30 μ M	24-48 h	ENN A1 foi a mais citotóxica, enquanto ENN A, B1 e B4 foram menos citotóxicas entre as eniatinas testadas.	(MECA <i>et al.</i> , 2011)
CCRF-CEM	BEA	1-10 μ M	24 h	Aumento da atividade da caspase-3 de maneira dose-dependente. A maior dose aumentou a liberação de citocromo C da mitocôndria em um padrão tempo-dependente.	(JOW <i>et al.</i> , 2004)

Células da granulosa de bovinos	BEA e FB1	0-10 μM	48 h	BEA inibiu a proliferação celular e diminuiu fortemente a produção de esteroides. FB1 inibiu fracamente a produção de estradiol e não influenciou os efeitos de BEA.	(ALBONICO <i>et al.</i> , 2017)
Células da granulosa de suínos	BEA and AOH	0,3-20 μM	24 h	Na ausência do fluido folicular (FF), a viabilidade celular diminuiu para ambas as micotoxinas. A presença do FF com AOH manteve a viabilidade celular, mas o FF com BEA não teve efeito citoprotetor.	(SANTOS <i>et al.</i> , 2015)
Células dendríticas humanas e macrófagos	BEA, ENN B e MON	0,1-80 μM (BEA e MON) e 0,1-10 μM (ENN B)	2-8 d	BEA e ENN B foram citotóxicas para essas células. O processo de diferenciação de monócitos em células dendríticas imaturas não foi perturbado. Células dendríticas expostas a BEA e ENN B apresentaram aumento da secreção de IL10 e diminuição da capacidade de endocitose.	(FICHEUX <i>et al.</i> , 2013)
CHO-K1	BEA	0.625, 1.25, 2.5, 5, 10, and 20 μM	24-72 h	Diminuição da viabilidade celular de maneira tempo-dependente, parada do ciclo celular em fase G0/G1, danos ao DNA e aumento da atividade de enzimas antioxidantes.	(MALLEBRERA <i>et al.</i> , 2016)
CHO-K1	BEA	0.1-5 μM	24 h	Aumento das atividades de GST e GPx e diminuição das atividades de GR e GSH após 24h. N-acetilcisteína (NAC) é um eliminador eficaz de BEA.	(MALLEBRERA <i>et al.</i> , 2014)
CHO-K1	BEA	0.1-5 μM	24-72 h	O pré-tratamento com resveratrol (RSV) antes da exposição a BEA causou um efeito citoprotetor e diminuiu a produção de ERO. A BEA sozinha induziu a peroxidação lipídica aumentando os níveis de MDA, mas o pré-tratamento com RSV diminuiu os níveis de MDA.	(MALLEBRERA <i>et al.</i> , 2015)
CHO-K1	BEA, PAT e STE	0,75-20 μM (BEA), 0,049-6,25 μM (PAT) e 1,56-75 μM (STE)	24-72 h	A associação de 2 ou 3 micotoxinas diminuiu a viabilidade celular de forma dose-dependente. Valores de IC ₅₀ de 2,9 μM para PAT, 10,7 (24 h) a 2,2 μM (72 h) e de 25 (24 h) a 12,5 μM (72 h) para BEA e STE, respectivamente.	(ZOUAOU <i>et al.</i> , 2016)
CHO-K1	BEA, PAT e ZEA	1-100 μM (BEA), 0,2-25 (PAT) e 1,5-150 μM (ZEA)	2-48 h	Todas as micotoxinas foram citotóxicas de maneira dose-dependente. Aumento da produção intracelular de ERO e de MDA após a exposição a BEA e PAT de maneira dependente da concentração e do tempo.	(FERRER <i>et al.</i> , 2009)
Fibroblastos embrionários de camundongo	ENN B1	0,625–40 $\mu\text{mol/L}$	24 h	Desestabilização do complexo LAMP-2 na membrana lisossômica, resultando na alcalinização dos lisossomos, vazamento de componentes associados à autofagia mediada por chaperonas no citosol.	(OLIVEIRA <i>et al.</i> , 2019)

H295R e células de Leydig neonatal de suínos	ENN B	0,01–100 μM	24-72 h	Diminuição da viabilidade celular em ambos os tipos de celulares na maior dose (100 μM). Parada do ciclo celular na fase S e diminuição na produção de progesterona, testosterona e cortisol.	(KALAYOU <i>et al.</i> , 2015)
H4IIE, RTH-149 e PLHC-1	BEA, DON, e OTA	0,00076-25 μM (BEA) e 0,003-100 μM (DON e OTA)	24 h	As linhagens celulares de peixes e mamíferos foram muito sensíveis às micotoxinas. Diminuição da viabilidade celular na seguinte ordem: BEA = DON > OTA. Todas as micotoxinas mostraram um forte efeito antagonista no receptor da tireoide. BEA teve um efeito antagonista fraco no receptor de androgênio e OTA produziu uma curva dose-responsiva bifásica no receptor de estrogênio.	(GARCÍA-HERRANZ <i>et al.</i> , 2019)
HepG2	BEA e ENN (A1 e B1)	1,5-3 μM	24-72 h	Parada do ciclo celular em G1, diminuição do percentual apoptótico-necrótico de células e perda do potencial de membrana mitocondrial.	(JUAN-GARCÍA <i>et al.</i> , 2015)
HepG2	BEA e OTA	0-25 μM (BEA) e 0-100 μM (OTA)	24-72 h	Citotoxicidade de BEA foi maior que de OTA. Efeitos aditivos e sinérgicos com a associação das duas micotoxinas. Parada do ciclo celular em fase G0/G1 para a associação.	(JUAN-GARCÍA <i>et al.</i> , 2019)
HepG2 e Balb 3T	ENN B	1,5-100 μM	24-48 h	Diminuição da viabilidade celular e alteração do metabolismo energético.	(JONSSON <i>et al.</i> , 2016)
HepG2, H4IIE, Hct116 e C6	BEA	0,1-25 μM	4-24 h	Alta citotoxicidade para todas as linhagens celulares. Em células H4IIE, induziu apoptose, inibiu a atividade de NF-kB e modulou MAPKs. Nas células C6, causou morte celular por necrose.	(WÄTJEN <i>et al.</i> , 2014)
HL-60 e U-937	BEA	0,1-300 μM	4-24 h	Diminuição da viabilidade celular tempo e dose-dependentes.	(CALÒ <i>et al.</i> , 2004)
HL-60, A549, GLC-4 e KB-3-1	BEA e ENN	0,5-10 μM	24 h	Diversos ensaios celulares e moleculares indicaram que o estresse oxidativo não contribuiu para a citotoxicidade induzida por ENN e BEA. As micotoxinas induziram atividade antioxidante moderada.	(DORNETSHUBER <i>et al.</i> , 2009a)
IPEC-J2	BEA e ENN (A, A1, B e B1)	0-100 μM	24 h	As células foram altamente sensíveis à BEA e ENN A. A ENN B foi a micotoxina menos citotóxica entre todas as micotoxinas testadas.	(FRAEYMAN <i>et al.</i> , 2018)
IPEC-J2	BEA, ENN (A, A1, B e B1), API, AFN, DON, MON, rubrofusarina, equisetina e bikaverina	0-10 μM	24-72 h	Diminuição da resistência elétrica transepitelial (TEER) na seguinte ordem: API > ENN B > BEA = DON > ENN B1 > ENN A > AFN = ENN A1 > moniliformina = equisetina = bikaverina = rubrofusarina. Nenhum efeito citotóxico foi observado após 72h.	(SPRINGLER <i>et al.</i> , 2016)

Jukart-T	BEA	1,5-5 μ M	24 h	Danos mitocondriais, afetando a cadeia respiratória e levando a apoptose através da cascata de caspases.	(ESCRIVÁ <i>et al.</i> , 2018)
Jukart-T	BEA e ENN B	1-15 μ M	24-72 h	BEA diminuiu a viabilidade celular a partir de 3 μ M, enquanto ENN B diminuiu a viabilidade celular apenas com 15 μ M. Apenas BEA apresentou distúrbios do ciclo celular e células apoptóticas e apoptóticas/necróticas aumentadas.	(MANYES <i>et al.</i> , 2018)
Jukart-T	BEA e ENN B	0,1-1,5 μ M	24 h	Alterações transcricionais a nível mitocondrial foram observadas após a co-exposição a BEA e ENN B, incluindo a regulação negativa de genes relacionados à atividade antioxidante.	(ESCRIVÁ <i>et al.</i> , 2019)
Jukart-T	ENN B	1,5-5 μ M	24 h	Genes envolvidos em processos biológicos, funções moleculares e vias relacionadas ao metabolismo mitocondrial e respiração foram significativamente alterados.	(ALONSO-GARRIDO <i>et al.</i> , 2018)
Oócitos, células cumulus e embriões de suínos	BEA	0-10 μ M	44 h	BEA foi tóxica para embriões, oócitos e células cumulus em concentrações superiores a 0,5 μ M, mas exerceu efeitos diferentes nos três tipos celulares.	(SCHOEVERS <i>et al.</i> , 2016)
PBCEC, HBMEC e CCF-STTG1	ENN B e B1	0,1-10 μ M	48 h	As células CCF-STTG1 foram mais sensíveis que as células endoteliais, e apenas ENN B aumentou a atividade da caspase-3 nas células CCF-STTG1. O transporte das micotoxinas através da barreira hematoencefálica revelou altas taxas de influxo para ambas as micotoxinas.	(KRUG <i>et al.</i> , 2018)
PK15	BEA, FB1 e OTA	0,05, 0,5 e 5 μ g/ml	24-48 h	Diminuição da viabilidade celular e aumento dos níveis de GSH e TBARS de maneira concentração e tempo-dependentes. O tratamento combinado com BEA, FB1 e OTA resultou em efeitos aditivos, especialmente após uma exposição de 24 h.	(KLARIĆ <i>et al.</i> , 2007)
RAW264.7	BEA	0-4,5 μ M	24 h	BEA inibiu a resposta inflamatória de macrófagos pela inibição da via do fator de transcrição NF- κ B.	(YOO <i>et al.</i> , 2017)
V79	ENN B, DON, PAT, OTA, ZEA e CIT	0,1–100 μ M	24-48 h	Diminuição da viabilidade celular na seguinte ordem: DON ENN B > PAT > OTA > ZEA > CIT. Nenhum potencial genotóxico significativo da ENN B foi revelado. Fragmentação nuclear induzida por ENN B em baixas concentrações submicromolares.	(FÖLLMANN <i>et al.</i> , 2009)

737 Alternariol (AOH), citrinina (CIT), desoxinivalenol (DON), fumonisina B1 (FB1), fusaproliferina (FUS), moniliformina (MON), ocratoxina
738 A (OTA), patulina (PAT), esterigmatocistina (STE), zearalenona (ZEA).

739 Em células IPEC-J2 de suínos, foi testado a resistência elétrica
740 transepitelial (TEER), e os resultados indicaram que a TEER foi maior para ENN B,
741 seguido de BEA > ENN B1 > ENN A > ENN A1 (SPRINGLER *et al.*, 2016). As células
742 IPEC-J2 também apresentaram maior sensibilidade à BEA e ENN A, tendo menor
743 viabilidade celular após 24h de exposição a essas micotoxinas em várias doses,
744 enquanto na exposição à ENN B, em alta concentração (100 μ M), as células
745 apresentavam viabilidade de 83% após 24 horas (FRAEYMAN *et al.*, 2018b).

746 Em células HepG2, os efeitos de BEA, ENN A1 e B1 após 24-72 horas
747 foram avaliados. BEA e ENN A1 causaram a interrupção do potencial de membrana
748 mitocondrial e ENN B1 promoveu a parada do ciclo celular em fase G1 de maneira
749 tempo dependente (JUAN-GARCÍA *et al.*, 2015).

750 Ainda em relação ao ciclo celular, nas células Caco-2, as ENN A e A1
751 apresentaram maior toxicidade que ENN B1 e BEA, sendo que ENN B teve o menor
752 efeito citotóxico nessas células. ENN A, A1 e B1 induziram danos ao DNA e parada
753 do ciclo celular na fase G₂/M nas concentrações 1,5 e 3 μ M (PROSPERINI *et al.*,
754 2013b).

755 A exposição à BEA também causou parada do ciclo celular nas fases
756 G₀/G₁ de células HepG2, aumentou a apoptose, alterou o potencial de membrana
757 mitocondrial e causou danos ao DNA de células CHO-K1 (JUAN-GARCÍA *et al.*, 2015;
758 MALLEBRERA *et al.*, 2016). Já em células HepG2 tratadas com BEA e/ou OTA, houve
759 acúmulo de células nas fases G₀/G₁ e S para OTA e a combinação de BEA + OTA,
760 mas para BEA isoladamente não houve acúmulo celular, demonstrando que a
761 combinação das duas teve um efeito aditivo e sinérgico (JUAN-GARCÍA *et al.*, 2019).

762 Em doses de 2,5-10 μ M, BEA foi capaz de produzir alterações
763 cromossômicas e micronúcleos em linfócitos de humanos e células IPEC-J2
764 (PROSPERINI *et al.*, 2013a; SPRINGLER *et al.*, 2016). Em fibroblastos embrionários
765 de camundongo, a exposição à ENN B1 (0,625–40 μ mol/L) por 24 horas
766 desestabilizou o complexo LAMP-2 na membrana lisossômica, o que resultou na
767 alcalinização dos lisossomos e vazamento de componentes associados à autofagia
768 mediada por chaperonas no citoplasma dessas células (OLIVEIRA *et al.*, 2019).

769 Em uma linhagem de linfócitos T (Jurkat), BEA teve maior toxicidade
770 do que ENN B, a exposição a essas micotoxinas variou de 24 a 72 horas. BEA também
771 provocou alterações no ciclo celular e nas mitocôndrias, enquanto ENN B não causou
772 mudanças no ciclo celular e as alterações mitocondriais ocorreram apenas em doses
773 mais altas (15 μ M) e com maior tempo de exposição (72 horas) (MANYES *et al.*, 2018).

774 BEA e ENNs também possuem efeito imunomodulador (FRAEYMAN
775 *et al.*, 2017; MALLEBRERA *et al.*, 2018; PROSPERINI *et al.*, 2017), aumentando a
776 secreção de interleucina 10 (IL-10) e interferindo na migração de células dendríticas.
777 A fagocitose de macrófagos também foi prejudicada pela exposição a essas
778 micotoxinas (FICHEUX; SIBIRIL; PARENT-MASSIN, 2013). A exposição por 24 horas
779 com BEA também inibiu a resposta inflamatória de macrófagos RAW 265.7, por inibir
780 a via do fator de transcrição NF- κ B (YOO; KIM; CHO, 2017).

781 A ENN B alterou significativamente a expressão de genes em células
782 Jurkat. Mais de 245 genes, entre eles os genes de processos metabólicos, como
783 cadeia de transporte elétrico, fosforilação oxidativa e respiração celular, estavam
784 alterados (ALONSO-GARRIDO *et al.*, 2018). Nessas células, o tratamento com BEA
785 também alterou a expressão de vários genes envolvidos no metabolismo celular. Entre
786 eles, 77 genes responsáveis pela cadeia respiratória foram inibidos, 21 genes de
787 apoptose e 12 genes relacionados com a atividade das caspases tiveram maior
788 expressão, principalmente das caspases 8, 9 e 10 (ESCRIVÁ *et al.*, 2018).

789 Quando considerada uma associação entre BEA + ENN B em células
790 Jukart, essa associação apresentou menos alterações na expressão de genes
791 mitocondriais do que a exposição isolada de cada micotoxina. No entanto, a
792 associação provou ser mais prejudicial para o estado oxidativo, uma vez que esse
793 tratamento diminuiu a expressão de genes relacionados com a atividade antioxidante
794 e aumentou a expressão de genes oxidantes (ESCRIVÁ *et al.*, 2019).

795 Estudos demonstraram que BEA e ENNs estimulam a produção de
796 ERO, que levam a alterações oxidativas como a peroxidação lipídica e diminuição de
797 glutathiona (GSH) em diferentes tipos celulares (IVANOVA *et al.*, 2012; KLARIĆ *et al.*,
798 2007; PROSPERINI *et al.*, 2013a, 2013b). A peroxidação lipídica após exposição à
799 BEA, FB1 e OTA, em células animais, foi comprovada primeiramente em células

800 renais PK-15. Após 24 horas, OTA causou aumento da peroxidação lipídica e após 48
801 horas isso também ocorreu com BEA e FB1. A diminuição de GSH foi detectada em
802 24 horas e uma combinação das três micotoxinas teve efeito aditivo (KLARIĆ *et al.*,
803 2007).

804 Em células CHO-K1 e HepG2 também foram reportados aumento da
805 produção de ERO e da atividade de superóxido dismutase (SOD) e catalase (CAT)
806 assim como aumento da peroxidação lipídica nessas células e diminuição dos níveis
807 de enzimas antioxidantes (KLARIĆ *et al.*, 2007; MALLEBRERA *et al.*, 2015, 2016;
808 MALLEBRERA; FONT; RUIZ, 2014). Quando comparada com PAT e ZEA, a BEA teve
809 citotoxicidade intermediária, sendo PAT a mais tóxica e ZEA a que causou menos
810 danos em células CHO-K1, essa citotoxicidade foi associada à formação de ERO e
811 peroxidação lipídica (FERRER *et al.*, 2009).

812 Quanto ao uso de diferentes substâncias antioxidantes, em um estudo
813 foi testado o efeito de N-acetilcisteína (NAC) sobre células CHO-K1 expostas à BEA,
814 os resultados mostraram que NAC foi capaz de impedir a diminuição de enzimas
815 antioxidantes pela BEA (MALLEBRERA; FONT; RUIZ, 2014). Outro tratamento,
816 utilizando resveratrol, antes da exposição à BEA, foi capaz de diminuir a
817 citotoxicidade, a formação de ERO e a peroxidação lipídica em células CHO-K1
818 (MALLEBRERA *et al.*, 2015). Em doses intravenosas de 5 mg/kg em camundongos,
819 ocorreu aumento na produção de ERO, que levou à apoptose dos blastocistos. Mas
820 quando foi associado um tratamento com NAC, houve interrupção efetiva na produção
821 de ERO (HUANG; WANG; CHAN, 2019).

822 No entanto, em células cancerígenas de útero (KB-3-1) e de leucemia
823 promielocítica (HL-60), a BEA exerceu um efeito antioxidante, diminuindo a produção
824 de ERO e os danos observados pela intensidade na cauda do teste de cometa
825 (DORNETSHUBER *et al.*, 2009a). Em células Jurkat, não foram encontradas
826 alterações oxidativas após 72 horas de exposição à BEA e ENN B, mas BEA produziu
827 mais quebra de DNA, evidenciada na cauda do teste de cometa (MANYES *et al.*,
828 2018). Por conta desses resultados controversos e dos poucos estudos sobre
829 estresse oxidativo com essas micotoxinas estarem disponíveis, mais estudos em
830 relação a esse assunto são desejáveis.

831 A apoptose celular após exposição à BEA foi confirmada em várias
832 linhagens celulares (DORNETSHUBER *et al.*, 2009b; KLARIĆ *et al.*, 2007;
833 MALLEBRERA *et al.*, 2015; PROSPERINI *et al.*, 2013a; WÄTJEN *et al.*, 2014). Alguns
834 dos principais reguladores da apoptose são as caspases e ficou demonstrado que
835 BEA é capaz de aumentar a atividade da caspase-3 (JOW *et al.*, 2004), aumentando
836 a taxa de apoptose por meio de alterações morfológicas e fragmentação do DNA nas
837 células. Na linhagem celular de leucemia linfoblástica (CCRF-CEM), a ativação da
838 caspase-3, por conta da liberação do citocromo C mitocondrial, foi o principal indutor
839 da apoptose (JOW *et al.*, 2004), já em células PK15 e Jurkat, houve ativação das
840 caspases 3 e 7 (MANYES *et al.*, 2018; WÄTJEN *et al.*, 2014).

841 Também foi constatado que a apoptose induzida por BEA é regulada
842 pelo equilíbrio entre a expressão de genes pró (Bax, Bad e BaK) e anti-apoptóticos
843 (Bcl-2) em células cancerígenas pulmonares (NSCLC A549) (LIN *et al.*, 2005b). Os
844 genes da família Bcl-2 também são importantes na manutenção da integridade da
845 membrana mitocondrial, quando as células foram expostas à BEA, houve diminuição
846 do potencial de membrana das mitocôndrias, indicando que isso deve ocorrer para
847 que haja liberação do citocromo C no citosol (JOW *et al.*, 2004; LIN *et al.*, 2005a;
848 MALLEBRERA *et al.*, 2015; PROSPERINI *et al.*, 2013a, 2013b).

849 Em células do sistema nervoso de humanos (HBMEC e CCF-STTG1)
850 e de suínos (PBCEC), as ENN B e B1 foram capazes de atravessar a barreira
851 hematoencefálica e atingir o parênquima cerebral. Dentre os três tipos celulares, CCF-
852 STTG1 apresentou maior sensibilidade para as micotoxinas e apenas ENN B causou
853 aumento da atividade da caspase-3 (KRUG *et al.*, 2018).

854 Estudos sugerem que BEA e ENNs exercem citotoxicidade no sistema
855 reprodutivo. O tratamento com BEA prejudicou o desenvolvimento de oócitos e
856 embriões de suínos (SANTOS *et al.*, 2015; SCHOEVERS *et al.*, 2016). Foi
857 comprovado que BEA afetou de maneira diferente células cumulus, oócitos e
858 embriões de suínos, por isso, acredita-se que o mecanismo de toxicidade seja
859 diferente nos vários estágios embrionários (SCHOEVERS *et al.*, 2016). Em
860 blastocistos de camundongos, a ENN B1 (1-10 µM) aumentou a taxa de apoptose e a
861 reabsorção embrionário pós-implantação. Quando administrada via intravenosa (1-5
862 mg/kg/d) por quatro dias, a ENN B1 causou apoptose dos blastocistos por danos

863 oxidativos e prejudicou o desenvolvimento embrionário, com degradação do embrião
864 (HUANG; WANG; CHAN, 2019).

865 Em células da granulosa de bovinos, a BEA inibiu a síntese de
866 estradiol e progesterona nas concentrações 3 e 10 μM , na dose 10 μM houve
867 diminuição marcante do número células da granulosa, suprimindo a expressão dos
868 genes CYP19A1 e CYP11A1 (ALBONICO *et al.*, 2017). Além disso, a ENN B suprimiu
869 a secreção de cortisol, testosterona e progesterona em células de adenocarcinoma
870 adrenocortical de humanos da linhagem H295R, em doses maiores que 10 μM as
871 células de Leydig também reduziram a produção de testosterona e estradiol
872 (KALAYOU *et al.*, 2015).

873 Elas também exercem efeito antimicrobiano em micro-organismos
874 patogênicos e probióticos. A BEA inibe o crescimento de bactérias patogênicas como
875 *Escherichia coli*, *Enterococcus faecium*, *Salmonella enterica*, *Shigella dysenteriae*,
876 *Listeria monocytogenes*, *Yersinia enterocolitica*, *Clostridium perfringens* e
877 *Pseudomonas aeruginosa* (MECA *et al.*, 2010). Enquanto as ENN A, A1 e B1 são
878 capazes de inibir o crescimento de micro-organismos como: *Streptococcus*
879 *thermophilus*, *Bifidobacterium* spp. e *Lactobacillus* spp. (ROIG *et al.*, 2014).

880 2.4.2.3 Estudos *in vivo*

881 A administração por três dias de doses altas (50, 100 ou 200 mg/kg
882 peso vivo) de BEA ou ENN B por gavagem oral induziu apenas efeitos tóxicos leves
883 no fígado de camundongos (MARANGHI *et al.*, 2018). A ingestão de uma dieta
884 contaminada com 2.352 $\mu\text{g}/\text{kg}$ de ENN B, por três semanas, não causou efeitos
885 negativos na morfologia intestinal, nem lesões histológicas no fígado de frangos de
886 corte. Além disso, a taxa de transferência de ENN B para o tecido hepático nesses
887 animais foi baixo, o que indica que o consumo de frangos contaminados com ENN B
888 não é o principal contribuinte para a contaminação alimentar em humanos
889 (FRAEYMAN *et al.*, 2018a).

890 Estudos *in vivo* confirmaram a capacidade imunomoduladora de BEA
891 e ENNs em roedores. Em ratos alimentados com ração contaminada por ENN A (465
892 mg/kg) por quatro semanas, houve modulação na expressão de antígenos de
893 superfície de linfócitos no sangue periférico, aumento do número de células CD4⁺ e

894 diminuição da citotoxicidade de células CD8⁺ (JUAN *et al.*, 2014). Em camundongos
895 com colite induzida, a administração intraperitoneal de BEA (2-4 mg/kg) por 1 semana
896 induziu a apoptose de linfócitos T e diminuiu a secreção de TNF- α e interferon gama
897 (IFN- γ), BEA também atenuou a inflamação induzida e impediu a formação de
898 alterações histopatológicas no cólon dos animais tratados (WU *et al.*, 2013).

899 As ENNs também são capazes de levar a alterações a nível
900 transcricional. Em ratos Wistar, a administração orofaríngea aguda (8 h) de ENNs (A,
901 A1, B e B1) em dose única em concentrações moderadas (256, 353, 540 e 296 $\mu\text{g/mL}$
902 de ENN A, A1, B e B1, respectivamente) ou altas (513, 706, 1.021 e 593 $\mu\text{g/mL}$ de
903 ENN A, A1, B e B1, respectivamente) levou a alterações transcricionais no estômago,
904 cólon, fígado e rim desses animais de genes relacionados a cadeia de transporte de
905 elétrons, apoptose, estresse oxidativo, inflamação e integridade da barreira intestinal
906 (CIMBALO *et al.*, 2021).

907 Outro efeito exercido por BEA e as ENNs é o seu potencial
908 anticarcinogênico, com a indução da apoptose e a interrupção da sinalização da via
909 das MAPKs em células de hepatoma H4IIE (WÄTJEN *et al.*, 2014) e o envolvimento
910 dos genes p53 e p21 na apoptose de diversos tipos de células tumorais humanas
911 (DORNETSHUBER *et al.*, 2007). Esse potencial também foi demonstrado *in vivo* em
912 camundongos, a ENN B teve grande efeito sinérgico com uma droga inibidora de
913 quinases (Sorafenib[®]) contra o câncer cervical (DORNETSHUBER-FLEISS *et al.*,
914 2015).

915 Em camundongos enxertados com células cancerígenas de intestinos
916 (CT-26) ou de útero (KB-3-1), o grupo tratado com BEA teve tumores menores em
917 relação ao grupo não tratado, além disso, constatou-se que houve necrose tecidual e
918 acúmulo de BEA nas regiões tumorais desses animais (HEILOS *et al.*, 2017). O papel
919 anticarcinogênico dessas micotoxinas deve ser mais explorado a fim de que elas se
920 tornem componentes importantes na terapia de tumores.

921 3 REFERÊNCIAS

- 922 AJANDOUZ, E.; BERDAH, S.; MOUTARDIER, V.; BEGE, T.; BIRNBAUM, D.;
923 PERRIER, J.; DI PASQUALE, E.; MARESCA, M. Hydrolytic Fate of 3/15-
924 Acetyldeoxynivalenol in Humans: Specific Deacetylation by the Small Intestine and
925 Liver Revealed Using in Vitro and ex Vivo Approaches. **Toxins**, v. 8, n. 8, p. 232, 28
926 jul. 2016. Disponível em: <<http://www.mdpi.com/2072-6651/8/8/232>>.
- 927 AKBARI, P.; BRABER, S.; VARASTEHE, S.; ALIZADEH, A.; GARSSSEN, J.; FINK-
928 GREMMELS, J. The Intestinal Barrier as an Emerging Target in the Toxicological
929 Assessment of Mycotoxins. **Archives of Toxicology**, v. 91, n. 3, p. 1007–1029, 2017.
- 930 ALASSANE-KPEMBI, I.; GEREZ, J. R.; COSSALTER, A.-M.; NEVES, M.; LAFFITTE,
931 J.; NAYLIES, C.; LIPPI, Y.; KOLF-CLAUW, M.; BRACARENSE, A. P. L.; PINTON, P.;
932 OSWALD, I. P. Intestinal Toxicity of the Type B Trichothecene Mycotoxin Fusarenon-
933 X: Whole Transcriptome Profiling Reveals New Signaling Pathways. **Scientific**
934 **Reports**, v. 7, n. 1, p. 7530, 8 dez. 2017a. Disponível em:
935 <<https://www.nature.com/articles/s41598-017-07155-2>>.
- 936 ALASSANE-KPEMBI, I.; PUEL, O.; PINTON, P.; COSSALTER, A.-M.; CHOU, T.-C.;
937 OSWALD, I. P. Co-exposure to low doses of the food contaminants deoxynivalenol
938 and nivalenol has a synergistic inflammatory effect on intestinal explants. **Archives of**
939 **Toxicology**, v. 91, n. 7, p. 2677–2687, 3 jul. 2017b. Disponível em:
940 <<http://link.springer.com/10.1007/s00204-016-1902-9>>.
- 941 ALBONICO, M.; SCHUTZ, L. F.; CALONI, F.; CORTINOVIS, C.; SPICER, L. J. In Vitro
942 Effects of the Fusarium Mycotoxins Fumonisin B1 and Beauvericin on Bovine
943 Granulosa Cell Proliferation and Steroid Production. **Toxicon**, v. 128, p. 38–45, 2017.
- 944 ALONSO-GARRIDO, M.; ESCRIVÁ, L.; MANYES, L.; FONT, G. Enniatin B Induces
945 Expression Changes in the Electron Transport Chain Pathway Related Genes in
946 Lymphoblastic T-Cell Line. **Food and Chemical Toxicology**, v. 121, n. September, p.
947 437–443, 2018.
- 948 AWAD, W. A.; BOHM, J.; RAZZAZI-FAZELI, E.; GHAREEB, K.; ZENTEK, J. Effect of
949 Addition of a Probiotic Microorganism to Broiler Diets Contaminated with
950 Deoxynivalenol on Performance and Histological Alterations of Intestinal Villi of Broiler
951 Chickens. **Poultry Science**, v. 85, n. 6, p. 974–979, 1 jun. 2006.
- 952 AWAD, W. A.; GHAREEB, K.; DADAK, A.; HESS, M.; BÖHM, J. Single and Combined
953 Effects of Deoxynivalenol Mycotoxin and a Microbial Feed Additive on Lymphocyte
954 DNA Damage and Oxidative Stress in Broiler Chickens. **PLoS ONE**, v. 9, n. 1, p.
955 e88028, 2014.
- 956 BAI, Y.; MA, K.; LI, J.; LI, J.; BI, C.; SHAN, A. Deoxynivalenol exposure induces liver
957 damage in mice: Inflammation and immune responses, oxidative stress, and protective
958 effects of *Lactobacillus rhamnosus* GG. **Food and Chemical Toxicology**, v. 156, p.
959 112514, 1 out. 2021. Disponível em:
960 <<https://linkinghub.elsevier.com/retrieve/pii/S0278691521005470>>.
- 961 BARREIROS, A. L. B. S.; DAVID, J. P. Estresse Oxidativo: Relação Entre Geração De
962 Espécies Reativas E Defesa Do Organismo. **Química Nova**, v. 29, n. 1, p. 113–123,
963 2006.
- 964 BERTERO, A.; SPICER, L. J.; CALONI, F. Fusarium Mycotoxins and In Vitro Species-
965 Specific Approach with Porcine Intestinal and Brain In Vitro Barriers: A review. **Food**
966 **and Chemical Toxicology**, v. 121, n. September, p. 666–675, 2018.
- 967 BHATERIA, M.; KARSAULIYA, K.; SONKER, A. K.; YAHAVI, C.; SINGH, S. P.
968 Cytochrome P450 isoforms contribution, plasma protein binding, toxicokinetics of

- 969 enniatin A in rats and in vivo clearance prediction in humans. **Food and Chemical**
970 **Toxicology**, v. 164, p. 112988, 1 jun. 2022. Disponível em:
971 <<https://linkinghub.elsevier.com/retrieve/pii/S0278691522001867>>.
- 972 BIOMIN, 2021. BIOMIN Mycotoxin Survey Q3 2021 Results. Acesso em.
973 <https://www.biomin.net/science-hub/biomin-mycotoxin-survey-q3-2021-results/>.
974 (Acessado em: 19 de novembro de 2021).
- 975 BIRBEN, E.; SAHINER, U. M.; SACKESEN, C.; ERZURUM, S.; KALAYCI, O.
976 Oxidative Stress and Antioxidant Defense. **World Allergy Organization Journal**, v.
977 5, n. January, p. 9–19, 2012.
- 978 BODEA, G. O. D.; MUNTEANU, M. C.; DINU, D.; SERBAN, A. I.; ROMING, F. I.;
979 COSTACHE, M.; DINISCHIOTU, A. **Influence of deoxynivalenol on the oxidative**
980 **status of HepG2 cells****Romanian Biotechnological Letters**. [s.l.: s.n.].
- 981 BOUHET, S.; OSWALD, I. P. The Effects of Mycotoxins, Fungal Food Contaminants,
982 on the Intestinal Epithelial Cell-derived Innate Immune Response. **Veterinary**
983 **Immunology and Immunopathology**, v. 108, n. 1–2, p. 199–209, out. 2005.
- 984 BRACARENSE, A. P. F. L.; BASSO, K. M.; DA SILVA, E. O.; PAYROS, D.; OSWALD,
985 I. P. Deoxynivalenol in the Liver and Lymphoid Organs of Rats: Effects of Dose and
986 Duration on Immunohistological Changes. **World Mycotoxin Journal**, v. 10, n. 1, p.
987 89–96, 2017.
- 988 BRACARENSE, A. P. F. L.; LUCIOLI, J.; GRENIER, B.; DROCIUNAS PACHECO, G.;
989 MOLL, W. D.; SCHATZMAYR, G.; OSWALD, I. P. Chronic ingestion of deoxynivalenol
990 and fumonisin, alone or in interaction, induces morphological and immunological
991 changes in the intestine of piglets. **British Journal of Nutrition**, v. 107, n. 12, p. 1776–
992 1786, 2012.
- 993 BRACARENSE, A. P. F. L.; PIERRON, A.; PINTON, P.; GEREZ, J. R.;
994 SCHATZMAYR, G.; MOLL, W. D.; ZHOU, T.; OSWALD, I. P. Reduced Toxicity of 3-
995 epi-deoxynivalenol and De-epoxy-deoxynivalenol through Deoxynivalenol Bacterial
996 Biotransformation: In Vivo Analysis in Piglets. **Food and Chemical Toxicology**, v.
997 140, n. December 2019, p. 111241, 2020.
- 998 BRASIL, Instrução normativa nº 88, de 28 de março de 2021. Estabelece os limites
999 máximos tolerados (LMT) de contaminantes em alimentos. Brasília. Agência Nacional
1000 de Vigilância Sanitária – ANVISA, [2021]. Acesso em:
1001 [https://www.in.gov.br/en/web/dou/-/instrucao-normativa-in-n-88-de-26-de-marco-de-](https://www.in.gov.br/en/web/dou/-/instrucao-normativa-in-n-88-de-26-de-marco-de-2021-31165559)
1002 [2021-31165559](https://www.in.gov.br/en/web/dou/-/instrucao-normativa-in-n-88-de-26-de-marco-de-2021-31165559)
- 1003 BROWNING, T. H.; TRIER, J. S. Organ Culture of Mucosal Biopsies of Human Small
1004 Intestine. **The Journal of Clinical Investigation**, v. 48, p. 1423–1431, 1969.
- 1005 BRYDEN, W. L. Mycotoxin Contamination of the Feed Supply Chain: Implications for
1006 Animal Productivity and Feed Security. **Animal Feed Science and Technology**, v.
1007 173, n. 1–2, p. 134–158, abr. 2012. Disponível em:
1008 <<http://linkinghub.elsevier.com/retrieve/pii/S0377840111005037>>.
- 1009 CALÒ, L.; FORNELLI, F.; RAMIRES, R.; NENNA, S.; TURSI, A.; CAIAFFA, M. F.;
1010 MACCHIA, L. Cytotoxic Effects of the Mycotoxin Beauvericin to Human Cell Lines of
1011 Myeloid Origin. **Pharmacological Research**, v. 49, n. 1, p. 73–77, 2004.
- 1012 CANO, P. M.; SEEBOTH, J.; MEURENS, F.; COGNIE, J.; ABRAMI, R.; OSWALD, I.
1013 P.; GUZYLACK-PIRIOU, L. Deoxynivalenol as a New Factor in the Persistence of
1014 Intestinal Inflammatory Diseases: An Emerging Hypothesis through Possible
1015 Modulation of Th17-Mediated Response. **PLoS ONE**, v. 8, n. 1, p. e53647, 10 jan.
1016 2013. Disponível em: <<https://dx.plos.org/10.1371/journal.pone.0053647>>.
- 1017 CHEN, F.; MA, Y.; XUE, C.; MA, J.; XIE, Q.; WANG, G.; BI, Y.; CAO, Y. **Veterinary**
1018 **Science The combination of deoxynivalenol and zearalenone at permitted feed**

- 1019 **concentrations causes serious physiological effects in young pigs***J. Vet. Sci.*
1020 [s.l: s.n.].
- 1021 CIMBALO, A.; ALONSO-GARRIDO, M.; FONT, G.; FRANGIAMONE, M.; MANYES, L.
1022 Transcriptional Changes after Enniatins A, A1, B and B1 Ingestion in Rat Stomach,
1023 Liver, Kidney and Lower Intestine. **Foods**, v. 10, n. 7, p. 1630, 14 jul. 2021. Disponível
1024 em: <<https://www.mdpi.com/2304-8158/10/7/1630>>.
- 1025 COOPER, S. E. J.; WILSON, S.; FEIGHERY, C. F. Twenty-Four Hour Ex Vivo Culture
1026 of Celiac Duodenal Biopsies. *Em: Celiac Disease: Methods ans Protocols*. New
1027 York, NY: Humana Press, 2015. p. 47–51.
- 1028 DARWISH, W. S.; CHEN, Z.; LI, Y.; TAN, H.; CHIBA, H.; HUI, S.-P. Deoxynivalenol-
1029 induced alterations in the redox status of HepG2 cells: identification of lipid
1030 hydroperoxides, the role of Nrf2-Keap1 signaling, and protective effects of zinc.
1031 **Mycotoxin Research**, v. 36, n. 3, p. 287–299, 18 ago. 2020. Disponível em:
1032 <<http://link.springer.com/10.1007/s12550-020-00392-x>>.
- 1033 DE GRAAF, I. A. M.; OLINGA, P.; DE JAGER, M. H.; MEREMA, M. T.; DE KANTER,
1034 R.; VAN DE KERKHOF, E. G.; GROOTHUIS, G. M. M. Preparation and incubation of
1035 precision-cut liver and intestinal slices for application in drug metabolism and toxicity
1036 studies. **Nature Protocols**, v. 5, n. 9, p. 1540–1551, 19 set. 2010. Disponível em:
1037 <<http://www.nature.com/articles/nprot.2010.111>>.
- 1038 DEVREESE, M.; BROEKAERT, N.; DE MIL, T.; FRAEYMAN, S.; DE BACKER, P.;
1039 CROUBELS, S. Pilot Toxicokinetic Study and Absolute Oral Bioavailability of the
1040 Fusarium Mycotoxin Enniatin B1 in Pigs. **Food and Chemical Toxicology**, v. 63, p.
1041 161–165, 2014.
- 1042 DEVREESE, M.; DE BAERE, S.; DE BACKER, P.; CROUBELS, S. Quantitative
1043 Determination of the Fusarium Mycotoxins Beauvericin, Enniatin A, A1, B and B1 in
1044 Pig Plasma Using High Performance Liquid Chromatography-Tandem Mass
1045 Spectrometry. **Talanta**, v. 106, p. 212–219, 2013. Disponível em:
1046 <<http://dx.doi.org/10.1016/j.talanta.2012.11.068>>.
- 1047 DÖLL, S.; SCHRICKX, J. A.; VALENTA, H.; DÄNICKE, S.; FINK-GREMMELS, J.
1048 Interactions of Deoxynivalenol and Lipopolysaccharides on Cytotoxicity Protein
1049 Synthesis and Metabolism of DON in Porcine Hepatocytes and Kupffer Cell Enriched
1050 Hepatocyte Cultures. **Toxicology Letters**, v. 189, n. 2, p. 121–129, set. 2009.
- 1051 DORNETSHUBER, R.; HEFFETER, P.; KAMYAR, M. R.; PETERBAUER, T.;
1052 BERGER, W.; LEMMENS-GRUBER, R. Enniatin Exerts p53-Dependent Cytostatic
1053 and p53-Independent Cytotoxic Activities Against Human Cancer Cells. **Chemical**
1054 **Research in Toxicology**, v. 20, n. 3, p. 465–473, 2007.
- 1055 DORNETSHUBER, R.; HEFFETER, P.; LEMMENS-GRUBER, R.; ELBLING, L.;
1056 MARKO, D.; MICKSCHE, M.; BERGER, W. Oxidative Stress and DNA Interactions are
1057 Not Involved in Enniatin- and Beauvericin-Mediated Apoptosis Induction. **Molecular**
1058 **Nutrition and Food Research**, v. 53, n. 9, p. 1112–1122, 2009a.
- 1059 DORNETSHUBER, R.; HEFFETER, P.; SULYOK, M.; SCHUMACHER, R.; CHIBA, P.;
1060 KOPP, S.; KOELLENSPERGER, G.; MICKSCHE, M.; LEMMENS-GRUBER, R.;
1061 BERGER, W. Interactions Between ABC-Transport Proteins and the Secondary
1062 Fusarium Metabolites Enniatin and Beauvericin. **Molecular Nutrition and Food**
1063 **Research**, v. 53, n. 7, p. 904–920, 2009b.
- 1064 DORNETSHUBER-FLEISS, R.; HEILOS, D.; MOHR, T.; RICHTER, L.; SÜSSMUTH,
1065 R. D.; ZLESAK, M.; NOVICKY, A.; HEFFETER, P.; LEMMENS-GRUBER, R.;
1066 BERGER, W. The Naturally Born Fusariotoxin Enniatin B and Sorafenib Exert
1067 Synergistic Activity Against Cervical Cancer In Vitro and In Vivo. **Biochemical**
1068 **Pharmacology**, v. 93, n. 3, p. 318–331, 2015.

- 1069 EFSA, E. P. on C. in the F. C. (CONTAM); KNUTSEN, H. K.; ALEXANDER, J.;
1070 BARREGÅRD, L.; BIGNAMI, M.; BRÜSCHWEILER, B.; CECCATELLI, S.; COTTRILL,
1071 B.; DINOVI, M.; GRASL-KRAUPP, B.; HOGSTRAND, C.; HOOGENBOOM, L. (Ron);
1072 NEBBIA, C. S.; OSWALD, I. P.; PETERSEN, A.; ROSE, M.; ROUDOT, A.;
1073 SCHWERDTLE, T.; VLEMINCKX, C.; VOLLMER, G.; WALLACE, H.; DE SAEGER,
1074 S.; ERIKSEN, G. S.; FARMER, P.; FREMY, J.; GONG, Y. Y.; MEYER, K.; NAEGELI,
1075 H.; PARENT-MASSIN, D.; RIETJENS, I.; VAN EGMOND, H.; ALTIERI, A.; ESKOLA,
1076 M.; GERGLOVA, P.; RAMOS BORDAJANDI, L.; BENKOVA, B.; DÖRR, B.;
1077 GKRILLAS, A.; GUSTAVSSON, N.; VAN MANEN, M.; EDLER, L. Risks to human and
1078 animal health related to the presence of deoxynivalenol and its acetylated and modified
1079 forms in food and feed. **EFSA Journal**, v. 15, n. 9, set. 2017. Disponível em:
1080 <<http://doi.wiley.com/10.2903/j.efsa.2017.4718>>.
- 1081 EKATAKSIN, W.; WAKE, K. Liver units in three dimensions: I. organization of
1082 argyrophilic connective tissue skeleton in porcine Liver with particular reference to
1083 the ?compound hepatic lobule? **American Journal of Anatomy**, v. 191, n. 2, p. 113–
1084 153, jun. 1991. Disponível em: <<http://doi.wiley.com/10.1002/aja.1001910202>>.
- 1085 ERIKSEN, G. S.; PETTERSSON, H.; LINDBERG, J. E. Absorption, metabolism and
1086 excretion of 3-acetyl don in pigs. **Archives of Animal Nutrition**, v. 57, n. 5, p. 335–
1087 345, out. 2003. Disponível em:
1088 <<http://www.tandfonline.com/doi/abs/10.1080/00039420310001607699>>.
- 1089 ESCRIVÁ, L.; ALONSO-GARRIDO, M.; FONT, G.; MANYES, L. Transcriptional Study
1090 After Beauvericin and Enniatin B Combined Exposure in Jurkat T Cells. **Food and**
1091 **Chemical Toxicology**, v. 130, n. April, p. 122–129, ago. 2019.
- 1092 ESCRIVÁ, L.; JENNEN, D.; CAIMENT, F.; MANYES, L. Transcriptomic Study of the
1093 Toxic Mechanism Triggered by Beauvericin in Jurkat Cells. **Toxicology Letters**, v.
1094 284, n. September 2017, p. 213–221, 2018. Disponível em:
1095 <<https://doi.org/10.1016/j.toxlet.2017.11.035>>.
- 1096 ESKOLA, M.; KOS, G.; ELLIOTT, C. T.; HAJŠLOVÁ, J.; MAYAR, S.; KRŠKA, R.
1097 Worldwide contamination of food-crops with mycotoxins: Validity of the widely cited
1098 'FAO estimate' of 25%. **Critical Reviews in Food Science and Nutrition**, v. 60, n.
1099 16, p. 2773–2789, 7 set. 2020. Disponível em:
1100 <<https://doi.org/10.1080/10408398.2019.1658570>>.
- 1101 EUROPEAN COMMISSION. Commission Recommendation of 17 August 2006 on the
1102 Presence of Deoxynivalenol, Zearalenone, Ochratoxin A, T-2 and HT-2 and
1103 Fumonisin in Products Intended for Animal Feeding. **Official Journal of the**
1104 **European Union**, v. 299, n. March 2005, p. 7–9, 2006.
- 1105 EUROPEAN FOOD SAFETY AUTHORITY (EFSA). Scientific Opinion on the risks to
1106 human and animal health related to the presence of beauvericin and enniatins in food
1107 and feed. **EFSA Journal**, v. 12, n. 8, p. 3802, ago. 2014. Disponível em:
1108 <<http://doi.wiley.com/10.2903/j.efsa.2014.3802>>.
- 1109 FAVERO, G. del; WOELFLINGSEDER, L.; BRAUN, D.; PUNTSCHER, H.; KÜTT, M.-
1110 L.; DELLAFIORA, L.; WARTH, B.; PAHLKE, G.; DALL'ASTA, C.; ADAM, G.; MARKO,
1111 D. Response of intestinal HT-29 cells to the trichothecene mycotoxin deoxynivalenol
1112 and its sulfated conjugates. **Toxicology Letters**, v. 295, p. 424–437, 1 out. 2018.
1113 Disponível em: <<https://linkinghub.elsevier.com/retrieve/pii/S0378427418314917>>.
- 1114 FERNÁNDEZ-BLANCO, C.; ELMO, L.; WALDNER, T.; RUIZ, M. Cytotoxic Effects
1115 Induced by Patulin, Deoxynivalenol and Toxin T2 Individually and in Combination in
1116 Hepatic Cells (HepG2). **Food and Chemical Toxicology**, v. 120, p. 12–23, 2018.
1117 Disponível em: <<https://doi.org/10.1016/j.fct.2018.06.019>>.
- 1118 FERNÁNDEZ-BLANCO, C.; FONT, G.; RUIZ, M. J. Interaction Effects of Enniatin B,

- 1119 Deoxynivalenol and Alternariol in Caco-2 Cells. **Toxicology Letters**, v. 241, p. 38–48,
1120 2016.
- 1121 FERRER, E.; JUAN-GARCÍA, A.; FONT, G.; RUIZ, M. J. Reactive Oxygen Species
1122 Induced by Beauvericin, Patulin and Zearalenone in CHO-K1 Cells. **Toxicology in**
1123 **Vitro**, v. 23, n. 8, p. 1504–1509, 2009.
- 1124 FICHEUX, A. S.; SIBIRIL, Y.; PARENT-MASSIN, D. Effects of Beauvericin, Enniatin b
1125 and Moniliformin on Human Dendritic Cells and Macrophages: An In vitro Study.
1126 **Toxicon**, v. 71, p. 1–10, 2013. Disponível em:
1127 <<http://dx.doi.org/10.1016/j.toxicon.2013.04.024>>.
- 1128 FÖLLMANN, W.; BEHM, C.; DEGEN, G. H. The emerging Fusarium Toxin Enniatin B:
1129 In-Vitro Studies on its Genotoxic Potential and Cytotoxicity in V79 Cells in Relation to
1130 Other Mycotoxins. **Mycotoxin Research**, v. 25, n. 1, p. 11–19, 2009.
- 1131 FRAEYMAN, S.; CROUBELS, S.; DEVREESE, M.; ANTONISSEN, G. Emerging
1132 Fusarium and Alternaria Mycotoxins: Occurrence, Toxicity and Toxicokinetics. **Toxins**,
1133 v. 9, n. 7, p. 228, 18 jul. 2017.
- 1134 FRAEYMAN, S.; CROUBELS, S.; DEVREESE, M.; DUCATELLE, R.; RYCHLIK, M.;
1135 ANTONISSEN, G. Chronic Dietary Intake of Enniatin B in Broiler Chickens Has Low
1136 Impact on Intestinal Morphometry and Hepatic Histology, and Shows Limited Transfer
1137 to Liver Tissue. **Toxins**, v. 10, n. 1, p. 1–11, 2018a.
- 1138 FRAEYMAN, S.; DEVREESE, M.; ANTONISSEN, G.; DE BAERE, S.; RYCHLIK, M.;
1139 CROUBELS, S. Comparative Oral Bioavailability, Toxicokinetics, and
1140 Biotransformation of Enniatin B1 and Enniatin B in Broiler Chickens. **Journal of**
1141 **Agricultural and Food Chemistry**, v. 64, n. 38, p. 7259–7264, 2016.
- 1142 FRAEYMAN, S.; MEYER, E.; DEVREESE, M.; ANTONISSEN, G.; DEMEYERE, K.;
1143 HAESBROUCK, F.; CROUBELS, S. Comparative In Vitro Cytotoxicity of the
1144 Emerging Fusarium Mycotoxins Beauvericin and Enniatins to Porcine Intestinal
1145 Epithelial Cells. **Food and Chemical Toxicology**, v. 121, n. June, p. 566–572, 2018b.
1146 Disponível em: <<https://doi.org/10.1016/j.fct.2018.09.053>>.
- 1147 FRANKIČ, T.; SALOBIR, J.; REZAR, V. The effect of vitamin E supplementation on
1148 reduction of lymphocyte DNA damage induced by T-2 toxin and deoxynivalenol in
1149 weaned pigs. **Animal Feed Science and Technology**, v. 141, n. 3–4, p. 274–286, 1
1150 abr. 2008. Disponível em:
1151 <<https://linkinghub.elsevier.com/retrieve/pii/S037784010700226X>>.
- 1152 GARCÍA-HERRANZ, V.; VALDEHITA, A.; NAVVAS, J. M.; FERNÁNDEZ-CRUZ, M. L.
1153 Cytotoxicity Against Fish and Mammalian Cell Lines and Endocrine Activity of the
1154 Mycotoxins Beauvericin, Deoxynivalenol and Ochratoxin-A. **Food and Chemical**
1155 **Toxicology**, v. 127, n. January, p. 288–297, 2019.
- 1156 GÄUMANN, E.; ROTH, S.; ETTLINGER, L. Enniatin, ein neues, gegen Mykobakterien
1157 wirksames Antibiotikum. **Experientia**, v. 3, p. 202–203, 1947.
- 1158 GAUTHIER, T.; WACHÉ, Y.; LAFFITTE, J.; TARANU, I.; SAEEDIKOUZEHKONANI,
1159 N.; MORI, Y.; OSWALD, I. P. Deoxynivalenol Impairs the Immune Functions of
1160 Neutrophils. **Molecular Nutrition and Food Research**, v. 57, n. 6, p. 1026–1036,
1161 2013.
- 1162 GEREZ, J. R.; CAMACHO, T.; BRUNALDI MARUTANI, V. H.; NASCIMENTO DE
1163 MATOS, R. L.; HOHMANN, M. S.; VERRI JÚNIOR, W. A.; BRACARENSE, A. P. F. R.
1164 L. Ovarian toxicity by fusariotoxins in pigs: Does it imply in oxidative stress?
1165 **Theriogenology**, v. 165, p. 84–91, abr. 2021. Disponível em:
1166 <<https://www.sciencedirect.com/science/article/pii/S0093691X21000546>>.
- 1167 GEREZ, J. R.; DESTO, S. S.; BRACARENSE, A. P. F. R. L. Deoxynivalenol induces
1168 toxic effects in the ovaries of pigs: An ex vivo approach. **Theriogenology**, v. 90, p. 94–

- 1169 100, mar. 2017. Disponível em:
1170 <<http://dx.doi.org/10.1016/j.theriogenology.2016.10.023>>.
- 1171 GEREZ, J. R.; PINTON, P.; CALLU, P.; GROSJEAN, F.; OSWALD, I. P.;
1172 BRACARENSE, A. P. F. L. Deoxynivalenol Alone or in Combination with Nivalenol and
1173 Zearalenone Induce Systemic Histological Changes in Pigs. **Experimental and**
1174 **Toxicologic Pathology**, v. 67, n. 2, p. 89–98, fev. 2015.
- 1175 GISSEN, P.; ARIAS, I. M. Structural and functional hepatocyte polarity and liver
1176 disease. **Journal of Hepatology**, v. 63, n. 4, p. 1023–1037, 2015. Disponível em:
1177 <<http://dx.doi.org/10.1016/j.jhep.2015.06.015>>.
- 1178 GRENIER, B.; LOUREIRO-BRACARENSE, A.-P.; LUCIOLI, J.; PACHECO, G. D.;
1179 COSSALTER, A.-M.; MOLL, W.-D.; SCHATZMAYR, G.; OSWALD, I. P. Individual and
1180 Combined Effects of Subclinical Doses of Deoxynivalenol and Fumonisin in Piglets.
1181 **Molecular Nutrition & Food Research**, v. 55, n. 5, p. 761–771, maio 2011.
- 1182 GROVE, J. F. Macrocyclic Trichothecenes. **Natural Product Reports**, v. 10, n. 5, p.
1183 429, 1993.
- 1184 GRUBER-DORNINGER, C.; NOVAK, B.; NAGL, V.; BERTHILLER, F. Emerging
1185 Mycotoxins: Beyond Traditionally Determined Food Contaminants. **Journal of**
1186 **Agricultural and Food Chemistry**, v. 65, n. 33, p. 7052–7070, 2017.
- 1187 GUO, W.; GU, X.; TONG, Y.; WANG, X.; WU, J.; CHANG, C. Protective effects of
1188 mannan/ β -glucans from yeast cell wall on the deoxynivalenol-induced oxidative stress
1189 and autophagy in IPEC-J2 cells. **International Journal of Biological**
1190 **Macromolecules**, v. 135, p. 619–629, 15 ago. 2019. Disponível em:
1191 <<https://linkinghub.elsevier.com/retrieve/pii/S0141813019319117>>.
- 1192 HAMILL, R. L.; HIGGINS, C. E.; BOAZ, H. E.; GORMAN, M. The Structure of
1193 Beauvericin, A New Depsipeptide Antibiotic Toxic to *Artemia Salina*. **Tetrahedron**
1194 **Letters**, v. 10, n. 49, p. 4255–4258, jan. 1969.
- 1195 HEILOS, D.; RODRÍGUEZ-CARRASCO, Y.; ENGLINGER, B.; TIMELTHALER, G.;
1196 VAN SCHOONHOVEN, S.; SULYOK, M.; BOECKER, S.; SÜSSMUTH, R. D.;
1197 HEFFETER, P.; LEMMENS-GRUBER, R.; DORNETSHUBER-FLEISS, R.; BERGER,
1198 W. The Natural Fungal Metabolite Beauvericin Exerts Anticancer Activity In Vivo: A
1199 Pre-Clinical Pilot Study. **Toxins**, v. 9, n. 9, p. 1–15, 2017.
- 1200 HELKE, K. L.; SWINDLE, M. M. Animal models of toxicology testing: the role of pigs.
1201 **Expert Opinion on Drug Metabolism & Toxicology**, v. 9, n. 2, p. 127–139, 10 fev.
1202 2013.
- 1203 HORNBUCKLE, W. E.; SIMPSON, K. W.; TENNANT, B. C. Gastrointestinal Function.
1204 *Em*: KANEKO, J.; HARVEY, J.; BRUSS, M. **Clinical Biochemistry of Domestic**
1205 **Animals**. 6th. ed. San Diego: Elsevier, 2008. p. 413–457.
- 1206 HUANG, C. H.; WANG, F. T.; CHAN, W. H. Enniatin B1 Exerts Embryotoxic Effects on
1207 Mouse Blastocysts and Induces Oxidative Stress and Immunotoxicity During Embryo
1208 Development. **Environmental Toxicology**, v. 34, n. 1, p. 48–59, 2019.
- 1209 IVANOVA, L.; EGGE-JACOBSEN, W. M.; SOLHAUG, A.; THOEN, E.; FÆSTE, C. K.
1210 Lysosomes as a Possible Target of Enniatin B-Induced Toxicity in Caco-2 Cells.
1211 **Chemical Research in Toxicology**, v. 25, n. 8, p. 1662–1674, 2012.
- 1212 IVANOVA, L.; UHLIG, S.; DEVREESE, M.; CROUBELS, S.; FÆSTE, C. K.
1213 Biotransformation of the Mycotoxin Enniatin B1 in Pigs: A Comparative In Vitro and In
1214 Vivo Approach. **Food and Chemical Toxicology**, v. 105, p. 506–517, 2017.
- 1215 JESTOI, M. Emerging Fusarium-Mycotoxins Fusaproliferin, Beauvericin, Enniatins,
1216 and Moniliformin - A Review. **Critical Reviews in Food Science and Nutrition**, v. 48,
1217 n. 1, p. 21–49, 2008.
- 1218 JONSSON, M.; JESTOI, M.; ANTHONI, M.; WELLING, A.; LOIVAMAA, I.;

- 1219 HALLIKAINEN, V.; KANKAINEN, M.; LYSØE, E.; KOIVISTO, P.; PELTONEN, K.
1220 Fusarium mycotoxin enniatin B: Cytotoxic effects and changes in gene expression
1221 profile. **Toxicology in Vitro**, v. 34, p. 309–320, 1 ago. 2016. Disponível em:
1222 <<https://linkinghub.elsevier.com/retrieve/pii/S0887233316300844>>.
- 1223 JOW, G. M.; CHOU, C. J.; CHEN, B. F.; TSAI, J. H. Beauvericin Induces Cytotoxic
1224 Effects in Human Acute Lymphoblastic Leukemia Cells Through Cytochrome C
1225 Release, Caspase 3 Activation: The Causative Role of Calcium. **Cancer Letters**, v.
1226 216, n. 2, p. 165–173, 2004.
- 1227 JUAN, C.; MANYES, L.; FONT, G.; JUAN-GARCÍA, A. Evaluation of Immunologic
1228 Effect of Enniatin A and Quantitative Determination in Feces, Urine and Serum on
1229 Treated Wistar Rats. **Toxicon**, v. 87, p. 45–53, 2014.
- 1230 JUAN-GARCÍA, A.; RUIZ, M.-J.; FONT, G.; MANYES, L. Enniatin A1, enniatin B1 and
1231 beauvericin on HepG2: Evaluation of toxic effects. **Food and Chemical Toxicology**,
1232 v. 84, p. 188–196, out. 2015. Disponível em:
1233 <<https://linkinghub.elsevier.com/retrieve/pii/S0278691515300521>>.
- 1234 JUAN-GARCÍA, A.; TOLOSA, J.; JUAN, C.; RUIZ, M.-J. Cytotoxicity, Genotoxicity and
1235 Disturbance of Cell Cycle in HepG2 Cells Exposed to OTA and BEA: Single and
1236 Combined Actions. **Toxins**, v. 11, n. 6, p. 341, 14 jun. 2019.
- 1237 JUNQUEIRA, L. C.; CARNEIRO, J. **Histologia Básica**. 11. ed. Rio de Janeiro:
1238 Guanabara Koogan, 2008. 535 p.
- 1239 KALAISELVI, P.; RAJASHREE, K.; BHARATHI PRIYA, L.; PADMA, V. V.
1240 Cytoprotective effect of epigallocatechin-3-gallate against deoxynivalenol-induced
1241 toxicity through anti-oxidative and anti-inflammatory mechanisms in HT-29 cells. **Food**
1242 **and Chemical Toxicology**, v. 56, p. 110–118, jun. 2013. Disponível em:
1243 <<https://linkinghub.elsevier.com/retrieve/pii/S0278691513000902>>.
- 1244 KALAYOU, S.; NDOSSI, D.; FRIZZELL, C.; GROSETH, P. K.; CONNOLLY, L.;
1245 SØRLIE, M.; VERHAEGEN, S.; ROPSTAD, E. An Investigation of the Endocrine
1246 Disrupting Potential of Enniatin B Using In Vitro Bioassays. **Toxicology Letters**, v.
1247 233, n. 2, p. 84–94, 2015.
- 1248 KANG, R.; LI, R.; DAI, P.; LI, Z.; LI, Y.; LI, C. Deoxynivalenol Induced Apoptosis and
1249 Inflammation of IPEC-J2 Cells by Promoting ROS Production. **Environmental**
1250 **Pollution**, v. 251, p. 689–698, 2019. Disponível em:
1251 <<https://doi.org/10.1016/j.envpol.2019.05.026>>.
- 1252 KATIKA, M. R.; HENDRIKSEN, P. J. M.; SHAO, J.; VAN LOVEREN, H.;
1253 PEIJNENBURG, A. Transcriptome analysis of the human T lymphocyte cell line Jurkat
1254 and human peripheral blood mononuclear cells exposed to deoxynivalenol (DON):
1255 New mechanistic insights. **Toxicology and Applied Pharmacology**, v. 264, n. 1, p.
1256 51–64, 2012. Disponível em: <<http://dx.doi.org/10.1016/j.taap.2012.07.017>>.
- 1257 KHOSHAL, A. K.; NOVAK, B.; MARTIN, P. G. P.; JENKINS, T.; NEVES, M.;
1258 SCHATZMAYR, G.; OSWALD, I. P.; PINTON, P. Co-Occurrence of DON and
1259 Emerging Mycotoxins in Worldwide Finished Pig Feed and Their Combined Toxicity in
1260 Intestinal Cells. **Toxins**, v. 11, n. 12, p. 727, 11 dez. 2019.
- 1261 KINSER, S.; LI, M.; JIA, Q.; PESTKA, J. J. Truncated Deoxynivalenol-Induced Splenic
1262 Immediate Early Gene Response in Mice Consuming (n-3) Polyunsaturated Fatty
1263 Acids. **The Journal of Nutritional Biochemistry**, v. 16, n. 2, p. 88–95, fev. 2005.
1264 Disponível em: <<https://linkinghub.elsevier.com/retrieve/pii/S0955286304001834>>.
- 1265 KLARIĆ, M. Š.; PEPELJNJAK, S.; DOMIJAN, A. M.; PETRIK, J. Lipid Peroxidation and
1266 Glutathione Levels in Porcine Kidney PK15 Cells After Individual and Combined
1267 Treatment with Fumonisin B1, Beauvericin and Ochratoxin A. **Basic and Clinical**
1268 **Pharmacology and Toxicology**, v. 100, n. 3, p. 157–164, 2007.

- 1269 KOLF-CLAUW, M.; CASTELLOTE, J.; JOLY, B.; BOURGES-ABELLA, N.;
 1270 RAYMOND-LETRON, I.; PINTON, P.; OSWALD, I. P. Development of a pig jejunal
 1271 explant culture for studying the gastrointestinal toxicity of the mycotoxin
 1272 deoxynivalenol: Histopathological analysis. **Toxicology in Vitro**, v. 23, n. 8, p. 1580–
 1273 1584, dez. 2009. Disponível em:
 1274 <<https://linkinghub.elsevier.com/retrieve/pii/S0887233309001751>>.
- 1275 KÖNIGS, M.; SCHWERDT, G.; GEKLE, M.; HUMPF, H. Effects of the Mycotoxin
 1276 Deoxynivalenol on Human Primary Hepatocytes. **Molecular Nutrition & Food
 1277 Research**, v. 52, n. 7, p. 830–839, jul. 2008.
- 1278 KRISHNASWAMY, R.; DEVARAJ, S. N.; PADMA, V. V. Lutein protects HT-29 cells
 1279 against Deoxynivalenol-induced oxidative stress and apoptosis: Prevention of NF-κB
 1280 nuclear localization and down regulation of NF-κB and Cyclo-Oxygenase – 2
 1281 expression. **Free Radical Biology and Medicine**, v. 49, n. 1, p. 50–60, jul. 2010.
 1282 Disponível em: <<https://linkinghub.elsevier.com/retrieve/pii/S0891584910001905>>.
- 1283 KRUG, I.; BEHRENS, M.; ESSELEN, M.; HUMPF, H. U. Transport of Enniatin B and
 1284 Enniatin B1 Across the Blood-Brain Barrier and Hints for Neurotoxic Effects in Cerebral
 1285 Cells. **PLoS ONE**, v. 13, n. 5, p. 1–17, 2018.
- 1286 KRUMDIECK, C. L.; SANTOS, J. E. dos; HO, K.-J. A new instrument for the rapid
 1287 preparation of tissue slices. **Analytical Biochemistry**, v. 104, n. 1, p. 118–123, maio
 1288 1980. Disponível em:
 1289 <<https://linkinghub.elsevier.com/retrieve/pii/0003269780902845>>.
- 1290 KUBES, P.; JENNE, C. Immune Responses in the Liver. **Annual Review of
 1291 Immunology**, v. 36, n. 1, p. 247–277, 26 abr. 2018. Disponível em:
 1292 <<http://www.annualreviews.org/doi/10.1146/annurev-immunol-051116-052415>>.
- 1293 LALLÈS, J.-P.; BOUDRY, G.; FAVIER, C.; LE FLOC'H, N.; LURON, I.; MONTAGNE,
 1294 L.; OSWALD, I. P.; PIÉ, S.; PIEL, C.; SÈVE, B. Gut Function and Dysfunction in Young
 1295 Pigs: Physiology. **Animal Research**, v. 53, n. 4, p. 301–316, jul. 2004.
- 1296 LEWCZUK, B.; PRZYBYLSKA-GORNOWICZ, B.; GAJECKA, M.; TARGOŃSKA, K.;
 1297 ZIÓŁKOWSKA, N.; PRUSIK, M.; GAJECKI, M. Histological Structure of Duodenum in
 1298 Gilts Receiving Low Doses of Zearalenone and Deoxynivalenol in Feed. **Experimental
 1299 and Toxicologic Pathology**, v. 68, n. 2–3, p. 157–166, 2016a.
- 1300 LEWCZUK, B.; PRZYBYLSKA-GORNOWICZ, B.; GAJECKA, M.; TARGOŃSKA, K.;
 1301 ZIÓŁKOWSKA, N.; PRUSIK, M.; GAJECKI, M. Histological Structure of Duodenum in
 1302 Gilts Receiving Low Doses of Zearalenone and Deoxynivalenol in Feed. **Experimental
 1303 and Toxicologic Pathology**, v. 68, n. 2–3, p. 157–166, 2016b.
- 1304 LIN, H. I.; LEE, Y. J.; CHEN, B. F.; TSAI, M. C.; LU, J. L.; CHOU, C. J.; JOW, G. M.
 1305 Involvement of Bcl-2 Family, Cytochrome C and Caspase 3 in Induction of Apoptosis
 1306 by Beauvericin in Human Non-Small Cell Lung Cancer Cells. **Cancer Letters**, v. 230,
 1307 n. 2, p. 248–259, 2005a.
- 1308 LIN, H.; LEE, Y.; CHEN, B.; TSAI, M.; LU, J.; CHOU, C.; JOW, G. Involvement of Bcl-
 1309 2 family, cytochrome and caspase 3 in induction of apoptosis by beauvericin in human
 1310 non-small cell lung cancer cells. **Cancer Letters**, v. 230, n. 2, p. 248–259, 18 dez.
 1311 2005b.
- 1312 LUCIOLI, J.; PINTON, P.; CALLU, P.; LAFFITTE, J.; GROSJEAN, F.; KOLF-CLAUW,
 1313 M.; OSWALD, I. P.; BRACARENSE, A. P. F. R. L. The food contaminant
 1314 deoxynivalenol activates the mitogen activated protein kinases in the intestine: Interest
 1315 of ex vivo models as an alternative to in vivo experiments. **Toxicon**, v. 66, p. 31–36,
 1316 maio 2013. Disponível em:
 1317 <<https://linkinghub.elsevier.com/retrieve/pii/S0041010113000585>>.
- 1318 LUO, S.; TERCIOLO, C.; BRACARENSE, A. P. F. L.; PAYROS, D.; PINTON, P.;

- 1319 OSWALD, I. P. In Vitro and In Vivo Effects of a Mycotoxin, Deoxynivalenol, and a Trace
1320 Metal, Cadmium, Alone or in a Mixture on the Intestinal Barrier. **Environment**
1321 **International**, v. 132, nov. 2019.
- 1322 LYKKESFELDT, J.; SVENDSEN, O. Oxidants and Antioxidants in Disease: Oxidative
1323 Stress in Farm Animals. **The Veterinary Journal**, v. 173, p. 502–511, 2007.
- 1324 MAIDANA, L.; GEREZ, J. R.; EL, R.; PINHO, F.; PUEL, O.; OSWALD, I. P.; PAULA,
1325 A.; BRACARENSE, F. R. L. Effects of Patulin and Ascladiol on Porcine Intestinal
1326 Mucosa : An Ex Vivo Approach. **Food and Chemical Toxicology**, v. 98, p. 189–194,
1327 2016. Disponível em: <<http://dx.doi.org/10.1016/j.fct.2016.10.001>>.
- 1328 MALLEBRERA, B.; BRANDOLINI, V.; FONT, G.; RUIZ, M. J. Cytoprotective Effect of
1329 Resveratrol Diastereomers in CHO-K1 Cells Exposed to Beauvericin. **Food and**
1330 **Chemical Toxicology**, v. 80, p. 319–327, 2015.
- 1331 MALLEBRERA, B.; FONT, G.; RUIZ, M. J. Disturbance of Antioxidant Capacity
1332 Produced by Beauvericin in CHO-K1 Cells. **Toxicology Letters**, v. 226, n. 3, p. 337–
1333 342, 2014.
- 1334 MALLEBRERA, B.; JUAN-GARCIA, A.; FONT, G.; RUIZ, M. J. Mechanisms of
1335 Beauvericin Toxicity and Antioxidant Cellular Defense. **Toxicology Letters**, v. 246, p.
1336 28–34, 2016. Disponível em: <<http://dx.doi.org/10.1016/j.toxlet.2016.01.013>>.
- 1337 MALLEBRERA, B.; PROSPERINI, A.; FONT, G.; RUIZ, M. J. In Vitro Mechanisms of
1338 Beauvericin Toxicity: A Review. **Food and Chemical Toxicology**, v. 111, n.
1339 November 2017, p. 537–545, jan. 2018.
- 1340 MANYES, L.; ESCRIVÁ, L.; RUIZ, M. J.; JUAN-GARCÍA, A. Beauvericin and Enniatin
1341 B Effects on a Human Lymphoblastoid Jurkat T-cell Model. **Food and Chemical**
1342 **Toxicology**, v. 115, n. February, p. 127–135, maio 2018. Disponível em:
1343 <<https://linkinghub.elsevier.com/retrieve/pii/S0278691518301534>>.
- 1344 MARANGHI, F.; TASSINARI, R.; NARCISO, L.; TAIT, S.; ROCCA, C. Ia; FELICE, G.
1345 di; BUTTERONI, C.; CORINTI, S.; BARLETTA, B.; CORDELLI, E.; PACCHIEROTTI,
1346 F.; ELEUTERI, P.; VILLANI, P.; HEGARAT, L. Ie; FESSARD, V.; REALE, O. In vivo
1347 toxicity and genotoxicity of beauvericin and enniatins. Combined approach to study in
1348 vivo toxicity and genotoxicity of mycotoxins beauvericin (BEA) and enniatin B (ENNB).
1349 **EFSA Supporting Publications**, v. 15, n. 5, maio 2018. Disponível em:
1350 <<http://doi.wiley.com/10.2903/sp.efs.2018.EN-1406>>.
- 1351 MARESCA, M. From the Gut to the Brain: Journey and Pathophysiological Effects of
1352 the Food-Associated Trichothecene Mycotoxin Deoxynivalenol. **Toxins**, v. 5, n. 4, p.
1353 784–820, 23 abr. 2013. Disponível em: <<http://www.mdpi.com/2072-6651/5/4/784>>.
- 1354 MARESCA, M.; PINTON, P.; AJANDOUZ, E. H.; MENARD, S.; FERRIER, L.;
1355 OSWALD, I. P. Overview and Comparison of Intestinal Organotypic Models, Intestinal
1356 Cells, and Intestinal Explants Used for Toxicity Studies. *Em*: **Current Topics in**
1357 **Microbiology and Immunology**. [s.l.] Springer Science and Business Media
1358 Deutschland GmbH, 2018. p. 247–264.
- 1359 MARESCA, M.; YAHY, N.; YOUNÈS-SAKR, L.; BOYRON, M.; CAPORICCIO, B.;
1360 FANTINI, J. Both Direct and Indirect Effects Account for the Pro-Inflammatory Activity
1361 of Enteropathogenic Mycotoxins on the Human Intestinal Epithelium: Stimulation of
1362 Tnterleukin-8 Secretion, Potentiation of Interleukin-1 β Effect and Increase in the
1363 Transepithelial. **Toxicology and Applied Pharmacology**, v. 228, n. 1, p. 84–92, abr.
1364 2008. Disponível em:
- 1365 <<https://linkinghub.elsevier.com/retrieve/pii/S0041008X07005157>>.
- 1366 MARIN, S.; RAMOS, A. J.; CANO-SANCHO, G.; SANCHIS, V. Mycotoxins:
1367 Occurrence, Toxicology, and Exposure Assessment. **Food and Chemical**
1368 **Toxicology**, v. 60, p. 218–237, out. 2013. Disponível em:

- 1369 <<http://dx.doi.org/10.1016/j.fct.2013.07.047>>.
- 1370 MAYER, E.; NOVAK, B.; SPRINGLER, A.; SCHWARTZ-ZIMMERMANN, H. E.; NAGL,
1371 V.; REISINGER, N.; HESSENBERGER, S.; SCHATZMAYR, G. Effects of
1372 Deoxynivalenol (DON) and its Microbial Biotransformation Product Deepoxy-
1373 deoxynivalenol (DOM-1) on a Trout, Pig, mouse, and Human Cell Line. **Mycotoxin**
1374 **Research**, v. 33, n. 4, p. 297–308, 2017.
- 1375 MCMICHAEL, M. A. Oxidative Stress, Antioxidants, and Assessment of Oxidative
1376 Stress in Dogs and Cats. **Journal of the American Veterinary Medical Association**,
1377 v. 231, n. 5, p. 714–720, set. 2007.
- 1378 MECA, G.; FONT, G.; RUIZ, M. J. Comparative cytotoxicity study of enniatins A, A1,
1379 A2, B, B1, B4 and J3 on Caco-2 cells, Hep-G2 and HT-29. **Food and Chemical**
1380 **Toxicology**, v. 49, n. 9, p. 2464–2469, set. 2011. Disponível em:
1381 <<http://dx.doi.org/10.1016/j.fct.2011.05.020>>.
- 1382 MECA, G.; SOSPEDRA, I.; SORIANO, J. M.; RITIENI, A.; MORETTI, A.; MAÑES, J.
1383 Antibacterial Effect of the Bioactive Compound Beauvericin Produced by *Fusarium*
1384 *proliferatum* on Solid Medium of Wheat. **Toxicon**, v. 56, n. 3, p. 349–354, 2010.
- 1385 MIKAMI, O.; YAMAGUCHI, H.; MURATA, H.; NAKAJIMA, Y.; MIYAZAKI, S. Induction
1386 of Apoptotic Lesions in Liver and Lymphoid Tissues and Modulation of Cytokine mRNA
1387 Expression by Acute Exposure to Deoxynivalenol in Piglets. **Journal of Veterinary**
1388 **Science**, v. 11, n. 1, p. 107–113, 2010.
- 1389 MISHRA, S.; DWIVEDI, P. D.; PANDEY, H. P.; DAS, M. Role of Oxidative Stress in
1390 Deoxynivalenol Induced Toxicity. **Food and Chemical Toxicology**, v. 72, p. 20–29,
1391 2014. Disponível em: <<http://dx.doi.org/10.1016/j.fct.2014.06.027>>.
- 1392 MOON, Y. Vomitoxin-Induced Cyclooxygenase-2 Gene Expression in Macrophages
1393 Mediated by Activation of ERK and p38 but Not JNK Mitogen-Activated Protein
1394 Kinases. **Toxicological Sciences**, v. 69, n. 2, p. 373–382, 1 out. 2002. Disponível em:
1395 <<https://academic.oup.com/toxsci/article-lookup/doi/10.1093/toxsci/69.2.373>>.
- 1396 MORETTI, A.; PASCALE, M.; LOGRIECO, A. F. Mycotoxin risks under a climate
1397 change scenario in Europe. **Trends in Food Science & Technology**, v. 84, p. 38–40,
1398 1 fev. 2019. Disponível em:
1399 <<https://linkinghub.elsevier.com/retrieve/pii/S0924224417304090>>.
- 1400 MOROOKA, N.; URATSUJI, N.; YOSHIZAWA, T.; YAMAMOTO, H. Studies on the
1401 toxic effects of barley infected with *Fusarium* spp. **Journal of The Food Hygienic**
1402 **Society of Japan**, v. 13, n. 5, p. 368–375, 1972. Disponível em:
1403 <https://www.jstage.jst.go.jp/article/shokueishi1960/13/5/13_5_368/_pdf>. Acesso
1404 em: 17 dez. 2021.
- 1405 NARVÁEZ, A.; CASTALDO, L.; IZZO, L.; PALLARÉS, N.; RODRÍGUEZ-CARRASCO,
1406 Y.; RITIENI, A. Deoxynivalenol contamination in cereal-based foodstuffs from Spain:
1407 Systematic review and meta-analysis approach for exposure assessment. **Food**
1408 **Control**, v. 132, p. 108521, 1 fev. 2022. Disponível em:
1409 <<https://linkinghub.elsevier.com/retrieve/pii/S0956713521006599>>.
- 1410 NIELSEN, C.; LIPPKE, H.; DIDIER, A.; DIETRICH, R.; MÄRTLBAUER, E. Potential of
1411 deoxynivalenol to induce transcription factors in human hepatoma cells. **Molecular**
1412 **Nutrition & Food Research**, v. 53, n. 4, p. 479–491, abr. 2009. Disponível em:
1413 <<http://doi.wiley.com/10.1002/mnfr.200800475>>.
- 1414 NOVAK, B.; RAINER, V.; SULYOK, M.; HALTRICH, D.; SCHATZMAYR, G.; MAYER,
1415 E. Twenty-Eight Fungal Secondary Metabolites Detected in Pig Feed Samples: Their
1416 Occurrence, Relevance and Cytotoxic Effects In Vitro. **Toxins**, v. 11, n. 9, p. 537, 14
1417 set. 2019. Disponível em: <<https://www.mdpi.com/2072-6651/11/9/537>>.
- 1418 NOVAK, B.; VATZIA, E.; SPRINGLER, A.; PIERRON, A.; GERNER, W.; REISINGER,

- 1419 N.; HESSENBERGER, S.; SCHATZMAYR, G.; MAYER, E. Bovine Peripheral Blood
1420 Mononuclear Cells are More Sensitive to Deoxynivalenol Than Those Derived from
1421 Poultry and Swine. **Toxins**, v. 10, n. 4, p. 1–14, 2018.
- 1422 NOVAK, E. A.; MOLLEN, K. P. **Mitochondrial dysfunction in inflammatory bowel**
1423 **disease** *Frontiers in Cell and Developmental Biology* Frontiers Media S.A., 1 out.
1424 2015.
- 1425 OLIVEIRA, C. A. F.; IVANOVA, L.; SOLHAUG, A.; FÆSTE, C. K. Enniatin B1-Induced
1426 Lysosomal Membrane Permeabilization in Mouse Embryonic Fibroblasts. **Mycotoxin**
1427 **Research**, 1 jul. 2019.
- 1428 OSSELAERE, A.; SANTOS, R.; HAUTEKIET, V.; DE BACKER, P.; CHIERS, K.;
1429 DUCATELLE, R.; CROUBELS, S. Deoxynivalenol Impairs Hepatic and Intestinal Gene
1430 Expression of Selected Oxidative Stress, Tight Junction and Inflammation Proteins in
1431 Broiler Chickens, but Addition of an Adsorbing Agent Shifts the Effects to the Distal
1432 Parts of the Small Intestine. **PLoS ONE**, v. 8, n. 7, p. e69014, 26 jul. 2013. Disponível
1433 em: <<https://dx.plos.org/10.1371/journal.pone.0069014>>.
- 1434 OSWALD, I. P.; MARIN, D. E.; BOUHET, S.; PINTON, P.; TARANU, I.; ACCENSI, F.
1435 Immunotoxicological risk of mycotoxins for domestic animals. **Food Additives and**
1436 **Contaminants**, v. 22, n. 4, p. 354–360, abr. 2005. Disponível em:
1437 <<http://www.tandfonline.com/doi/abs/10.1080/02652030500058320>>.
- 1438 PAVELESCU, L. A. On Reactive Oxygen Species Measurement in Living Systems.
1439 **Journal of Medicine and Life**, v. 8, p. 38–42, 2015.
- 1440 PAVENTI, G.; PIZZUTO, R.; PASSARELLA, S. The Occurrence of L-lactate
1441 Dehydrogenase in the Inner Mitochondrial Compartment of Pig Liver. **Biochemical**
1442 **and Biophysical Research Communications**, v. 489, n. 2, p. 255–261, jul. 2017.
- 1443 PAYROS, D.; ALASSANE-KPEMBI, I.; PIERRON, A.; LOISEAU, N.; PINTON, P.;
1444 OSWALD, I. P. Toxicology of deoxynivalenol and its acetylated and modified forms.
1445 **Archives of Toxicology**, v. 90, n. 12, p. 2931–2957, 23 dez. 2016. Disponível em:
1446 <<http://link.springer.com/10.1007/s00204-016-1826-4>>.
- 1447 PESTKA, J. J. Deoxynivalenol-Induced Proinflammatory Gene Expression:
1448 Mechanisms and Pathological Sequelae. **Toxins**, v. 2, n. 6, p. 1300–1317, 1 jun.
1449 2010a. Disponível em: <<http://www.mdpi.com/2072-6651/2/6/1300>>.
- 1450 PESTKA, J. J. Deoxynivalenol: mechanisms of action, human exposure, and
1451 toxicological relevance. **Archives of Toxicology**, v. 84, n. 9, p. 663–679, 27 set.
1452 2010b. Disponível em: <<http://link.springer.com/10.1007/s00204-010-0579-8>>.
- 1453 PESTKA, J. J.; SMOLINSKI, A. T. Deoxynivalenol: Toxicology and Potential Effects on
1454 Humans. **Journal of Toxicology and Environmental Health, Part B**, v. 8, n. 1, p.
1455 39–69, 14 dez. 2005. Disponível em:
1456 <<http://www.tandfonline.com/doi/abs/10.1080/10937400590889458>>.
- 1457 PIERRON, A.; BRACARENSE, A. P. F. L.; COSSALTER, A. M.; LAFFITTE, J.;
1458 SCHWARTZ-ZIMMERMANN, H. E.; SCHATZMAYR, G.; PINTON, P.; MOLL, W. D.;
1459 OSWALD, I. P. Deepoxy-deoxynivalenol Retains Some Immune-modulatory
1460 Properties of the Parent Molecule Deoxynivalenol in Piglets. **Archives of Toxicology**,
1461 v. 92, n. 11, p. 3381–3389, 2018.
- 1462 PIERRON, A.; MIMOUN, S.; MURATE, L. S.; LOISEAU, N.; LIPPI, Y.; BRACARENSE,
1463 A. P. F. L.; LIAUBET, L.; SCHATZMAYR, G.; BERTHILLER, F.; MOLL, W. D.;
1464 OSWALD, I. P. Intestinal toxicity of the masked mycotoxin deoxynivalenol-3- β -d-
1465 glucoside. **Archives of Toxicology**, v. 90, n. 8, p. 2037–2046, 2016.
- 1466 PINTON, P.; ACCENSI, F.; BEAUCHAMP, E.; COSSALTER, A. M.; CALLU, P.;
1467 GROSJEAN, F.; OSWALD, I. P. Ingestion of Deoxynivalenol (DON) Contaminated
1468 Feed Alters the Pig Vaccinal Immune Responses. **Toxicology Letters**, v. 177, n. 3, p.

- 1469 215–222, abr. 2008.
- 1470 PINTON, P.; NOUGAYRÈDE, J.-P.; DEL RIO, J.-C.; MORENO, C.; MARIN, D. E.;
- 1471 FERRIER, L.; BRACARENSE, A.-P.; KOLF-CLAUW, M.; OSWALD, I. P. The food
- 1472 contaminant deoxynivalenol, decreases intestinal barrier permeability and reduces
- 1473 claudin expression. **Toxicology and Applied Pharmacology**, v. 237, n. 1, p. 41–48,
- 1474 15 maio 2009. Disponível em:
- 1475 <<https://linkinghub.elsevier.com/retrieve/pii/S0041008X09001045>>.
- 1476 PINTON, P.; OSWALD, I. P. Trichothecenes on the Intestine : A Review. **Toxins**, v. 6,
- 1477 p. 1615–1643, 2014.
- 1478 PRELUSKY, D. B.; ROTTER, B. A.; ROTTER, R. G.; MILLER; TRENHOLM, H. L.
- 1479 Toxicology in mycotoxins. Em: MILLER, J. D.; TRENHOLM, H. **Mycotoxin in grain**.
- 1480 [s.l: s.n.]p. 458–458.
- 1481 PROSPERINI, A.; BERRADA, H.; RUIZ, M. J.; CALONI, F.; COCCINI, T.; SPICER, L.
- 1482 J.; PEREGO, M. C.; LAFRANCONI, A. A Review of the Mycotoxin Enniatin B.
- 1483 **Frontiers in Public Health**, v. 5, n. November, p. 1–11, 16 nov. 2017.
- 1484 PROSPERINI, A.; JUAN-GARCÍA, A.; FONT, G.; RUIZ, M. J. Beauvericin-Induced
- 1485 Cytotoxicity via ROS Production and Mitochondrial Damage in Caco-2 Cells.
- 1486 **Toxicology Letters**, v. 222, n. 2, p. 204–211, 2013a.
- 1487 PROSPERINI, A.; JUAN-GARCÍA, A.; FONT, G.; RUIZ, M. J. Reactive Oxygen
- 1488 Species Involvement in Apoptosis and Mitochondrial Damage in Caco-2 Cells Induced
- 1489 by Enniatins A, A1, B and B1. **Toxicology Letters**, v. 222, n. 1, p. 36–44, 2013b.
- 1490 Disponível em: <<http://dx.doi.org/10.1016/j.toxlet.2013.07.009>>.
- 1491 PUPPEL, K.; KAPUSTA, A.; KUCZYNSKA, B. The Etiology of Oxidative Stress in the
- 1492 Various Species of Animals , A Review. **Journal of the Science of Food and**
- 1493 **Agriculture**, v. 95, p. 2179–2184, 2014.
- 1494 RANDALL, K. J.; TURTON, J.; FOSTER, J. R. Explant culture of gastrointestinal tissue:
- 1495 a review of methods and applications. **Cell Biology and Toxicology**, v. 27, n. 4, p.
- 1496 267–284, 8 ago. 2011. Disponível em: <[http://link.springer.com/10.1007/s10565-011-](http://link.springer.com/10.1007/s10565-011-9187-5)
- 1497 [9187-5](http://link.springer.com/10.1007/s10565-011-9187-5)>.
- 1498 REDDY, K. E.; JEONG, J. Y.; LEE, Y.; LEE, H.-J.; KIM, M. S.; KIM, D.-W.; JUNG, H.
- 1499 J.; CHOE, C.; OH, Y. K.; LEE, S. D. Deoxynivalenol- and zearalenone-contaminated
- 1500 feeds alter gene expression profiles in the livers of piglets. **Asian-Australasian**
- 1501 **Journal of Animal Sciences**, v. 31, n. 4, p. 595–606, 1 abr. 2018. Disponível em:
- 1502 <<http://ajas.info/journal/view.php?doi=10.5713/ajas.17.0466>>.
- 1503 REN, Z.; DENG, H.; DENG, Y.; LIANG, Z.; DENG, J.; ZUO, Z.; HU, Y.; SHEN, L.; YU,
- 1504 S.; CAO, S. Combined Effects of Deoxynivalenol and Zearalenone on Oxidative Injury
- 1505 and Apoptosis in Porcine Splenic Lymphocytes In Vitro. **Experimental and**
- 1506 **Toxicologic Pathology**, v. 69, n. 8, p. 612–617, out. 2017. Disponível em:
- 1507 <<http://dx.doi.org/10.1016/j.etp.2017.05.008>>.
- 1508 RENNER, L.; KAHLERT, S.; TESCH, T.; BANNERT, E.; FRAHM, J.; BARTA-
- 1509 BÖSZÖRMÉNYI, A.; KLUSS, J.; KERSTEN, S.; SCHÖNFELD, P.; ROTHKÖTTER,
- 1510 H.-J.; DÄNICKE, S. Chronic DON exposure and acute LPS challenge: effects on
- 1511 porcine liver morphology and function. **Mycotoxin Research**, v. 33, n. 3, p. 207–218,
- 1512 4 ago. 2017. Disponível em: <<http://link.springer.com/10.1007/s12550-017-0279-9>>.
- 1513 RODRÍGUEZ-CARRASCO, Y.; HEILOS, D.; RICHTER, L.; SÜSSMUTH, R. D.;
- 1514 HEFFETER, P.; SULYOK, M.; KENNER, L.; BERGER, W.; DORNETSHUBER-
- 1515 FLEISS, R. Mouse Tissue Distribution and Persistence of the Food-Born Fusariotoxins
- 1516 Enniatin B and Beauvericin. **Toxicology Letters**, v. 247, p. 35–44, 2016.
- 1517 ROIG, M.; MECA, G.; MARÍN, R.; FERRER, E.; MAÑES, J. Antibacterial Activity of the
- 1518 Emerging Fusarium Mycotoxins Enniatins A, A1, A2, B, B1, and B4 on Probiotic

- 1519 Microorganisms. **Toxicon**, v. 85, p. 1–4, 2014.
- 1520 RUSSO, C.; BRACARENSE, A. P. F. R. L. Oxidative Stress in Dogs. **Semina:**
1521 **Ciências Agrárias**, v. 37, n. 3, p. 1431–1440, 2016.
- 1522 RUSSO, I.; ZEPPA, P.; IOVINO, P.; DEL GIORNO, C.; ZINGONE, F.; BUCCI, C.;
1523 PUZZIELLO, A.; CIACCI, C. The Culture of Gut Explants: A Model to Study the
1524 Mucosal Response. **Journal of Immunological Methods**, v. 438, p. 1–10, 2016.
- 1525 SANTOS, R. R.; SCHOEVERS, E. J.; WU, X.; ROELEN, B. A. J.; FINK-GREMMELS,
1526 J. The Protective Effect of Follicular Fluid Against the Emerging Mycotoxins Alternariol
1527 and Beauvericin. **World Mycotoxin Journal**, v. 8, n. 4, p. 445–450, 2015.
- 1528 SCHOEVERS, E. J.; SANTOS, R. R.; FINK-GREMMELS, J.; ROELEN, B. A. J.
1529 Toxicity of Beauvericin on Porcine Oocyte Maturation and Preimplantation Embryo
1530 Development. **Reproductive Toxicology**, v. 65, p. 159–169, 2016.
- 1531 SERGENT, T.; PARYS, M.; GARSOU, S.; PUSSEMIER, L.; SCHNEIDER, Y.-J.;
1532 LARONDELLE, Y. Deoxynivalenol transport across human intestinal Caco-2 cells and
1533 its effects on cellular metabolism at realistic intestinal concentrations. **Toxicology**
1534 **Letters**, v. 164, n. 2, p. 167–176, 1 jul. 2006. Disponível em:
1535 <<https://linkinghub.elsevier.com/retrieve/pii/S037842740500425X>>.
- 1536 SILVA, E. O. da; GEREZ, J. R.; DRAPE, T. do C.; BRACARENSE, A. P. F. R. L. Phytic
1537 Acid Decreases Deoxynivalenol and Fumonisin B1-Induced Changes on Swine Jejunal
1538 Explants. **Toxicology Reports**, v. 1, p. 284–292, 2014. Disponível em:
1539 <<https://linkinghub.elsevier.com/retrieve/pii/S2214750014000213>>.
- 1540 SILVA, E. O. da; GEREZ, J. R.; HOHMANN, M. S. N.; VERRI, W. A.; BRACARENSE,
1541 A. P. F. R. L. Phytic Acid Decreases Oxidative Stress and Intestinal Lesions Induced
1542 by Fumonisin B1 and Deoxynivalenol in Intestinal Explants of Pigs. **Toxins**, v. 11, n.
1543 1, p. 18, 4 jan. 2019.
- 1544 SKIEPKO, N.; PRZYBYLSKA-GORNOWICZ, B.; GAJĘCKA, M.; GAJĘCKI, M.;
1545 LEWCZUK, B. Effects of Deoxynivalenol and Zearalenone on the Histology and
1546 Ultrastructure of Pig Liver. **Toxins**, v. 12, n. 7, p. 463, 20 jul. 2020. Disponível em:
1547 <<https://www.mdpi.com/2072-6651/12/7/463>>.
- 1548 SOBROVA, P.; ADAM, V.; VASATKOVA, A.; BEKLOVA, M.; ZEMAN, L.; KIZEK, R.
1549 Deoxynivalenol and its Toxicity. **Interdisciplinary Toxicology**, v. 3, n. 3, p. 94–99, 1
1550 jan. 2010. Disponível em: <[http://content.sciendo.com/view/journals/intox/3/3/article-](http://content.sciendo.com/view/journals/intox/3/3/article-p94.xml)
1551 [p94.xml](http://content.sciendo.com/view/journals/intox/3/3/article-p94.xml)>.
- 1552 SOUZA, M. de; BAPTISTA, A. A. S.; VALDIVIEZO, M. J. J.; JUSTINO, L.; MENCK-
1553 COSTA, M. F.; FERRAZ, C. R.; DA GLORIA, E. M.; VERRI, W. A.; BRACARENSE, A.
1554 P. F. R. L. Lactobacillus spp. Reduces Morphological Changes and Oxidative Stress
1555 Induced by Deoxynivalenol on the Intestine and Liver of Broilers. **Toxicon**, v. 185, n.
1556 July, p. 203–212, 2020. Disponível em:
1557 <<https://doi.org/10.1016/j.toxicon.2020.07.002>>.
- 1558 SPRINGLER, A.; VRUBEL, G. J.; MAYER, E.; SCHATZMAYR, G.; NOVAK, B. Effect
1559 of Fusarium-Derived Metabolites on the Barrier Integrity of Differentiated Intestinal
1560 Porcine Epithelial Cells (IPEC-J2). **Toxins**, v. 8, n. 11, 2016.
- 1561 STADNYK, A. W. Intestinal Epithelial Cells as a Source of Inflammatory Cytokines and
1562 Chemokines. **Canadian Journal of Gastroenterology**, v. 16, n. 4, p. 241–246, 2002.
1563 Disponível em: <<http://www.hindawi.com/journals/cjgh/2002/941087/abs/>>.
- 1564 STEADMAN, R. H.; BRAUNFELD, M.; PARK, H. Liver and Gastrointestinal
1565 Physiology. *Em: Pharmacology and Physiology for Anesthesia*. 2nd. ed. [s.l.]
1566 Elsevier, 2019. p. 630–644.
- 1567 SUGITA-KONISHI, Y.; PESTKA, J. J. Differential Upregulation of TNF-alpha, IL-6, and
1568 IL-8 Production by Deoxynivalenol (Vomitoxin) and other 8-Ketotrichothecenes in a

- 1569 Human Macrophage Model. **Journal of Toxicology and Environmental Health, Part**
1570 **A**, v. 64, n. 8, p. 619–636, 21 dez. 2001. Disponível em:
1571 <<http://www.tandfonline.com/doi/abs/10.1080/152873901753246223>>.
- 1572 SUN, L. H.; LEI, M. Y.; ZHANG, N. Y.; ZHAO, L.; KRUMM, C. S.; QI, D. S. Hepatotoxic
1573 effects of mycotoxin combinations in mice. **Food and Chemical Toxicology**, v. 74, p.
1574 289–293, 2014. Disponível em: <<http://dx.doi.org/10.1016/j.fct.2014.10.020>>.
- 1575 SUN, L.-H.; LEI, M.; ZHANG, N.-Y.; GAO, X.; LI, C.; KRUMM, C. S.; QI, D.-S. Individual
1576 and combined cytotoxic effects of aflatoxin B1, zearalenone, deoxynivalenol and
1577 fumonisin B1 on BRL 3A rat liver cells. **Toxicon**, v. 95, p. 6–12, mar. 2015. Disponível
1578 em: <<http://dx.doi.org/10.1016/j.toxicon.2014.12.010>>.
- 1579 TANG, M.; YUAN, D.; LIAO, P. Berberine improves intestinal barrier function and
1580 reduces inflammation, immunosuppression, and oxidative stress by regulating the NF-
1581 κ B/MAPK signaling pathway in deoxynivalenol-challenged piglets. **Environmental**
1582 **Pollution**, v. 289, p. 117865, 15 nov. 2021. Disponível em:
1583 <<https://linkinghub.elsevier.com/retrieve/pii/S0269749121014470>>.
- 1584 TARANU, I.; MARIN, D. E.; BURLACU, R.; PINTON, P.; DAMIAN, V.; OSWALD, I. P.
1585 Comparative Aspects of In Vitro Proliferation of Human and Porcine Lymphocytes
1586 Exposed to Mycotoxins. **Archives of Animal Nutrition**, v. 64, n. 5, p. 383–393, out.
1587 2010. Disponível em:
1588 <<http://www.tandfonline.com/doi/abs/10.1080/1745039X.2010.492140>>.
- 1589 TENNANT, B. C.; CENTER, S. A. Hepatic Function. *Em*: KANEKO, J.; HARVEY, J.;
1590 BRUSS, M. **Clinical Biochemistry of Domestic Animals**. 6th. ed. San Diego:
1591 Elsevier, 2008. p. 379–412.
- 1592 THRALL, M. A.; WEISER, G.; ALLISON, R. W.; CAMPBELL, T. W. **Hematologia e**
1593 **Bioquímica Clínica Veterinária**. 2. ed. São Paulo: ROCA LTDA, 2015. 678 p.
- 1594 TIEMANN, U.; BRÜSSOW, K. P.; KÜCHENMEISTER, U.; JONAS, L.; PÖHLAND, R.;
1595 REISCHAUER, A.; JÄGER, K.; DÄNICKE, S. Changes in the Spleen and Liver of
1596 Pregnant Sows and Full-Term Piglets After Feeding Diets Naturally Contaminated with
1597 Deoxynivalenol and Zearalenone. **Veterinary Journal**, v. 176, n. 2, p. 188–196, 2008.
- 1598 TOLOSA, J.; RODRÍGUEZ-CARRASCO, Y.; RUIZ, M. J.; VILA-DONAT, P. Multi-
1599 mycotoxin occurrence in feed, metabolism and carry-over to animal-derived food
1600 products: A review. **Food and Chemical Toxicology**, v. 158, p. 112661, 1 dez. 2021.
1601 Disponível em: <<https://linkinghub.elsevier.com/retrieve/pii/S0278691521006943>>.
- 1602 TONSHIN, A. A.; TEPLOVA, V. V.; ANDERSSON, M. A.; SALKINOJA-SALONEN, M.
1603 S. The Fusarium Mycotoxins Enniatins and Beauvericin Cause Mitochondrial
1604 Dysfunction by Affecting the Mitochondrial Volume Regulation, Oxidative
1605 Phosphorylation and Ion Homeostasis. **Toxicology**, v. 276, n. 1, p. 49–57, 2010.
- 1606 URBANIAK, M.; WAŚKIEWICZ, A.; STĘPIEŃ, Ł. Fusarium Cyclodepsipeptide
1607 Mycotoxins: Chemistry, Biosynthesis, and Occurrence. **Toxins**, v. 12, n. 12, p. 765, 3
1608 dez. 2020. Disponível em: <<https://www.mdpi.com/2072-6651/12/12/765>>.
- 1609 VACLAVIKOVA, M.; MALACHOVA, A.; VEPRIKOVA, Z.; DZUMAN, Z.;
1610 ZACHARIASOVA, M.; HAJŠLOVA, J. ‘Emerging’ mycotoxins in cereals processing
1611 chains: Changes of enniatins during beer and bread making. **Food Chemistry**, v. 136,
1612 n. 2, p. 750–757, 15 jan. 2013. Disponível em:
1613 <<https://linkinghub.elsevier.com/retrieve/pii/S0308814612013155>>.
- 1614 VAN DE WALLE, J.; ROMIER, B.; LARONDELLE, Y.; SCHNEIDER, Y. J. Influence of
1615 deoxynivalenol on NF- κ B activation and IL-8 secretion in human intestinal Caco-2
1616 cells. **Toxicology Letters**, v. 177, n. 3, p. 205–214, 2008.
- 1617 WANG, S.; WU, K.; XUE, D.; ZHANG, C.; RAJPUT, S. A.; QI, D. Mechanism of
1618 deoxynivalenol mediated gastrointestinal toxicity: Insights from mitochondrial

- 1619 dysfunction. **Food and Chemical Toxicology**, v. 153, n. January, p. 112214, 2021.
1620 Disponível em: <<https://doi.org/10.1016/j.fct.2021.112214>>.
- 1621 WÄTJEN, W.; DEBBAB, A.; HOHLFELD, A.; CHOVOLOU, Y.; PROKSCH, P. The
1622 Mycotoxin Beauvericin Induces Apoptotic Cell Death in H4IIE Hepatoma Cells
1623 Accompanied by an Inhibition of NF- κ B-Activity and Modulation of MAP-Kinases.
1624 **Toxicology Letters**, v. 231, n. 1, p. 9–16, 2014.
- 1625 WENTZEL, J. F.; LOMBARD, M. J.; DU PLESSIS, L. H.; ZANDBERG, L. Evaluation of
1626 the cytotoxic properties, gene expression profiles and secondary signalling responses
1627 of cultured cells exposed to fumonisin B1, deoxynivalenol and zearalenone
1628 mycotoxins. **Archives of Toxicology**, v. 91, n. 5, p. 2265–2282, 18 maio 2017.
1629 Disponível em: <<http://link.springer.com/10.1007/s00204-016-1872-y>>.
- 1630 WU, X. F.; XU, R.; OUYANG, Z. J.; QIAN, C.; SHEN, Y.; WU, X. D.; GU, Y. H.; XU, Q.;
1631 SUN, Y. Beauvericin Ameliorates Experimental Colitis by Inhibiting Activated T Cells
1632 via Downregulation of the PI3K/Akt Signaling Pathway. **PLoS ONE**, v. 8, n. 12, 2013.
- 1633 YANG, J.; ZHU, C.; YE, J.; LV, Y.; WANG, L.; CHEN, Z.; JIANG, Z. Protection of
1634 Porcine Intestinal-Epithelial Cells from Deoxynivalenol-Induced Damage by
1635 Resveratrol via the Nrf2 Signaling Pathway. **Journal of Agricultural and Food
1636 Chemistry**, v. 67, n. 6, p. 1726–1735, 13 fev. 2019. Disponível em:
1637 <<https://pubs.acs.org/doi/10.1021/acs.jafc.8b03662>>.
- 1638 YANG, W.; YU, M.; FU, J.; BAO, W.; WANG, D.; HAO, L.; YAO, P.; NÜSSLER, A. K.;
1639 YAN, H.; LIU, L. Deoxynivalenol induced oxidative stress and genotoxicity in human
1640 peripheral blood lymphocytes. **Food and Chemical Toxicology**, v. 64, p. 383–396,
1641 fev. 2014. Disponível em:
1642 <<https://linkinghub.elsevier.com/retrieve/pii/S027869151300834X>>.
- 1643 YOO, S.; KIM, M.-Y.; CHO, J. Y. Beauvericin, a Cyclic Peptide, Inhibits Inflammatory
1644 Responses in Macrophages by Inhibiting the NF- κ B Pathway. **Korean Journal of
1645 Physiology and Pharmacology**, v. 21, n. 4, p. 449–456, 2017.
- 1646 YUAN, L.; MU, P.; HUANG, B.; LI, H.; MU, H.; DENG, Y. EGR1 is essential for
1647 deoxynivalenol-induced G2/M cell cycle arrest in HepG2 cells via the ATF3 Δ Zip2a/2b-
1648 EGR1-p21 pathway. **Toxicology Letters**, v. 299, n. June, p. 95–103, 2018. Disponível
1649 em: <<https://doi.org/10.1016/j.toxlet.2018.09.012>>.
- 1650 ZACHARY, J. F.; MCGAVIN, M. D. **Bases Da Patologia Em Veterinária**. 2. ed. Rio
1651 de Janeiro: Elsevier, 2013.
- 1652 ZHANG, K.; HORNEF, M. W.; DUPONT, A. The intestinal epithelium as guardian of
1653 gut barrier integrity. **Cellular Microbiology**, v. 17, n. 11, p. 1561–1569, 1 nov. 2015.
1654 Disponível em: <<https://onlinelibrary.wiley.com/doi/10.1111/cmi.12501>>.
- 1655 ZHANG, X.; JIANG, L.; GENG, C.; CAO, J.; ZHONG, L. The Role of Oxidative Stress
1656 in Deoxynivalenol-induced DNA Damage in HepG2 Cells. **Toxicon**, v. 54, n. 4, p. 513–
1657 518, 2009. Disponível em: <<http://dx.doi.org/10.1016/j.toxicon.2009.05.021>>.
- 1658 ZOUAOUI, N.; MALLEBRERA, B.; BERRADA, H.; ABID-ESSEFI, S.; BACHA, H.;
1659 RUIZ, M. J. Cytotoxic Effects Induced by Patulin, Sterigmatocystin and Beauvericin on
1660 CHO-K1 Cells. **Food and Chemical Toxicology**, v. 89, p. 92–103, 2016.
1661

1662 **4 HIPÓTESE**

1663 H_0 : A exposição a doses realistas de DON, BEA e ENNs não causa
1664 alterações tóxicas no fígado e intestino de suínos.

1665 H_1 : A exposição a doses realistas de DON, BEA e ENNs causa
1666 alterações tóxicas no fígado e intestino de suínos.

1667 5 OBJETIVOS

1668 5.1 OBJETIVO GERAL

1669 Verificar os efeitos tóxicos de DON e das micotoxinas emergentes
1670 BEA e ENNs em suínos.

1671 5.2 OBJETIVOS ESPECÍFICOS

1672 Avaliar a performance animal em suínos alimentados com dieta
1673 contaminada com DON, BEA e ENNs.

1674 Avaliar aspectos histológicos do intestino, fígado e linfonodos de
1675 suínos alimentados com dieta contaminada com DON, BEA e ENNs.

1676 Identificar alterações nos parâmetros plasmáticos e na expressão de
1677 genes no intestino e fígado de suínos tratados com DON, BEA e ENNs.

1678 Identificar alterações na microbiota intestinal de suínos tratados com
1679 DON, BEA e ENNs.

1680 Avaliar a viabilidade celular de células hepáticas humanas expostas
1681 ao DON e às micotoxinas emergentes.

1682 Avaliar o aspecto histológico do novo modelo de explantes de fígado
1683 de suínos cortados com precisão expostos ao DON e às micotoxinas emergentes.

1684 Identificar alterações na expressão de genes dos explantes de fígado
1685 de suínos e células hepáticas humanas expostos ao DON e às micotoxinas
1686 emergentes.

1 **6 ARTIGO A – EFFECTS OF FUSARIUM METABOLITES BEAUVERICIN AND**
 2 **ENNIATINS ALONE OR IN MIXTURE WITH DEOXYNIVALENOL ON**
 3 **WEANING PIGLETS**

4 **Effects of *Fusarium* metabolites beauvericin and enniatins**
 5 **alone or in mixture with deoxynivalenol on weaning**
 6 **piglets**

7 **Barbara Novak^{1,*+}, Amanda Lopes Hasuda^{2,3,+}, Mahdi Ghanbari¹, Viviane Mayumi Maruo^{3,4},**
 8 **Ana Paula F. R. L. Bracarense², Manon Neves³, Caroline Emsenhuber¹, Silvia Wein¹, Isabelle**
 9 **P. Oswald³, Philippe Pinton³ and Dian Schatzmayr¹**

10 ¹ BIOMIN Research Center, Technopark 1, 3430 Tulln, Austria; barbara.novak@dsm.com (B.N.);
 11 mahdi.ghanbari@dsm.com (M.G.); caroline.emsenhuber@dsm.com (C.E.); silvia.wein@dsm.com (S.W.);
 12 dian.schatzmayr@dsm.com (D.S.)

13 ² Laboratory of Animal Pathology, State University of Londrina, P.O. Box 10.011, Londrina, PR 86057-970,
 14 Brazil; amanda.lopeshasuda@uel.br (A.L.); anapaula@uel.br (A.B.)

15 ³ Toxalim (Research Centre in Food Toxicology), Université de Toulouse, INRA, ENVT, INP-Purpan, UPS,
 16 31027 Toulouse, France; manon.neves@gmail.com (M.N.); isabelle.oswald@inrae.fr (IPO);
 17 philippe.pinton@inrae.fr (P.P.);

18 ⁴ Universidade Federal do Tocantins, Araguaína 77824-838, Brazil; vivimaruo@mail.uft.edu.br (V.M.)

19 * Corresponding author: barbara.novak@dsm.com, Tel.: +43 2272 81166 0

20 + Contributed equally to this work

21 Received: 21 October 2021; Accepted: 25 November 2021; Published: 27 November 2021.

22 **Abstract:** The impact of the *Fusarium*-derived metabolites beauvericin, enniatin B and B1 (EB)
 23 alone or in combination with deoxynivalenol (DON) was investigated in 28-29 days old weaning
 24 piglets over a time period of 14 days. The co-application of EB and DON (EB+DON) led to a
 25 significant decrease in the weight gain of the animals. Liver enzyme activities in plasma were
 26 significantly decreased at day 14 in piglets receiving the EB+DON-containing diets compared to
 27 piglets receiving the control diet. All mycotoxin-contaminated diets led to moderate to severe
 28 histological lesions in the jejunum, the liver and lymph nodes. Shotgun metagenomics revealed a
 29 significant effect of EB-application on the gut microbiota. Our results provide novel insights into
 30 the harmful impact of emerging mycotoxins alone or with DON on the performance, gut health and
 31 immunological parameters in pigs.

32 **Keywords:** biomarker of effect, cyclic hexadepsipeptides, fungal metabolites, gut microbiota,
 33 histological alterations, mycotoxins

35 **1. Introduction**

36 Cyclic hexadepsipeptides such as enniatins (ENNs) and beauvericin (BEA) are secondary fungal
 37 metabolites produced by different fungal genera, but mainly by *Fusarium* species and are considered

1 as emerging mycotoxins (Jestoi, 2008b; Urbaniak et al., 2020). Over the past decade, these
2 ionophoric and lipophilic compounds have been the subject of controversy in the literature due to
3 their many detrimental and beneficial effects (Caloni et al., 2020; Gruber-Dorninger et al., 2017b;
4 Křížová et al., 2021). On the one hand, they showed cytotoxic, oxidative, proinflammatory and
5 genotoxic effects in numerous cell lines and impaired the gut barrier function of intestinal cells
6 (Albonico et al., 2016; Juan-García et al., 2015; Khoshal et al., 2019; Manyes et al., 2018; Novak et
7 al., 2019; Prosperini et al., 2013; Springler et al., 2016). On the other side, they are also known to
8 possess antibacterial, antifungal and insecticidal properties (Olleik et al., 2019; Urbaniak et al., 2020).

9 As they occur ubiquitously in feed and food samples, the European Food and Safety Agency
10 (EFSA) published a scientific opinion on their risk as early as 2014, but no regulations or guidelines
11 have been established to date (EFSA, 2014). This is mainly a result of the lack of *in vivo* experiments
12 and long-exposure studies in mammals. The main challenges to perform such *in vivo* trials is the lack
13 of naturally contaminated culture material and the economic feasibility to obtain an affordable amount
14 of those toxins. BEA, enniatin B (ENN B) and enniatin B1 (ENN B1) were detected to 83%, 71%
15 and 69%, respectively, of 1113 feed samples recently analyzed (Kovalsky et al., 2016). Another study
16 found a similarly high prevalence of 82 % for ENN B and ENN B1, and 67% for BEA in 1141 finished
17 feed samples for swine (Novak et al., 2019). Furthermore, several studies have been published
18 showing different occurrence of those mycotoxins in different geographic regions, different feed
19 commodities and feed destined for different species (Hietaniemi et al., 2016; Juan et al., 2016;
20 Mahnine et al., 2011; Serrano et al., 2013). Concentrations of ENNs and BEA vary from low $\mu\text{g}/\text{kg}$
21 to high mg/kg ranges, depending on feed type, climate, country and weather conditions (Medina et
22 al., 2017; Santini et al., 2012; Urbaniak et al., 2020). Furthermore, co-occurrence with more
23 investigated and regulated *Fusarium* mycotoxins, such as deoxynivalenol (DON), was already
24 described (Khoshal et al., 2019; Spanic et al., 2020; Yoshinari et al., 2016). DON is one of the most
25 prevalent mycotoxins detected in 55% to 95% of analyzed feed stuff depending on the region with
26 several described negative effects on animals' health, performance, and immune system (Holanda

27 and Kim, 2021). Among the known 29 analogues of ENNs, ENN B and B1 seem to occur more often
28 than the others (Novak et al., 2019; Reisinger et al., 2019).

29 The aim of this study was to investigate the short-term effects of the emerging mycotoxins BEA,
30 ENN B and ENN B1 alone (EB), and together with the regulated mycotoxin DON (EB+DON) on the
31 performance and feed consumption as well as on the intestine and liver of piglets. We chose 28-29
32 days old piglets for the study, as they are in a critical phase during the first weeks after weaning
33 (Campbell et al., 2013) and thus, are more susceptible to mycotoxins and infectious diseases (Pierron
34 et al., 2016a). Due to the known antibiotic properties of the used emerging mycotoxins, we further
35 investigated their impact on the fecal microbiome by applying a shotgun metagenomics approach.
36 Finally, we analyzed the effect of the mycotoxins on several clinical blood parameters, gene
37 expression in liver and jejunum tissue, as well as histology of liver, intestine and lymph nodes.

38 2. *Materials and Methods*

39 2.1. *Chemical and reagents*

40 Culture material containing 4.67 g/kg beauvericin and 2.50 g/kg enniatins was prepared by Dr.
41 Roman Labudá from the BiMM institute (Bioactive Microbial Metabolites, UFT Tulln, Austria). In
42 brief, 200 g corn kernels were mixed with 200 mL deionized water and soaked for 60 min under room
43 temperature ($23\text{ }^{\circ}\text{C} \pm 1\text{ }^{\circ}\text{C}$) in polypropylene plastic bags (200 x 300 mm, Roth) before autoclaving
44 at standard conditions ($121\text{ }^{\circ}\text{C}$ for 20 min). The autoclaved corn material was then transferred into
45 disposable PD 1200 Microboxes (Nevele, Belgium). A *Fusarium oxysporum* strain RL 108 (personal
46 collection of Dr. Roman Labudá) was used as a production organism. Inoculation was performed with
47 100 μL conidial suspension (1.0×10^5 conidia/mL) per box, followed by cultivation in darkness at 25
48 $^{\circ}\text{C}$ for 4 weeks. At the end of cultivation, the cultures were exposed to $75\text{ }^{\circ}\text{C}$ for 2 hours (closed
49 boxes) and consequently to $70\text{ }^{\circ}\text{C}$ (open boxes) for the next 4 days till complete dryness. Heat
50 deactivation and drying was performed in a thermostat with forced air circulation (Binder, Germany).
51 The dried cultures were then transferred into a 30 L capacity bag, thoroughly mixed and crushed into
52 smaller pieces. The material was then ground in the mill (Retsch GM 200, Germany), sieved, and

53 further homogenized before final sampling. During the milling process, from every portion of freshly
54 ground material (ca. 100 g), several grams were taken as aliquots and all such aliquots were
55 consequently mixed (homogenized) before preparing the final representative sample. The final
56 representative sample (10 g) in duplication was then transferred into 250 mL capacity Erlenmeyer
57 flasks and extracted with 100 mL of solvent mix (ACN:H₂O:AcOH, 70:29:1) by rotary agitating at
58 160 rpm for 60 min. An aliquot of 100 µL was taken, diluted, and filtered for LC-MS/MS analysis.

59 Culture material with a DON concentration of 15.48 g/kg was obtained by Romer Labs (Tulln,
60 Austria) and produced according to a publication from the year 1994 (ALTPETER; POSSELT, 1994).

61 The LC-MS grade eluents used within the analytical method were purchased as followed:
62 acetonitrile (VWR chemicals, USA), methanol (Honeywell Riedel-de-Haën™, Germany), formic
63 acid (Honeywell Riedel-de-Haën™, Germany) and ammonium formate (Merck, Germany).

64 2.2. *Animal and study design*

65 All procedures related to the animal experiment were performed according to Austrian law and
66 following the European Guidelines for the Care and Use of Animals for Research Purpose. The
67 experiment was approved by the office of the Lower Austrian Region Government, Group of
68 Agriculture and Forestry, Department of Agricultural Law (approval code LF1-TVG-57/015-2019)
69 and carried out at the Center of Applied Animal Nutrition (BIOMIN Holding GmbH, Tulln, Austria).

70 Thirty-two crossbred piglets (Breed Ö-HYB-F1 [Landrace x Large White] x Pietrain, 28-29 days
71 old, average weight 7.32 ± 0.72 kg, mixed sex) were obtained from a local swine producer. Piglets
72 were randomly grouped pairwise in metabolic cages (8 animals/group), had free access to water and
73 were allowed to acclimatize for five days. Feed was provided twice daily in the morning and evening
74 for *ad libitum* intake. Prior to the start of the experiment, the feed was mixed with the respective
75 contaminated culture material and tested for mycotoxin contamination by a multi-toxin LC-MS/MS
76 method (Sulyok et al., 2020).

77 After an adaptation period of 5 days, piglets received control feed; DON-contaminated feed;
78 enniatin B, B1 and beauvericin (EB)-contaminated diet or an EB+DON-contaminated diet for a period
79 of 14 days (for mycotoxin concentrations see table 1).

80 **Table 1.** Mycotoxin concentration in the respective diet

Group \ Toxin	BEA	ENN B + B1	DON	ZEN	FB1
Control	4	161	92	<LOQ	<LOQ
DON	5	186	2524	342	<LOQ
EB	2570	1345	93	<LOQ	<LOQ
EB + DON	3578	1830	2034	263	<LOQ

Concentrations in $\mu\text{g}/\text{kg}$

<LOQ = below limit of quantification

81
82 Blood of each piglet was collected after 7 days (D7) and 14 days (D14) on the experimental
83 diets, respectively. Samples were aliquoted and stored at $-80\text{ }^{\circ}\text{C}$ until analysis. For blood sampling,
84 about 8 mL full blood was taken with Li-Heparin tubes (S-Monovette 9 mL, Sarstedt, cat. no.
85 02.1065) and immediately cooled to $4\text{ }^{\circ}\text{C}$. After transfer to the laboratory, samples were centrifuged
86 at $2,000 \times g$ for 20 min at $4\text{ }^{\circ}\text{C}$ and plasma was aliquoted á 500 μL to labeled 1.5 mL tubes and frozen
87 to -80°C . Determination of the respective parameters was done within the next 2 months.

88 Feces samples were taken at the end of the trial from individual piglets during euthanasia
89 (D15/16). About 1 g were transferred into a homemade nucleic acid preservation buffer (NAP) and
90 stored at room temperature for microbiome analysis.

91 *2.3. Metagenomic analysis*

92 DNA from individual fecal samples was extracted using the QIAamp PowerFecal kit (Qiagen,
93 Crawley, West Sussex, UK) which as shown in a recent study, has minimum effects on the microbial
94 community structure and promising results in terms of the DNA integrity for pig feces samples (Wegl
95 et al., 2021). Briefly, 0.25 mg of digesta/fecal sample was added to the dry bead tube containing 750
96 μL of bead solution and gently vortexed. C1 solution was added, briefly vortexed, and incubated at
97 $65\text{ }^{\circ}\text{C}$ for 10 min. Samples were shaken in Mo Bio Vortex Adapter Genie2 at maximum speed for 5
98 min. Samples were centrifuged at $13,000 \times g$ for 1 min, the supernatant transferred to the 2 mL
99 collection tube and the remainder of the protocol was followed as recommended by the manufacturer.
100 All samples were eluted in 100 μL 10 mM Tris-buffer pH 8.0 after being incubated for 5 min for
101 maximum elution efficiency. The total DNA concentration in each extract were determined

102 fluorometrically using Qubit™ dsDNA BR assay kit on a Qubit™ 2.0 fluorometer (Invitrogen™,
103 Unites States) and purity was assessed via 260/280 and 260/230 absorbance ratios determined via
104 spectrophotometry (NanoDrop® ND-1000, Thermo Fisher Scientific, United States).

105 For the size-selected ONT library, 600 ng of genomic DNA was used and quality was controlled
106 using Agilent 4200 TapeStation. The DNA was sheared using Covaris g-Tubes to generate >7-8 kb
107 fragments (Covaris, Inc., Woburn, Ma, USA). After clean-up, DNA was repaired and end-prepared
108 using the NEBNext FFPE DNA Repair kit (New England BioLabs, Ipswich, MA, USA). AMPure
109 XP beads were added to the repaired DNA and incubated on a Hula mixer at RT for 30 min, followed
110 by two washes with 70% EtOH. Beads were then resuspended with 61 µL of nuclease-free (NF) water
111 and incubated on a Hula mixer at RT for 30 min. Then, 61 µL of the eluate was transferred into a
112 clean 1.5 ml Eppendorf tube. The resulting DNA was quantified using the Qubit HS DNA kit. Adapter
113 ligation and clean-up was performed using the Ligation Sequencing Kit SQK-LSK109 (Oxford
114 Nanopore Technologies, Oxford, United Kingdom) with a slightly changed protocol. In brief, ligation
115 buffer, NEBNext Quick T4 DNA ligase, and adapter mix were added to the repaired DNA and
116 incubated at RT for 10 min and then overnight at 4°C. The ligated sample was purified using 100 µL
117 of AMPure XP beads during a 30 min incubation at RT on the Hula mixer, two bead washing steps
118 using the kit-provided wash buffer and resuspension of the beads in 40 µL of elution buffer at RT for
119 30 min on the Hula mixer. Then, 40 µL of the eluate was transferred into a clean 1.5 mL tube. The
120 library was then sequenced on a MK1C device (software version 20.03) using R10 flow cell
121 sequencing chemistry, resulting in 11,653,936 1D reads with the quality score >8. Taxonomic profiles
122 of the demultiplexed reads and taxa relative abundance estimated were generated using Kraken2
123 (Wood et al., 2019) and Bracken (Lu et al., 2017). The R-packages phyloseq (v. 1.30.0) (Mcmurdie
124 and Holmes, 2013), was used for microbiota data handling and calculating alpha (observed richness
125 and Shannon index) and beta diversity.

126 *2.4. Histological analysis*

127 After euthanasia, samples of jejunum, colon, liver, and lymph nodes were collected from all
128 treatments and fixed in 10% buffered formalin for histopathological evaluation. After fixation, the

129 tissues were dehydrated in a graded series of alcohol, cleared and diaphanized by xylol, and embedded
130 in paraffin for histological sections. Afterwards, 5- μ m sections were stained with hematoxylin and
131 eosin or alcian blue for histological analysis. Histological changes were evaluated using a lesion score
132 scale, considering the injury intensity as described by Terciolo et al. (2019). The lesion score was
133 established by considering the degree of severity (severity factor) and the extent of each lesion
134 (according to intensity or observed frequency, scored from 0 to 3). For each lesion, the score of the
135 extent was multiplied by the severity factor.

136 The morphometric analysis of the number of goblet cells and villi height were adapted from
137 Bracarense *et al.* (2012). Goblet cells were counted randomly in ten fields per slide at 60X
138 magnification. Villi height was measured randomly on ten villi using a MOTIC Image Plus 2.0 MLW
139 image analysis system (MOTIC Image Plus Motic Instruments, Richmond, Canada).

140 *2.5. Immunoassays and biochemical analysis*

141 A human free IGF-I/IGF-1 immunoassay (Cat. No. DG100B, R&D Systems, Minneapolis,
142 USA), a human FABP2/I-FABP immunoassay (Quantikine[®] ELISA, Cat. No. DFBP20, R&D
143 Systems, Minneapolis, USA) and a porcine zonulin immunoassay (Cat. No. MBS2607498,
144 MyBioSource, San Diego, USA) were used. The detection limits are indicated as 0.01 ng/mL, 3.63
145 pg/mL and 0.5 ng/mL, respectively. Determination of the respective protein was done according to
146 the manufacturer's protocol using lithium-heparin plasma taken on D7 and D14. Plasma biochemistry
147 was determined at D7 and D14 at GenoToul-Anexplo platform (Toulouse, France) with a Pentra 400
148 Clinical Chemistry benchtop analyzer (Horiba, Les Ulis, France).

149 *2.6. Expression of jejunal and liver mRNA by real-time PCR*

150 RT-qPCR assays were performed as previously described (Maruo et al., 2018). Primers obtained
151 from previous studies or designed using PrimerQuest[®] software were purchased from Sigma (Table
152 2). Data were analyzed with the LinRegPCR 2016.2 program. The expression values of the genes of
153 interest were normalized against three housekeeping genes: hypoxanthine phosphoribosyltransferase

154 1 (HPRT1), topoisomerase (DNA) II beta (TOP2B) and hydroxymethylbilane synthase (HMBS) and
 155 validated with NormFinder software. Gene expression was expressed relatively to the control group.

156 **Table 2.** Primer sequences of genes used for qRT-PCR analysis of the jejunum (J) and liver (L)

Target gene	Primer sequence (5'-3')	mRNA	Reference
Nitric oxide synthase 2 (NOS2)	F GAGAGGCAGAGGCTTGAGAC R TGGAGGAGCTGATGGAGTAG	ENSSSCT00000065180.2	present study
Interferon gamma (IFNG)	F TGGTAGCTCTGGGAACTGAATG R GGCTTTGCGCTGGATCTG	ENSSSCT00070017081.1	(Gourbeyre et al., 2015)
Apoptosis inducing factor mitochondria associated 1 (AIFM1)	F ATCATCTGCTCCAGAAGGA R AGTGCCCTCCACCAATGA	ENSSSCT00000013838.4	present study
Superoxide Dismutase 1 (SOD1)	F ATCATGGATTCCATGTCCATCAG R GGACCTGCACTGGTACAGCC	ENSSSCG00000021355	present study
Tumor protein p53 (TP53)	F AAAAGAAGAAGCCACTGGATGG R GTTCACGCCACCGATCT	ENSSSCT00000019534.4	present study
Tumor Necrosis Factor alpha (TNFA)	F ACTGCACTTCGAGGTTATCGG R GGCGACGGGCTTATCTGA	ENSSSCT00070048157.1	(Gourbeyre et al., 2015)
Toll-like receptor 9 (TLR9)	F CACGACAGCCGAATAGCAC R GGGAACAGGGAGCAGAGC	ENSSSCT00000012516.5	present study
Interleukin 1A (IL1A)	F GCCAATGACACAGAAGAAGA R ATGCACTGGTGGTTGATG	ENSSSCT00000008863.3	(Pierron et al., 2016b)
Nuclear Factor Kappa B (NFkB)	F CCTCCACAAGGCAGCAAATAG R TCCACACCGCTGTACAGA	ENSSSCT000000033438	(Maruo et al., 2018)
Mitogen-activated protein kinase 8 (MAPK8)	F GTGGAATCAAGCACCTTCACTCT R GGGCTTTAAGTCCCGATGAATA	ENSSSCT000000036610.1	present study
Transforming growth factor beta 1 (TGFB1)	F GGATACCAACTACTGCTTCAG R GGTTTCATGAATCCACTTCCA	ENSSSCT000000036469.3	(Gourbeyre et al., 2015)
Interleukin 10 (IL10)	F GGCCCAAGTGAAGAGTTTCTTTC R CAACAAGTCGCCCATCTGGT	ENSSSCT000000017049.5	(Pierron et al., 2016b)
Interleukin 8 (IL8)	F GCTCTCTGTGAGGCTGCAGTTC R AAGGTGTGGAATGCGTATTTATGC	ENSSSCG000000008953	(Cano et al., 2013)
Peptide YY (PYY)	F CTGCGCCACTACCTCAACCT R GGGAAGAGCAGTTTGGAGAGAA	ENSSSCT000000030078.3	present study
Cholecystokinin (CCK)	F AAAGCACCTTCTGGCCGAGT R GGTCACCTATTCTGTGGCTGGG	ENSSSCT000000012346.4	present study
Insulin like growth factor 1 (IGF1)	F TTCAGTTTCGTGTGCGGAGAC R CGTACCCTGTGGGCTTGTTG	ENSSSCT000000083279.1	present study
Ghrelin (GHRL)	F AGAAGACAGTGGTGAGGTGGAA G R TGAACCGGATTTCCAGCTTG	ENSSSCT000000012660	present study
Insulin like growth factor binding protein 1 (IGFBP1)	F ACCGACATCAAGAAGTGGAAGG R CACTTTGTAGAGTTCTCGCTGGC	ENSSSCT000000018209.3	present study
Gastric inhibitory polypeptide (GIP)	F CTCCTGGCAGTGGCGCTA R GTGGAATCTGGAGTGACCCTCT	ENSSSCT000000030856.3	present study
Leptin (LEP)	F TTTCACACATGCAGTCTGTCTCC R AAGTCCAAACCGGTGACCCT	ENSSSCT00015057529.1	present study
Interleukin 1B (IL1B)	F ATGCTGAAGGCTCTCCACCTC R TTGTTGCTATCATCTCCTTGACAC	ENSSSCT00070040964.1	(Maruo et al., 2018)
Interleukin 6 (IL6)	F TTCACCTCTCCGGACAAAACCTG R TCTGCCAGTACCTCCTTGCTGT	ENSSSCT000000023544.3	(Gourbeyre et al., 2015)

Caspase 3 (CASP3)	F	ATAATAAGAACTTTGATAAAAAAT		
	R	ACCGGAATG	NM_214131.1	present study
		TCCACATCTGTACCAGATCGACA		
		T		
Oxidative stress induced growth inhibitor 1 (OSGIN)	F	CATTGGCAACGGTCCC	ENSSSCT00000066181.2	present study
	R	TATAGCCTGAGAGCAGGTAG		
NADH dehydrogenase subunit 2 (MT-ND2)	F	GCCTCCACTATCAGGATTTATG	ENSSSCT00000019664.4	present study
	R	GGAGTAGGCTAGTCGTATGT		
Mitochondrially encoded cytochrome c oxidase III (MT-CO3)	F	GCACTAGGCGTATACTTCAC	ENSSSCT00000019677.1	present study
	R	CCCTGTAGCCACAAAGAAA		
Mitochondrially encoded cytochrome c oxidase I (MT-CO1)	F	CTTCCACCATCCTTCTATTAC	ENSSSCT00000019670.1	present study
	R	GGGCTAAGTTTCCAGCTAAA		
ATP synthase F0 subunit 6 (MT-ATP6)	F	CACCCACCACAACTATC	ENSSSCT00070061678.1	present study
	R	GTGTTCTTGTGGTAGAAA		
Cytochrome b (MT-CYB)	F	TAGGAGACCCAGACAACTAC	ENSSSCT00000019689.3	present study
	R	GTAGAATAGCGTAGGCGAATAA		
Mitochondrially Encoded NADH Dehydrogenase 1 (MT-ND1)	F	CATACCCACGATTCCGATAC	ENSSSCT00000019660.4	present study
	R	AGGGAGTGAGATGTGTCATA		
RNA, Ribosomal 45S Cluster 2 (MT-RNR2)	F	TCCAGGTCGGTTTCTATCT	NC_026992.1	present study
	R	GGTAGGTCCTTTCTCTTG		
Hypoxanthine phosphoribosyltransferase 1 (HPRT1)	F	CTGACCTGCTGGATTACA	ENSSSCT00065066899.1	present study
	R	CCCGTTGACTGGTCATTA		
Topoisomerase (DNA) II beta (TOP2B)	F	AAGGGCGAGAGGTCAATGAT	ENSSSCT00015080370.1	(Park et al., 2015)
	R	ACATCTTCTCGTTCTTGCGC		
Hydroxymethylbilane synthase (HMBS)	F	AGGATGGGCAACTCTACCTG	ENSSSCT00000060506.2	(Wang et al., 2018)
	R	GATGGTGGCCTGCATAGTCT		

157 2.7. Statistical analysis

158 Performance and feed conversion data were evaluated in the software R-3.5. Boxplots were used
159 to visually inspect the data distribution, variability, and outliers. The model assumptions (normality,
160 homoscedasticity, and independence) were inspected via the residual plots. Mixed Effects Models
161 and Generalized Least Squares with subsequent multiple comparisons were used as indicated to test
162 for differences between groups. The significance level was defined as $p < 0.05$, and $p \geq 0.05$ to < 0.10
163 were considered as tendencies. All histology statistical analyses were performed using GraphPad
164 Prism 9.0.2 software (GraphPad Software Inc., La Jolla, USA). Data were expressed as mean \pm SEM
165 (standard error of the mean) for normal distribution or median and interquartile range when data were
166 not normally distributed. They were submitted to statistical analysis, using normality (Shapiro–Wilk)
167 and homogeneity (Bartlett) tests. Significant differences were assessed by one-way ANOVA followed
168 by Tukey’s test for parametric data and by Kruskal-Wallis test followed by Dunn’s test for non-
169 parametric data. Statistical analysis for all other results were performed by GraphPad Prism 7.05
170 (GraphPad Software Inc., La Jolla, USA). Values were analyzed for normality (Shapiro–Wilk) as

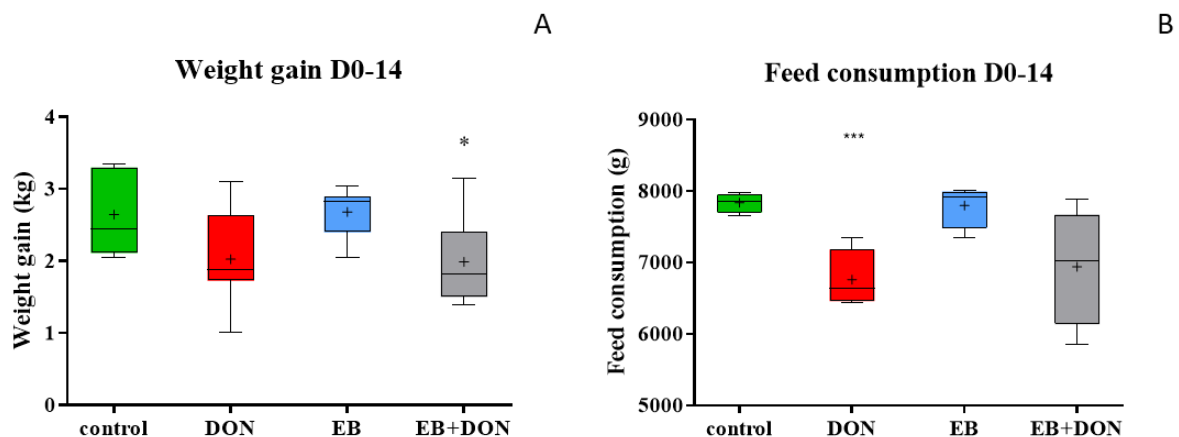
171 well as homogeneity of variance (Levene Statistics). Normally distributed homogeneous data were
 172 analyzed by one-way ANOVA (Dunnett's multiple comparison test). If normal distribution was
 173 violated, the Kruskal-Wallis Test was used. Outliers were identified by Grubbs' test and removed, if
 174 applicable.

175 3. Results

176 3.1. Growth performance

177 During the entire study period, the mean body weight gain significantly differed between the
 178 groups (Mixed Effects Model, $p = 0.006$). Compared to the control, the weight gain was significantly
 179 lower in the EB+DON group (Mixed Effects Model, multiple comparisons, $p = 0.039$) and tended to
 180 be lower in the DON group ($p = 0.062$) (Figure 1A). The DON group did differ significantly in the
 181 feed consumption per cage during the entire study period if compared to the control group ($p = 0.001$).
 182 In the EB-DON group, a slight decrease in feed consumption was determined as well (by trend, $p =$
 183 0.076) (Figure 1B).

184



185 **Figure 1.** Boxplot of the body weight gain of piglets (A; $n = 8$) and feed consumption of two piglets
 186 per cage (B; $n = 4$) during a time period of D0-14. The box represents the interquartile range (IQR:
 187 50 % of data are found between Q1 to Q3). A line within the box indicates the median. The
 188 lines/whiskers outside the box extend by $Q1 - 1.5 \times IQR$ (25 % of data) and $Q3 + 1.5 \times IQR$ (25 %
 189 of data). The + indicates the mean of the group. Significant differences to the control are indicated
 190 with * $p \leq 0.05$, ** $p \leq 0.01$, *** $p \leq 0.001$.
 191

192 3.2. Plasma parameters

193 Plasma biochemical parameters revealing liver injury (activities of alkaline phosphatase, ALP;
194 alanine aminotransferase, ALT; aspartate aminotransferase, AST), liver function (concentrations of
195 albumin and total protein), lipid profile, kidney function and metabolism were assessed at D7 and
196 D14 (Table 3).

197 On D7, a significant increase in albumin concentration was seen in piglets that received either
198 of the EB-containing diets from 445.1 ± 31.4 and 453.4 ± 26.9 $\mu\text{mol/L}$, respectively compared to
199 404.6 ± 24.7 $\mu\text{mol/L}$ in the control. Additionally, total protein was higher in the EB group (55.9 ± 3.0
200 g/L) compared to the control (50.3 ± 3.9 g/L). Plasma calcium was slightly, but significantly higher
201 in piglets that received the EB+DON diet (2.46 ± 0.12 mmol/L) compared to the control (2.30 ± 0.09
202 mmol/L).

203 On D14, the liver enzymes ALP, AST and ALT were affected by the mycotoxin-contaminated
204 diets (Table 3). The most remarkable results were observed in the EB+DON group with a decrease
205 of in 21 - 30% for each of the three enzymes compared to the control group.

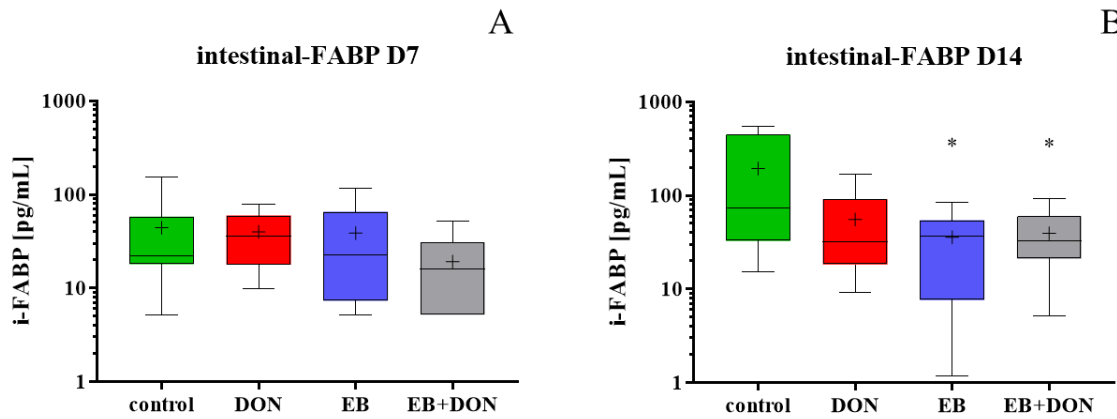
Table 3. Plasma biochemical analysis at D7 (left side) and D14 (right side)

	Animal groups (time and diet)							
	Control D7	DON D7	EB D7	EB+DON D7	Control D14	DON D14	EB D14	EB+DON D14
Alkaline phosphatase (U/L)	313.8±91.5	231.2±51.4	238.6±68.5	236.5±86.7	410.1±91.5	293.6±51.0*	326.3±94.8	288.6±95.7*
Alanine aminotransferase (U/L)	32.6±5.3	31.6±4.3	31.4±7.1	31±6.8	57.8±9.4	49.4±8.35	45.6±5.9*	45.8±9.4*
Aspartate aminotransferase (U/L)	33.1±8.5	34.8±5.9	31.8±7.6	28.3±5.3	49.3±7.4	46.8±6.0	40.8±6.0	38.6±5.7*
Albumin (µmol/L)	404.6±24.7	437.5±38.2	445.1±31.4*	453.4±26.9*	430±42.7	453.4±18.0	443.2±14.6	461.4±28.2
Total proteins (g/L)	50.3±3.9	52.2±3.3	55.9±3.0*	52.5±2.3	48.4±3.6	48.9±3.2	48.8±2.3	48.6±2.1
Urea (mmol/L)	0.95±0.21	1.90±1.27	1.91±1.14	1.74±0.68	0.82±0.173	0.86±0.28	0.55±0.12	1.06±0.3
Glucose PAP (mmol/L)	6.05±0.53	5.75±0.39	5.96±0.49	5.66±0.33	6.43±0.46	6.20±0.58	6.45±0.74	5.93±0.48
Cholesterol (mmol/L)	1.81±0.24	1.84±0.34	1.97±0.28	1.96±0.29	2.05±0.27	2.01±0.25	1.92±0.41	1.95±0.27
HDL (mmol/L)	0.97±0.13	0.94±0.14	1.06±0.14	1.05±0.14	1.15±0.11	1.13±0.12	1.08±0.23	1.13±0.17
LDL (mmol/L)	0.65±0.12	0.71±0.20	0.73±0.13	0.71±0.15	0.79±0.14	0.77±0.18	0.74±0.16	0.71±0.10
Triglycerides (mmol/L)	0.47±0.05	0.43±0.08	0.70±0.36	0.49±0.10	0.4±0.10	0.40±0.08	0.35±0.06	0.48±0.14
Creatinine (µmol/L)	117.9±19.2	124.1±18.8	118.7±12.8	110.3±14.7	120.8±16.2	123.4±24.9	113.7±10.1	120.1±16.3
Uric acid (µmol/L)	13.9±7.5	15.0±6.8	15.9±8.8	17.4±6.5	19.4±14.7	18.6±13.6	18.9±10.9	17.5±9.2
Calcium (mmol/L)	2.30±0.09	2.36±0.05	2.39±0.07	2.46±0.12*	2.64±0.16	2.64±0.11	2.59±0.13	2.55±0.13
Phosphorus (mmol/L)	2.24±0.10	2.22±0.19	2.32±0.15	2.39±0.20	2.77±0.16	2.84±0.17	2.80±0.22	2.85±0.24

Values are means ± SD. Comparison between control group and animals exposed to contaminated diets. n=8; Significant differences are indicated with * $p \leq 0.05$ (marked in red and italics).

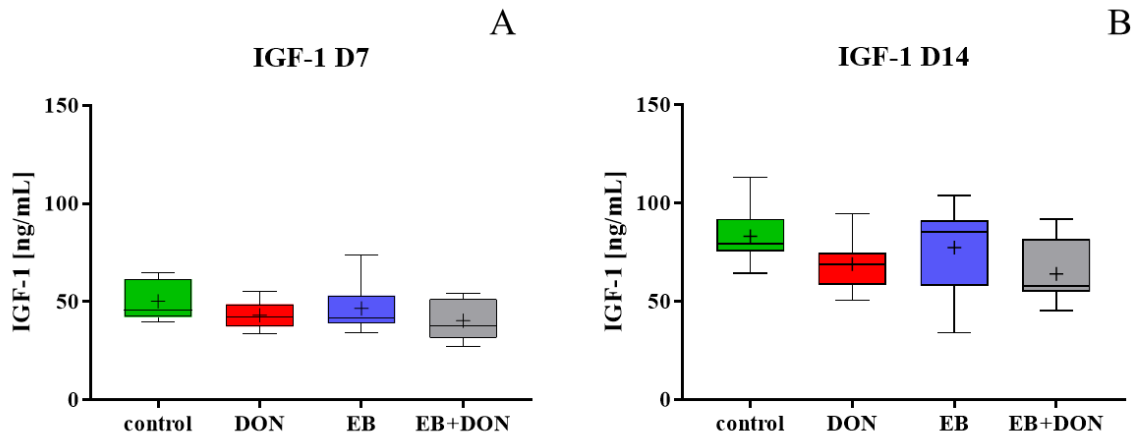
239 Potential biomarkers for gut health and growth, such as the intestinal-fatty acid binding protein (i-
240 FABP), the tight junction protein regulator zonulin (ZON) and the insulin-like growth factor 1 (IGF-1)
241 were analyzed in heparin plasma samples taken on D7 and D14 (Figures 2 – 4).

242 As shown in Figure 2, the i-FABP concentration was significantly decreased in the EB group ($p =$
243 0.028) and the EB+DON group ($p = 0.032$) on D14 compared to the control. This protein was also
244 reduced in the DON-fed group, but not significantly ($p = 0.059$). IGF-1 protein, which might be a
245 parameter for growth reduction, was not significantly affected by the different diets on any sampling
246 day. However, p -value between control and EB+DON group was 0.092 on D14, which could indicate a
247 declining trend. Likewise, a decrease of in IGF-1 mean values in the DON group on both days is evident,
248 from 50.1 ng/mL (control) to 43.1 ng/mL (D7) and from 83.1 ng/mL (control) to 68.9 ng/mL,
249 respectively (Figure 3). ZON, described as permeability marker in chronic bowel diseases, did not
250 vary between the groups, although a decreasing trend was seen in the DON group ($p = 0.099$) on D14
251 (Figure 4).



252

Figure 2. Intestinal-fatty acid binding protein (pg/mL) measured in heparin plasma samples from D7 (A) and D14 (B); n = 8; Significant differences are indicated with * $p \leq 0.05$.



253

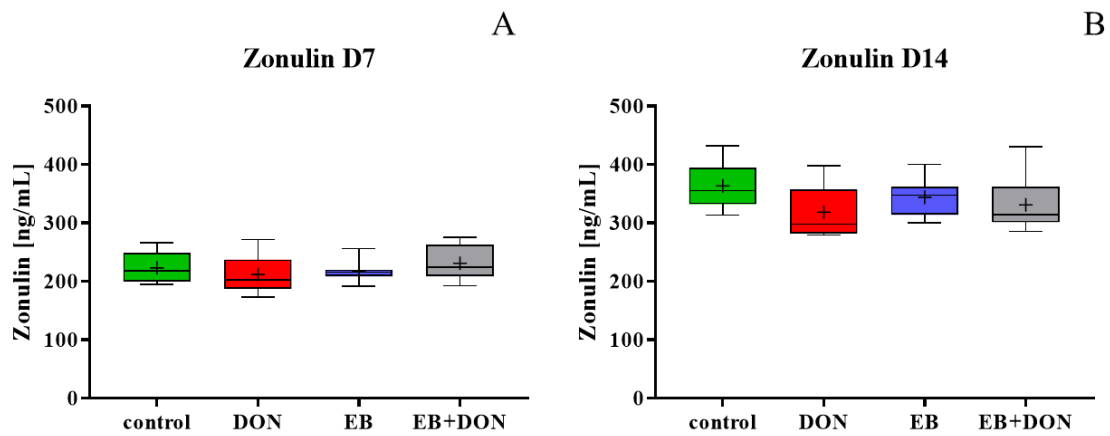
Figure 3. IGF-1 concentration (ng/mL) measured in heparin plasma samples from D7 (A) and D14 (B); n = 8.

254

255

256

257



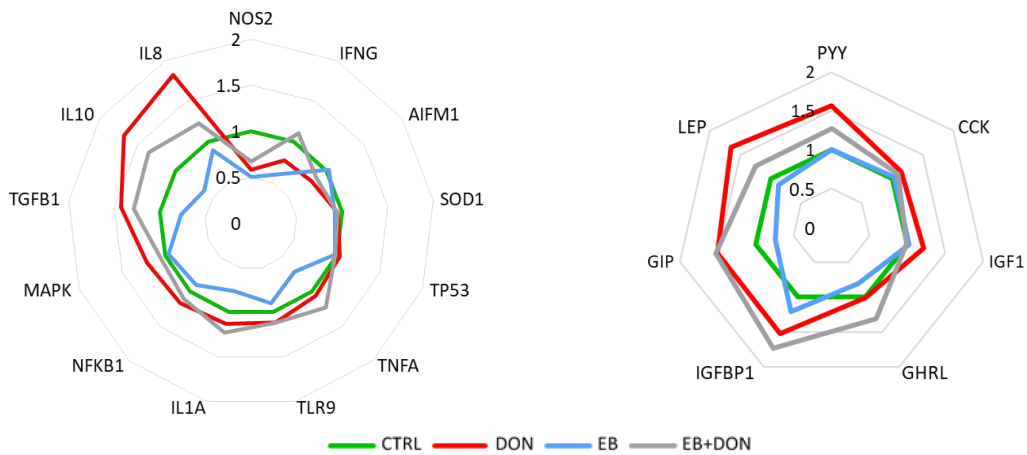
258

Figure 4. Zonulin concentration (ng/mL) measured in heparin plasma samples from D7 (A) and D14 (B); n = 8.

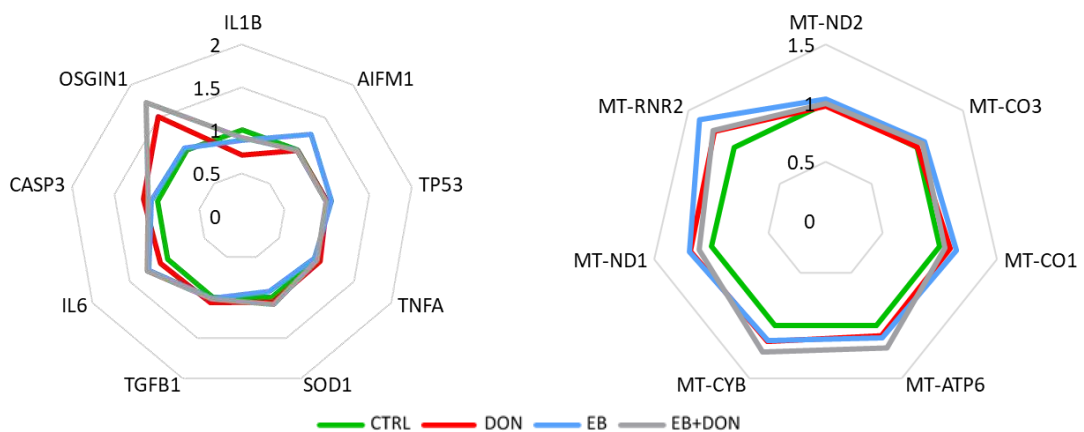
259 3.3. mRNA expression in jejunum and liver tissue

260 The mRNA expression of genes related to immune response (NOS2, IFNG, AIFM1, SOD1, TP53,
 261 TNFA, TLR9, IL1A, NFKB1, MAPK, TGFB1, IL10, IL8) as well as to satiety and growth (PYY, CCK,
 262 IGF1, GHRL, IGFBP1, GIP, LEP) was analyzed in the jejunum. The results are presented in Figure 5.
 263 Expression profile of most genes showed a slight, but not significant upregulation in the DON group or
 264 the EB+DON group.

265 In the liver tissue, the expression of genes coding for inflammatory mediators (IL1B, AIFM1, TP53,
 266 TNFA, SOD1, TGFB1, IL6, CASP3, OSGIN1) and of mitochondrial genes (MT-ND2, MT-CO3, MT-
 267 CO1, MT-ATP6, MT-CYB, MT-ND1, MT-RNR2) was affected but to a lesser extent (Figure 6).
 268 Oxidative Stress Induced Growth Inhibitor 1 (OSGIN1) tended to be up-regulated in the two groups
 269 receiving DON.



270 **Figure 5.** mRNA expression of selected genes in the jejunum of animals fed a control or contaminated
 271 diet. Mean values of gene expression levels for the control group are set to 1.



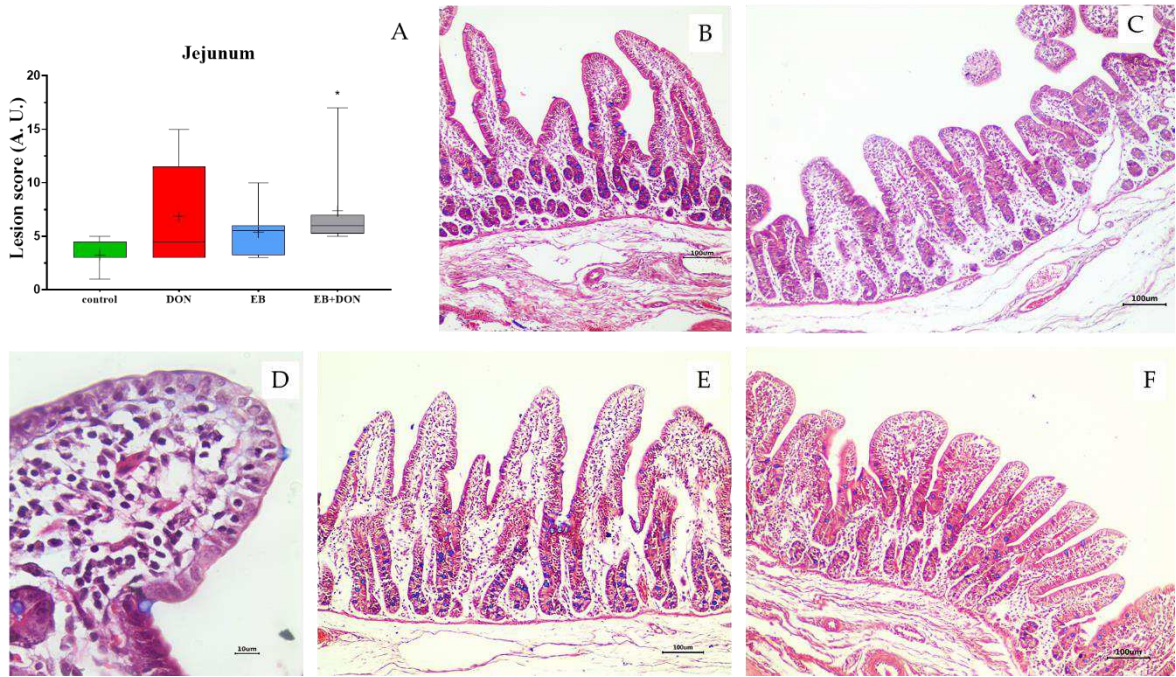
272 **Figure 6.** mRNA expression of selected genes in the liver of animals fed a control or contaminated
 273 diet. Mean values of gene expression levels for the control group are set to 1.

274 3.4. *Histology*

275 In jejunum, a significant increase ($p = 0.007$) in the lesion score was detected in animals fed the
276 multi-toxin contaminated diet (EB+DON) compared to the control (Figure 7A). Control animals showed
277 well-delineated villi lined by columnar enterocytes (Figure 7B), while changes such as lymphatic vessel
278 dilation and interstitial edema with mild intensity were also observed in these animals. Animals fed the
279 DON-contaminated diet showed villi atrophy, as well as flattening and cytoplasmic vacuolation of
280 enterocytes (Figure 7C). In animals that received the EB diet, cytoplasmic vacuolation of enterocytes
281 was the most frequently observed change (Figure 7D). Animals receiving the EB+DON-contaminated
282 diet showed mainly villi atrophy and vacuolation of enterocytes (Figure 7E). A significant decrease in
283 the number of goblet cells in the jejunum was observed in DON-fed animals ($p = 0.029$, Figure 8A).
284 Furthermore, villi height was decreased in the DON- ($p = 0.008$) and EB+DON-fed ($p = 0.022$) groups
285 (Figure 8B).

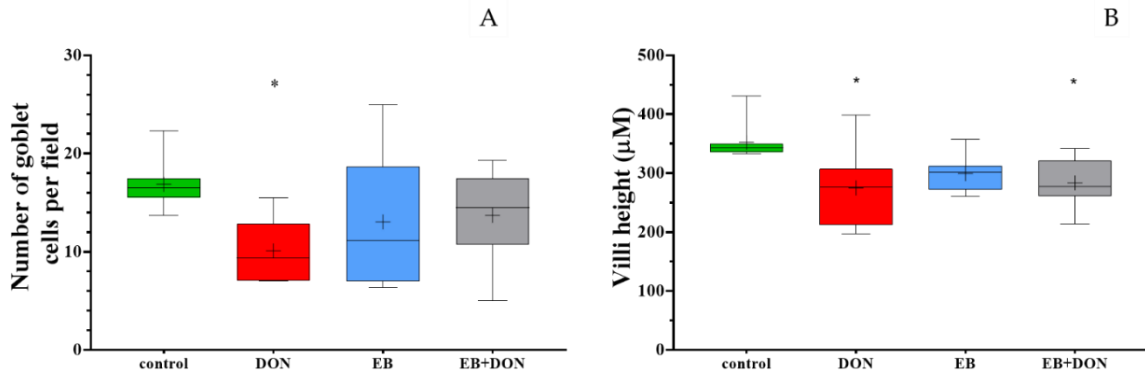
286 Colon samples were analyzed, however, no significant difference was observed in the lesion score
287 between treatments (Figure 9A). The control group showed a normal histological structure (Figure 9B).
288 The main histological findings in pigs fed the mycotoxin-contaminated diets were edema of the lamina
289 propria, flattening and cytoplasmic vacuolation of apical enterocytes as well as focal areas of enterocytes
290 necrosis (Figure 9C-E).

291

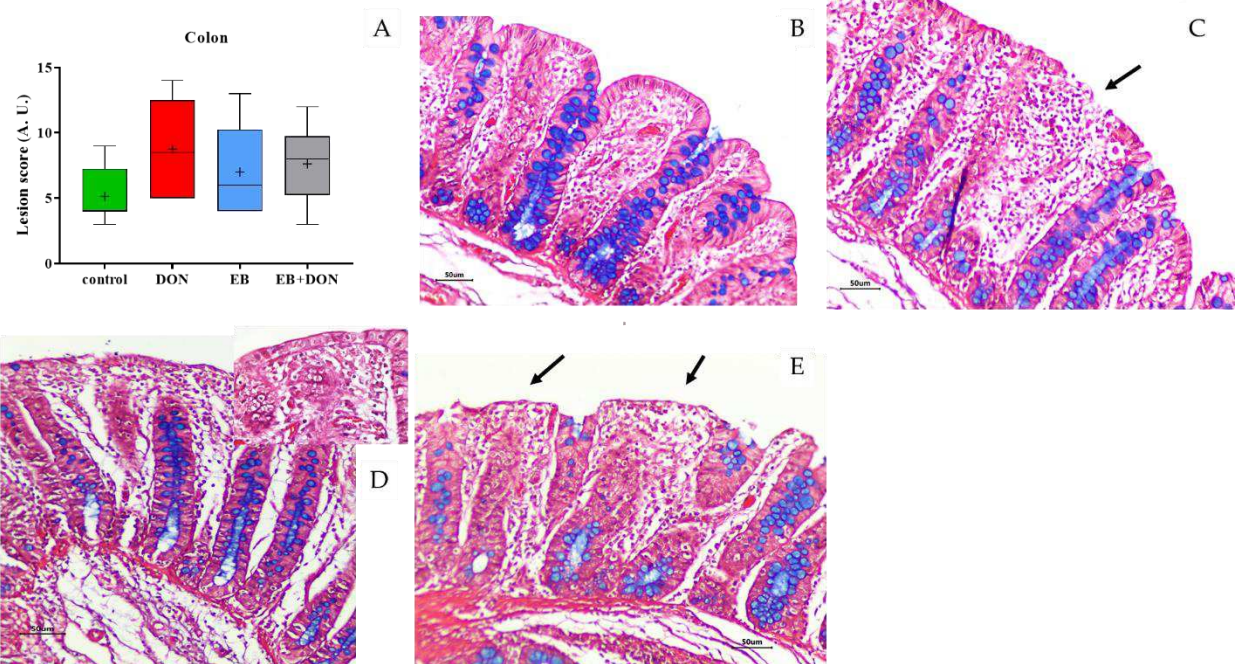


292
 293 **Figure 7.** Lesion score of jejunum tissue (A, n = 8) and histological images of experimental groups.
 294 Control (B) showing a normal aspect of villi; DON (C) with villi atrophy and edema of lamina propria;
 295 EB (D) showing enterocyte flattening; EB+DON showing edema of lamina propria (E) and villi atrophy
 296 (F). Alcian blue staining. Scale bar 100 μ m (B, C, E, F), 10 μ m (D). Significant differences are indicated
 297 with * $p \leq 0.05$.

298



299
 300 **Figure 8.** Number of goblet cells per field (A) and villi height (B) in the jejunum (n = 8). Significant
 301 differences are indicated with * $p \leq 0.05$.



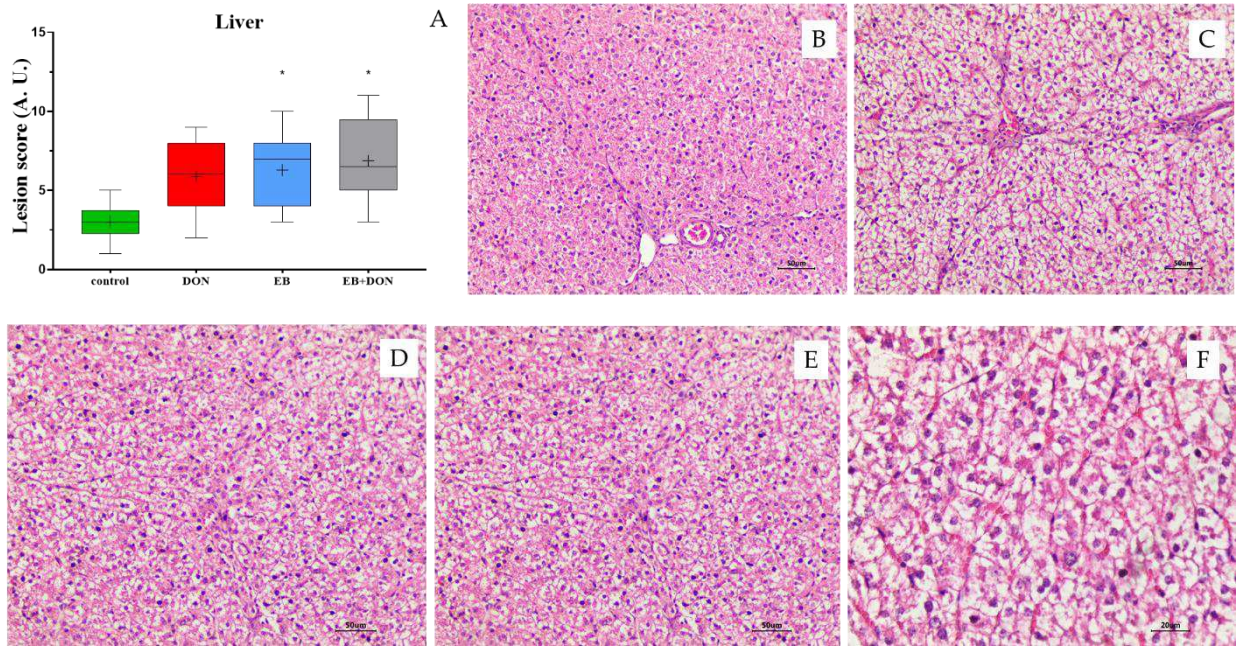
302
303
304
305
306

Figure 9. Lesion score of colon tissue (A). Control: Normal aspect of colon (B). DON: Edema of the lamina propria, focal necrosis of enterocytes (arrow) (C). EB: Edema of lamina propria, flattening of enterocytes. Insert: Flattening of enterocytes (D). EB+DON: Multifocal flattening of enterocytes and necrosis (arrows) (E). Alcian blue staining. Scale bar 50 μm.

307
308

In the liver, animals fed EB and EB+DON diets showed a significant increase ($p = 0.043$ and $p = 0.011$, respectively) in histological changes when compared to the control (Figure 10A). Control animals showed well-organized hepatocytes forming trabeculae, while mild cytoplasmic vacuolation of hepatocytes was frequently detected in this group (Figure 10B). Animals receiving the contaminated diets showed mainly moderate to severe vacuolation of hepatocytes and megalocytosis (Figure 10C-F). Apoptosis of hepatocytes and focal necrosis were also detected in DON and EB+DON groups (Figure 10C+E).

309
310
311
312
313
314



315
 316 **Figure 10.** Lesion score of liver tissue (A) and histological images of control (B) showing a normal
 317 aspect of liver; DON (C) showing diffuse and severe vacuolar degeneration of hepatocytes; EB (D)
 318 showing moderate vacuolar degeneration of hepatocytes; EB+DON showing moderate vacuolar
 319 degeneration of hepatocytes (E) and megalocytosis (F). Hematoxylin and Eosin (H&E) staining. Scale
 320 bar 100 μm (B-E), 20 μm (F). Significant differences are indicated with * $p \leq 0.05$.

321

322

323

324

325

326

A significant increase in histological changes ($p = 0.022$) was detected in lymph nodes of animals exposed to DON in comparison to control. Lymph nodes of control animals presented a histological aspect within normal limits. In pigs fed the DON or EB+DON contaminated diets, the main findings were lymphoid depletion and apoptosis, while in the EB group lymphoid hyperplasia was the most frequent change (Figure 11).

327

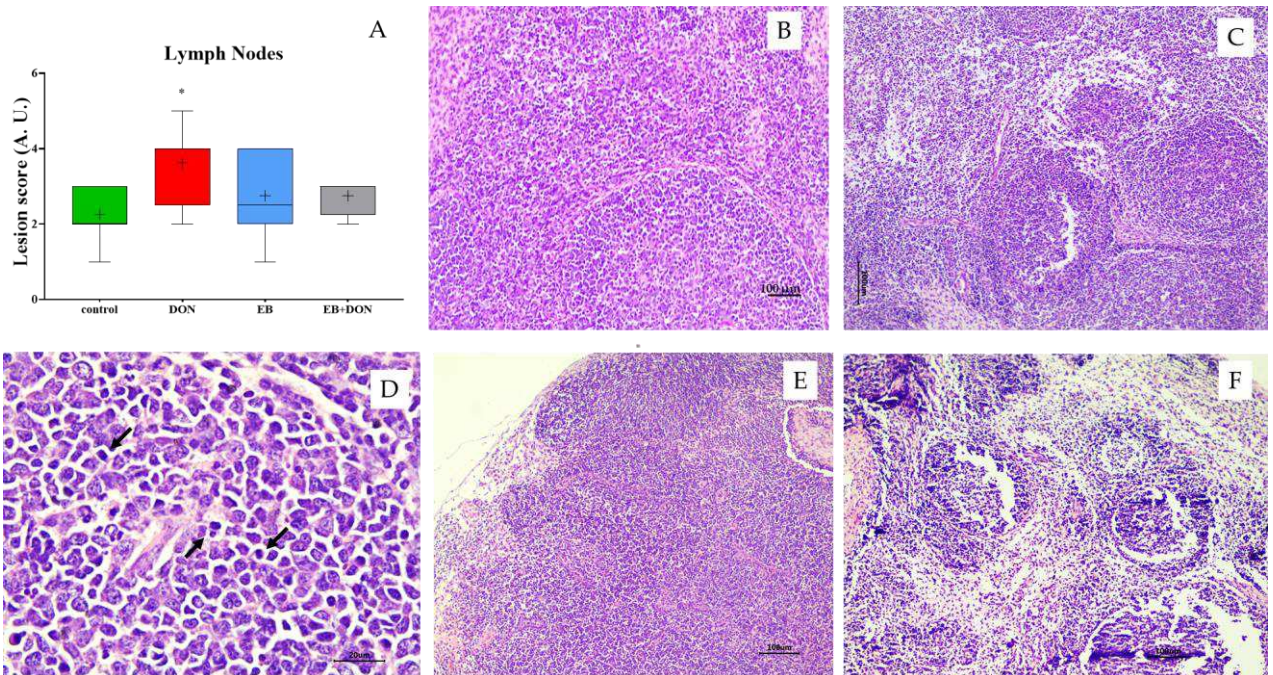


Figure 11. Lesion score of lymph nodes tissue (A) and histological images of control (B) showing a normal aspect of lymph node; DON showing lymphoid depletion (C) and lymphocyte apoptosis (D); EB (E) showing lymphoid hyperplasia; EB+DON (F) showing severe lymphoid depletion. Hematoxylin and Eosin (H&E) staining. Scale bar 100 µm (B, C, E and F), 20 µm (D). Significant differences are indicated with * $p \leq 0.05$.

328 3.5. Metagenomic data of the fecal microbiome

329 Mycotoxin applications substantially impacted the diversity and structure of fecal microbiota in
 330 weaned piglets. Shotgun metagenomics of 32 collected fecal samples using the MK1C platform
 331 generated over 11 million 1D reads with the quality score > 8 with a mean number of about 300 k reads
 332 per sample. Taxonomic profiling of the fecal samples in terms of the most abundant microbial phyla and
 333 species is shown in Figure 12. In total, 1,945 different microbial species were observed, of which
 334 Firmicutes, followed by Ascomycota and Proteobacteria, were the most dominant members of the
 335 piglet's fecal microbiota. Interestingly, the phyla Actinobacteria was more dominant in the EB group
 336 which goes along with a reduction in Ascomycota (Figure 12A). In regard to the most abundant species,
 337 *Aureobasidium namibiae* completely disappeared in the EB and EB+DON groups, while the
 338 *Mycobacterium branderi* is found in a remarkable amount in the EB group, but not in the others (Figure
 339 12B).

340

341

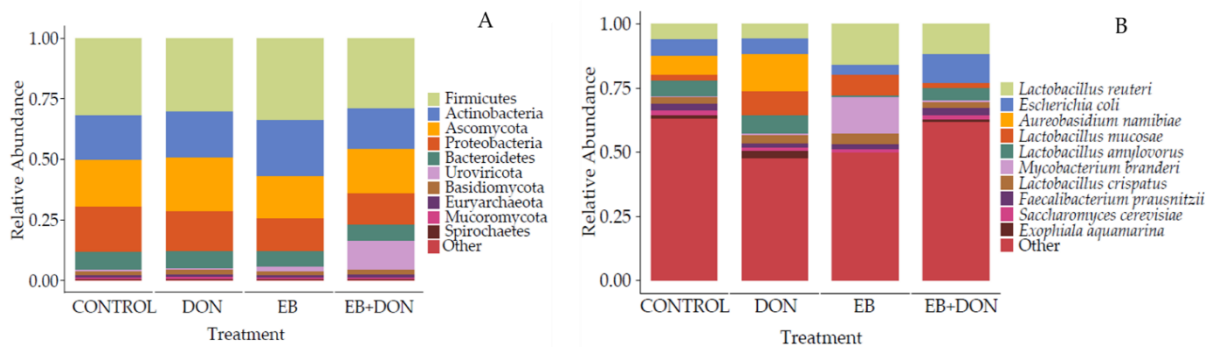


Figure 12. Relative abundance of 10 most abundant microbial phyla (A) and microbial species (B) found in the fecal microbiome of pigs fed with the different diets.

342

343

344

345

346

347

348

349

350

351

352

353

354

355

356

Permutational Multivariate Analysis of Variance (PERMANOVA) statistical analysis calculated on Bray–Curtis dissimilarity matrices from Kraken2 and Bracken data showed that the difference in the treatment groups of the piglets explained 14% of the variation in fecal microbiota profiles of the piglets in the current study ($R^2 = 0.13351$, $p = 0.005$), showing a significant impact of the applied mycotoxins on the structure and community membership of the piglet’s fecal microbiota. Furthermore, pairwise post-hoc comparisons (<https://rdrr.io/github/GuillemSalazar/-EcolUtils/man/adonis.pair.html>) showed that among different groups, fecal microbiota of the piglets in the EB group showed the most significant difference in the profiles of the relative abundance of taxa compared to the animals in the control group (control vs EB, $R^2 = 0.10$, FDR-corrected $p = 0.005$), followed by DON (control vs DON, $R^2 = 0.072$, FDR-corrected $p = 0.02$) and EB+DON (control vs EBD, $R^2 = 0.068$, FDR-corrected $p = 0.02$). In line with the observation from the beta diversity analysis, a significant effect of mycotoxins contamination on the alpha diversity indices was observed, with the EB+DON resulted in a significantly lower microbial diversity (measured by Shannon index, $p = 0.004$ and 0.088 , respectively) and richness (measured by Observed index, $p = 0.035$ for EB) in the fecal microbiota of the piglets (Figure 13).

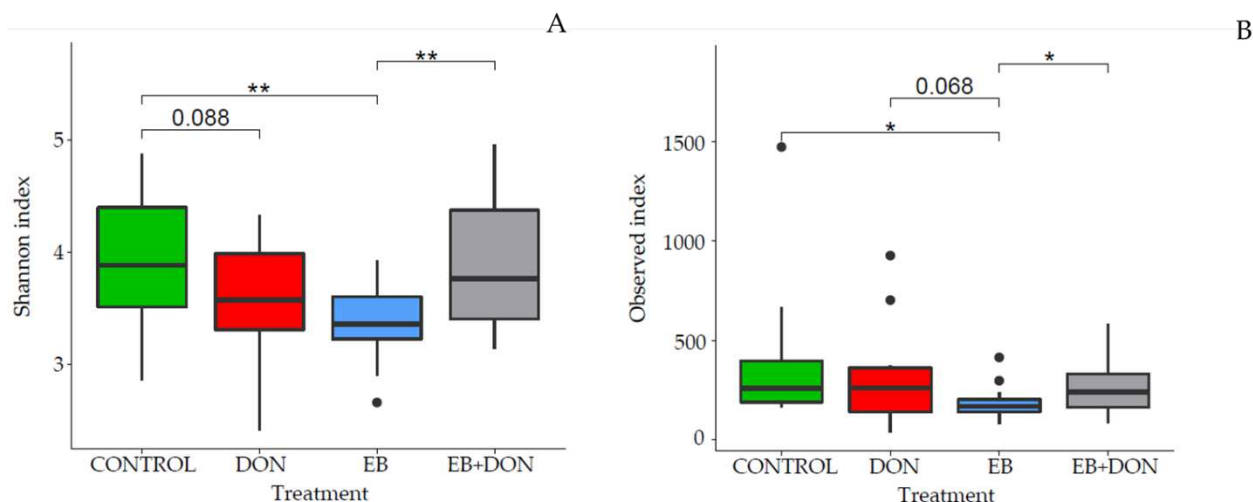


Figure 13 Alpha diversity analysis of the taxa in pig fecal microbiome (**A**: Shannon index, **B**: observed index); $n = 8$; * $p \leq 0.05$, ** $p \leq 0.01$, *** $p \leq 0.001$

357

358

359

4. Discussion

360

361

362

363

364

365

366

367

368

369

370

371

372

373

374

375

376

In this study, we investigated, for the first time the effects of a diet contaminated with the emerging mycotoxins enniatin B, enniatin B1 and beauvericin (EB) on piglets. As enniatins (ENNs) and BEA frequently co-occur with the regulated *Fusarium* mycotoxin DON (Kovalsky et al., 2016; Lindblad et al., 2013), we included a combinatory group to determine possible combined effects. We used a BEA concentration of 2570 $\mu\text{g}/\text{kg}$ and 3578 $\mu\text{g}/\text{kg}$, as well as a joint ENN B and ENN B1 concentration of 1345 $\mu\text{g}/\text{kg}$ and 1830 $\mu\text{g}/\text{kg}$ in the EB and EB+DON group, respectively. In the field, BEA is found in rather low concentrations (~ 100 $\mu\text{g}/\text{kg}$), however, also highly contamination up to 26300 $\mu\text{g}/\text{kg}$ were already determined in specific feed stuff and countries. Regarding ENN B and B1, the usual contamination is higher with detected maximum levels of 81100 $\mu\text{g}/\text{kg}$ and 795000 $\mu\text{g}/\text{kg}$, respectively (Fraeyman et al., 2017). However, concentrations are difficult to compare as many variables have to be considered such as feed stuff, country region, detection analytical method, sampling as well as weather and storage conditions.

As a first indicator, we determined weight gain and feed consumption of the animals. In the 14 experimental days, the weight gain of 2.64 ± 0.56 kg in the control group was significantly decreased to only 1.99 ± 0.60 kg in the EB+DON group but remained constant in the EB group with 2.68 ± 0.34 kg. As with 2.03 ± 0.66 kg the weight gain in the DON group was also low (by trend, Figure 1A), the observed negative effect of EB+DON derived due to an enhanced intake of DON through the gut barrier,

377 triggered by the ionophoric properties of the emerging mycotoxins (Tonshin et al., 2010). Also *in vitro*
378 experiments showed synergistic effects of ENNs with DON on the gut integrity in intestinal porcine
379 epithelial cells (Springler et al., 2016). The direct reason might be the reduced feed consumption in both
380 DON groups. Animals which received the DON-contaminated diet ate 6763 ± 404 g of feed on average;
381 EB+DON-fed animals only 6943 ± 832 g (Figure 1B). A significant difference was detected only for
382 the DON group compared to the control (7839 ± 135 g). A lower consumption of DON-contaminated
383 feed has been described by several other scientists (FAO/WHO, 2001; Prelusky, 1997; Rotter et al.,
384 1996; Trenholm et al., 1994) and is believed to be a consequence of the impact of DON on satiety
385 hormones, such as peptide YY (PYY) and cholecystokinin (CCK) (Flannery et al., 2012; Knutsen et al.,
386 2017). However, only a slight, but not statistically significant up-regulation of the expression of genes
387 coding for satiety and growth hormones was observed (Figure 6), which could be a matter of sampling
388 time point (Taylor et al., 2019). One of the most remarkable effects of DON is the anorexia and also
389 emesis that are elicited by the direct action on the central nervous system and by the indirect action of
390 enteroendocrine cells that secretes several gut hormones (Terciolo et al., 2018).

391 In general, due to the inter-individual variability and the limited number of animals in this trial, the
392 number of genes whose expression was significantly regulated by the ingestion of a mycotoxin-
393 contaminated diet was limited. However, the tendency of some genes to be upregulated was consistent
394 with previously described effects of DON. Increased production of cytokines upon DON exposure has
395 already been demonstrated in human cells (Maresca et al., 2008), in porcine intestinal cells (Cano et al.,
396 2013), in jejunal explants from pigs (Pierron et al., 2016b) as well as *in vivo* in pigs and mice (Azcona-
397 Olivera et al., 1995; Bracarense et al., 2012, 2020; Pierron et al., 2018). In the present study, a 2-weeks-
398 week exposure to ~ 2 ppm DON showed a tendency to elicit a pro-inflammatory response. As
399 zearalenone (ZEN) concentration with 342 and 263 $\mu\text{g}/\text{kg}$, respectively, in both DON groups was quite
400 high, an impact of ZEN on inflammation mediators could be possible (Pistol et al., 2015). However,
401 clinical effects on estrogenic parameters such as an estrogenic effect increased, swollen vulva in female
402 pigs as described for ZEN were not detected (Gajecki, 2002). Since ZEN is not known to elicit any
403 effect on our analyzed parameters, we assume that our findings are mainly caused by EB and/or DON.
404 Most interestingly, co-exposure to EB seemed to reduce the inflammatory potential of DON and led to

405 a down-regulation of cytokines (Figure 6), possibly due to their ionophoric properties disrupting several
406 functions of cells (EFSA, 2014). Antagonistic cytotoxic effects of DON and EB have already been
407 described in IPEC-1 cells (Khoshal et al., 2019). Our results, both on feed consumption and growth and
408 on mRNA expression, corroborate the indirect action of hormones on the anorexic mechanism of DON
409 and, again, the association with EB partially antagonized this effect. Recent studies have highlighted the
410 involvement of mitochondrial genes in the acute toxicity of DON (Wang et al., 2021), BEA and ENNs
411 (Alonso-Garrido et al., 2018; Escrivá et al., 2018, 2019) in cultured cells. Our experiment indicates that
412 the expression of these genes was also slightly exacerbated upon *in vivo* chronic exposure to the toxins
413 (Figure 6).

414 Besides tissue samples from different organs, we also took plasma samples at the middle and at the end
415 of the trial. Increased concentrations of albumin and total proteins were observed in pigs exposed to EB
416 at D7 (Table 3). Co-exposure to EB and DON showed a similar effect on albumin but not on total
417 proteins (Table 3). Albumin has a turnover of about 25 days and there is a relative consensus in the
418 literature that hyperalbuminemia, an increase of in the albumin concentration in serum is mainly due to
419 dehydration (Busher, 1990; Levitt and Levitt, 2016). Increased serum albumin levels in our trial could
420 be due to the ionophoric effect of ENNs and BEA on cell membranes leading to a disturbance of osmosis.
421 The lack of increase of in total protein concentration in the EB+DON group could be related to the well-
422 characterized inhibitory effect of DON on protein synthesis after its binding to the ribosome (Payros et
423 al., 2016). The increase in albumin level in the EB+DON group accompanied an increase of in
424 circulating calcium (Table 3). The lack of an increase in calcium in the EB group could be due to the
425 fact that BEA increases cytoplasmic calcium concentration, thereby reducing the amount of circulating
426 calcium (Chen et al., 2006). These effects seem to be temporary since no differences between the groups
427 were seen at D14.

428 At D14, the ALP concentration was decreased in DON-receiving groups (Table 3), although usually
429 an increase in liver enzyme activity is associated with liver damage (Giannini et al., 2005). An
430 explanation could be that enzymes increase rapidly after the first days of exposure and on D14, the
431 activity has already dropped to a lower level. A positive correlation between food consumption and
432 serum ALP was reported previously (Amacher, 2002). So, the decreased feed consumption may have

433 led to a reduction in serum ALP in this study. Another reason could be a zinc deficiency elicited by an
434 inadequate absorption and which correlates with a low ALP (Cho et al., 2007). ALP activity is a good
435 marker of intestinal function. Indeed, it was shown to be higher in rat intestinal mucosa than in liver
436 (Ramaiah, 2007). ALP participates in the metabolism of vitamin B6 which is a co-factor for both ALT
437 and AST (Ono et al., 1995). In fact, both groups exhibiting ALP reduction (DON, EB-DON) also
438 presented reductions in ALT and AST activity (Table 3). (EB-DON). Although an increase in liver
439 enzyme activity is associated with liver injury, also reductions on ALT and AST activities have been
440 seen in cases of chronic liver diseases usually associated with other pre-existent condition such as kidney
441 disease (Ono et al., 1995).

442 We additionally analyzed the effects of mycotoxin-contaminated diets on proteins in porcine
443 plasma associated with growth or gut barrier functionality, i.e. i-FABP, IGF-1 and ZON, in the porcine
444 plasma. IGF-1 is known to correlate with growth performance and a reduction of this biomarker has
445 been already described upon DON exposure (Pestka, 2010; Voss, 2010). However, in our study, no
446 significant impact of mycotoxin-contaminated diets on IGF-1 in serum was seen (Figure 4), although
447 trends were determined in the DON group on both sampling days as well as in the EB+DON group on
448 D14. Additionally, the IGF-1 mRNA expression in jejunum was slightly increased (Figure 5), which is
449 in accordance with a previous study in mice, in which a higher gene expression in the liver was observed,
450 but circulating IGF-1 was decreased (Amuzie and Pestka, 2009).

451 ZON, a widely-discussed biomarker for mucosal barrier integrity (Fasano, 2020), has been
452 described in humans suffering from inflammatory bowel disease (Caviglia et al., 2018). In DON-fed
453 piglets a significant increase in ZON was associated with the damaging effect of this mycotoxin on the
454 gut barrier (Wang et al., 2018). In contrast to our expectations, we observed a slightly lower ZON level
455 in the DON group (318.7 ng/mL) compared to the control group (363.6 ng/mL). This has also been
456 shown in another study in patients with chronic kidney diseases and the authors of this study
457 hypothesized that low ZON concentration is caused by impaired defensive mechanisms due to a
458 suppressed immune system (Lukaszyk et al., 2018).

459 As another biomarker for intestinal permeability, we analyzed i-FABP, which is considered to be
460 released into the blood stream from damaged mucosal tissue (Funaoka et al., 2010). Again, we detected

461 a significant decrease of in i-FABP in both EB-containing diets on D14, instead of the expected increase
462 (Figure 2). However, Lau *et al.* also reported an unexpected decrease inof i-FABP plasma levels with a
463 parallel increased gene expression in the jejunum (Lau et al., 2016). They hypothesized that increased
464 i-FABP levels could be a result of an increased production by enterocytes rather than tissue damage.
465 Furthermore, EB inhibit protein biosynthesis (Olleik et al., 2019) and thereby, might lead to a reduced
466 i-FABP plasma concentration.

467 As blood parameters alone can be difficult to interpret due to limitations in methods, dependence
468 on sampling time point and choosing the right parameter (Celi et al., 2019), we additionally investigated
469 the extent of histological lesions in selected organs. As the intestine and the liver are the main sites of
470 drug metabolism (Chhabra, 1979), we focused on jejunum, colon, liver and additionally on lymph nodes.
471 DON-containing diets led to significant changes in the jejunum seen as villi atrophy, flattening and
472 cytoplasmic vacuolation of enterocytes, reduced number of goblet cells and shorter villi (Figures 8A+B).
473 This is in accordance with several other studies (Bracarense et al., 2012; Pinton and Oswald, 2014;
474 Gerez et al., 2015; Przybylska-Gornowicz et al., 2018). The most frequent change observed in EB-fed
475 animals was vacuolation of enterocytes. This change may be associated with the ionophoric properties
476 of ENNs and BEA resulting in an imbalance of cell membrane permeability. Enniatins have the ability
477 to incorporate into cell membranes forming cation selective pores with high affinity to Na⁺ (Kouri et
478 al., 2003). Increases in cytosolic Na⁺ is followed by intracellular water rise and cell swelling (Myers et
479 al., 2012). No significant effects were seen in the histological part of colon tissue between the different
480 groups. Most likely, the parent fungal compounds were already metabolized into less-toxic substances
481 as known for DON and its metabolite deepoxy-DON (DOM-1) (Bracarense et al., 2020). In general, the
482 effects of EB were more significant on liver tissue than in the intestine (Figures 7 – 10), which might be
483 due to rapid absorption known for ENN B1, and its fast metabolism in the liver (Devreese et al., 2014).
484 Piglets receiving the EB-diets showed moderate to severe vacuolation of hepatocytes and megalocytosis
485 (Figure 10). This could be due to a possible bioaccumulation of lipophilic ENNs and BEA in fat-rich
486 tissue as seen in mice (Rodríguez-Carrasco et al., 2016) In addition, the administration of 50, 100 or 200
487 mg/kg b.w. of BEA or ENN B by oral gavage in mice induced mild toxic effects in the liver (Maranghi
488 et al., 2018). However, those doses are very high and perhaps mice may be more tolerant to these

489 mycotoxins than pigs, but it is hard to make this conclusion confirm due to the lack of *in vivo* studies
490 with emerging mycotoxins. In total, apoptosis and necrosis were detected only in animals fed the DON-
491 diets. An increase in the lesion score of piglets fed with DON-diets was reported previously (Mikami et
492 al., 2010; Pierron et al., 2018; Bracarense et al., 2020), but apoptosis was not present in the liver of rats
493 despite the increased lesion score in this organ (Bracarense et al., 2017). In lymph nodes, a significant
494 increase in the histological score was detected in DON-exposed animals showing lymphoid depletion
495 and apoptosis (Figure 11). This is in accordance with several studies performed by our group, which
496 found that DON increased the lesion score in the lymph nodes in both, piglets and rats (Bracarense et
497 al., 2017, 2020; Gerez et al., 2015; Mikami et al., 2010; Pierron et al., 2016). In this study, lymphoid
498 hyperplasia was frequent in the EB group, but the lesion score did not differ from the control group
499 (Figure 11).

500 The antibiotic activity of ENNs and BEA against mostly several gram-positive bacteria and fungi
501 due to their ionophoric properties has already been studied (Olleik et al., 2019; Sy-Cordero et al., 2012),
502 and could explain differences in fecal microbiome between groups in our study. The fecal microbiome
503 of animals receiving the EB diet showed a lower diversity compared to the control group, but also
504 compared to the EB+DON group. Therefore, it is tempting to speculate that DON antagonized the
505 antibiotic effect of EB. Furthermore, a change in the microbial pattern was seen in all mycotoxin-
506 containing groups (Figure 12). This life stage of pigs, only two weeks after weaning, is crucial as the
507 microbial flora is not fully developed which can lead to higher susceptibility to diarrhea, weight loss
508 and mortality (Rhouma et al., 2017). The importance of the intestinal gut microbiome has been studied
509 more extensively in the last decade due to development of the "omics" methodologies. Therefore, we
510 already know the strong correlation between a high diverse microbiota and appropriate functions such
511 as enhanced feed efficiency, production of volatile fatty acids, resistance against pathogenic bacteria
512 and improved immune system (Ghanbari et al., 2019; Guevarra et al., 2019; Kraler et al., 2016; Stokes,
513 2017; Yang et al., 2017). One study showed that DON, applied in a concentration of 2.8 mg/kg, changed
514 the microflora balance and modified the richness index in 9-week-old pigs, but did not influence the
515 diversity (Waché et al., 2009). In our study, DON alone also led to a slight decrease of in the diversity
516 of taxa, but not significantly ($p = 0.088$) and in the EB+DON group no effect was found (Figure 13). A

517 higher translocation of a pathogenic *Escherichia coli* strain was seen *in vitro* using intestinal porcine
518 cells (IPEC-1), when treated with DON (Pinton et al., 2009). The relative abundance of *E. coli* in the
519 DON group was not increased (Figure 12). However, in animals that received DON+EB, an increase in
520 *E. coli* abundance was seen. Another remarkable alteration in EB-fed piglets was the increase of in
521 *Actinobacteria* and *Mycobacterium branderi* with a parallel decrease in *Ascomycota* and the species
522 *Aureobasidium namibiae*. An alteration of the mycobiome (the fungal part of the microbiome) has been
523 associated with several diseases in humans (Chin et al., 2020). There is not much literature about the
524 species *M. branderi*, belonging to the phylum *Actinobacteria*, except that it is a potential pathogen first
525 isolated from human respiratory tract (Koukila-Kahkola et al., 1995). Also, the abundant *Lactobacillus*
526 species *L. amylovorus* known to exhibit positive probiotic activities in weaning piglets (Konstantinov et
527 al., 2006) was reduced only in the EB-fed group, but not in the EB+DON group. On the other hand, the
528 relative abundance of *L. reuteri* was increased in the EB group and also, to a lesser extent, in the
529 EB+DON group compared to the control and the DON group. *L. reuteri* is a lactic acid bacterium and
530 proven to reduce *Cryptosporidium parvum*-induced diarrhea in piglets (Casas and Dobrogosz, 2000).
531 This is in contrast to a recent publication (Reddy et al., 2018), in which *Lactobacillus* was significantly
532 more abundant in piglets fed a DON-diet (7.38 mg/kg) compared to the control. However, in this study
533 8-week-old piglets were used for a 4-week trial with a quite high DON contamination, which is in
534 contrast to our approach.

535 5. Conclusion

536 All together it could be seen that a contaminated diet including EB led to a decrease in the diversity
537 of the gut microbiome as well as to a shift in certain fungal, viral, and bacterial genera in weaning piglets.
538 Interestingly, these effects were not so evident when DON was additionally included in the diet, which
539 indicates a combinatory effect. The EB+DON combinatory diet of EB+DON significantly decreased the
540 weight gain within the short period of 14 days, which was not seen in the EB or DON groups.
541 Furthermore, all mycotoxins-receiving animals showed moderate to severe histological changes in the
542 intestine, the liver, and the lymph nodes to different extents, although plasma biomarkers were not as
543 clearly affected. Our study shows that the emerging mycotoxins alone, but also with the frequently co-

544 occurring metabolite DON, impact the growth performance, lead to organ lesions and to an alteration of
545 microbial community composition for which later consequences have to be in the focus of further
546 studies. Therefore, regarding the high prevalence and co-occurrence of EB with regulated mycotoxins
547 in different feed commodities, more *in vivo* results must be generated also in other animal species to
548 provide sufficient data for a reliable risk assessment.

549

550 **Author Contributions:** For research articles with several authors, a short paragraph specifying their
551 individual contributions must be provided. The following statements should be used “Conceptualization,
552 B.N., A.L., P.P. and D.S.; methodology, B.N., A.L., M.N. and C.E.; validation, B.N. and A.L.; formal
553 analysis, B.N., A.L., M.G., A.B., V.M. and P.P.; data curation, B.N., A.L., M.G., A.B., V.M. and P.P.;
554 writing—original draft preparation, B.N. and A.L.; writing—review and editing, B.N., A.L., A.B., S.W.,
555 P.P. and IPO.; visualization, B.N. and A.L.; supervision, IPO. and D.S.; project administration, B.N.
556 and A.L.; funding acquisition, B.N., A.L., IPO and P.P. All authors have read and agreed to the published
557 version of the manuscript.

558 **Funding:** “This research was funded by Austrian Research Promotion Agency (FFG) via the research
559 project Early Stage, grant number 879467 and by the French ANR project “EmergingMyco” (ANR-18-
560 CE34-0014). Amanda L. Hasuda received a fellowship from the Coordenação de Aperfeiçoamento de
561 Pessoal de Nível Superior-CAPES/Cofecub (Grant 0389/2019). This study was financed in part by the
562 Coordenação de Aperfeiçoamento de Pessoal de Nível Superior - Brasil (CAPES) - Finance Code 001.”

563 **Acknowledgments:** The authors would like to express their gratitude towards Josef Bandion, Ida
564 Gradner, Christina Gruber, Heinz Heidegger, Daniel Pasteiner, Lukas Moser for practical support during
565 the animal experiment. Furthermore, we would like to thank Valentina Rainer for her support during the
566 analysis.

567 **Conflicts of Interest:** The authors declare no conflict of interest.

568 *References*

- 569 Ajamian, M., Steer, D., Rosella, G., Gibson, P.R., 2019. Serum zonulin as a marker of intestinal mucosal
570 barrier function: May not be what it seems. *PLoS One*.
571 <https://doi.org/10.1371/journal.pone.0210728>
- 572 Albonico, M., Schutz, L.F., Cortinovis, C., Caloni, F., Spicer, L.J., 2016. In vitro effects of beauvericin
573 alone and combined with fumonisin B1 on bovine granulosa cell proliferation and steroidogenesis.
574 *Toxicol. Lett.* <https://doi.org/10.1016/j.toxlet.2016.06.1854>
- 575 Alonso-Garrido, M., Escrivá, L., Manyes, L., Font, G., 2018. Enniatin B induces expression changes in
576 the electron transport chain pathway related genes in lymphoblastic T-cell line. *Food Chem.*
577 *Toxicol.* <https://doi.org/10.1016/j.fct.2018.09.018>
- 578 Altpeter, F., Posselt, U.K., 1994. Production of high quantities of 3-acetyldeoxynivalenol and
579 deoxynivalenol. *Appl. Microbiol. Biotechnol.* <https://doi.org/10.1007/BF01982524>
- 580 Amacher, D.E., 2002. A toxicologist's guide to biomarkers of hepatic response. *Hum. Exp. Toxicol.*
581 <https://doi.org/10.1191/0960327102ht247oa>
- 582 Amuzie, C.J., Pestka, J.J., 2009. Suppression of insulin-like growth factor acid-labile subunit
583 expression-A novel mechanism for deoxynivalenol-induced growth retardation. *Toxicol. Sci.*
584 <https://doi.org/10.1093/toxsci/kfp225>
- 585 Azcona-Olivera, J.I., Ouyang, Y., Murtha, J., Chu, F.S., Pestka, J.J., 1995. Induction of cytokine
586 mRNAs in mice after oral exposure to the trichothecene vomitoxin (deoxynivalenol): Relationship
587 to toxin distribution and protein synthesis inhibition. *Toxicol. Appl. Pharmacol.*
588 <https://doi.org/10.1006/taap.1995.1132>
- 589 Bertero, A., Fossati, P., Tedesco, D.E.A., Caloni, F., 2020. Beauvericin and Enniatins: In Vitro Intestinal
590 Effects. *Toxins (Basel)*. <https://doi.org/10.3390/toxins12110686>
- 591 Bracarense, A.P.F., Lucioli, J., Grenier, B., Drociunas Pacheco, G., Moll, W., Schatzmayr, G., Oswald,
592 I.P., 2012. Chronic ingestion of deoxynivalenol and fumonisin, alone or in interaction, induces
593 morphological and immunological changes in the intestine of piglets. *Br. J. Nutr.* 107, 1776–1786.
594 <https://doi.org/10.1017/S0007114511004946>
- 595 Bracarense, A.P.F.L., Lucioli, J., Grenier, B., Drociunas Pacheco, G., Moll, W.D., Schatzmayr, G.,
596 Oswald, I.P., 2012. Chronic ingestion of deoxynivalenol and fumonisin, alone or in interaction,
597 induces morphological and immunological changes in the intestine of piglets. *Br. J. Nutr.*
598 <https://doi.org/10.1017/S0007114511004946>
- 599 Bracarense, A.P.F.L., Pierron, A., Pinton, P., Gerez, J.R., Schatzmayr, G., Moll, W.D., Zhou, T.,
600 Oswald, I.P., 2020. Reduced toxicity of 3-epi-deoxynivalenol and de-epoxy-deoxynivalenol
601 through deoxynivalenol bacterial biotransformation: In vivo analysis in piglets. *Food Chem.*
602 *Toxicol.* <https://doi.org/10.1016/j.fct.2020.111241>
- 603 Busher, J.T., 1990. Serum Albumin and Globulin, *Clinical Methods: The History, Physical, and*
604 *Laboratory Examinations.*
- 605 Caloni, F., Fossati, P., Anadón, A., Bertero, A., 2020. Beauvericin: The beauty and the beast. *Environ.*
606 *Toxicol. Pharmacol.* <https://doi.org/10.1016/j.etap.2020.103349>
- 607 Campbell, J.M., Crenshaw, J.D., Polo, J., 2013. The biological stress of early weaned piglets. *J. Anim.*
608 *Sci. Biotechnol.* <https://doi.org/10.1186/2049-1891-4-19>
- 609 Cano, P.M., Seeboth, J., Meurens, F., Cognie, J., Abrami, R., Oswald, I.P., Guzylack-Piriou, L., 2013.
610 Deoxynivalenol as a new factor in the persistence of intestinal inflammatory diseases: an emerging
611 hypothesis through possible modulation of Th17-mediated response. *PLoS One* 8, e53647.
- 612 Casas, I.A., Dobrogosz, W.J., 2000. Validation of the Probiotic Concept: *Lactobacillus reuteri* confers
613 broad-spectrum protection against disease in humans and animals. *Microb. Ecol. Health Dis.*
614 <https://doi.org/10.1080/08910600050216246-1>
- 615 Caviglia, G.P., Dughera, F., Ribaldone, D.G., Rosso, C., Abate, M.L., Pellicano, R., Bresso, F., Smedile,
616 A., Saracco, G.M., Astegiano, M., 2018. Serum zonulin in patients with inflammatory bowel
617 disease: A pilot study. *Minerva Med.* <https://doi.org/10.23736/S0026-4806.18.05787-7>
- 618 Celi, P., Verlhac, V., Pérez Calvo, E., Schmeisser, J., Klünter, A.M., 2019. Biomarkers of
619 gastrointestinal functionality in animal nutrition and health. *Anim. Feed Sci. Technol.*
620 <https://doi.org/10.1016/j.anifeedsci.2018.07.012>
- 621 Chen, B.F., Tsai, M.C., Jow, G.M., 2006. Induction of calcium influx from extracellular fluid by

- 622 beauvericin in human leukemia cells. *Biochem. Biophys. Res. Commun.*
623 <https://doi.org/10.1016/j.bbrc.2005.11.166>
- 624 Chhabra, R.S., 1979. Intestinal absorption and metabolism of xenobiotics. *Environ. Health Perspect.*
625 <https://doi.org/10.1289/ehp.793361>
- 626 Chin, V.K., Yong, V.C., Chong, P.P., Amin Nordin, S., Basir, R., Abdullah, M., 2020. Mycobiome in
627 the Gut: A Multiperspective Review. *Mediators Inflamm.* <https://doi.org/10.1155/2020/9560684>
- 628 Cho, Y.-E., Lomeda, R.-A.R., Ryu, S.-H., Sohn, H.-Y., Shin, H.-I., Beattie, J.H., Kwun, I.-S., 2007.
629 Zinc deficiency negatively affects alkaline phosphatase and the concentration of Ca, Mg and P in
630 rats. *Nutr. Res. Pract.* <https://doi.org/10.4162/nrp.2007.1.2.113>
- 631 Devreese, M., Broekaert, N., De Mil, T., Fraeyman, S., De Backer, P., Croubels, S., 2014. Pilot
632 toxicokinetic study and absolute oral bioavailability of the Fusarium mycotoxin enniatin B1 in
633 pigs. *Food Chem. Toxicol.* <https://doi.org/10.1016/j.fct.2013.11.005>
- 634 EFSA, 2014a. Scientific Opinion on the risks to human and animal health related to the presence of
635 beauvericin and enniatins in food and feed. *EFSA J.* <https://doi.org/10.2903/j.efsa.2012.2605>.
- 636 EFSA, 2014b. Scientific Opinion on the risks to human and animal health related to the presence of
637 beauvericin and enniatins in food and feed. *EFSA J.* 12, 3802.
638 <https://doi.org/10.2903/j.efsa.2012.2605>.
- 639 Escrivá, L., Alonso-Garrido, M., Font, G., Manyes, L., 2019. Transcriptional study after Beauvericin
640 and Enniatin B combined exposure in Jurkat T cells. *Food Chem. Toxicol.*
641 <https://doi.org/10.1016/j.fct.2019.05.018>
- 642 Escrivá, L., Jennen, D., Caiment, F., Manyes, L., 2018. Transcriptomic study of the toxic mechanism
643 triggered by beauvericin in Jurkat cells. *Toxicol. Lett.* <https://doi.org/10.1016/j.toxlet.2017.11.035>
- 644 FAO/WHO, 2001. Safety evaluation of certain mycotoxins in food / prepared by the fifty-sixth meeting
645 of the Joint FAO/WHO Expert Committee on Food Additives (JECFA). *Food Agric. Organ.*
- 646 Fasano, A., 2020. All disease begins in the (leaky) gut: Role of zonulin-mediated gut permeability in
647 the pathogenesis of some chronic inflammatory diseases. *F1000Research.*
648 <https://doi.org/10.12688/f1000research.20510.1>
- 649 Flannery, B.M., Clark, E.S., Pestka, J.J., 2012. Anorexia induction by the trichothecene deoxynivalenol
650 (vomitin) is mediated by the release of the gut satiety hormone peptide YY. *Toxicol. Sci.*
651 <https://doi.org/10.1093/toxsci/kfs255>
- 652 Funaoka, H., Kanda, T., Fujii, H., 2010. Intestinal fatty acid-binding protein (I-FABP) as a new
653 biomarker for intestinal diseases. *Rinsho Byori.*
- 654 Gerez, J.R., Pinton, P., Callu, P., Grosjean, F., Oswald, I.P., Bracarense, A.P.F.L., 2015. Deoxynivalenol
655 alone or in combination with nivalenol and zearalenone induce systemic histological changes in
656 pigs. *Exp. Toxicol. Pathol.* <https://doi.org/10.1016/j.etp.2014.10.001>
- 657 Gruber-Dorninger, C., Novak, B., Nagl, V., Berthiller, F., 2017. Emerging Mycotoxins: Beyond
658 Traditionally Determined Food Contaminants. *J. Agric. Food Chem.*
659 <https://doi.org/10.1021/acs.jafc.6b03413>
- 660 Guevarra, R.B., Lee, J.H., Lee, S.H., Seok, M.J., Kim, D.W., Kang, B.N., Johnson, T.J., Isaacson, R.E.,
661 Kim, H.B., 2019. Piglet gut microbial shifts early in life: Causes and effects. *J. Anim. Sci.*
662 *Biotechnol.* <https://doi.org/10.1186/s40104-018-0308-3>
- 663 Hietaniemi, V., Rämö, S., Yli-Mattila, T., Jestoi, M., Peltonen, S., Kartio, M., Sieviläinen, E., Koivisto,
664 T., Parikka, P., 2016. Updated survey of Fusarium species and toxins in Finnish cereal grains. *Food*
665 *Addit. Contam. - Part A Chem. Anal. Control. Expo. Risk Assess.*
666 <https://doi.org/10.1080/19440049.2016.1162112>
- 667 Jestoi, M., 2008. Emerging fusarium-mycotoxins fusaproliferin, beauvericin, enniatins, and
668 moniliformin - A review. *Crit. Rev. Food Sci. Nutr.* <https://doi.org/10.1080/10408390601062021>
- 669 Juan-García, A., Juan, C., König, S., Ruiz, M.J., 2015. Cytotoxic effects and degradation products of
670 three mycotoxins: Alternariol, 3-acetyl-deoxynivalenol and 15-acetyl-deoxynivalenol in liver
671 hepatocellular carcinoma cells. *Toxicol. Lett.* <https://doi.org/10.1016/j.toxlet.2015.03.003>
- 672 Juan, C., Covarelli, L., Beccari, G., Colasante, V., Mañes, J., 2016. Simultaneous analysis of twenty-six
673 mycotoxins in durum wheat grain from Italy. *Food Control.*
674 <https://doi.org/10.1016/j.foodcont.2015.10.032>
- 675 Khoshal, Abdullah Khan, Novak, B., Martin, P.G.P., Jenkins, T., Neves, M., Schatzmayr, G., Oswald,
676 I.P., Pinton, P., 2019. Co-occurrence of DON and emerging mycotoxins in worldwide finished pig

- 677 feed and their combined toxicity in intestinal cells. *Toxins* (Basel).
678 <https://doi.org/10.3390/toxins11120727>
- 679 Khoshal, A.K., Novak, B., Martin, P.G.P., Jenkins, T., Neves, M., Schatzmayr, G., Oswald, I.P., Pinton,
680 P., 2019. Co-occurrence of DON and emerging mycotoxins in worldwide finished pig feed and
681 their combined toxicity in intestinal cells. *Toxins* (Basel). 11.
682 <https://doi.org/10.3390/toxins11120727>
- 683 Konstantinov, S.R., Poznanski, E., Fuentes, S., Akkermans, A.D.L., Smidt, H., de Vos, W.M., 2006.
684 *Lactobacillus sobrius* sp. nov., abundant in the intestine of weaning piglets. *Int. J. Syst. Evol.*
685 *Microbiol.* <https://doi.org/10.1099/ijms.0.63508-0>
- 686 Koukila-Kahkola, P., Springer, B., Bottger, E.C., Paulin, L., Jantzen, E., Katila, M.L., 1995.
687 *Mycobacterium branderi* sp. nov., a new potential human pathogen. *Int. J. Syst. Bacteriol.*
688 <https://doi.org/10.1099/00207713-45-3-549>
- 689 Kovalsky, P., Kos, G., Nährer, K., Schwab, C., Jenkins, T., Schatzmayr, G., Sulyok, M., Krska, R.,
690 2016. Co-occurrence of regulated, masked and emerging mycotoxins and secondary metabolites
691 in finished feed and maize—An extensive survey. *Toxins* (Basel).
692 <https://doi.org/10.3390/toxins8120363>
- 693 Křížová, L., Dadáková, K., Dvořáčková, M., Kašparovský, T., 2021. Feedborne Mycotoxins
694 Beauvericin and Enniatins and Livestock Animals. *Toxins* (Basel).
695 <https://doi.org/10.3390/toxins13010032>
- 696 Lau, E., Marques, C., Pestana, D., Santoalha, M., Carvalho, D., Freitas, P., Calhau, C., 2016. The role
697 of I-FABP as a biomarker of intestinal barrier dysfunction driven by gut microbiota changes in
698 obesity. *Nutr. Metab.* <https://doi.org/10.1186/s12986-016-0089-7>
- 699 Levitt, D.G., Levitt, M.D., 2016. Human serum albumin homeostasis: A new look at the roles of
700 synthesis, catabolism, renal and gastrointestinal excretion, and the clinical value of serum albumin
701 measurements. *Int. J. Gen. Med.* <https://doi.org/10.2147/IJGM.S102819>
- 702 Lindblad, M., Gidlund, A., Sulyok, M., Börjesson, T., Krska, R., Olsen, M., Fredlund, E., 2013.
703 Deoxynivalenol and other selected fusarium toxins in swedish wheat - occurrence and correlation
704 to specific fusarium species. *Int. J. Food Microbiol.*
705 <https://doi.org/10.1016/j.ijfoodmicro.2013.07.002>
- 706 Lukaszyk, E., Lukaszyk, M., Koc-Zorawska, E., Bodzenta-Lukaszyk, A., Malyszko, J., 2018. Zonulin,
707 inflammation and iron status in patients with early stages of chronic kidney disease. *Int. Urol.*
708 *Nephrol.* <https://doi.org/10.1007/s11255-017-1741-5>
- 709 Mahnine, N., Meca, G., Elabidi, A., Fekhaoui, M., Saoiabi, A., Font, G., Mañes, J., Zinedine, A., 2011.
710 Further data on the levels of emerging *Fusarium* mycotoxins enniatins (A, A1, B, B1), beauvericin
711 and fusaproliferin in breakfast and infant cereals from Morocco. *Food Chem.*
712 <https://doi.org/10.1016/j.foodchem.2010.06.058>
- 713 Manyes, L., Escrivá, L., Ruiz, M.J., Juan-García, A., 2018. Beauvericin and enniatin B effects on a
714 human lymphoblastoid Jurkat T-cell model. *Food Chem. Toxicol.*
715 <https://doi.org/10.1016/j.fct.2018.03.008>
- 716 Maresca, M., Yahi, N., Younes-Sakr, L., Boyron, M., Caporiccio, B., Fantini, J., 2008. Both direct and
717 indirect effects account for the pro-inflammatory activity of enteropathogenic mycotoxins on the
718 human intestinal epithelium: Stimulation of interleukin-8 secretion, potentiation of interleukin-
719 1beta effect and increase in the transepithel. *Toxicol Appl Pharmacol* 228, 84–92.
720 <https://doi.org/10.1016/j.taap.2007.11.013>
- 721 Maruo, V.M., Bracarense, A.P., Metayer, J.P., Vilarino, M., Oswald, I.P., Pinton, P., 2018. Ergot
722 alkaloids at doses close to EU regulatory limits induce alterations of the liver and intestine. *Toxins*
723 (Basel). <https://doi.org/10.3390/toxins10050183>
- 724 Medina, A., Akbar, A., Baazeem, A., Rodriguez, A., Magan, N., 2017. Climate change, food security
725 and mycotoxins: Do we know enough? *Fungal Biol. Rev.*
726 <https://doi.org/10.1016/j.fbr.2017.04.002>
- 727 Novak, B., Rainer, V., Sulyok, M., Haltrich, D., Schatzmayr, G., Mayer, E., 2019. Twenty-eight fungal
728 secondary metabolites detected in pig feed samples: Their occurrence, relevance and cytotoxic
729 effects in vitro. *Toxins* (Basel). <https://doi.org/10.3390/toxins11090537>
- 730 Olleik, H., Nicoletti, C., Lafond, M., Courvoisier-Dezord, E., Xue, P., Hijazi, A., Baydoun, E., Perrier,
731 J., Maresca, M., 2019. Comparative structure-activity analysis of the antimicrobial activity,

- 732 cytotoxicity, and mechanism of action of the fungal cyclohexadepsipeptides enniatins and
733 beauvericin. *Toxins (Basel)*. <https://doi.org/10.3390/toxins11090514>
- 734 Ono, K., Ono, T., Matsumata, T., 1995. The pathogenesis of decreased aspartate aminotransferase and
735 alanine aminotransferase activity in the plasma of hemodialysis patients: The role of vitamin B6
736 deficiency. *Clin. Nephrol.*
- 737 Payros, D., Alassane-Kpembi, I., Pierron, A., Loiseau, N., Pinton, P., Oswald, I.P., 2016. Toxicology of
738 deoxynivalenol and its acetylated and modified forms. *Arch. Toxicol.*
739 <https://doi.org/10.1007/s00204-016-1826-4>
- 740 Pestka, J.J., 2010. Deoxynivalenol: Mechanisms of action, human exposure, and toxicological
741 relevance. *Arch. Toxicol.* <https://doi.org/10.1007/s00204-010-0579-8>
- 742 Pierron, Alix, Alassane-Kpembi, I., Oswald, I.P., 2016. Impact of mycotoxin on immune response and
743 consequences for pig health. *Anim. Nutr.* <https://doi.org/10.1016/j.aninu.2016.03.001>
- 744 Pierron, A., Bracarense, A.P.F.L., Cossalter, A.M., Laffitte, J., Schwartz-Zimmermann, H.E.,
745 Schatzmayr, G., Pinton, P., Moll, W.D., Oswald, I.P., 2018. Deepoxy-deoxynivalenol retains some
746 immune-modulatory properties of the parent molecule deoxynivalenol in piglets. *Arch. Toxicol.*
747 <https://doi.org/10.1007/s00204-018-2293-x>
- 748 Pierron, A., Mimoun, S., Murate, L.S., Loiseau, N., Lippi, Y., Bracarense, A.F., Liaubet, L., Schatzmayr,
749 G., Berthiller, F., Moll, W.D., Oswald, I.P., 2016. Intestinal toxicity of the masked mycotoxin
750 deoxynivalenol-3-beta-D-glucoside. *Arch. Toxicol.* 90, 2037–2046.
751 <https://doi.org/10.1007/s00204-015-1592-8> 10.1007/s00204-015-1592-8 [pii]
- 752 Pinton, P., Nougayrède, J.P., Del Rio, J.C., Moreno, C., Marin, D.E., Ferrier, L., Bracarense, A.P., Kolf-
753 Clauw, M., Oswald, I.P., 2009. The food contaminant deoxynivalenol, decreases intestinal barrier
754 permeability and reduces claudin expression. *Toxicol. Appl. Pharmacol.*
755 <https://doi.org/10.1016/j.taap.2009.03.003>
- 756 Pinton, P., Oswald, I.P., 2014. Effect of deoxynivalenol and other type B trichothecenes on the intestine:
757 A review. *Toxins (Basel)*. <https://doi.org/10.3390/toxins6051615>
- 758 Prelusky, D.B., 1997. Effect of intraperitoneal infusion of deoxynivalenol on feed consumption and
759 weight gain in the pig. *Nat. Toxins*. <https://doi.org/10.1002/nt.7>
- 760 Prosperini, A., Juan-García, A., Font, G., Ruiz, M.J., 2013. Beauvericin-induced cytotoxicity via ROS
761 production and mitochondrial damage in Caco-2 cells. *Toxicol. Lett.*
762 <https://doi.org/10.1016/j.toxlet.2013.07.005>
- 763 Przybylska-Gornowicz, B., Lewczuk, B., Prusik, M., Hanuszewska, M., Petruszewicz-Kosińska, M.,
764 Gajęcka, M., Zielonka, Ł., Gajęcki, M., 2018. The effects of deoxynivalenol and zearalenone on
765 the pig large intestine. A light and electron microscopy study. *Toxins (Basel)*.
766 <https://doi.org/10.3390/toxins10040148>
- 767 Ramaiah, S.K., 2007. A toxicologist guide to the diagnostic interpretation of hepatic biochemical
768 parameters. *Food Chem. Toxicol.* <https://doi.org/10.1016/j.fct.2007.06.007>
- 769 Reddy, K.E., Jeong, J.Y., Song, J., Lee, Y., Lee, H.J., Kim, D.W., Jung, H.J., Kim, K.H., Kim, Minji,
770 Oh, Y.K., Lee, S.D., Kim, Minseok, 2018. Colon microbiome of pigs fed diet contaminated with
771 commercial purified deoxynivalenol and zearalenone. *Toxins (Basel)*.
772 <https://doi.org/10.3390/toxins10090347>
- 773 Reisinger, N., Schürer-Waldheim, S., Mayer, E., Debevere, S., Antonissen, G., Sulyok, M., Nagl, V.,
774 2019. Mycotoxin occurrence in maize silage—a neglected risk for bovine gut health? *Toxins (Basel)*.
775 <https://doi.org/10.3390/toxins11100577>
- 776 Rhouma, M., Fairbrother, J.M., Beaudry, F., Letellier, A., 2017. Post weaning diarrhea in pigs: Risk
777 factors and non-colistin-based control strategies. *Acta Vet. Scand.* <https://doi.org/10.1186/s13028-017-0299-7>
- 779 Rodríguez-Carrasco, Y., Heilos, D., Richter, L., Süßmuth, R.D., Heffeter, P., Sulyok, M., Kenner, L.,
780 Berger, W., Dornetshuber-Fleiss, R., 2016. Mouse tissue distribution and persistence of the food-
781 born fusariotoxins Enniatin B and Beauvericin. *Toxicol. Lett.*
782 <https://doi.org/10.1016/j.toxlet.2016.02.008>
- 783 Rotter, B.A., Prelusky, D.B., Pestka, J.J., 1996. Toxicology of deoxynivalenol (vomitoxin). *J Toxicol*
784 *Env. Heal.*
- 785 Santini, A., Meca, G., Uhlig, S., Ritieni, A., 2012. Fusaproliferin, beauvericin and enniatins: Occurrence
786 in food—A review. *World Mycotoxin J.* <https://doi.org/10.3920/WMJ2011.1331>

- 787 Serrano, A.B., Font, G., Mañes, J., Ferrer, E., 2013. Emerging *Fusarium* mycotoxins in organic and
788 conventional pasta collected in Spain. *Food Chem. Toxicol.*
789 <https://doi.org/10.1016/j.fct.2012.09.034>
- 790 Spanic, V., Katanic, Z., Sulyok, M., Krska, R., Puskas, K., Vida, G., Drezner, G., Šarkanj, B., 2020.
791 Multiple fungal metabolites including mycotoxins in naturally infected and *Fusarium*-inoculated
792 wheat samples. *Microorganisms*. <https://doi.org/10.3390/microorganisms8040578>
- 793 Springler, A., Vrabel, G.J., Mayer, E., Schatzmayr, G., Novak, B., 2016. Effect of *Fusarium*-derived
794 metabolites on the barrier integrity of differentiated intestinal porcine epithelial cells (IPEC-J2).
795 *Toxins (Basel)*. <https://doi.org/10.3390/toxins8110345>
- 796 Stokes, C.R., 2017. The development and role of microbial-host interactions in gut mucosal immune
797 development. *J. Anim. Sci. Biotechnol.* <https://doi.org/10.1186/s40104-016-0138-0>
- 798 Streit, E., Schwab, C., Sulyok, M., Naehrer, K., Krska, R., Schatzmayr, G., 2013. Multi-mycotoxin
799 screening reveals the occurrence of 139 different secondary metabolites in feed and feed
800 ingredients. *Toxins (Basel)*. <https://doi.org/10.3390/toxins5030504>
- 801 Sulyok, M., Stadler, D., Steiner, D., Krska, R., 2020. Validation of an LC-MS/MS-based dilute-and-
802 shoot approach for the quantification of > 500 mycotoxins and other secondary metabolites in food
803 crops: challenges and solutions. *Anal. Bioanal. Chem.* <https://doi.org/10.1007/s00216-020-02489-9>
- 804
- 805 Sy-Cordero, A.A., Pearce, C.J., Oberlies, N.H., 2012. Revisiting the enniatins: A review of their
806 isolation, biosynthesis, structure determination and biological activities. *J. Antibiot. (Tokyo)*.
807 <https://doi.org/10.1038/ja.2012.71>
- 808 Taylor, S.C., Nadeau, K., Abbasi, M., Lachance, C., Nguyen, M., Fenrich, J., 2019. The Ultimate qPCR
809 Experiment: Producing Publication Quality, Reproducible Data the First Time. *Trends Biotechnol.*
810 <https://doi.org/10.1016/j.tibtech.2018.12.002>
- 811 Terciolo, C., Bracarense, A.P., Souto, P.C.M.C., Cossalter, A.M., Dopavogui, L., Loiseau, N., Oliveira,
812 C.A.F., Pinton, P., Oswald, I.P., 2019. Fumonisin at doses below EU regulatory limits induce
813 histological alterations in piglets. *Toxins (Basel)*. <https://doi.org/10.3390/toxins11090548>
- 814 Terciolo, C., Maresca, M., Pinton, P., Oswald, I.P., 2018. Review article: Role of satiety hormones in
815 anorexia induction by Trichothecene mycotoxins. *Food Chem. Toxicol.*
816 <https://doi.org/10.1016/j.fct.2018.09.034>
- 817 Tonshin, A.A., Teplova, V. V., Andersson, M.A., Salkinoja-Salonen, M.S., 2010. The *Fusarium*
818 mycotoxins enniatins and beauvericin cause mitochondrial dysfunction by affecting the
819 mitochondrial volume regulation, oxidative phosphorylation and ion homeostasis. *Toxicology*.
820 <https://doi.org/10.1016/j.tox.2010.07.001>
- 821 Trenholm, H.L., Thompson, B.K., Foster, B.C., Charmley, L.L., Hartin, K.E., Coppock, R.W.,
822 Albassam, M.A., 1994. Effects of feeding diets containing *Fusarium* (naturally) contaminated
823 wheat or pure deoxynivalenol (DON) in growing pigs. *Can. J. Anim. Sci.*
824 <https://doi.org/10.4141/cjas94-049>
- 825 Urbaniak, M., Waskiewicz, A., Stepien, Ł., 2020. *Fusarium* cyclodepsipeptide mycotoxins: Chemistry,
826 biosynthesis, and occurrence. *Toxins (Basel)*. <https://doi.org/10.3390/toxins12120765>
- 827 Voss, K.A., 2010. A new perspective on deoxynivalenol and growth suppression. *Toxicol. Sci.*
828 <https://doi.org/10.1093/toxsci/kfp287>
- 829 Waché, Y.J., Valat, C., Postollec, G., Bougeard, S., Burel, C., Oswald, I.P., Fravallo, P., 2009. Impact of
830 deoxynivalenol on the intestinal microflora of pigs. *Int. J. Mol. Sci.*
831 <https://doi.org/10.3390/ijms10010001>
- 832 Wang, S., Wu, K., Xue, D., Zhang, C., Rajput, S.A., Qi, D., 2021. Mechanism of deoxynivalenol
833 mediated gastrointestinal toxicity: Insights from mitochondrial dysfunction. *Food Chem. Toxicol.*
834 153, 112214. <https://doi.org/10.1016/j.fct.2021.112214>
- 835 Wang, S., Yang, J., Zhang, B., Wu, K., Yang, A., Li, C., Zhang, J., Zhang, C., Rajput, S.A., Zhang, N.,
836 Sun, L., Qi, D., 2018. Deoxynivalenol impairs porcine intestinal host defense peptide expression
837 in weaned piglets and IPEC-J2 cells. *Toxins (Basel)*. <https://doi.org/10.3390/toxins10120541>
- 838 Yang, H., Huang, X., Fang, S., He, M., Zhao, Y., Wu, Z., Yang, M., Zhang, Z., Chen, C., Huang, L.,
839 2017. Unraveling the fecal microbiota and metagenomic functional capacity associated with feed
840 efficiency in pigs. *Front. Microbiol.* <https://doi.org/10.3389/fmicb.2017.01555>
- 841 Yoshinari, T., Suzuki, Y., Sugita-Konishi, Y., Ohnishi, T., Terajima, J., 2016. Occurrence of beauvericin

842 and enniatins in wheat flour and corn grits on the Japanese market, and their co-contamination
843 with type B trichothecene mycotoxins. Food Addit. Contam. - Part A Chem. Anal. Control. Expo.
844 Risk Assess. <https://doi.org/10.1080/19440049.2016.1228126>

1 **7 ARTIGO B – DEOXYNIVALENOL INDUCES APOPTOSIS AND INFLAMMATION**
2 **IN THE LIVER: ANALYSIS USING PRECISION-CUT LIVER SLICES**

3 **Deoxynivalenol induces apoptosis and inflammation in the**
4 **liver: Analysis using precision-cut liver slices**

5 **Amanda Lopes Hasuda^{1,2*}, Elodie Person², Abdullah Khoshal², Sandrine Bruel², Sylvie Puel²,**
6 **Isabelle P. Oswald^{2*}, Ana Paula F. R. L. Bracarense¹, Philippe Pinton²**

7 ¹Laboratory of Animal Pathology, Londrina State University, P.O. Box 10.011, Londrina, PR 86057-970, Brazil;
8 amanda.lopeshasuda@uel.br (A.L.H.) anapaula@uel.br (A.P.B.)

9 ² TOXALIM (UMR 1331), Institut National de Recherche pour l'Agriculture l'Alimentation et
10 l'Environnement Centre Occitanie-Toulouse, UPS, 31027 Toulouse, France; elodie.person@inrae.fr (EP),
11 a.khoshal@outlook.com (AK); Sylvie.Puel@inrae.fr (S.P.); isabelle.oswald@inrae.fr (I.P.O.);
12 philippe.pinton@inrae.fr (P.P.)

13 *Corresponding authors: amanda.lopeshasuda@uel.br, isabelle.oswald@inrae.fr

14 Received: 27 January 2022; Accepted: 16 March 2022; Published: 18 March 2022;

15 **ABSTRACT:** Deoxynivalenol (DON) is one of the most common mycotoxins in cereals and their by-
16 products. Its adverse effects on animal and human health have been extensively studied in the intestine,
17 but little attention has been paid to another target organ for mycotoxins, the liver, which is potentially
18 exposed after intestinal absorption and enterohepatic circulation. To assess DON's toxicity in an ex vivo
19 model structurally and physiologically closer to the whole liver, we developed a pig precision-cut liver
20 slices (PCLS) model. PCLS contain all cell types and maintain intercellular and cell-matrix interactions,
21 among other architectural features of the liver. The human HepG2 cell line was used for comparison.
22 We observed that after a short exposure, DON reduced the cell viability of HepG2 and induced the
23 expression of genes involved in apoptosis, inflammation, and oxidative stress. When PCLS were
24 exposed to DON, damage to the tissues was observed, with no changes in markers of liver function or
25 injury. Exposure to the toxin also triggered liver inflammation and apoptosis, effects already observed
26 in pigs fed a DON-contaminated diet. Overall, these data demonstrate that DON had toxic effects on a
27 liver cell line and on whole liver tissue, consistent with the effect observed during in vivo exposure.
28 They also indicate that pig PCLS is a relevant and sensitive model to investigate the liver toxicity of
29 food contaminants.

30 **Keywords:** cell death, liver, explants, histology, inflammation, apoptosis, mycotoxins

31

32 **1. Introduction**

33 Mycotoxins are toxic secondary metabolites produced by fungi, mainly by *Aspergillus*,
34 *Penicillium*, *Alternaria*, *Fusarium*, and *Claviceps*. They are the most frequently occurring natural
35 contaminants in human food and animal feed. They are highly resistant to various food processes

1 including cooking, and therefore end up on our plates (Payros et al., 2021a). Estimates show that 60-
2 80% of food crops worldwide are contaminated with mycotoxins (Eskola et al., 2020).

3 Among mycotoxins, deoxynivalenol (DON) is the most prevalent member of the trichothecene
4 family. It is mainly produced by *Fusarium graminearum* and *F. culmorum* (Knutsen et al., 2017). In
5 Europe, DON was detected in almost half of 26,613 cereal samples collected from 21 countries, with
6 the highest levels observed in wheat, maize, and oat grains (Knutsen et al., 2017). Similarly, in the
7 southern region of Brazil, one of the largest crops producing regions, 48% of the maize samples analyzed
8 were contaminated with this toxin (Oliveira et al., 2017).

9 In 2017, EFSA set a tolerable daily intake (TDI) of 1 µg/kg of body weight/day for the sum of DON
10 and its modified forms (Knutsen et al., 2017). Data obtained at the European and national levels indicate
11 that this TDI may be exceeded in some parts of the population, particularly children (Knutsen et al.,
12 2017; Narváez et al., 2022; Vin et al., 2020); indicating that exposure to DON is of concern for humans.

13 At the molecular level, DON binds to the 60S ribosomal subunit, inducing ribotoxic stress,
14 inhibiting protein synthesis, and activating mitogen-activated protein kinases and their downstream
15 pathways (Pestka, 2010a). Vomiting and bloody diarrhea have been reported following acute exposure
16 to DON (Pestka, 2010b; Ruan et al., 2020). Chronic exposure to the toxin reduces food consumption
17 and weight gain and induces neuroendocrine changes (Payros et al., 2016; Terciolo et al., 2018),
18 alteration of the immune system (Pinton et al., 2008), and disturbance of intestinal morphology and
19 functions (Pinton and Oswald, 2014; Robert et al., 2017).

20 The effect of DON on the liver is poorly described even though it can be a target for mycotoxins.
21 The functional capacities of this organ are mainly related to anabolic and catabolic processes including
22 energy metabolism and xenobiotics detoxification, storage and circulation of nutrients, as well as protein
23 synthesis and bile production. *In vitro* studies with hepatic human cells lines have focused on
24 cytotoxicity, apoptotic, and transcription factors (Fernández-Blanco et al., 2018; Mayer et al., 2017;
25 Smith et al., 2017a, 2017b; Zhang et al., 2009). The only study on human primary hepatocytes
26 demonstrated cytotoxicity, decreased albumin secretion, and increased apoptosis (Königs et al., 2008).
27 *In vivo* animal trials showed that ingestion of DON targets the liver; oral exposure to the toxin alters the
28 liver morphology, induces an inflammatory response, increases apoptosis and oxidative stress

29 (Bracarense et al., 2017; Gerez et al., 2015; Grenier et al., 2011; Souza et al., 2020; Sun et al., 2014).

30 In the context of reducing the number of experimental animals (3Rs principles), *ex vivo* organ
31 culture is a powerful model that preserves normal histological structure (Maresca et al., 2018). Indeed,
32 large numbers of explants can be prepared from a single animal, thus reducing the number of animals,
33 and allowing multiple tests. The advantage of *ex vivo* approaches for the intestine has been demonstrated
34 through observation of reproducible toxic effects of mycotoxins, including DON (Alassane-Kpembé et
35 al., 2017a, 2017b; Gerez et al., 2021; Pierron et al., 2022; Silva et al., 2019, 2014). Precision-cut liver
36 slices (PCLS) are a physiologically relevant *ex vivo* model for hepatic studies (Palma et al., 2019). This
37 model has features close to the *in vivo* situation, including the conservation of the complex 3D liver
38 structure, as well as cell–cell and cell–matrix interactions. Moreover, PCLS provides the possibility to
39 work with a complete multicellular liver model including hepatocytes, Kupffer cells, stellate cells,
40 cholangiocytes, and liver sinusoidal endothelial cells. As normal metabolism is necessary for
41 morphological preservation, structural integrity is a valid criterion to demonstrate a successful culture
42 (Starokozhko et al., 2015). Methodologies and parameters to produce and culture PCLS have been
43 optimized over the past decades (de Graaf et al., 2010; Dewyse et al., 2021). It is now considered that
44 PCLS provides a useful *ex vivo* tool to obtain multiple read-outs and that it is relevant for studies
45 investigating liver functionality, toxicity, chronic liver diseases, and potential adverse effects on the
46 immune system (Dewyse et al., 2021; Kasper et al., 2005; Wu et al., 2018). However, studies using *ex*
47 *vivo* models from the liver are scarce and their advantage in analyzing the effects of mycotoxins remains
48 to be demonstrated.

49 The objective of this work was thus to study the impact of DON on the liver using a liver slice
50 model. In this model, histological damages, hepatic biomarkers, and changes in gene expression were
51 evaluated. HepG2 cells, which are widely used for hepatotoxicity studies, were used for comparison.

52 **2. Materials and methods**

53 *2.1 Mycotoxin*

54 DON was acquired from Sigma-Aldrich (Saint Quentin Fallavier, France), dissolved in dimethyl
55 sulfoxide (DMSO) (Sigma-Aldrich), and stored at -20°C until use. Except for cytotoxicity assays, the

56 DON working concentration was 10 μ M, in accordance with our previous studies performed in different
57 experimental models and tissues (Bracarense et al., 2020; Gerez et al., 2021, 2017).

58 *2.2 In vitro* assay

59 To evaluate DON hepatotoxicity and gene expression, *in vitro* assays were performed using HepG2,
60 a human liver cancer cell line (Sigma, 85011430). Cells were maintained as previously described (Luo
61 et al., 2019) for gene expression analysis. To assess the cytotoxicity, HepG2 cells were seeded in 96-
62 white-well flat-bottom cell culture plates (Greiner, Courtaboeuf, France) (10^3 cells/well in 100 μ L
63 culture medium). After 24 h, the medium was replaced by a complete medium (without fetal calf serum)
64 containing DON or vehicle (DMSO) and incubated for 4, 24, and 48 h. The cytotoxic effects of DON
65 were determined by measuring the reducing potential of living cells, and hence their metabolism, using
66 the RealTime-Glo™ MT Cell Viability Assay (Promega, Charbonnières-les-Bains, France). Six
67 biological replicates were performed.

68 For gene expression analysis, cells were incubated for 4 h with the mycotoxin or vehicle, lysed with
69 Extract All (Eurobio, Les Ulis, France), and stored at -80°C prior to mRNA extraction. Six biological
70 replicates were performed.

71 *2.3 Preparation of liver slices*

72 Animal experimentation procedures were approved by the Ethics Committee of Pharmacology-
73 Toxicology of Toulouse-Midi-Pyrénées in animal experimentation (Toxcométhique)
74 (APAFIS#N2016080314392462), in accordance with the European Directive on the protection of
75 animals used for scientific purposes.

76 Liver slices (PCLS) were prepared from liver lateral lobe resected from nine euthanized male 4–5-
77 weeks-old piglets. The lobe was immediately flushed with an ice-cold sodium chloride solution (0.9%
78 NaCl) to limit ischemia and remove hemoglobin.

79 To improve their viability during coring, slicing, and storage procedures, the liver slices were
80 maintained in Krebs-Henseleit ice-cold buffer supplemented with NaHCO_3 (2.1 g/L) and $\text{CaCl}_2 \cdot 2\text{H}_2\text{O}$
81 (0.373 g/L), previously bubbled with carbogen for 1 h. Eight-millimeter diameter cores were cut out and
82 transferred to the Krumdieck tissue slicer (Alabama Research and Development, AL, USA) where 250

83 μm thick slices were cut (de Graaf et al., 2010). Damaged slices were discarded, and perfect slices
 84 underwent homeostasis recovery during a 1 h regeneration step in ice-cold William's E Medium
 85 supplemented with 1% glutamine and 0.5% gentamycin (Eurobio) bubbled in carbogen. The slices were
 86 deposited in 12-wells culture plates (1 slice per well) for 4 h in 2 mL of complete William's E Medium
 87 previously bubbled in carbogen and containing 10 μM DON or vehicle. Incubation took place at 37°C
 88 under a 95% O₂ and 5% CO₂-controlled atmosphere.

89 After the incubation period, the cell culture medium was collected and frozen to detect hepatic
 90 injury markers. Some liver slices were snap-frozen and stored at -80°C until transcriptomic analyses.
 91 Others were fixed for 24 h in 4% buffered formaldehyde (VWR, Rosny-sous-Bois, France) and stored
 92 in 70% ethanol for histology and immunohistochemical experiments.

93 2.3.1 Histological evaluation

94 PCLS incubated for four hours were dehydrated in a series of alcohol solutions of increasing
 95 concentration and embedded in paraffin for histological examination. Sections of 5 μm were stained
 96 with hematoxylin and eosin (HE) and mounted with coverslips for histological analysis. A
 97 morphological lesion score as described by Bracarense et al. (2012) and Terciolo et al. (2019) was used
 98 to evaluate histological changes in the liver. The extent of each lesion (according to the intensity or the
 99 frequency observed, scored from 0 to 3) and the severity factor were used to establish the lesion score
 100 scale (Table 1).

101 **Table 1.** Histological criteria used to establish liver lesion score.

Type of lesion	Severity factor	Maximal score
Disorganization of hepatic cords	1	33
Inflammatory infiltrate	1	
Cytoplasmic vacuolation	1	
Nuclear vacuolation	1	
Megalocytosis	2	
Apoptosis	2	
Necrosis	3	

102 The maximum lesion score was obtained by multiplying the lesion's maximum extent level by the
 103 organ's maximum severity factor. The lesion score was obtained by multiplying the severity factor by
 104 the extent of the lesion.

105
 106

107 2.3.2 Hepatic biomarkers

108 To assess liver damage and function, hepatic enzyme activity and protein concentration were
109 evaluated in the medium after a 4 h incubation period. Alanine transaminase (ALT), aspartate
110 aminotransferase (AST), alkaline phosphatase (ALP), lactate dehydrogenase (LDH) activities, and total
111 protein (TP) concentrations were determined on a Pentra 400 chemistry analyzer (Horiba, Les Ulis,
112 France) at the Anexplo Platform in Toulouse (France).

113 2.3.3 Immunohistochemical assessment of apoptosis

114 Apoptosis was assessed on liver slices by immunohistochemical analysis using the antibody anti-
115 cleaved caspase-3 (CCasp3) (clone Asp 175, 1:200 dilution, Cell Signaling Technology, Beverly, MA)
116 and the procedures previously described (Bracarense et al., 2017). Cells with positive immunostaining
117 were counted in five random fields per section at 400x magnification, as described previously (Gerez et
118 al., 2015).

119 2.4 Expression of mRNA encoding genes by real-time qPCR

120 The RNA from tissue and cells was extracted as already described (Grenier et al., 2012). The
121 concentration and quality of the samples were analyzed, and reverse transcription and real-time qPCR
122 were performed as previously described (Maruo et al., 2018) using specific primers sequences purchased
123 from Sigma (Tables 2 and 3). Most of the primers were specifically designed for this experiment.

124 2.4.1 Total RNA Extraction and Reverse Transcription

125 PCLS were lysed using 1 mL of Extract-All with ceramic beads (MP Biomedicals, Illkirch, France).
126 Total RNA from PCLS and HepG2 assays were purified, and their concentration and integrity were
127 determined as previously described (Maruo *et al.*, 2018). For each sample, 2 µg of total RNA was
128 reverse transcribed into cDNA and diluted 1:20 with nuclease-free/injection water (Ambion, Austin,
129 TX) and stored at -20°C until use.

130 2.4.2 Quantitative Real-time PCR (qPCR) Analysis

131 To quantify mRNA expression levels, RT-qPCR was performed using a Viia™ 7 thermocycler
132 (Applied Biosystems, California). The specificity of the qPCR products was assessed at the end of the

133 reactions by analyzing the dissociation curves. TOP2B and ACTB for PCLS samples, and GAPDH and
 134 PPIA for HepG2 cells were selected for their stable expression upon treatments, assessed with
 135 NormFinder software (Andersen et al., 2004), and used as reference genes. Non-reverse transcribed
 136 RNA was used as non-template control (NTC) for verification of the genomic DNA amplification signal.
 137 Data from qPCR were analyzed with the LinRegPCR 2016 program enabling the determination of the
 138 starting concentrations (N0) based on the observed PCR efficiency values. mRNA expression levels in
 139 samples exposed to DON were expressed relative to the mean of the control (Maruo et al., 2018).

140 **Table 2:** Table of human primer sequences used for RT-qPCR analysis (F: Forward; R: Reverse)

Gene symbol	Gene name	Primer sequence	mRNA	References
FOS	AP-1 Transcription Factor Subunit	F: ACGCGCAGGACTTCTGCAC R: GAATGAAGTTGGCACTGGAGAC	AH003773.2	Present study
ATF3	Activating Transcription Factor 3	F: GCGACGAGAAAGAAATAAG R: CAGCTTCTCCGACTCTTT	NM_001674.4	Present study
HNF4	Hepatocyte Nuclear Factor 4 Alpha	F: CAGATGATCGAGCAGATCCA R: CGTTGGTTCCCATATGTTCC	X76930.1	Present study
CASP3	Caspase 3	F: GAGGCCGACTTCTTGTAT R: CAAAGCGACTGGATGAAC	NM_004346.4	Present study
CASP 9	Caspase 9	F: CACACCCAGTGACATCTTT R: AGGGTCTCAACGTACCA	AB020979.1	Present study
CAT	Catalase	F: CTTGACCCAAGCAACAT R: GGGACAGTTCACAGGTATATG	NM_001752.4	Present study
SOD2	Superoxide Dismutase 2	F: GGTGGCTTGGTTTCAATAAG R: GTGCTCCCACACATCAAT	NM_000636.4	Present study
HMOX1	Heme Oxygenase 1	F: CAGGCAGAGGGTGATAGA R: CTCCTGCAACTCCTCAAAG	NM_002133	Present study
IL8	Interleukin 8	F: GATTTCTGCAGCTCTGTG R: GTGGAAAGGTTTGGAGTATG	NM_000584	Present study
TNF α	Tumor Necrosis Factor Alpha	F: CCTGTAGCCCATGTTGTA R: CCAGCTGGTTATCTCTCA	NM_000594	Present study
NF- κ B	Nuclear Factor Kappa B	F: GAGCAACCTAAACAGAGAGG R: TTGACCTGAGGGTAAGACT	NM_003998.4	Present study
CCL20	C-C Motif Chemokine Ligand 20	F: GGCTGCTTTGATGTCAGT R: GAAGAATACGGTCTGTGTATCC	NM_001130046.2	Present study
PPIA	Peptidylprolyl Isomerase A	F: GTCAACCCACCGTGTCTTC R: TTTCTGCTGTCTTTGGGACCTTG	ENST00000355968	Present study

GAPDH	Glyceraldehyde-3-Phosphate Dehydrogenase	F: TCAAGGCTGAGAACGGGAAG R: CCACTTGATTTTGGAGGGATCTC	NM_002046	Luo et al., 2021
-------	--	---	-----------	------------------

141

142 **Table 3:** Table of pig primer sequences used for RT-qPCR analysis (F: Forward; R: Reverse)

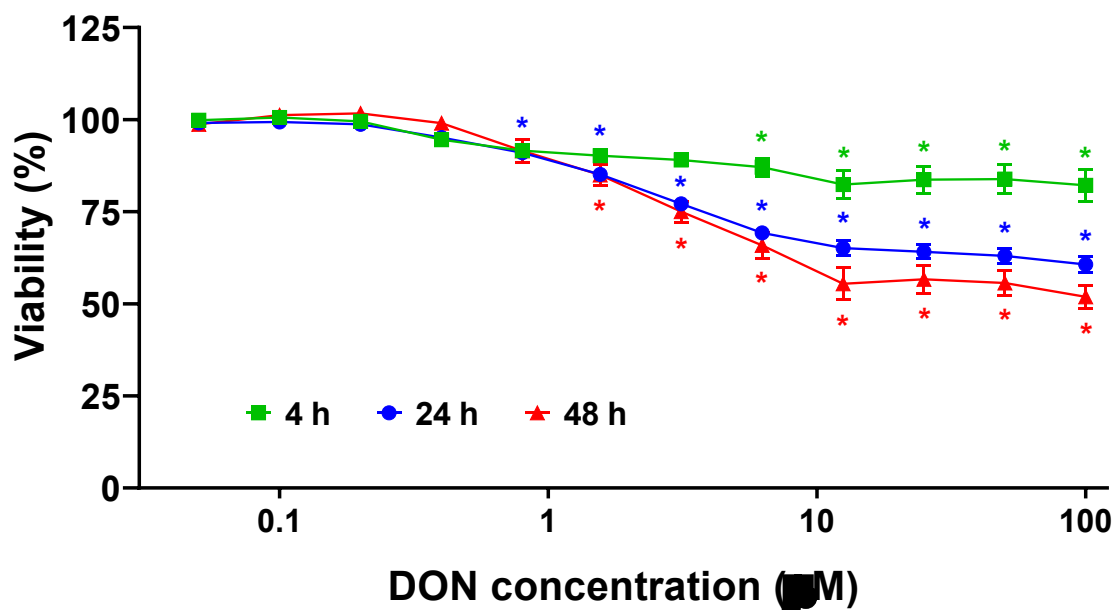
Gene symbol	Gene name	Primer sequence	mRNA	References
FOS	AP-1 Transcription Factor Subunit	F: CACTGTGAACAGATCAGC R: GAAGTCGGTCAGTTCTTTC	ENSSSCT000000 14174.4	Present study
ATF3	Activating Transcription Factor 3	F: TGAGGTTCCGCCATCCA R: TACCTCGGCTTTTCGTGA	ENSSSCT000000 33171.2	Present study
HNF4	Hepatocyte Nuclear Factor 4 Alpha	F: TACTGCAGGCTCAAGAAGTG R: CTGCTATCCTCGTAGCTTGAC	NM_001044571.1	Present study
IL1 α	Interleukin 1 Alpha	F: GCCAATGACACAGAAGAAGA R: ATGCACTGGTGGTTGATG	NM_214029	Pierron et al., 2022
IL8	Interleukin 8	F: GCTCTCTGTGAGGCTGCAGTTC R: AAGGTGTGGAATGCGTATTTATGC	NM_213867	Grenier et al., 2011
TNF α	Tumor necrosis factor alpha	F: ACTGCACTTCGAGGTTATCGG R: GGCGACGGGCTTATCTGA	NM_214022	Cano et al. 2013
NF- κ B	Nuclear Factor Kappa B	F: CCTCCACAAGGCAGCAAATAG R: TCCACACCGCTGTCACAGA	ENSSSCT000000 33438	Alassane-Kpembi et al, 2017a
CCL20	C-C Motif Chemokine Ligand 20	F: GCTCCTGGCTGCTTTGATGTC R: CATTGGCGAGCTGCTGTGTG	NM_001024589	Meurens et al., 2009
ACTB	Actin B	F: GCACCACACCTTCTACA R: ATCTGGGTCATCTTCTCAC	ENSSSCT000000 08324.1	Present study
TOP2B	DNA Topoisomerase II Beta	F: AAGGGCGAGAGGTCAATGAT R: ACATCTTCTCGTTCTTGCGC	ENSSSCT000150 80370.1	Park et al., 2015

143 *2.5 Statistical analysis*

144 All statistical analyses were performed using GraphPad Prism 9.0.2 software (GraphPad Software
145 Inc., La Jolla, USA). Data are expressed as mean \pm SEM (standard error of the mean). Significant
146 differences were assessed by one-way ANOVA followed by Tukey's test for cytotoxicity and by the
147 unpaired Student's t-test for parametric data and Mann Whitney test for non-parametric data for all the
148 other analyses. p-value \leq 0.05 was considered statistically significant.

149 **3. Results**150 *3.1 Effects of DON on HepG2 cells*

151 DON cytotoxicity was first evaluated on human liver cells (Figure 1). After 4 h exposure to DON,
 152 the viability of HepG2 cells decreased significantly at concentrations of 6.25 μM (12% reduction) to
 153 100 μM (17% reduction). After 24 h, viability decreased after DON exposure from 0.8 (9% reduction)
 154 to 100 μM (40% reduction). DON showed higher cytotoxic effects after 48 h exposure from 1.6 to 100
 155 μM (15% and 50% inhibition, respectively).



156

157 **Figure 1.** Toxicity of DON in HepG2 cells evaluated by measurement of the reducing potential of cells
 158 (RealTime-Glo™ MT Cell Viability Assay) after 4, 24, and 48 h. Cell viability is expressed as % of
 159 control cells. Data are presented as mean \pm SEM of six replicates, * $p \leq 0.05$.

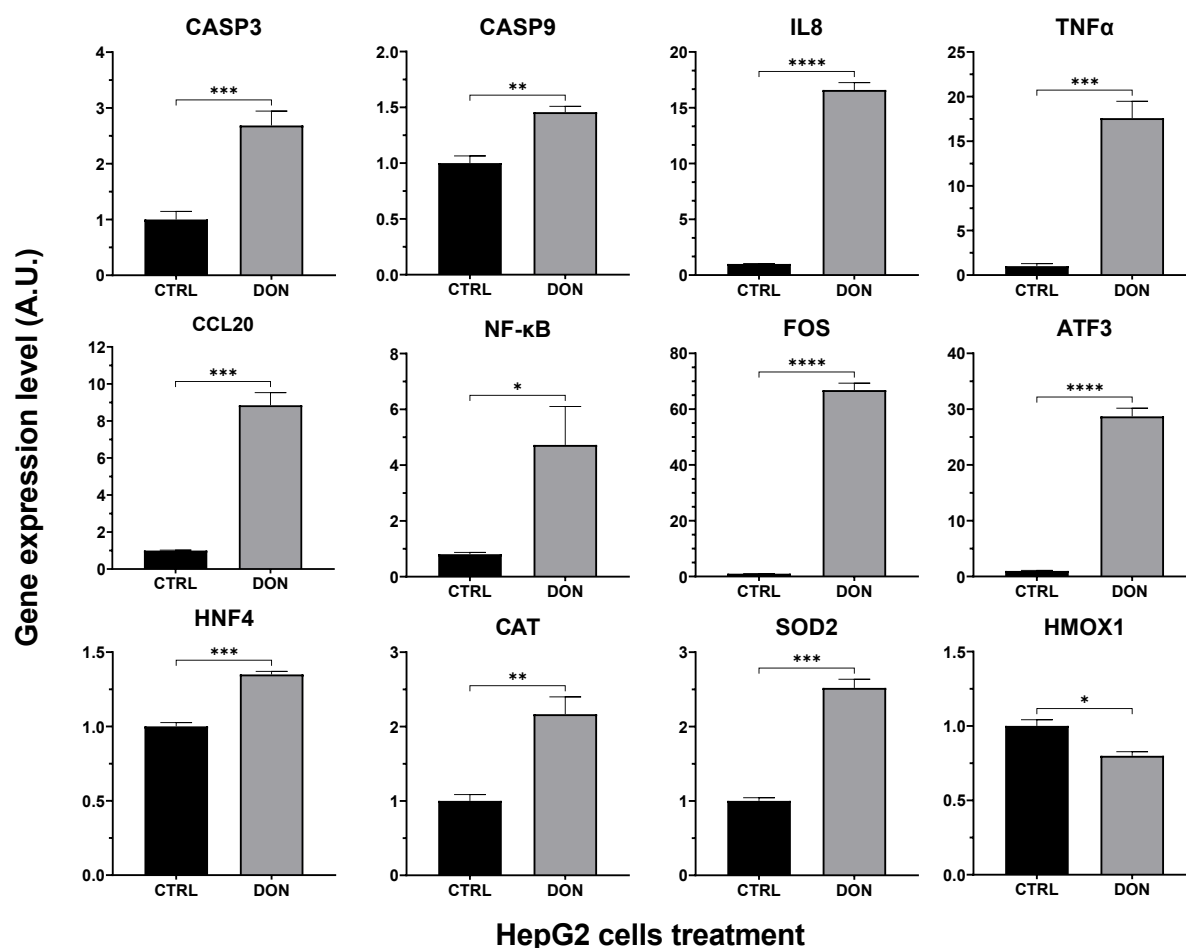
160

161 To complete the analysis of the hepatic toxicity of DON, the abundance of genes involved in
 162 apoptosis, inflammation, and oxidative stress were evaluated by RT-qPCR. The liver is exposed to a
 163 multitude of xenobiotics, including mycotoxins. Being the primary target tissue and main metabolizer
 164 of many xenobiotics, it is very sensitive to tissue injury leading to cell apoptosis. We thus evaluated the
 165 expression of genes involved in apoptosis. We observed that the expression of caspase-3 (CASP3) and
 166 caspase-9 (CASP9) increased in HepG2 exposed to DON (2.7- and 1.4-fold, respectively) (Figure 2).

167 Besides its metabolic role, the liver is also a key tissue involved in the immune system (Kubes and
 168 Jenne, 2018). For this reason, we also assessed the expression of cytokine genes. Upon exposure to
 169 DON, increased expression of interleukin 8 (IL8) (16.6-fold), tumor necrosis factor α (TNF α) (17.6-
 170 fold), and the C-C motif chemokine ligand 20 (CCL20) (8.8-fold) was observed, but no changes in

171 interleukin 1 α (IL1 α) (Figure 2). The expression of the transcription factor nuclear factor-kappa B (NF-
 172 κ B) (4.7-fold), which controls the transcription of many inflammatory cytokines, was also found to be
 173 up-regulated upon exposure to DON (Figure 2). Similarly, the Fos proto-oncogene (FOS) (66.8-fold),
 174 the expression of activating transcription factor 3 (ATF3) (28.7-fold), and of hepatocyte nuclear factor
 175 4 α (HNF4) (1.3-fold) were increased upon exposure to DON (Figure 2).

176 DON, like other mycotoxins, can induce oxidative stress in the liver. Thus, the last set of genes
 177 tested concerned enzymes involved in oxidative stress. In HepG2 cells, a significant increase (2.2-fold)
 178 only in the catalase (CAT) and superoxide dismutase 2 (SOD2) (2.5-fold) genes, and a (0.7-fold)
 179 decrease in heme oxygenase 1 (HMOX1) were observed (Figure 2).



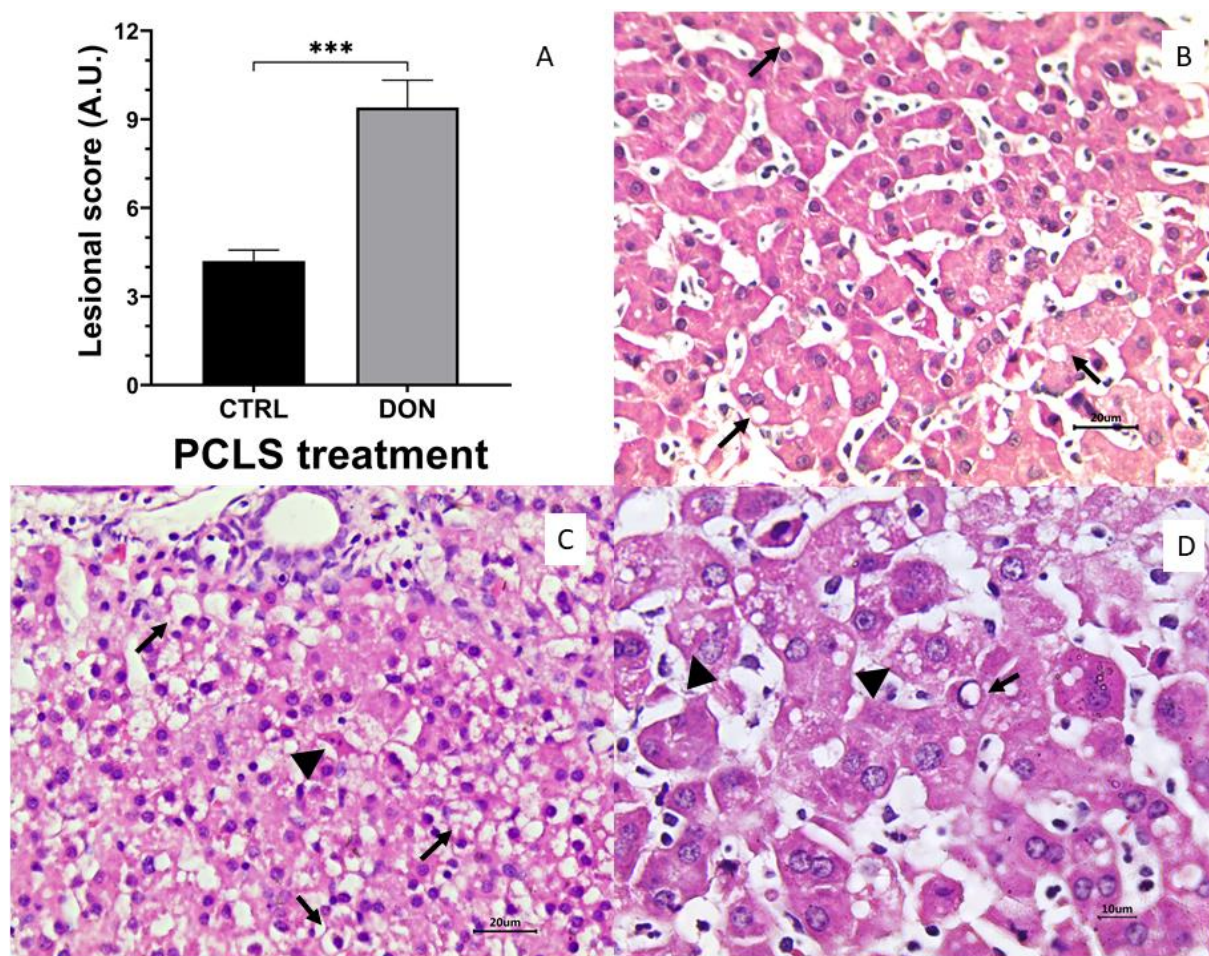
180

181 **Figure 2.** Apoptosis, inflammatory, transcription factors, and oxidative stress mRNA levels measured
 182 by RT-PCR in HepG2 cells exposed or not to 10 μ M DON for 4 h. Data are presented as mean \pm SEM
 183 of six replicates, * $p \leq 0.05$, ** $p \leq 0.01$, *** $p \leq 0.001$, and **** $p \leq 0.0001$.

184 3.2 Effects of DON on PCLS

185 To not limit our observations to a hepatic cell line, experiments were also performed on porcine
 186 PCLS. This later model has the advantage to include all liver cell types within the context of a preserved
 187 hepatic architecture, including the conservation of intercellular and cell-matrix interactions (de Graaf et
 188 al., 2010).

189 The hepatic effects of DON were first assessed histologically. A significant increase in the lesion
 190 score was observed in DON-treated PCLS ($p \leq 0.001$). The main histological changes in PCLS were
 191 disorganization of hepatic cords, apoptosis, and cytoplasmic vacuolation of hepatocytes (Figure 3).
 192 Despite damages to the tissue, we observed no significant increase in biomarkers of liver injury (alanine
 193 transaminase - ALT, aspartate aminotransferase – AST, and lactate dehydrogenase - LDH), cholestasis
 194 (alkaline phosphatase - ALP), or hepatic function (total proteins) in the PCLS supernatant upon DON
 195 treatment (Supplementary data - Table S1).

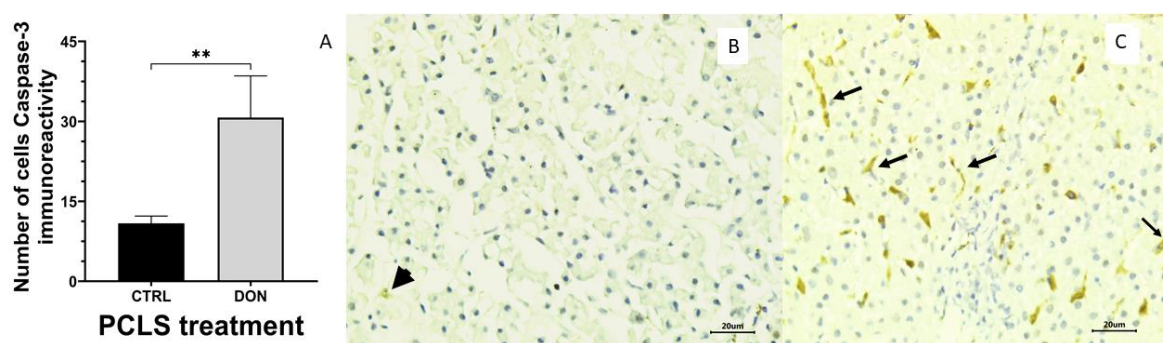


196

197 **Figure 3.** Effects of 4 h DON exposure on PCLS. A- Lesion score (A.U. – arbitrary units). Data are
 198 presented as mean \pm SEM of five different animals, *** $p \leq 0.001$. B- control group. Mild disorganization
 199 of hepatocytes trabeculae and cytoplasmic vacuolation (arrows). HE. Scale bar 20 μ m. C – DON group.

200 Moderate cytoplasmic vacuolation of hepatocytes (arrows) and apoptosis (arrowhead). HE. Scale bar 20
 201 μm . D- DON group. Cytoplasmic vacuolation (arrowheads) and nuclear vacuolation (arrows) of
 202 hepatocytes. HE. Scale bar 10 μm .

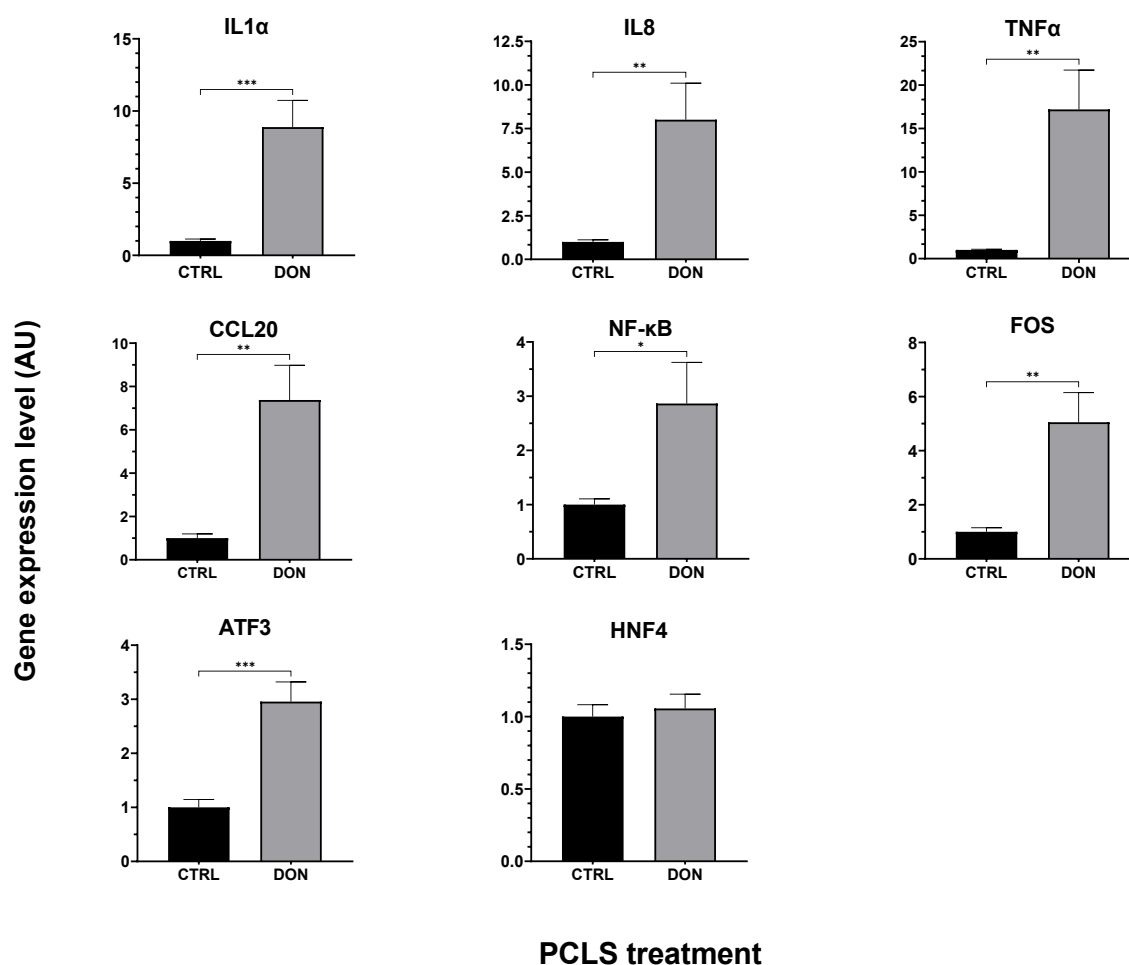
203 Because apoptosis was an important histological finding in DON-exposed PCLS, we sought to
 204 confirm activation of a cysteine protease, caspase-3 (CASP3), a key effector in cell apoptosis. A
 205 significant increase in CASP3 immunostaining was observed in the treated group ($p \leq 0.01$) compared to
 206 the control (Figure 4). The brownish immunostaining was randomly distributed in hepatocytes and
 207 Kupffer cells.



208

209 **Figure 4.** Analysis of apoptosis in PCLS. A- Mean number of immunoreactive cells for CASP3 in
 210 PCLS/field. Data are presented as mean \pm SEM of five different animals), $**p \leq 0.01$. B–C-
 211 Immunoperoxidase staining. B- control group. Mild positive CASP3 staining (arrowhead). Scale bar 20
 212 μm . C- DON group. Moderate CASP3 positive staining in hepatocytes and Kupffer cells (arrows). Scale
 213 bar 20 μm .

214 Next, we investigated the effect of DON on gene expression. As already observed in HepG2 cells,
 215 exposure of PCLS to 10 μM DON stimulates the expression of IL8 (8-fold), TNF α (17.2-fold), and
 216 CCL20 (7.4-fold) (Figure 5). In these samples, DON also induced the expression of IL1 α (8.9-fold).
 217 Like HepG2, DON upregulated in PCLS the transcription factors NF- κB , FOS, and ATF3 (2.9-, 5-, and
 218 3-fold, respectively) (Figure 5).



219

220 **Figure 5.** Inflammatory and transcription factors mRNA levels measured by RT-PCR in PCLS exposed
 221 or not to DON for 4 h. Data are mean ± SEM from 9 different animals. *p ≤ 0.05, **p ≤ 0.01, and ***p
 222 ≤ 0.001.

223 By contrast in PCLS, no significant differences were observed in the expression of any of the
 224 oxidative stress genes analyzed (data not shown).

225 4. Discussion

226 Many studies have reported an effect of DON on the intestine and the lymphoid organs (Luo et al.,
 227 2019; Novak et al., 2021; Pinton and Oswald, 2014), but investigations on the impact of DON on the
 228 liver are scarce. The present study evaluated the effects of DON on liver tissue, particularly PCLS. The
 229 human hepatocyte cell line, HepG2, was used for comparison.

230 Due to the difficulties in accessing human liver samples, the study was performed on porcine PCLS.
 231 Pig is considered a good model for extrapolation to humans (Helke and Swindle, 2013). PCLS retain

232 the original three-dimensional structure of the liver, preserve hepatocytes and Kupffer cells as well as
233 cellular crosstalk and cell-matrix interactions (de Graaf et al., 2010). PCLS thus appear to be highly
234 suitable for studies of the toxic effects of food contaminants. This model has two main advantages, (i)
235 cultured explants are in line with 3R principles, as one animal allows the assessment of multiple doses
236 and (ii) it gives access to a fully differentiated three-dimensional model for histopathology assessment.
237 A few studies using rat PCLS have addressed the effects of mycotoxins, one assessed the effect of
238 fumonisin B1 on sphingoid base (Norred et al., 1996), another one the impact of aflatoxins on RNA
239 synthesis (Friedman et al., 1997), and a third one described the metabolization of *Alternaria* toxins into
240 potentially toxic compounds (Burkhardt et al., 2011).

241 A cytotoxic effect of DON was observed in HepG2 cells at low concentrations (0.8-1.6 μM),
242 regardless of the duration of exposure (4, 24, and 48 h). The decrease observed at these low
243 concentrations after 24 h is in agreement with the results of previous studies (Darwish et al., 2020;
244 Mayer et al., 2017) indicating that short exposure to realistic doses of DON alters hepatic cells.

245 Damages to the tissue were observed in PCLS exposed to DON, despite the short time of exposure
246 (4 h), but no changes in markers of liver function or injury. Thus, histology can be considered a sensitive
247 endpoint for liver damage. In PCLS, disorganization of hepatic cords, apoptosis, and cytoplasmic
248 vacuolation of hepatocytes were observed after 4 h of exposure to 10 μM DON. These histological
249 changes are similar to those obtained in subchronic *in vivo* trials. Indeed, disorganization of hepatic
250 cords, apoptosis, cytoplasmic and nuclear vacuolation of hepatocytes, megalocytosis, and focal necrosis
251 were observed in piglets or gilts fed diets contaminated with 0.012 to 3 mg/kg DON for one to six weeks
252 (Bracarense et al., 2020; Gerez et al., 2015; Grenier et al., 2011; Pierron et al., 2018; Skiepkowski et al.,
253 2020).

254 The cytoplasmic vacuolation observed in PCLS may be related to the DON-induced impairment of
255 mitochondrial function (Springler et al., 2017). Indeed, mitochondrial dysfunction leads to failure of the
256 Na^+/K^+ -ATPase pump causing an influx of Na^+ , Ca^{+2} , and water into the cytosol, inducing, cytoplasmic
257 vacuolation (Miller and Zachary, 2017). Moreover, an increased number of apoptotic hepatocytes and
258 cells in hepatic sinusoids was observed in gilts exposed to a fusariotoxins-contaminated diet (Dolenšek
259 et al., 2021).

260 Apoptosis observed in PCLS was confirmed by immunostaining of CASP3. Liver apoptosis has
261 already been reported in piglets injected intra-venously with DON (Mikami et al., 2010) as well as in
262 mice and pigs fed a DON-contaminated diet (Bracarense et al., 2017; Gerez et al., 2015; Sun et al.,
263 2014). Apoptosis can occur via different pathways (Elmore, 2007). The extrinsic pathway induced by
264 transmembrane death-receptor interactions activates CASP8 and subsequently CASP3. The intrinsic or
265 mitochondrial pathway involves intracellular signals such as p53, resulting in the activation of CASP9
266 and subsequently of CASP3 (van Cruchten and van den Broeck, 2002). In the present study, we observed
267 upregulation of both CASP3 and CAPS9. CASP9 activation suggests that in the liver the intrinsic
268 pathway is involved in DON-induced apoptosis, as already demonstrated in the intestine (Payros et al.,
269 2021b). In the same way as observed for the histological evaluation of PCLS exposed to DON, it should
270 be noted that the evaluation of apoptosis has revealed similar effects to those observed *in vivo* in different
271 species.

272 DON is known to activate the inflammatory response. Indeed, DON-induced ribotoxic stress leads
273 to the activation of the MAPK1/2 pathway, which in turn activates several immediate-early genes and
274 induces the production of cytokines, the expression of cyclooxygenase-2 (COX2), and apoptosis
275 (Pestka, 2010a; Pierron et al., 2016) in different target organs (Payros et al., 2016; Pestka, 2010a). In
276 the present study, we observed overexpression of various cytokines in both HepG2 and PCLS. Such
277 pro-inflammatory expression patterns have already been observed in the liver of pigs and rats fed a
278 DON-contaminated diet (Abdel-Wahhab et al., 2015; Chen et al., 2008). In our study, IL1 α gene
279 expression was only upregulated in PCLS. This difference might be due to the presence of Kupffer cells
280 in hepatic tissue that are known to produce high levels of this cytokine (Bilzer et al., 2006) in the liver
281 (Bai et al., 2021). The IL1 α was also shown to be expressed in the intestine after *in vivo* exposure to
282 DON (Pestka, 2010b). Taken together, these results show that pro-inflammatory cytokines are sensitive
283 markers when the liver is exposed to DON and that such inflammation can be observed *in vitro*
284 (hepatocytes), *ex vivo* (PCLS), and *in vivo*.

285 Concerning transcription factors, DON-activation of MAPK pathway activates immediate-early
286 genes, such as FOS and ATF3, in turn promoting the expression of COX2, cytokines, and apoptosis
287 (Nielsen et al., 2009; Smith et al., 2017b; Sun et al., 2015; Yuan et al., 2018). In the present study, we

288 demonstrated an increase in the expression of FOS, ATF3 in PCLS, and of HNF4 only, in the cells.
289 ATF3 reveals endoplasmic reticulum (ER) stress. In absence of relief of ER, cells can go into apoptosis
290 (Holtz et al., 2006; Li et al., 2006). FOS is highly induced in HepG2 cells, probably due to its
291 stabilization by sustained extracellular signal-regulated kinase (ERK) signaling (Murphy et al., 2002).
292 In HepG2 cells, but not in PCLS, we observed increased expression of HNF4, a transcription factor that
293 controls the expression of several hepatic-specific genes involved in hepatic metabolism (Madec et al.,
294 2011; Petrescu et al., 2002). The cancerous origin of HepG2 cells, which involves different demands on
295 metabolic processes (Coller, 2014), could explain the high induction of these transcription factors.

296 **5. Conclusions**

297 We observed that short exposure to DON reduces HepG2 cells viability and induces toxic effects
298 on hepatic cells and liver tissue. In particular, we demonstrated that in accordance with the effects
299 observed in pigs fed a DON-contaminated diet, this toxin induces the expression of genes involved in
300 liver apoptosis and inflammation and histological damages.

301 To the best of our knowledge, this is the first study to use PCLS for the identification of DON toxic
302 effects on liver structure and functions.

303 Pig PCLS is a promising model to study the effects of DON, and potentially other mycotoxins on
304 the liver. It enables the demonstration of histomorphological and molecular effects at realistic dietary
305 levels, in very good accordance with data obtained in in vivo trials. As pig is a good model for
306 extrapolation to humans and is very sensitive to mycotoxins, particularly to DON, our results are
307 relevant for progressing towards a better assessment of human consumers' risk related to mycotoxins.

308 **Author Contributions:** “Conceptualization, A.L.H, P.P., A.P.B, and I.P.O.; methodology, P.P., A.L.H.,
309 A.K., E.P. S.B.; validation, A.L.H., S.P., and A.K.; formal analysis, A.L.H., P.P., and A.P.B.;
310 investigation, A.L.H., A.P.B, P.P., A.K., S.P., S.B. and E.P.; resources, A.P.B. and P.P.; data curation,
311 A.L.H. and P.P.; writing—original draft preparation, A.L.H.; writing—review and editing, A.L.H,
312 A.P.B., P.P., and I.P.O.; visualization, A.L.H. and P.P.; supervision, A.P.B and I.P.O.; project
313 administration, A.L.H, P.P.; funding acquisition, A.P.B., I.P.O., and P.P. All authors have read and
314 agreed to the published version of the manuscript.”

315 **Funding:** A.L.H received a fellowship from the Coordenação de Aperfeiçoamento de Pessoal de Nível
316 Superior-CAPES/Cofecub, grant number 0389/2019. This research was supported by the ANR grant
317 “EmergingMyco” (ANR-18-CE34-0014).

318 **Acknowledgments:** The authors would like to express their gratitude to the residents and Ricardo L. N.
319 de Matos in the Laboratory of Animal Pathology (UEL) for their practical support during histological
320 analyses, to Mikael Albin (INRAE-Toxalim) for animal experiment phases and to Claire Naylies and
321 Yannick Lippi for their contribution to qPCR experiments performed at GeT-TRiX Genopole Toulouse
322 Midi-Pyrénées facility.

323 **Appendix A:** Supplementary data to this article can be found online at: [https://doi.](https://doi.org/10.1016/j.fct.2022.112930)
324 [org/10.1016/j.fct.2022.112930](https://doi.org/10.1016/j.fct.2022.112930).

325 **Conflicts of Interest:** The authors have no conflict of interest to declare.

326 **References**

- 327 Abdel-Wahhab, M.A., El-Kady, A.A., Hassan, A.M., Abd El-Moneim, O.M., Abdel-Aziem, S.H., 2015.
 328 Effectiveness of Activated Carbon and Egyptian Montmorillonite in the Protection Against
 329 Deoxynivalenol-induced Cytotoxicity and Genotoxicity in Rats. *Food and Chemical Toxicology*
 330 83, 174–182. <https://doi.org/10.1016/j.fct.2015.06.015>
- 331 Alassane-Kpembi, I., Gerez, J.R., Cossalter, A.-M., Neves, M., Laffitte, J., Naylies, C., Lippi, Y., Kolf-
 332 Clauw, M., Bracarense, A.P.L., Pinton, P., Oswald, I.P., 2017a. Intestinal Toxicity of the Type B
 333 Trichothecene Mycotoxin Fusarenon-X: Whole Transcriptome Profiling Reveals New Signaling
 334 Pathways. *Scientific Reports* 7, 7530. <https://doi.org/10.1038/s41598-017-07155-2>
- 335 Alassane-Kpembi, I., Puel, O., Pinton, P., Cossalter, A.-M., Chou, T.-C., Oswald, I.P., 2017b. Co-
 336 exposure to low doses of the food contaminants deoxynivalenol and nivalenol has a synergistic
 337 inflammatory effect on intestinal explants. *Archives of Toxicology* 91, 2677–2687.
 338 <https://doi.org/10.1007/s00204-016-1902-9>
- 339 Andersen, C.L., Jensen, J.L., Ørntoft, T.F., 2004. Normalization of Real-Time Quantitative Reverse
 340 Transcription-PCR Data: A Model-Based Variance Estimation Approach to Identify Genes Suited
 341 for Normalization, Applied to Bladder and Colon Cancer Data Sets. *Cancer Research* 64, 5245–
 342 5250. <https://doi.org/10.1158/0008-5472.CAN-04-0496>
- 343 Bai, Y., Ma, K., Li, Jibo, Li, Jianping, Bi, C., Shan, A., 2021. Deoxynivalenol exposure induces liver
 344 damage in mice: Inflammation and immune responses, oxidative stress, and protective effects of
 345 *Lactobacillus rhamnosus* GG. *Food and Chemical Toxicology* 156, 112514.
 346 <https://doi.org/10.1016/j.fct.2021.112514>
- 347 Bilzer, M., Roggel, F., Gerbes, A.L., 2006. Role of Kupffer Cells in Host Defense and Liver Disease.
 348 *Liver International* 26, 1175–1186. <https://doi.org/10.1111/j.1478-3231.2006.01342.x>
- 349 Bracarense, A.P.F.L., Basso, K.M., da Silva, E.O., Payros, D., Oswald, I.P., 2017. Deoxynivalenol in
 350 the Liver and Lymphoid Organs of Rats: Effects of Dose and Duration on Immunohistological
 351 Changes. *World Mycotoxin Journal* 10, 89–96. <https://doi.org/10.3920/WMJ2016.2094>
- 352 Bracarense, A.P.F.L., Luciola, J., Grenier, B., Drociunas Pacheco, G., Moll, W.D., Schatzmayr, G.,
 353 Oswald, I.P., 2012. Chronic ingestion of deoxynivalenol and fumonisin, alone or in interaction,
 354 induces morphological and immunological changes in the intestine of piglets. *British Journal of*
 355 *Nutrition* 107, 1776–1786. <https://doi.org/10.1017/S0007114511004946>
- 356 Bracarense, A.P.F.L., Pierron, A., Pinton, P., Gerez, J.R., Schatzmayr, G., Moll, W.D., Zhou, T.,
 357 Oswald, I.P., 2020. Reduced Toxicity of 3-epi-deoxynivalenol and De-epoxy-deoxynivalenol
 358 through Deoxynivalenol Bacterial Biotransformation: In Vivo Analysis in Piglets. *Food and*
 359 *Chemical Toxicology* 140, 111241. <https://doi.org/10.1016/j.fct.2020.111241>
- 360 Burkhardt, B., Wittenauer, J., Pfeiffer, E., Schauer, U.M.D., Metzler, M., 2011. Oxidative metabolism
 361 of the mycotoxins alternariol and alternariol-9-methyl ether in precision-cut rat liver slices in vitro.
 362 *Molecular Nutrition & Food Research* 55, 1079–1086. <https://doi.org/10.1002/mnfr.201000487>
- 363 Chen, F., Ma, Y., Xue, C., Ma, J., Xie, Q., Wang, G., Bi, Y., Cao, Y., 2008. The combination of
 364 Deoxynivalenol and Zearalenone at Permitted Feed Concentrations Causes Serious Physiological
 365 Effects in Young Pigs. *Journal of Veterinary Science* 9, 39. <https://doi.org/10.4142/jvs.2008.9.1.39>
- 366 Coller, H.A., 2014. Is Cancer a Metabolic Disease? *The American Journal of Pathology* 184, 4–17.
 367 <https://doi.org/10.1016/j.ajpath.2013.07.035>
- 368 Darwish, W.S., Chen, Z., Li, Y., Tan, H., Chiba, H., Hui, S.-P., 2020. Deoxynivalenol-induced
 369 alterations in the redox status of HepG2 cells: identification of lipid hydroperoxides, the role of
 370 Nrf2-Keap1 signaling, and protective effects of zinc. *Mycotoxin Research* 36, 287–299.
 371 <https://doi.org/10.1007/s12550-020-00392-x>
- 372 de Graaf, I.A.M., Olinga, P., de Jager, M.H., Merema, M.T., de Kanter, R., van de Kerkhof, E.G.,

- 373 Groothuis, G.M.M., 2010. Preparation and incubation of precision-cut liver and intestinal slices
374 for application in drug metabolism and toxicity studies. *Nature Protocols* 5, 1540–1551.
375 <https://doi.org/10.1038/nprot.2010.111>
- 376 Dewyse, L., Reynaert, H., van Grunsven, L.A., 2021. Best Practices and Progress in Precision-Cut Liver
377 Slice Cultures. *International Journal of Molecular Sciences* 22, 7137.
378 <https://doi.org/10.3390/ijms22137137>
- 379 Dolenšek, T., Švara, T., Knific, T., Gombač, M., Luzar, B., Jakovac-Strajn, B., 2021. The Influence of
380 *Fusarium* Mycotoxins on the Liver of Gilts and Their Suckling Piglets. *Animals* 11, 2534.
381 <https://doi.org/10.3390/ani11092534>
- 382 Elmore, S., 2007. Apoptosis: A Review of Programmed Cell Death. *Toxicologic Pathology* 35, 495–
383 516. <https://doi.org/10.1080/01926230701320337>
- 384 Eskola, M., Kos, G., Elliott, C.T., Hajšlová, J., Mayar, S., Krska, R., 2020. Worldwide contamination
385 of food-crops with mycotoxins: Validity of the widely cited ‘FAO estimate’ of 25%. *Critical*
386 *Reviews in Food Science and Nutrition* 60, 2773–2789.
387 <https://doi.org/10.1080/10408398.2019.1658570>
- 388 Fernández-Blanco, C., Elmo, L., Waldner, T., Ruiz, M., 2018. Cytotoxic Effects Induced by Patulin,
389 Deoxynivalenol and Toxin T2 Individually and in Combination in Hepatic Cells (HepG2). *Food*
390 *and Chemical Toxicology* 120, 12–23. <https://doi.org/10.1016/j.fct.2018.06.019>
- 391 Friedman, L., Gaines, D.W., Chi, R.K., Smith, M.C., Braunberg, R.C., Thorpe, C.W., 1997.
392 INTERACTION OF AFLATOXINS AS MEASURED BY THEIR BIOCHEMICAL ACTION ON
393 RAT LIVER SLICES AND HEPATOCYTES. *Toxic Substance Mechanisms* 16, 15–42.
394 <https://doi.org/10.1080/107691897229775>
- 395 Gerez, J.R., Camacho, T., Brunaldi Marutani, V.H., Nascimento de Matos, R.L., Hohmann, M.S., Verri
396 Júnior, W.A., Bracarense, A.P.F.R.L., 2021. Ovarian toxicity by fusariotoxins in pigs: Does it
397 imply in oxidative stress? *Theriogenology* 165, 84–91.
398 <https://doi.org/10.1016/j.theriogenology.2021.02.003>
- 399 Gerez, J.R., Desto, S.S., Bracarense, A.P.F.R.L., 2017. Deoxynivalenol induces toxic effects in the
400 ovaries of pigs: An ex vivo approach. *Theriogenology* 90, 94–100.
401 <https://doi.org/10.1016/j.theriogenology.2016.10.023>
- 402 Gerez, J.R., Pinton, P., Callu, P., Grosjean, F., Oswald, I.P., Bracarense, A.P.F.L., 2015. Deoxynivalenol
403 Alone or in Combination with Nivalenol and Zearalenone Induce Systemic Histological Changes
404 in Pigs. *Experimental and Toxicologic Pathology* 67, 89–98.
405 <https://doi.org/10.1016/j.etp.2014.10.001>
- 406 Grenier, B., Bracarense, A.-P.F.L., Schwartz, H.E., Trumel, C., Cossalter, A.-M., Schatzmayr, G., Kolf-
407 Clauw, M., Moll, W.-D., Oswald, I.P., 2012. The low intestinal and hepatic toxicity of hydrolyzed
408 fumonisin B1 correlates with its inability to alter the metabolism of sphingolipids. *Biochemical*
409 *Pharmacology* 83, 1465–1473. <https://doi.org/10.1016/j.bcp.2012.02.007>
- 410 Grenier, B., Loureiro-Bracarense, A.-P., Luciola, J., Pacheco, G.D., Cossalter, A.-M., Moll, W.-D.,
411 Schatzmayr, G., Oswald, I.P., 2011. Individual and Combined Effects of Subclinical Doses of
412 Deoxynivalenol and Fumonisin in Piglets. *Molecular Nutrition & Food Research* 55, 761–771.
413 <https://doi.org/10.1002/mnfr.201000402>
- 414 Helke, K.L., Swindle, M.M., 2013. Animal models of toxicology testing: the role of pigs. *Expert*
415 *Opinion on Drug Metabolism & Toxicology* 9, 127–139.
416 <https://doi.org/10.1517/17425255.2013.739607>
- 417 Holtz, W.A., Turetzky, J.M., Jong, Y.-J.I., O’Malley, K.L., 2006. Oxidative stress-triggered unfolded
418 protein response is upstream of intrinsic cell death evoked by parkinsonian mimetics. *Journal of*
419 *Neurochemistry* 99, 54–69. <https://doi.org/10.1111/j.1471-4159.2006.04025.x>
- 420 Kasper, H.-U., Dries, V., Drebber, U., Kern, M.A., Dienes, H.P., Schirmacher, P., 2005. Precision cut

- 421 tissue slices of the liver as morphological tool for investigation of apoptosis. *In vivo* (Athens,
422 Greece) 19, 423–31.
- 423 Knutsen, H.K., Alexander, J., Barregård, L., Bignami, M., Brüschweiler, B., Ceccatelli, S., Cottrill, B.,
424 Dinovi, M., Grasl-Kraupp, B., Hogstrand, C., Hoogenboom, L. (Ron), Nebbia, C.S., Oswald, I.P.,
425 Petersen, A., Rose, M., Roudot, A., Schwerdtle, T., Vleminckx, C., Vollmer, G., Wallace, H., de
426 Saeger, S., Eriksen, G.S., Farmer, P., Fremy, J., Gong, Y.Y., Meyer, K., Naegeli, H., Parent-Massin,
427 D., Rietjens, I., van Egmond, H., Altieri, A., Eskola, M., Gergelova, P., Ramos Bordajandi, L.,
428 Benkova, B., Dörr, B., Gkrillas, A., Gustavsson, N., van Manen, M., Edler, L., 2017. Risks to
429 human and animal health related to the presence of deoxynivalenol and its acetylated and modified
430 forms in food and feed. *EFSA Journal* 15. <https://doi.org/10.2903/j.efsa.2017.4718>
- 431 Kubes, P., Jenne, C., 2018. Immune Responses in the Liver. *Annual Review of Immunology* 36, 247–
432 277. <https://doi.org/10.1146/annurev-immunol-051116-052415>
- 433 Li, J., Lee, B., Lee, A.S., 2006. Endoplasmic Reticulum Stress-induced Apoptosis. *Journal of Biological*
434 *Chemistry* 281, 7260–7270. <https://doi.org/10.1074/jbc.M509868200>
- 435 Luo, S., Terciolo, C., Bracarense, A.P.F.L., Payros, D., Pinton, P., Oswald, I.P., 2019. *In Vitro* and *In*
436 *Vivo* Effects of a Mycotoxin, Deoxynivalenol, and a Trace Metal, Cadmium, Alone or in a Mixture
437 on the Intestinal Barrier. *Environment International* 132, 105082.
438 <https://doi.org/10.1016/j.envint.2019.105082>
- 439 Luo, S., Terciolo, C., Neves, M., Puel, S., Naylies, C., Lippi, Y., Pinton, P., Oswald, I.P., 2021.
440 Comparative sensitivity of proliferative and differentiated intestinal epithelial cells to the food
441 contaminant, deoxynivalenol. *Environmental Pollution* 277, 116818.
442 <https://doi.org/10.1016/j.envpol.2021.116818>
- 443 Madec, S., Cerec, V., Plée-Gautier, E., Antoun, J., Glaise, D., Salaun, J.-P., Guguen-Guillouzo, C.,
444 Corlu, A., 2011. CYP4F3B Expression Is Associated with Differentiation of HepaRG Human
445 Hepatocytes and Unaffected by Fatty Acid Overload. *Drug Metabolism and Disposition* 39, 1987–
446 1996. <https://doi.org/10.1124/dmd.110.036848>
- 447 Maresca, M., Pinton, P., Ajandouz, E.H., Menard, S., Ferrier, L., Oswald, I.P., 2018. Overview and
448 Comparison of Intestinal Organotypic Models, Intestinal Cells, and Intestinal Explants Used for
449 Toxicity Studies, in: *Current Topics in Microbiology and Immunology*. Springer Science and
450 Business Media Deutschland GmbH, pp. 247–264. https://doi.org/10.1007/82_2018_142
- 451 Maruo, V., Bracarense, A.P.F.R.L., Metayer, J.-P., Vilarino, M., Oswald, I., Pinton, P., 2018. Ergot
452 Alkaloids at Doses Close to EU Regulatory Limits Induce Alterations of the Liver and Intestine.
453 *Toxins* 10, 183. <https://doi.org/10.3390/toxins10050183>
- 454 Mayer, E., Novak, B., Springler, A., Schwartz-Zimmermann, H.E., Nagl, V., Reisinger, N.,
455 Hessenberger, S., Schatzmayr, G., 2017. Effects of Deoxynivalenol (DON) and its Microbial
456 Biotransformation Product Deepoxy-deoxynivalenol (DOM-1) on a Trout, Pig, mouse, and Human
457 Cell Line. *Mycotoxin Research* 33, 297–308. <https://doi.org/10.1007/s12550-017-0289-7>
- 458 Mikami, O., Yamaguchi, H., Murata, H., Nakajima, Y., Miyazaki, S., 2010. Induction of Apoptotic
459 Lesions in Liver and Lymphoid Tissues and Modulation of Cytokine mRNA Expression by Acute
460 Exposure to Deoxynivalenol in Piglets. *Journal of Veterinary Science* 11, 107–113.
461 <https://doi.org/10.4142/jvs.2010.11.2.107>
- 462 Miller, M.A., Zachary, J.F., 2017. Mechanisms and Morphology of Cellular Injury, Adaptation, and
463 Death, in: Zachary, J.F. (Ed.), *Pathologic Basis of Veterinary Disease*. Elsevier, St. Louis, pp. 2-
464 43.e19. <https://doi.org/10.1016/B978-0-323-35775-3.00001-1>
- 465 Murphy, L.O., Smith, S., Chen, R.-H., Fingar, D.C., Blenis, J., 2002. Molecular interpretation of ERK
466 signal duration by immediate early gene products. *Nature Cell Biology* 4, 556–564.
467 <https://doi.org/10.1038/ncb822>
- 468 Narváez, A., Castaldo, L., Izzo, L., Pallarés, N., Rodríguez-Carrasco, Y., Ritieni, A., 2022.

- 469 Deoxynivalenol contamination in cereal-based foodstuffs from Spain: Systematic review and meta-
470 analysis approach for exposure assessment. *Food Control* 132, 108521.
471 <https://doi.org/10.1016/j.foodcont.2021.108521>
- 472 Nielsen, C., Lippke, H., Didier, A., Dietrich, R., Märtlbauer, E., 2009. Potential of deoxynivalenol to
473 induce transcription factors in human hepatoma cells. *Molecular Nutrition & Food Research* 53,
474 479–491. <https://doi.org/10.1002/mnfr.200800475>
- 475 Norred, W.P., Riley, R.T., Meredith, F.I., Bacon, C.W., Voss, K.A., 1996. Time- and dose-response
476 effects of the mycotoxin, fumonisin B1 on sphingoid base elevations in precision-cut rat liver and
477 kidney slices. *Toxicology in Vitro* 10, 349–358. [https://doi.org/10.1016/0887-2333\(96\)00013-6](https://doi.org/10.1016/0887-2333(96)00013-6)
- 478 Novak, B., Hasuda, A.L., Ghanbari, M., Mayumi Maruo, V., Bracarense, A.P.F.R.L., Neves, M.,
479 Emsenhuber, C., Wein, S., Oswald, I.P., Pinton, P., Schatzmayr, D., 2021. Effects of Fusarium
480 metabolites beauvericin and enniatins alone or in mixture with deoxynivalenol on weaning piglets.
481 *Food and Chemical Toxicology* 158, 112719. <https://doi.org/10.1016/j.fct.2021.112719>
- 482 Oliveira, M.S., Rocha, A., Sulyok, M., Krska, R., Mallmann, C.A., 2017. Natural Mycotoxin
483 Contamination of Maize (*Zea mays* L.) in the South Region of Brazil. *Food Control* 73, 127–132.
484 <https://doi.org/10.1016/j.foodcont.2016.07.033>
- 485 Palma, E., Doornebal, E.J., Chokshi, S., 2019. Precision-cut liver slices: a versatile tool to advance liver
486 research. *Hepatology International* 13, 51–57. <https://doi.org/10.1007/s12072-018-9913-7>
- 487 Payros, D., Alassane-Kpembé, I., Laffitte, J., Lencina, C., Neves, M., Bracarense, A.P., Pinton, P.,
488 Ménard, S., Oswald, I.P., 2021a. Dietary Exposure to the Food Contaminant Deoxynivalenol
489 Triggers Colonic Breakdown by Activating the Mitochondrial and the Death Receptor Pathways.
490 *Molecular Nutrition & Food Research* 2100191. <https://doi.org/10.1002/mnfr.202100191>
- 491 Payros, D., Alassane-Kpembé, I., Pierron, A., Loiseau, N., Pinton, P., Oswald, I.P., 2016. Toxicology of
492 deoxynivalenol and its acetylated and modified forms. *Archives of Toxicology* 90, 2931–2957.
493 <https://doi.org/10.1007/s00204-016-1826-4>
- 494 Payros, D., Garofalo, M., Pierron, A., Soler-Vasco, L., Al-Ayoubi, C., Maruo, V.M., Alassane-Kpembé,
495 I., Pinton, P., Oswald, I.P., 2021b. Les mycotoxines en alimentation humaine : un défi pour la
496 recherche. *Cahiers de Nutrition et de Diététique* 56, 170–183.
497 <https://doi.org/10.1016/j.cnd.2021.02.001>
- 498 Pestka, J.J., 2010a. Deoxynivalenol-Induced Proinflammatory Gene Expression: Mechanisms and
499 Pathological Sequelae. *Toxins* 2, 1300–1317. <https://doi.org/10.3390/toxins2061300>
- 500 Pestka, J.J., 2010b. Deoxynivalenol: mechanisms of action, human exposure, and toxicological
501 relevance. *Archives of Toxicology* 84, 663–679. <https://doi.org/10.1007/s00204-010-0579-8>
- 502 Petrescu, A.D., Hertz, R., Bar-Tana, J., Schroeder, F., Kier, A.B., 2002. Ligand Specificity and
503 Conformational Dependence of the Hepatic Nuclear Factor-4 α (HNF-4 α). *Journal of Biological*
504 *Chemistry* 277, 23988–23999. <https://doi.org/10.1074/jbc.M201241200>
- 505 Pierron, A., Bracarense, A.P.F.L., Cossalter, A.M., Laffitte, J., Schwartz-Zimmermann, H.E.,
506 Schatzmayr, G., Pinton, P., Moll, W.D., Oswald, I.P., 2018. Deepoxy-deoxynivalenol Retains
507 Some Immune-modulatory Properties of the Parent Molecule Deoxynivalenol in Piglets. *Archives*
508 *of Toxicology* 92, 3381–3389. <https://doi.org/10.1007/s00204-018-2293-x>
- 509 Pierron, A., Mimoun, S., Murate, L.S., Loiseau, N., Lippi, Y., Bracarense, A.P.F.L., Liaubet, L.,
510 Schatzmayr, G., Berthiller, F., Moll, W.D., Oswald, I.P., 2016. Intestinal toxicity of the masked
511 mycotoxin deoxynivalenol-3- β -d-glucoside. *Archives of Toxicology* 90, 2037–2046.
512 <https://doi.org/10.1007/s00204-015-1592-8>
- 513 Pierron, A., Neves, M., Puel, S., Lippi, Y., Soler, L., Miller, J.D., Oswald, I.P., 2022. Intestinal toxicity
514 of the new type A trichothecenes, NX and 3ANX. *Chemosphere* 288, 132415.
515 <https://doi.org/10.1016/j.chemosphere.2021.132415>
- 516 Pinton, P., Accensi, F., Beauchamp, E., Cossalter, A.M., Callu, P., Grosjean, F., Oswald, I.P., 2008.

- 517 Ingestion of Deoxynivalenol (DON) Contaminated Feed Alters the Pig Vaccinal Immune
518 Responses. *Toxicology Letters* 177, 215–222. <https://doi.org/10.1016/j.toxlet.2008.01.015>
- 519 Pinton, P., Oswald, I.P., 2014. Trichothecenes on the Intestine: A Review. *Toxins* 6, 1615–1643.
520 <https://doi.org/10.3390/toxins60>
- 521 Robert, H., Payros, D., Pinton, P., Théodorou, V., Mercier-Bonin, M., Oswald, I.P., 2017. Impact of
522 mycotoxins on the intestine: are mucus and microbiota new targets? *Journal of Toxicology and*
523 *Environmental Health, Part B* 20, 249–275. <https://doi.org/10.1080/10937404.2017.1326071>
- 524 Ruan, F., Chen, J.G., Chen, L., Lin, X. tian, Zhou, Y., Zhu, K. jing, Guo, Y.T., Tan, A.J., 2020. Food
525 Poisoning Caused by Deoxynivalenol at a School in Zhuhai, Guangdong, China, in 2019.
526 *Foodborne Pathogens and Disease* 17, 429–433. <https://doi.org/10.1089/fpd.2019.2710>
- 527 Silva, E.O. da, Gerez, J.R., Drape, T. do C., Bracarense, A.P.F.R.L., 2014. Phytic Acid Decreases
528 Deoxynivalenol and Fumonisin B1-Induced Changes on Swine Jejunal Explants. *Toxicology*
529 *Reports* 1, 284–292. <https://doi.org/10.1016/j.toxrep.2014.05.001>
- 530 Silva, E.O. da, Gerez, J.R., Hohmann, M.S.N., Verri, W.A., Bracarense, A.P.F.R.L., 2019. Phytic Acid
531 Decreases Oxidative Stress and Intestinal Lesions Induced by Fumonisin B1 and Deoxynivalenol
532 in Intestinal Explants of Pigs. *Toxins* 11, 18. <https://doi.org/10.3390/toxins11010018>
- 533 Skiepkó, N., Przybylska-Gornowicz, B., Gajęcka, M., Gajęcki, M., Lewczuk, B., 2020. Effects of
534 Deoxynivalenol and Zearalenone on the Histology and Ultrastructure of Pig Liver. *Toxins* 12, 463.
535 <https://doi.org/10.3390/toxins12070463>
- 536 Smith, M.-C., Hymery, N., Troadec, S., Pawtowski, A., Coton, E., Madec, S., 2017a. Hepatotoxicity of
537 fusariotoxins, alone and in combination, towards the HepaRG human hepatocyte cell line. *Food*
538 *and Chemical Toxicology* 109, 439–451. <https://doi.org/10.1016/j.fct.2017.09.022>
- 539 Smith, M.-C., Madec, S., Pawtowski, A., Coton, E., Hymery, N., 2017b. Individual and Combined
540 Toxicological Effects of Deoxynivalenol and Zearalenone on Human Hepatocytes in In Vitro
541 Chronic Exposure Conditions. *Toxicology Letters* 280, 238–246.
542 <https://doi.org/10.1016/j.toxlet.2017.08.080>
- 543 Souza, M. de, Baptista, A.A.S., Valdiviezo, M.J.J., Justino, L., Menck-Costa, M.F., Ferraz, C.R., da
544 Gloria, E.M., Verri, W.A., Bracarense, A.P.F.R.L., 2020. *Lactobacillus* spp. Reduces
545 Morphological Changes and Oxidative Stress Induced by Deoxynivalenol on the Intestine and Liver
546 of Broilers. *Toxicon* 185, 203–212. <https://doi.org/10.1016/j.toxicon.2020.07.002>
- 547 Springler, A., Hessenberger, S., Reisinger, N., Kern, C., Nagl, V., Schatzmayr, G., Mayer, E., 2017.
548 Deoxynivalenol and its metabolite deepoxy-deoxynivalenol: multi-parameter analysis for the
549 evaluation of cytotoxicity and cellular effects. *Mycotoxin Research* 33, 25–37.
550 <https://doi.org/10.1007/s12550-016-0260-z>
- 551 Starokozhko, V., Abza, G.B., Maessen, H.C., Merema, M.T., Kuper, F., Groothuis, G.M.M., 2015.
552 Viability, Function and Morphological Integrity of Precision-cut Liver Slices During Prolonged
553 Incubation: Effects of Culture Medium. *Toxicology in Vitro* 30, 288–299.
554 <https://doi.org/10.1016/j.tiv.2015.10.008>
- 555 Sun, L.-H., Lei, M., Zhang, N.-Y., Gao, X., Li, C., Krumm, C.S., Qi, D.-S., 2015. Individual and
556 combined cytotoxic effects of aflatoxin B1, zearalenone, deoxynivalenol and fumonisin B1 on BRL
557 3A rat liver cells. *Toxicon* 95, 6–12. <https://doi.org/10.1016/j.toxicon.2014.12.010>
- 558 Sun, L.H., Lei, M.Y., Zhang, N.Y., Zhao, L., Krumm, C.S., Qi, D.S., 2014. Hepatotoxic effects of
559 mycotoxin combinations in mice. *Food and Chemical Toxicology* 74, 289–293.
560 <https://doi.org/10.1016/j.fct.2014.10.020>
- 561 Terciolo, C., Maresca, M., Pinton, P., Oswald, I.P., 2018. Review article: Role of satiety hormones in
562 anorexia induction by Trichothecene mycotoxins. *Food and Chemical Toxicology* 121, 701–714.
563 <https://doi.org/10.1016/j.fct.2018.09.034>
- 564 van Cruchten, S., van den Broeck, W., 2002. Morphological and Biochemical Aspects of Apoptosis,

- 565 Oncosis and Necrosis. *Anatomia, Histologia, Embryologia: Journal of Veterinary Medicine Series*
566 *C* 31, 214–223. <https://doi.org/10.1046/j.1439-0264.2002.00398.x>
- 567 Vin, K., Rivière, G., Leconte, S., Cravedi, J.-P., Fremy, J.M., Oswald, I.P., Roudot, A.-C., Vasseur, P.,
568 Jean, J., Hulin, M., Sirot, V., 2020. Dietary exposure to mycotoxins in the French infant total diet
569 study. *Food and Chemical Toxicology* 140, 111301. <https://doi.org/10.1016/j.fct.2020.111301>
- 570 Wu, X., Roberto, J.B., Knupp, A., Kenerson, H.L., Truong, C.D., Yuen, S.Y., Brempelis, K.J., Tuefferd,
571 M., Chen, A., Horton, H., Yeung, R.S., Crispe, I.N., 2018. Precision-cut human liver slice cultures
572 as an immunological platform. *Journal of Immunological Methods* 455, 71–79.
573 <https://doi.org/10.1016/j.jim.2018.01.012>
- 574 Yuan, L., Mu, P., Huang, B., Li, H., Mu, H., Deng, Y., 2018. EGR1 is essential for deoxynivalenol-
575 induced G2/M cell cycle arrest in HepG2 cells via the ATF3 Δ Zip2a/2b-EGR1-p21 pathway.
576 *Toxicology Letters* 299, 95–103. <https://doi.org/10.1016/j.toxlet.2018.09.012>
- 577 Zhang, X., Jiang, L., Geng, C., Cao, J., Zhong, L., 2009. The Role of Oxidative Stress in
578 Deoxynivalenol-induced DNA Damage in HepG2 Cells. *Toxicicon* 54, 513–518.
579 <https://doi.org/10.1016/j.toxicicon.2009.05.021>
580

1 **8 ARTIGO C – EMERGING MYCOTOXINS INDUCE EX VIVO AND IN VITRO**
 2 **HEPATOTOXICITY IN PIGS PRECISION-CUT LIVER SLICES AND HEPG2**
 3 **CELLS**

4 **Emerging mycotoxins induce *ex vivo* and *in vitro***
 5 **hepatotoxicity in pigs precision-cut liver slices and HepG2**
 6 **cells**

7 **Amanda Lopes Hasuda^{1,2*}, Elodie Person², Abdullah Khoshal², Sandrine Bruel², Sylvie Puel²,**
 8 **Isabelle P. Oswald^{2*}, Ana Paula F. R. L. Bracarense¹, Philippe Pinton²**

9 ¹Laboratory of Animal Pathology, Londrina State University, P.O. Box 10.011, Londrina, PR 86057-970, Brazil;
 10 amanda.lopeshasuda@uel.br (A.L.H.) anapaula@uel.br (A.P.B.)

11 ² TOXALIM (UMR 1331), Institut National de Recherche pour l'Agriculture l'Alimentation et
 12 l'Environnement Centre Occitanie-Toulouse, UPS, 31027 Toulouse, France; elodie.person@inrae.fr (EP),
 13 a.khoshal@outlook.com (AK); Sylvie.Puel@inrae.fr (S.P.); isabelle.oswald@inrae.fr (I.P.O.);
 14 philippe.pinton@inrae.fr (P.P.)

15 *Corresponding authors: amanda.lopeshasuda@uel.br, isabelle.oswald@inrae.fr

16 Received: ; Accepted: ; Published: ;

17 **ABSTRACT:** Emerging mycotoxins are currently gaining more attention due to their high frequency
 18 of contamination in foods and grains. However, most data available in the literature are *in vitro*, with
 19 few *in vivo* results that do not allow establishing their regulation. Beauvericin (BEA), eniatins (ENNs),
 20 emodin (EMO), apicidin (API) and aurofusarin (AFN) are emerging mycotoxins frequently found
 21 contaminating food and there is growing interest in studying their impact on the liver, a key organ in the
 22 metabolization of these components. We used an *ex vivo* model of precision-cut liver slices (PCLS) to
 23 verify morphological and transcriptional changes after acute exposure (4 h) to these mycotoxins. The
 24 human liver cell line HepG2 was used for comparison purposes. Most of the emerging mycotoxins were
 25 cytotoxic to the cells, except for AFN. In cells, BEA and ENNs were able to increase the expression of
 26 genes related to transcription factors, inflammation, and hepatic metabolism. In the explants, only ENN
 27 B1 led to significant changes in the morphology and expression of few genes. Overall, our results
 28 demonstrate that BEA, ENNs and API have the potential to be hepatotoxic.

29 **Keywords:** cell death, histology, liver explants, non-regulated mycotoxins, swine.

30

31 **1. Introduction**

32 Toxic secondary fungal metabolites, as mycotoxins, can contaminate food and feed commodities
 33 (Marin et al., 2013). Grain contamination by mycotoxins can occur throughout the entire food chain
 34 process, including food processes such as cooking, as they are highly resistant to high temperatures
 35 (Payros et al., 2021).

1 As some of these mycotoxins, such as deoxynivalenol (DON), zearalenone (ZEN), fumonisins,
2 T-2/HT-2, aflatoxins, ochratoxin A (OTA), and patulin have toxic effects in the organism and occur
3 with high frequency in the food and feed grains, they are regulated in Europe (European Commission,
4 2006). However, some mycotoxins have recently "emerged", and they were not routinely determined,
5 nor regulated. Therefore, they are called emerging mycotoxins (Vaclavikova et al., 2013). A recent study
6 estimates that 60-80% of crops worldwide are contaminated by mycotoxins (Eskola et al., 2020), and
7 emerging mycotoxins are frequently associated with some other mycotoxins in contaminated crops
8 (Fraeyman et al., 2017).

9 The most frequent emerging mycotoxins found in grains are the *Fusarium*-toxins – beauvericin
10 (BEA – 12-100%), enniatins (ENNs – 96-100%), apicidin (API – 29-55%), aurofusarin (AFN – 62-
11 79%), moniliformin, fusaproliferin, culmorin, butenolide, and fusaric acid (Drakopoulos et al., 2021;
12 Gruber-Dorninger et al., 2017; Jestoi, 2008). Moreover, emodin (EMO – 63-74%), a mycotoxin
13 produced by many plants and *Aspergillus* species, is important because often contaminates pig feed and
14 grains, and it is probably the most ubiquitous anthraquinone found worldwide (Gruber-Dorninger et al.,
15 2017; Novak et al., 2019; Streit et al., 2013).

16 BEA and ENNs are cyclic hexadepsipeptides and their toxicity are related to their ionophore
17 properties by inserting into the cell membrane and forming cation-selective pores and consequently
18 interfering with cell homeostasis (Fraeyman et al., 2017). The mechanism and toxic effects of AFN and
19 API are poorly studied and understood. AFN belongs to the naphthoquinone group and had only
20 moderate toxicity to intestinal swine and human cells (Frandsen et al., 2006; Khoshal et al., 2019;
21 Vejdovszky et al., 2016). API is a cyclic tetrapeptide and a high toxicity for intestinal swine cells was
22 reported (Niehaus et al., 2014; Novak et al., 2019). EMO is a compound known to have beneficial effects
23 on cancer cells and is widely used in Chinese medicine for decades (Tuli et al., 2021).

24 *In vitro* studies in various cell types exposed to some of these mycotoxins were already published,
25 showing the cytotoxicity and genotoxicity, oxidative and inflammatory effects in intestinal, hepatic,
26 reproductive, neurological, and lymphocytic cells (Escrivá et al., 2018; Juan-García et al., 2019; Krug
27 et al., 2018; Liu et al., 2009; Prosperini et al., 2013a; Schoevers et al., 2016). Few *in vivo* studies about
28 the toxic and immune effects of some of these emerging mycotoxins were performed to date, mainly in

29 chicken and mice (Fraeyman et al., 2018a; Liu et al., 2009; Maranghi et al., 2018; Wu et al., 2013), and
30 recent studies in piglets and rats (Bhateria et al., 2022; Novak et al., 2021). The European Food Safety
31 Authority (EFSA) publish a scientific opinion in 2014 about the risk of BEA and ENNs to human and
32 animal health, but due to the shortage of *in vivo* data, no regulations were yet established (EFSA, 2014).

33 The lack of *in vivo* information needs to be fulfilled. Thinking of that and valuing the 3Rs
34 principle, *ex vivo* models are proven to be good substitutes for the use of several animals to assess
35 mycotoxin toxicity (Gerez et al., 2021; Pierron et al., 2022). The liver is a major organ that promotes
36 the detoxification of several toxic substances and the effects of mycotoxins in this organ are poorly
37 described. A recent study using a promising *ex vivo* model of precision-cut liver slices (PCLS) in the
38 toxic effects of DON showed that liver explants have good results that agree with *in vivo* experiments
39 (Hasuda et al., 2022).

40 This study aimed to investigate the effects of the emerging mycotoxins (BEA, ENN A1, ENN B,
41 ENN B1, EMO, AFN, and API) short exposure in PCLS explants. Histological and biochemical
42 changes, cytotoxicity, and gene expression were evaluated in these explants. The HepG2 cell, a hepatic
43 cell type that is widely used in toxicological studies, was used for comparison.

44 **2. Material and methods**

45 *2.1. Mycotoxin*

46 The mycotoxins BEA, ENN A1, ENN B, ENN B1, EMO, AFN, and API were acquired from
47 Sigma-Aldrich (Saint Quentin Fallavier, France), dissolved in dimethyl sulfoxide (DMSO) (Sigma-
48 Aldrich), and stored at -20 °C until use. Except for cytotoxicity assays, the mycotoxins' working
49 concentration was 10 µM, a dose that is cytotoxic according to a previous study performed by our
50 research team in intestinal cells (Khoshal et al., 2019).

51 *2.2. In vitro assay*

52 To evaluate the effects of emerging mycotoxins on hepatic toxicity and gene expression, *in vitro*
53 assays were performed using HepG2 cells, a human liver cancer cell line (Sigma, 85011430). Cells
54 were maintained as previously described (Luo et al., 2019) for gene expression analysis. To assess

55 the cytotoxicity, HepG2 cells were seeded in 96-white-well flat-bottom cell culture plates (Greiner,
56 Courtaboeuf, France) (10^3 cells/well in 100 μ L culture medium). After 24 h, the medium was
57 replaced by a complete medium (without fetal calf serum) containing crescent concentrations (0.1-
58 100 μ M) of BEA, ENN A1, ENN B, ENN B1, EMO, AFN, API, or vehicle (DMSO) and incubated
59 for 24 h. The cytotoxic effects of the emerging mycotoxins were determined by measuring the ATP
60 production, thus their metabolism, using the CellTiter-Glo[®] Luminiscent Cell Viability Assay
61 (Promega, Charbonnières-les-Bains, France). Six biological replicates were performed.

62 For gene expression analysis, cells were incubated for 4 h with the mycotoxins (BEA, ENN A1,
63 ENN B, ENN B1, EMO, AFN, and API) or vehicle, lysed with Extract All (Eurobio, Les Ulis,
64 France), and stored at -80 °C before mRNA extraction. Six biological replicates were performed.

65 *2.3. Preparation of liver explants*

66 Animal experimentation procedures were approved by the Ethics Committee of Pharmacology-
67 Toxicology of Toulouse-Midi-Pyrénées in animal experimentation (Toxcométhique)
68 (APAFIS#N2016080314392462), following the European Directive on the protection of animals
69 used for scientific purposes.

70 For liver explants sampling, six male 4–5-week-old crossbred piglets were euthanized to obtain
71 precision-cut liver slices (PCLS) that were prepared from the resected liver lateral lobe. The lobe
72 was immediately flushed with an ice-cold sodium chloride solution (0.9% NaCl) to limit ischemia
73 and remove hemoglobin.

74 All the procedures to prepare liver slices were made as described (Hasuda et al., 2022). The slices
75 were deposited in 12-well culture plates (1 slice per well) for 4 h in 2 mL of complete William's E
76 Medium previously bubbled in carbogen and containing 10 μ M of BEA, ENN A1, ENN B, ENN B1,
77 EMO, AFN, API, or vehicle. Incubation took place at 37 °C under a 95% O₂ and 5% CO₂-controlled
78 atmosphere.

79 After the incubation period, the culture medium was collected and frozen to measure liver injury
80 enzymes. Some liver slices were snap-frozen and stored at -80 °C until transcriptomic analyses.
81 Others were fixed for 24 h in 4% buffered formaldehyde (VWR, Rosny-sous-Bois, France) and

82 stored in 70% ethanol for histology analysis.

83 2.3.1. *Histological evaluation*

84 After four hours of incubation, the PCLS were dehydrated in a series of alcohol solutions of
85 increasing concentration and embedded in paraffin for histological examination. Sections of 5 μm
86 were stained with hematoxylin and eosin (HE) and mounted with coverslips for histological
87 analysis. A morphological lesion score as described by Bracarense et al. (2012) was used to evaluate
88 histological changes in the liver. The extent of each lesion (according to the intensity or the
89 observed frequency, scored from 0 to 3) and the severity factor were used to establish the lesion
90 score scale (Table 1).

91 **Table 1.** Histological criteria used to establish liver and intestinal lesion scores.

Organ	Type of lesion	Severity factor	Maximal score
Liver	Disorganization of hepatic cords	1	33
	Inflammatory infiltrate	1	
	Cytoplasmic vacuolation	1	
	Nuclear vacuolation	1	
	Megalocytosis	2	
	Apoptosis	2	
	Necrosis	3	

92 The maximum lesion score was obtained by multiplying the lesion's maximum extent level by the
93 organ's maximum severity factor. The lesion score was obtained by multiplying the severity factor
94 by the extent of the lesion.

95 2.3.2. *Liver biochemicals*

96 To assess liver damage and function, hepatic enzyme activity and protein concentration were
97 evaluated in the culture medium after a 4 h incubation period. Alanine transaminase (ALT),
98 aspartate aminotransferase (AST), alkaline phosphatase (ALP), lactate dehydrogenase (LDH)
99 activities, and total protein (TP) concentration were determined on a Pentra 400 chemistry analyzer
100 (Horiba, Les Ulis, France) at the Anexplo Platform in Toulouse (France).

101 2.4. *Expression of mRNA encoding genes by real-time qPCR*

102 Expression of mRNA encoding genes by real-time qPCR The RNA from tissue and cells was
103 extracted as already described in (Grenier et al., 2012). The concentration and quality of the samples

104 were analyzed, and reverse transcription and real-time qPCR were performed as previously
 105 described in (Maruo et al., 2018) using specific primers sequences purchased from Sigma (Tables
 106 2 and 3).

107 2.5. Total RNA extraction and reverse transcription

108 Total RNA extraction and reverse transcription PCLS were lysed using 1 mL of Extract-All
 109 with ceramic beads (MP Biomedicals, Illkirch, France). Total RNA from PCLS and HepG2 cells
 110 assays were purified, and their concentration and integrity were determined as previously described
 111 (Maruo et al., 2018). For each sample, 2 µg of total RNA was reverse transcribed into cDNA and
 112 diluted 1:20 with nuclease-free/injection water (Ambion, Austin, TX) and stored at -20 °C until
 113 use.

114 **Table 2:** Table of human primer sequences used for RT-qPCR analysis (F: Forward; R: Reverse).

Gene symbol	Gene name	Primer sequence	mRNA	References
ATF3	Activating Transcription Factor 3	F: GGCGACGAGAAAGAAATAAG R: CAGCTTCTCCGACTCTTT	NM_001674.4	(Hasuda et al., 2022)
CYP1A1	Cytochrome p450 1A1	F: GGTGTTAAGTGAGAAGGTGATTATC R: AGCAGGATAGCCAGGAAGAG	NM_000499.5	(Budin et al., 2021)
CYP3A4	Cytochrome p450 3A4	F: GGATCCATTCTTTCTCTCAATAA R: AATTTGTAAGTCTCTTGGAAAC	ENST00000651514.1	(Budin et al., 2021)
P53	Tumor protein 53	F: CGTGTGGAGTATTTGGATGAC R: TGTAGTGGATGGTGGTACAG	ENST00000617185.4	Present study
PPARα	Peroxisome proliferator-activated receptor alpha	F: AGCTTTGGCTTTACGGAATA R: AGGATAAGTCACCGAGGAG	NM_001001928.3	Present study
IL8	Interleukin 8	F: GATTTCTGCAGCTCTGTG R: GTGGAAAGGTTTGGAGTATG	NM_000584	(Hasuda et al., 2022)
TNFα	Tumor Necrosis Factor Alpha	F: CCTGTAGCCCATGTTGTA R: CCAGCTGGTTATCTCTCA	NM_000594	(Hasuda et al., 2022)
NF-κB	Nuclear Factor Kappa B	F: GAGCAACCTAAACAGAGAGG R: TTGACCTGAGGGTAAGACT R: GAAGAATACGGTCTGTGTATCC	NM_003998.4	(Hasuda et al., 2022)
PPIA	Peptidylprolyl Isomerase A	F: GTCAACCCACCGTGTCTCTC R: TTTCTGCTGTCTTTGGGACCTTG	ENST00000355968	(Hasuda et al., 2022)

GAPDH	Glyceraldehyde-3-Phosphate Dehydrogenase	F: TCAAGGCTGAGAACGGGAAG R: CCACTTGATTTTGGAGGGATCTC	NM_002046	(Luo et al., 2021)
-------	--	---	-----------	--------------------

115

116 **Table 3:** Table of pig primer sequences used for RT-qPCR analysis (F: Forward; R: Reverse).

Gene symbol	Gene name	Primer sequence	mRNA	References
ATF3	Activating Transcription Factor 3	F: TGAGGTTCCGCATCCA R: TACCTCGGCTTTCGTGA	ENSSSCT0000033171.2	(Hasuda et al., 2022)
CYP7A1	Cytochrome p450 7A1	F: GGATCCATTCTTTCTCTCAATAA R: AATTTGTAACCTTCTCTGGAAAC	ENST00000651500.1	Present study
CYP1A1	Cytochrome p450 1A1	F: GGATCCATTCTTTCTCTCAATAA R: AATTTGTAACCTTCTCTGGAAAC	ENST00000651602.1	Present study
IL1 α	Interleukin 1 Alpha	F: GCCAATGACACAGAAGAAGA R: ATGCACTGGTGGTTGATG	NM_214029	(Pierron et al., 2022)
IL8	Interleukin 8	F: GCTCTCTGTGAGGCTGCAGTTC R: AAGGTGTGGAATGCGTATTTATGC	NM_213867	(Grenier et al., 2011)
TNF α	Tumor necrosis factor alpha	F: ACTGCACTTCGAGGTTATCGG R: GGCGACGGGCTTATCTGA	NM_214022	(Cano et al., 2013)
NF- κ B	Nuclear Factor Kappa B	F: CCTCCACAAGGCAGCAAATAG R: TCCACACCGCTGTCACAGA	ENSSSCT00000033438	(Alassane-Kpembi et al., 2017a)
CCL20	C-C Motif Chemokine Ligand 20	F: GCTCCTGGCTGCTTTGATGTC R: CATTGGCGAGCTGCTGTGTG	NM_001024589	(Meurens et al., 2009)
ACTB	Actin β	F: GCACCACACCTTCTACA R: ATCTGGGTCATCTTCTCAC	ENSSSCT00000008324.1	(Hasuda et al., 2022)
TOP2B	DNA Topoisomerase II Beta	F: AAGGGCGAGAGGTCAATGAT R: ACATCTTCTCGTTCTTGCGC	ENSSSCT00015080370.1	(Park et al., 2015)

117

118 *2.6. Quantitative Real-time PCR (qPCR) Analysis*

119 To quantify mRNA expression levels, RT-qPCR was performed using a Viia™ 7 thermocycler
120 (Applied Biosystems, California). The specificity of the qPCR products was assessed at the end of
121 the reactions by analyzing the dissociation curves. TOP2B and ACTB for PCLS samples, and
122 GAPDH and PPIA for HepG2 cells were selected for their stable expression upon treatments,
123 assessed with NormFinder software (Andersen et al., 2004), and used as reference genes. Non-
124 reverse transcribed RNA was used as non-template control (NTC) for verification of the genomic

125 DNA amplification signal. Data from qPCR were analyzed with the LinRegPCR 2016 program
126 enabling the determination of the starting concentrations (N0) based on the observed PCR
127 efficiency values. mRNA expression levels in samples exposed to the micotoxins were expressed
128 relative to the mean of the control (Maruo et al., 2018).

129 *2.7. Statistical analysis*

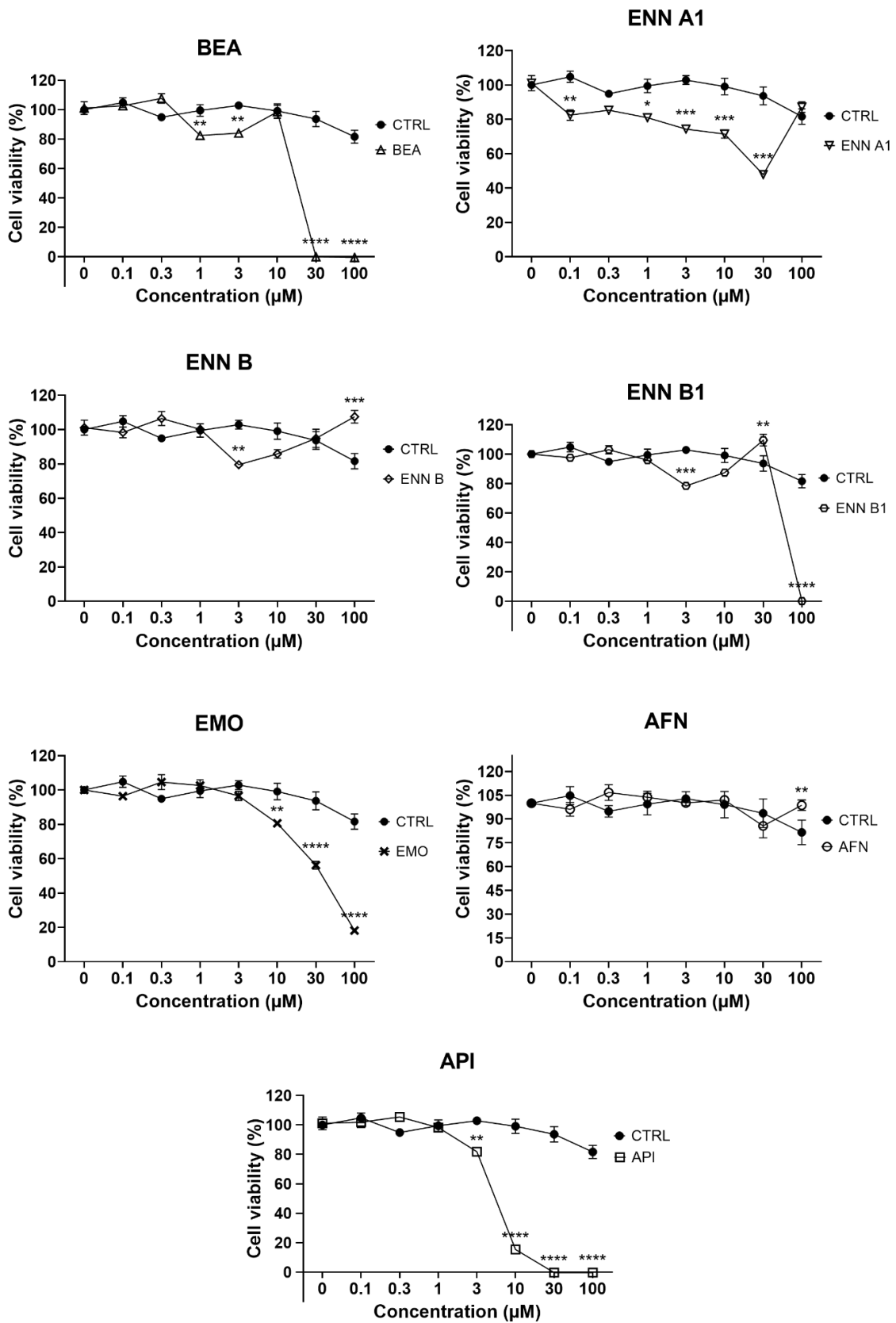
130 All statistical analyses were performed using GraphPad Prism 9.0.2 software (GraphPad
131 Software Inc., La Jolla, USA). Data were expressed as mean \pm SEM (standard error of the mean)
132 for normal distribution or median and interquartile range when data were not normally distributed.
133 They were submitted to statistical analysis, using normality (Shapiro–Wilk) and homogeneity
134 (Bartlett) tests. Significant differences were assessed by one-way ANOVA. Multiple comparisons
135 were performed by Bonferroni’s test for parametric data and by Kruskal-Wallis’ test followed by
136 Dunn’s test for nonparametric data. p-value ≤ 0.05 was considered statistically significant.

137 **3. Results**

138 *3.1. In vitro analysis*

139 *3.1.1. Cytotoxicity*

140 After 24 h of exposure all mycotoxins, except AFN, decreased the cell viability (Fig. 1). ENN
141 A1 and BEA showed the highest cytotoxicity, with a decrease in the viability from low
142 concentrations (0.1 and 1 μ M, respectively). AFN was not toxic for HepG2 cells in any
143 concentration. High concentrations of ENN B (100 μ M), AFN (100 μ M) and ENN B1 (30
144 μ M) stimulated the production of ATP in HepG2 cells.



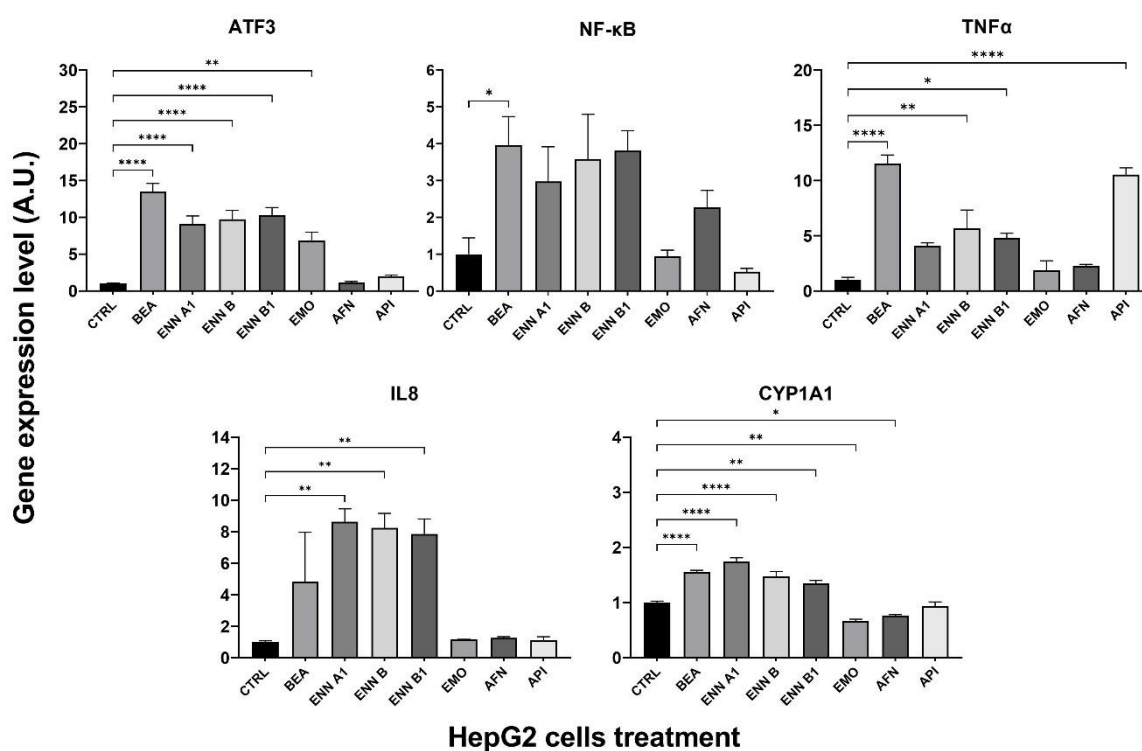
145
146
147
148

Figure 1. Toxicity of DON in HepG2 cells by CellTiter-Glo® Assay after 24h. Cell viability was evaluated by measurement of ATP and was expressed as % of control cells. Data are expressed as mean ± SEM of six replicates. *p<0.05, **p<0.01, ***p<0.001, and ****p<0.0001.

149 3.1.2. Gene expression

150 After 4 h incubation with a 10 μ M concentration, some of the tested emerging mycotoxins
 151 were able to change the expression of genes in HepG2 cells and PCLS.

152 In the cells, all the ENNs stimulated the expression of interleukin-8 (IL8) and tumor necrosis
 153 factor-alpha (TNF α), both inflammatory proteins. The overexpression of the last one was
 154 induced by BEA and API. BEA also increased the expression of the transcription nuclear factor
 155 kappa B (NF- κ B). In addition, BEA, ENNs, and EMO increased the expression of the
 156 activating transcription factor 3 (ATF3). BEA and the enniatins also increased a gene involved
 157 in hepatic metabolism, the CYP1A1, while AFN and EMO decreased the expression of this
 158 gene (Fig. 2).



159

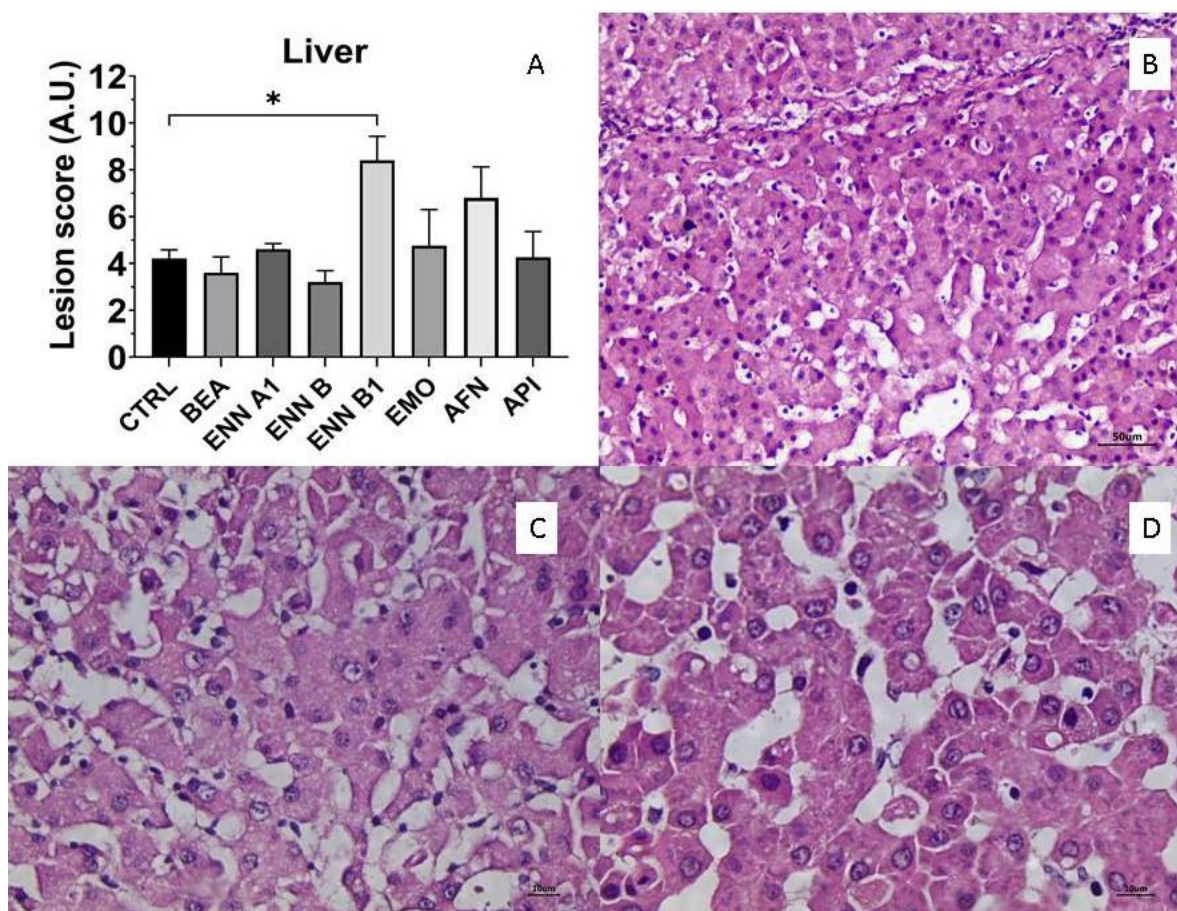
160 **Figure 2.** Inflammatory, transcription factors, and liver metabolism mRNA levels measured by RT-
 161 qPCR in HepG2 cells exposed or not to 10 μ M emerging mycotoxins for 4 h. Data are presented as mean
 162 \pm SEM of six replicates, ** $p \leq 0.01$, * $p \leq 0.05$, *** $p \leq 0.001$ and **** $p \leq 0.0001$.

163 3.2. Ex vivo analysis

164 3.2.1. Histology

165 Among all the tested mycotoxins, only ENN B1 increased the liver lesion score compared to

166 the control after 4 h incubation (Fig. 3). The main histological changes found in the liver were
 167 disorganization of hepatic cords, cytoplasmic vacuolation of hepatocytes, apoptosis,
 168 megalocytosis, nuclear vacuolation of hepatocytes, and inflammatory infiltrate.



169 **Figure 3.** Effects of emerging mycotoxins exposure on liver PCLS. A) Lesion score (A.U. – arbitrary
 170 units), data are presented as mean \pm SEM, n=6. B) control, mild disorganization of hepatic cords, HE,
 171 50 μ m bar. C) ENN B1, megalocytosis, HE, 10 μ m bar. D) ENN B1, nuclear vacuolation of hepatocytes,
 172 HE, 10 μ m bar.
 173

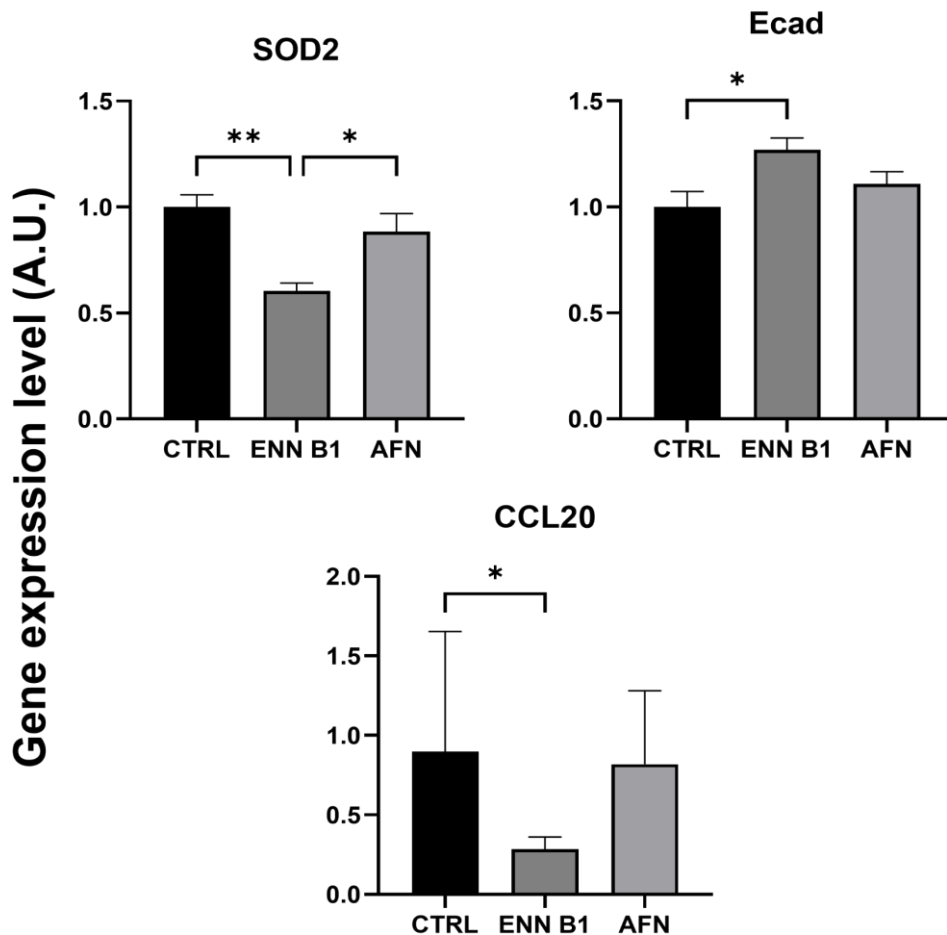
174 3.2.2. Liver biochemicals

175 The liver enzyme activity and total protein content had no significant changes among the
 176 groups (Supplementary material - Table S1).

177 3.2.3. Gene expression

178 In the PCLS, we decided to test only ENN B1 and AFN, which were the mycotoxins with the
 179 higher lesion score in histology for qPCR analysis. The expression of most genes was not
 180 changed by any mycotoxin. Only superoxide dismutase 2 (SOD2) and Chemokine (C-C motif)

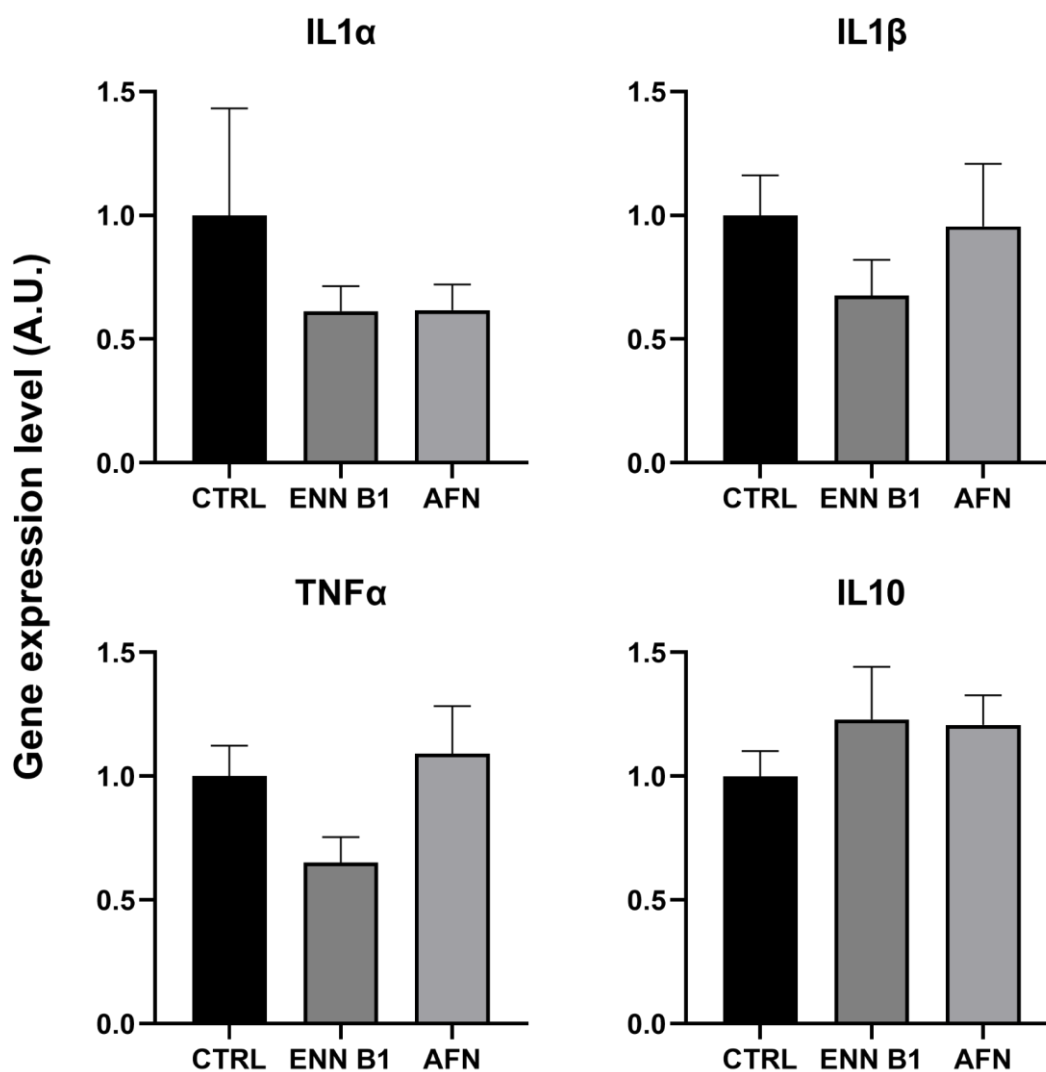
181 ligand 20 (CCL20) were downregulated and E-cadherin (Ecad) was upregulated with the ENN
 182 B1 treatment (Fig 4). The IL10 cytokine tended to increase with mycotoxin treatment (Fig 5),
 183 but with no significant changes as well as the other inflammatory genes that were not
 184 changed.



PCLS treatment

185

186 **Figure 4.** Significant changes in mRNA levels measured by RT-qPCR in PCLS exposed or not to 10
 187 μ M of ENN B1 and AFN for 4 h. Data are presented as mean \pm SEM (SOD2 and Ecad) or median \pm
 188 interquartile (CCL20), n=6, **p \leq 0.01 and *p \leq 0.05.



PCLS treatment

189

190 **Figure 5.** Cytokines mRNA levels measured by RT-qPCR in PCLS exposed or not to 10 μ M of ENN
 191 B1 and AFN for 4 h. Data are presented as mean \pm SEM, n=6.

192 4. Discussion

193 Cell viability is an important parameter to evaluate the toxicity of mycotoxins in *in vitro* studies.

194 In the present study, we have verified hepatocyte viability by a test (CellTiter-Glo[®]) that measures ATP

195 production by cells. The cytotoxicity observed after exposure to BEA and ENNs (A1, B, and B1) agrees

196 with what has already been described in previous studies with similar concentrations in intestinal (Caco-

197 2), liver (HepG2) and ovarian (CHO -K1) cells (Fraeyman et al., 2018b; Juan-García et al., 2019;

198 Zouaoui et al., 2016). Furthermore, BEA and ENNs (A, A1, B, and B1) can promote cell cycle arrest in

199 different phases, thus inhibiting the proliferation of intestinal cells (Prosperini et al., 2013a, 2013b).

200 The cytotoxicity presented by API in HepG2 cells has also been observed in intestinal cells
201 (Khoshal et al., 2019; Novak et al., 2019). The API toxicity mechanism is still not well elucidated, but
202 it is known that it has antiparasitic properties through the inhibition of histone deacetylase and
203 antiproliferative activity against various cancer cell lines (Han et al., 2000).

204 On the other hand, treatments with high concentrations of ENN B (100 μ M), ENN B1 (30 μ M),
205 and AFN (100 μ M), induced an increase in cell viability, indicating greater ATP production. It is known
206 that ENNs have ionophore properties, which can form pores in the mitochondrial membrane, and have
207 a greater affinity for the potassium ion (K^+), allowing the passage of this ion through the mitochondrial
208 membrane (Tonshin et al., 2010). Therefore, it is possible that there was an influx of K^+ into the
209 mitochondria, so the Na^+/K^+ ATPase pump needs more ATP to carry out the active transport of K^+ ions
210 from the extracellular environment to the cytoplasm in order to reestablish intracellular homeostasis
211 (Miller and Zachary, 2017).

212 Regarding AFN, previous results in IPEC-J2 cells exposed to 10 μ M of AFN show that cell
213 viability was not affected, even after 72 h (Springler et al., 2016). However, in Caco-2 cells, the same
214 concentration of AFN for 24 h was cytotoxic, decreasing cell viability measured by mitochondrial
215 activity by 51% (Vejdovszky et al., 2016). The present study appears to be one of the first to evaluate
216 the cytotoxicity of AFN in liver cells, and the differences in results between cell types suggest that
217 human liver cells may be more resistant than human intestinal cells.

218 In addition to cell viability, we also tested gene expression, but in a shorter exposure time (4h)
219 which was the same period that PCLS explants were exposed to treatments for comparison purposes.
220 The transcription factors-related genes (ATF3 and NF- κ B) were increased after exposure to BEA, ENNs
221 (A1, B, and B1), and EMO. ATF3 is related to endoplasmic reticulum (ER) stress. When there is no ER
222 relief, cells may undergo apoptosis (Li et al., 2006), which is an already described effect that BEA and
223 ENNs (A1 and B1) cause in HepG2 cells (Juan-García et al., 2015). Therefore, the higher rate of
224 apoptosis and overexpression of ATF3 may be related.

225 Furthermore, inflammatory genes (IL8 and TNF α) were tested and had an increase in their
226 expression with BEA, ENNs (A1, B, and B1), and API treatments. But in contradiction with our results,

227 in immune cells, BEA and ENNs stimulate IL10 secretion in macrophages and impair their phagocytic
228 capacity (Ficheux et al., 2013) and even lower concentrations of BEA (0.1-4.5 μ M) inhibited the NF-
229 κ B transcription factor pathway in macrophages (Yoo et al., 2017). It is possible that acute exposure
230 (4h) to BEA and ENNs exerts different effects since our results show an increase in the expression of
231 pro-inflammatory cytokines and transcription factors. While EMO and AFN did not increase the
232 expression of cytokines, it is likely that these mycotoxins are not hepatotoxic after a short exposure, as
233 they also did not cause a change in the morphology of the explants, nor the activity of liver enzymes.

234 The liver is the main organ to metabolize toxic compounds, including mycotoxins. In the liver,
235 there are several enzymes involved in the metabolism of these compounds, including cytochrome p450
236 (CYPs). Therefore, we investigated the effects of metabolic enzymes on emerging mycotoxins
237 metabolism in HepG2 cells. Even a short exposure (4h) to BEA and ENNs (A1, B, and B1) increased
238 CYP1A1 expression. In other kinds of liver and endocrine cells, ENN B was able to promote the same
239 effect. CYP1A1 is involved in an NADPH-dependent electron transport pathway and the metabolism of
240 ENN B in human, canine, and rat liver microsomes (Fæste et al., 2011; Kalayou et al., 2015).

241 In contrast, a decrease in the expression of CYP1A1 by EMO and AFN was observed. EMO
242 exerts a hepatoprotective effect in HepG2 cells against alcohol-induced damage by decreasing the
243 expression of CYP2E1 (Qian et al., 2011). Moreover, CYP1A2 is also involved in the metabolism of
244 EMO in the liver of rats (Zhou et al., 2023). Contrary to previous results, in which EMO exerted a
245 hepatotoxic effect (Wang et al., 2022), in the present study we demonstrated that CYP1A1 is also
246 affected by EMO in liver cells, but with a decrease in the expression of this gene. The difference can be
247 explained due to the short exposure time and the lower concentration used in the explants.

248 Studies regarding gene expression with AFN and API have practically not been carried out to
249 date. It is possible that AFN has also the same effect as EMO regarding CYP1A1 and that API can
250 produce inflammation in the liver by increasing TNF α expression based on the results found. Therefore,
251 the small amount of information available in the literature makes it even more important to further study
252 the effects of these mycotoxins.

253 Although *in vitro* studies are of great importance to assess the toxic effects of mycotoxins, they
254 do not fully replace studies in a living organism, where there are greater complexity and system

255 interactions. Therefore, we decided to use the *ex vivo* technique, in which there are fewer animals used
256 in experimentation, with good results like those found *in vivo* (Alassane-Kpembi et al., 2017b; Gerez et
257 al., 2021; Pierron et al., 2022).

258 Tissue damage was observed in PCLS exposed to ENN B1, despite the short time of exposure
259 (4 h), but no changes in the injury liver enzymes were verified. The PCLS model in the study of
260 mycotoxin toxicity has already proven effective in detecting the same histological changes found *in vivo*
261 (Hasuda et al., 2022). Increased lesion score and histological changes caused by ENNs and BEA have
262 already been reported *in vivo* in piglets (Novak et al., 2021). The same histological pattern was observed
263 in the present *ex vivo* study for ENN B1, thus corroborating previous results. ENN B1 is rapidly absorbed
264 orally, bioaccumulates, and is metabolized in the liver to be excreted (Devreese et al., 2014; Rodríguez-
265 Carrasco et al., 2016).

266 As only ENN B1 had a significant increase in lesion score and AFN was the other mycotoxin
267 with the highest lesion score, but without a significant increase, we decided to test the gene expression
268 only with these two mycotoxins to see if there was any change in the expression of genes related to liver
269 metabolism and health, inflammation, oxidative stress, and apoptosis. Despite the variety of genes
270 tested, only SOD2, CCL20, and Ecad changed with ENN B1 treatment.

271 SOD2 is an important antioxidant enzyme that has manganese as a cofactor and is present in the
272 mitochondria of aerobic cells (Zelko et al., 2002). SOD2 is a key molecule in cells because it provides
273 resistance against oxidative damage (Zou et al., 2017). In the intestine of Wistar rats, acute treatment (8
274 h) of ENNs led to a decrease in the expression of genes associated with the enzymatic antioxidant
275 defense system (SOD1 and GPx1) (Cimbalo et al., 2021). In PCLS explants, ENN B1 treatment also
276 impairs the enzymatic antioxidant system, with a decrease in SOD2.

277 CCL20 is an inflammatory chemokine related to lymphocyte attraction and it is negatively
278 regulated by IL10 secretion (Hieshima et al., 1997). In the present study, we found a downregulation of
279 CCL20, and a tendency to increase the IL10 expression with ENN B1 treatment, which could explain
280 the decrease in CCL20 expression.

281 Ecad is an important cell junction protein. In general, it decreases in the intestine of *in vivo* and
282 *ex vivo* studies with mycotoxins such as deoxynivalenol and fumonisin B1 (Basso et al., 2013; Lucioli

283 et al., 2013; Silva et al., 2019). However, in another study with pigs, acute mycotoxin exposure led to
284 an increase in Ecad expression (Bracarense et al., 2020). It is possible that an acute exposure leads to an
285 increase in Ecad as a way of trying to protect the organ, but in more chronic exposures, such as *in vivo*
286 studies, this expression decreases, as mycotoxins impair the structural integrity of the organ (Pinton et
287 al., 2009).

288 The lack of changes in the liver biochemicals and gene expression could be due to the short
289 exposure time in which the explants were submitted. Also, it is possible that an interindividual variability
290 could cause this lack of significance. More studies for a longer exposure time should be performed to
291 better understand the possible hepatotoxic effects that emerging mycotoxins, especially the poorly
292 studied ones like AFN and API, can develop. In addition, our results can contribute to *ex vivo* data to
293 aid in the establishment of regulation of emerging mycotoxins like BEA and ENNs.

294 **5. Conclusion**

295 . Taken together, our results indicate that emerging mycotoxins, particularly beauvericin,
296 enniatins, and apicidin have the potential to be hepatotoxic. These mycotoxins were able to decrease
297 cell viability and changed the expression of genes related to inflammation and hepatic metabolism in
298 human liver cells. In PCLS explants, ENN B1 in particular changed the liver morphology and the
299 expression of some genes after acute exposure. Although changes indicating loss of function or liver
300 damage were not identified in the supernatant of the medium in which the explants were cultured.

301 **References**

- 302 Alassane-Kpembi, I., Gerez, J.R., Cossalter, A.-M., Neves, M., Laffitte, J., Naylies, C., Lippi, Y., Kolf-
303 Clauw, M., Bracarense, A.P.L., Pinton, P., Oswald, I.P., 2017a. Intestinal toxicity of the type B
304 trichothecene mycotoxin fusarenon-X: whole transcriptome profiling reveals new signaling
305 pathways. *Sci Rep* 7, 7530. <https://doi.org/10.1038/s41598-017-07155-2>
- 306 Alassane-Kpembi, I., Puel, O., Pinton, P., Cossalter, A.-M., Chou, T.-C., Oswald, I.P., 2017b. Co-
307 exposure to low doses of the food contaminants deoxynivalenol and nivalenol has a synergistic
308 inflammatory effect on intestinal explants. *Arch Toxicol* 91, 2677–2687.
309 <https://doi.org/10.1007/s00204-016-1902-9>
- 310 Basso, K., Gomes, F., Bracarense, A., 2013. Deoxynivalenol and Fumonisin, Alone or in Combination,
311 Induce Changes on Intestinal Junction Complexes and in E-Cadherin Expression. *Toxins (Basel)*
312 5, 2341–2352. <https://doi.org/10.3390/toxins5122341>
- 313 Bhatia, M., Karsauliya, K., Sonker, A.K., Yahavi, C., Singh, S.P., 2022. Cytochrome P450 isoforms
314 contribution, plasma protein binding, toxicokinetics of enniatin A in rats and in vivo clearance
315 prediction in humans. *Food and Chemical Toxicology* 164, 112988.
316 <https://doi.org/10.1016/j.fct.2022.112988>
- 317 Bracarense, A.P.F.L., Luciola, J., Grenier, B., Drociunas Pacheco, G., Moll, W.D., Schatzmayr, G.,
318 Oswald, I.P., 2012. Chronic ingestion of deoxynivalenol and fumonisin, alone or in interaction,
319 induces morphological and immunological changes in the intestine of piglets. *British Journal of*
320 *Nutrition* 107, 1776–1786. <https://doi.org/10.1017/S0007114511004946>
- 321 Bracarense, A.P.F.L., Pierron, A., Pinton, P., Gerez, J.R., Schatzmayr, G., Moll, W.D., Zhou, T.,
322 Oswald, I.P., 2020. Reduced Toxicity of 3-epi-deoxynivalenol and De-epoxy-deoxynivalenol
323 through Deoxynivalenol Bacterial Biotransformation: In Vivo Analysis in Piglets. *Food and*
324 *Chemical Toxicology* 140, 111241. <https://doi.org/10.1016/j.fct.2020.111241>
- 325 Budin, C., Man, H.-Y., Al-Ayoubi, C., Puel, S., van Vugt-Lussenburg, B.M.A., Brouwer, A., Oswald,
326 I.P., van der Burg, B., Soler, L., 2021. Versicolorin A enhances the genotoxicity of aflatoxin B1 in
327 human liver cells by inducing the transactivation of the Ah-receptor. *Food and Chemical*
328 *Toxicology* 153, 112258. <https://doi.org/10.1016/j.fct.2021.112258>
- 329 Cano, P.M., Seeboth, J., Meurens, F., Cognie, J., Abrami, R., Oswald, I.P., Guzylack-Piriou, L., 2013.
330 Deoxynivalenol as a New Factor in the Persistence of Intestinal Inflammatory Diseases: An
331 Emerging Hypothesis through Possible Modulation of Th17-Mediated Response. *PLoS One* 8,
332 e53647. <https://doi.org/10.1371/journal.pone.0053647>
- 333 Cimbalo, A., Alonso-Garrido, M., Font, G., Frangiamone, M., Manyes, L., 2021. Transcriptional
334 Changes after Enniatins A, A1, B and B1 Ingestion in Rat Stomach, Liver, Kidney and Lower
335 Intestine. *Foods* 10, 1630. <https://doi.org/10.3390/foods10071630>
- 336 Devreese, M., Broekaert, N., de Mil, T., Fraeyman, S., de Backer, P., Croubels, S., 2014. Pilot
337 Toxicokinetic Study and Absolute Oral Bioavailability of the Fusarium Mycotoxin Enniatin B1 in
338 Pigs. *Food and Chemical Toxicology* 63, 161–165. <https://doi.org/10.1016/j.fct.2013.11.005>
- 339 Drakopoulos, D., Sulyok, M., Krska, R., Logrieco, A.F., Vogelgsang, S., 2021. Raised concerns about
340 the safety of barley grains and straw: A Swiss survey reveals a high diversity of mycotoxins and
341 other fungal metabolites. *Food Control* 125, 107919.
342 <https://doi.org/10.1016/j.foodcont.2021.107919>
- 343 Escrivá, L., Jennen, D., Caiment, F., Manyes, L., 2018. Transcriptomic Study of the Toxic Mechanism
344 Triggered by Beauvericin in Jurkat Cells. *Toxicol Lett* 284, 213–221.
345 <https://doi.org/10.1016/j.toxlet.2017.11.035>
- 346 Eskola, M., Kos, G., Elliott, C.T., Hajšlová, J., Mayar, S., Krska, R., 2020. Worldwide contamination
347 of food-crops with mycotoxins: Validity of the widely cited ‘FAO estimate’ of 25%. *Crit Rev Food*

- 348 Sci Nutr 60, 2773–2789. <https://doi.org/10.1080/10408398.2019.1658570>
- 349 European Commission, 2006. Commission Recommendation of 17 August 2006 on the Presence of
350 Deoxynivalenol, Zearalenone, Ochratoxin A, T-2 and HT-2 and Fumonisin in Products Intended
351 for Animal Feeding. Official Journal of the European Union 299, 7–9.
- 352 European Food Safety Authority (EFSA), 2014. Scientific Opinion on the risks to human and animal
353 health related to the presence of beauvericin and enniatins in food and feed. EFSA Journal 12, 3802.
354 <https://doi.org/10.2903/j.efsa.2014.3802>
- 355 Fæste, C.K., Ivanova, L., Uhlig, S., 2011. In Vitro Metabolism of the Mycotoxin Enniatin B in Different
356 Species and Cytochrome P450 Enzyme Phenotyping by Chemical Inhibitors. Drug Metabolism and
357 Disposition 39, 1768–1776. <https://doi.org/10.1124/dmd.111.039529>
- 358 Ficheux, A.S., Sibiril, Y., Parent-Massin, D., 2013. Effects of Beauvericin, Enniatin b and Moniliformin
359 on Human Dendritic Cells and Macrophages: An In vitro Study. Toxicol 71, 1–10.
360 <https://doi.org/10.1016/j.toxicol.2013.04.024>
- 361 Fraeyman, S., Croubels, S., Devreese, M., Antonissen, G., 2017. Emerging Fusarium and Alternaria
362 Mycotoxins: Occurrence, Toxicity and Toxicokinetics. Toxins (Basel) 9, 228.
363 <https://doi.org/10.3390/toxins9070228>
- 364 Fraeyman, S., Croubels, S., Devreese, M., Ducatelle, R., Rychlik, M., Antonissen, G., 2018a. Chronic
365 Dietary Intake of Enniatin B in Broiler Chickens Has Low Impact on Intestinal Morphometry and
366 Hepatic Histology, and Shows Limited Transfer to Liver Tissue. Toxins (Basel) 10, 1–11.
367 <https://doi.org/10.3390/toxins10010045>
- 368 Fraeyman, S., Meyer, E., Devreese, M., Antonissen, G., Demeyere, K., Haesebrouck, F., Croubels, S.,
369 2018b. Comparative In Vitro Cytotoxicity of the Emerging Fusarium Mycotoxins Beauvericin and
370 Enniatins to Porcine Intestinal Epithelial Cells. Food and Chemical Toxicology 121, 566–572.
371 <https://doi.org/10.1016/j.fct.2018.09.053>
- 372 Frandsen, R.J.N., Nielsen, N.J., Maolanon, N., Sorensen, J.C., Olsson, S., Nielsen, J., Giese, H., 2006.
373 The biosynthetic pathway for aurofusarin in *Fusarium graminearum* reveals a close link between
374 the naphthoquinones and naphthopyrones. Mol Microbiol 61, 1069–1080.
375 <https://doi.org/10.1111/j.1365-2958.2006.05295.x>
- 376 Gerez, J.R., Camacho, T., Brunaldi Marutani, V.H., Nascimento de Matos, R.L., Hohmann, M.S., Verri
377 Júnior, W.A., Bracarense, A.P.F.R.L., 2021. Ovarian toxicity by fusariotoxins in pigs: Does it
378 imply in oxidative stress? Theriogenology 165, 84–91.
379 <https://doi.org/10.1016/j.theriogenology.2021.02.003>
- 380 Grenier, B., Bracarense, A.-P.F.L., Schwartz, H.E., Trumel, C., Cossalter, A.-M., Schatzmayr, G., Kolf-
381 Clauw, M., Moll, W.-D., Oswald, I.P., 2012. The low intestinal and hepatic toxicity of hydrolyzed
382 fumonisin B1 correlates with its inability to alter the metabolism of sphingolipids. Biochem
383 Pharmacol 83, 1465–1473. <https://doi.org/10.1016/j.bcp.2012.02.007>
- 384 Grenier, B., Loureiro-Bracarense, A.-P., Luciola, J., Pacheco, G.D., Cossalter, A.-M., Moll, W.-D.,
385 Schatzmayr, G., Oswald, I.P., 2011. Individual and Combined Effects of Subclinical Doses of
386 Deoxynivalenol and Fumonisin in Piglets. Mol Nutr Food Res 55, 761–771.
387 <https://doi.org/10.1002/mnfr.201000402>
- 388 Gruber-Dorninger, C., Novak, B., Nagl, V., Berthiller, F., 2017. Emerging Mycotoxins: Beyond
389 Traditionally Determined Food Contaminants. J Agric Food Chem 65, 7052–7070.
390 <https://doi.org/10.1021/acs.jafc.6b03413>
- 391 Han, J.-W., Ahn, S.H., Park, S.H., Wang, S.Y., Bae, G.-U., Seo, D.-W., Kwon, H.-K., Hong, S., Lee,
392 H.Y., Lee, Y.-W., Lee, H.-W., 2000. Apicidin, a Histone Deacetylase Inhibitor, Inhibits
393 Proliferation of Tumor Cells via Induction of p21 WAF1/Cip1 and Gelsolin 1. Cancer Res 60,
394 6068–6074.
- 395 Hasuda, A.L., Person, E., Khoshal, A.K., Bruel, S., Puel, S., Oswald, I.P., Bracarense, A.P.F.R.L.,

- 396 Pinton, P., 2022. Deoxynivalenol induces apoptosis and inflammation in the liver: Analysis using
397 precision-cut liver slices. *Food and Chemical Toxicology* 163, 112930.
398 <https://doi.org/10.1016/j.fct.2022.112930>
- 399 Hieshima, K., Imai, T., Opendakker, G., van Damme, J., Kusuda, J., Tei, H., Sakaki, Y., Takatsuki, K.,
400 Miura, R., Yoshie, O., Nomiya, H., 1997. Molecular Cloning of a Novel Human CC Chemokine
401 Liver and Activation-regulated Chemokine (LARC) Expressed in Liver. *Journal of Biological*
402 *Chemistry* 272, 5846–5853. <https://doi.org/10.1074/jbc.272.9.5846>
- 403 Jestoi, M., 2008. Emerging Fusarium-Mycotoxins Fusaproliferin, Beauvericin, Enniatins, and
404 Moniliformin - A Review. *Crit Rev Food Sci Nutr* 48, 21–49.
405 <https://doi.org/10.1080/10408390601062021>
- 406 Juan-García, A., Ruiz, M.-J., Font, G., Manyes, L., 2015. Enniatin A1, enniatin B1 and beauvericin on
407 HepG2: Evaluation of toxic effects. *Food and Chemical Toxicology* 84, 188–196.
408 <https://doi.org/10.1016/j.fct.2015.08.030>
- 409 Juan-García, A., Tolosa, J., Juan, C., Ruiz, M.-J., 2019. Cytotoxicity, Genotoxicity and Disturbance of
410 Cell Cycle in HepG2 Cells Exposed to OTA and BEA: Single and Combined Actions. *Toxins*
411 (Basel) 11, 341. <https://doi.org/10.3390/toxins11060341>
- 412 Kalayou, S., Ndossi, D., Frizzell, C., Groseth, P.K., Connolly, L., Sørli, M., Verhaegen, S., Ropstad,
413 E., 2015. An Investigation of the Endocrine Disrupting Potential of Enniatin B Using In Vitro
414 Bioassays. *Toxicol Lett* 233, 84–94. <https://doi.org/10.1016/j.toxlet.2015.01.014>
- 415 Khoshal, A.K., Novak, B., Martin, P.G.P., Jenkins, T., Neves, M., Schatzmayr, G., Oswald, I.P., Pinton,
416 P., 2019. Co-Occurrence of DON and Emerging Mycotoxins in Worldwide Finished Pig Feed and
417 Their Combined Toxicity in Intestinal Cells. *Toxins* (Basel) 11, 727.
418 <https://doi.org/10.3390/toxins11120727>
- 419 Krug, I., Behrens, M., Esselen, M., Humpf, H.U., 2018. Transport of Enniatin B and Enniatin B1 Across
420 the Blood-Brain Barrier and Hints for Neurotoxic Effects in Cerebral Cells. *PLoS One* 13, 1–17.
421 <https://doi.org/10.1371/journal.pone.0197406>
- 422 Li, J., Lee, B., Lee, A.S., 2006. Endoplasmic Reticulum Stress-induced Apoptosis. *Journal of Biological*
423 *Chemistry* 281, 7260–7270. <https://doi.org/10.1074/jbc.M509868200>
- 424 Liu, Y.-X., Shen, N.-Y., Liu, C., Lv, Y., 2009. Immunosuppressive Effects of Emodin: An In Vivo and
425 In Vitro Study. *Transplant Proc* 41, 1837–1839. <https://doi.org/10.1016/j.transproceed.2009.02.090>
- 426 Luciola, J., Pinton, P., Callu, P., Laffitte, J., Grosjean, F., Kolf-Clauw, M., Oswald, I.P., Bracarense,
427 A.P.F.R.L., 2013. The food contaminant deoxynivalenol activates the mitogen activated protein
428 kinases in the intestine: Interest of ex vivo models as an alternative to in vivo experiments. *Toxicon*
429 66, 31–36. <https://doi.org/10.1016/j.toxicon.2013.01.024>
- 430 Luo, S., Terciolo, C., Neves, M., Puel, S., Naylies, C., Lippi, Y., Pinton, P., Oswald, I.P., 2021.
431 Comparative sensitivity of proliferative and differentiated intestinal epithelial cells to the food
432 contaminant, deoxynivalenol. *Environmental Pollution* 277, 116818.
433 <https://doi.org/10.1016/j.envpol.2021.116818>
- 434 Maranghi, F., Tassinari, R., Narciso, L., Tait, S., Rocca, C. la, Felice, G. di, Butteroni, C., Corinti, S.,
435 Barletta, B., Cordelli, E., Pacchierotti, F., Eleuteri, P., Villani, P., Hegarat, L. le, Fessard, V., Reale,
436 O., 2018. In vivo toxicity and genotoxicity of beauvericin and enniatins. Combined approach to
437 study in vivo toxicity and genotoxicity of mycotoxins beauvericin (BEA) and enniatin B (ENNB).
438 EFSA Supporting Publications 15. <https://doi.org/10.2903/sp.efsa.2018.EN-1406>
- 439 Marin, S., Ramos, A.J., Cano-Sancho, G., Sanchis, V., 2013. Mycotoxins: Occurrence, Toxicology, and
440 Exposure Assessment. *Food and Chemical Toxicology* 60, 218–237.
441 <https://doi.org/10.1016/j.fct.2013.07.047>
- 442 Maruo, V., Bracarense, A.P.F.R.L., Metayer, J.-P., Vilarino, M., Oswald, I., Pinton, P., 2018. Ergot
443 Alkaloids at Doses Close to EU Regulatory Limits Induce Alterations of the Liver and Intestine.

- 444 Toxins (Basel) 10, 183. <https://doi.org/10.3390/toxins10050183>
- 445 Meurens, F., Berri, M., Auray, G., Melo, S., Levast, B., Virlogeux-Payant, I., Chevaleyre, C., Gerdtts,
446 V., Salmon, H., 2009. Early immune response following *Salmonella enterica* subspecies *enterica*
447 serovar Typhimurium infection in porcine jejunal gut loops. *Vet Res* 40, 05.
448 <https://doi.org/10.1051/vetres:2008043>
- 449 Miller, M.A., Zachary, J.F., 2017. Mechanisms and Morphology of Cellular Injury, Adaptation, and
450 Death, in: Zachary, J.F. (Ed.), *Pathologic Basis of Veterinary Disease*. Elsevier, St. Louis, pp. 2-
451 43.e19. <https://doi.org/10.1016/B978-0-323-35775-3.00001-1>
- 452 Niehaus, E.-M., Janevska, S., von Bargen, K.W., Sieber, C.M.K., Harrer, H., Humpf, H.-U., Tudzynski,
453 B., 2014. Apicidin F: Characterization and Genetic Manipulation of a New Secondary Metabolite
454 Gene Cluster in the Rice Pathogen *Fusarium fujikuroi*. *PLoS One* 9, e103336.
455 <https://doi.org/10.1371/journal.pone.0103336>
- 456 Novak, B., Hasuda, A.L., Ghanbari, M., Mayumi Maruo, V., Bracarense, A.P.F.R.L., Neves, M.,
457 Emsenhuber, C., Wein, S., Oswald, I.P., Pinton, P., Schatzmayr, D., 2021. Effects of *Fusarium*
458 metabolites beauvericin and enniatins alone or in mixture with deoxynivalenol on weaning piglets.
459 *Food and Chemical Toxicology* 158, 112719. <https://doi.org/10.1016/j.fct.2021.112719>
- 460 Novak, B., Rainer, V., Sulyok, M., Haltrich, D., Schatzmayr, G., Mayer, E., 2019. Twenty-Eight Fungal
461 Secondary Metabolites Detected in Pig Feed Samples: Their Occurrence, Relevance and Cytotoxic
462 Effects In Vitro. *Toxins (Basel)* 11, 537. <https://doi.org/10.3390/toxins11090537>
- 463 Park, S.J., Kwon, S.G., Hwang, J.H., Park, D.H., Kim, T.W., Kim, C.W., 2015. Selection of appropriate
464 reference genes for RT-qPCR analysis in Berkshire, Duroc, Landrace, and Yorkshire pigs. *Gene*
465 558, 152–158. <https://doi.org/10.1016/j.gene.2014.12.052>
- 466 Payros, D., Alassane-Kpembé, I., Laffitte, J., Lencina, C., Neves, M., Bracarense, A.P., Pinton, P.,
467 Ménard, S., Oswald, I.P., 2021. Dietary Exposure to the Food Contaminant Deoxynivalenol
468 Triggers Colonic Breakdown by Activating the Mitochondrial and the Death Receptor Pathways.
469 *Mol Nutr Food Res* 2100191. <https://doi.org/10.1002/mnfr.202100191>
- 470 Pierron, A., Neves, M., Puel, S., Lippi, Y., Soler, L., Miller, J.D., Oswald, I.P., 2022. Intestinal toxicity
471 of the new type A trichothecenes, NX and 3ANX. *Chemosphere* 288, 132415.
472 <https://doi.org/10.1016/j.chemosphere.2021.132415>
- 473 Pinton, P., Nougayrède, J.-P., del Rio, J.-C., Moreno, C., Marin, D.E., Ferrier, L., Bracarense, A.-P.,
474 Kolf-Clauw, M., Oswald, I.P., 2009. The food contaminant deoxynivalenol, decreases intestinal
475 barrier permeability and reduces claudin expression. *Toxicol Appl Pharmacol* 237, 41–48.
476 <https://doi.org/10.1016/j.taap.2009.03.003>
- 477 Prosperini, A., Juan-García, A., Font, G., Ruiz, M.J., 2013a. Reactive Oxygen Species Involvement in
478 Apoptosis and Mitochondrial Damage in Caco-2 Cells Induced by Enniatins A, A1, B and B1.
479 *Toxicol Lett* 222, 36–44. <https://doi.org/10.1016/j.toxlet.2013.07.009>
- 480 Prosperini, A., Juan-García, A., Font, G., Ruiz, M.J., 2013b. Beauvericin-Induced Cytotoxicity via ROS
481 Production and Mitochondrial Damage in Caco-2 Cells. *Toxicol Lett* 222, 204–211.
482 <https://doi.org/10.1016/j.toxlet.2013.07.005>
- 483 Qian, Z.-J., Zhang, C., Li, Y.-X., Je, J.-Y., Kim, S.-K., Jung, W.-K., 2011. Protective Effects of Emodin
484 and Chrysophanol Isolated from Marine Fungus *Aspergillus* sp. on Ethanol-Induced Toxicity in
485 HepG2/CYP2E1 Cells. *Evidence-Based Complementary and Alternative Medicine* 2011, 1–7.
486 <https://doi.org/10.1155/2011/452621>
- 487 Rodríguez-Carrasco, Y., Heilos, D., Richter, L., Süßmuth, R.D., Heffeter, P., Sulyok, M., Kenner, L.,
488 Berger, W., Dornetshuber-Fleiss, R., 2016. Mouse Tissue Distribution and Persistence of the Food-
489 Born Fusariotoxins Enniatin B and Beauvericin. *Toxicol Lett* 247, 35–44.
490 <https://doi.org/10.1016/j.toxlet.2016.02.008>
- 491 Schoevers, E.J., Santos, R.R., Fink-Gremmels, J., Roelen, B.A.J., 2016. Toxicity of Beauvericin on

- 492 Porcine Oocyte Maturation and Preimplantation Embryo Development. *Reproductive Toxicology*
493 65, 159–169. <https://doi.org/10.1016/j.reprotox.2016.07.017>
- 494 Silva, E.O. da, Gerez, J.R., Hohmann, M.S.N., Verri, W.A., Bracarense, A.P.F.R.L., 2019. Phytic Acid
495 Decreases Oxidative Stress and Intestinal Lesions Induced by Fumonisin B1 and Deoxynivalenol
496 in Intestinal Explants of Pigs. *Toxins (Basel)* 11, 18. <https://doi.org/10.3390/toxins11010018>
- 497 Springler, A., Vrabel, G.J., Mayer, E., Schatzmayr, G., Novak, B., 2016. Effect of Fusarium-Derived
498 Metabolites on the Barrier Integrity of Differentiated Intestinal Porcine Epithelial Cells (IPEC-J2).
499 *Toxins (Basel)* 8. <https://doi.org/10.3390/toxins8110345>
- 500 Streit, E., Schwab, C., Sulyok, M., Naehrer, K., Krska, R., Schatzmayr, G., 2013. Multi-Mycotoxin
501 Screening Reveals the Occurrence of 139 Different Secondary Metabolites in Feed and Feed
502 Ingredients. *Toxins (Basel)* 5, 504–523. <https://doi.org/10.3390/toxins5030504>
- 503 Tonshin, A.A., Teplova, V. v., Andersson, M.A., Salkinoja-Salonen, M.S., 2010. The Fusarium
504 Mycotoxins Enniatins and Beauvericin Cause Mitochondrial Dysfunction by Affecting the
505 Mitochondrial Volume Regulation, Oxidative Phosphorylation and Ion Homeostasis. *Toxicology*
506 276, 49–57. <https://doi.org/10.1016/j.tox.2010.07.001>
- 507 Tuli, H.S., Aggarwal, V., Tuorkey, M., Aggarwal, D., Parashar, N.C., Varol, M., Savla, R., Kaur, G.,
508 Mittal, S., Sak, K., 2021. Emodin: A metabolite that exhibits anti-neoplastic activities by
509 modulating multiple oncogenic targets. *Toxicology in Vitro* 73, 105142.
510 <https://doi.org/10.1016/j.tiv.2021.105142>
- 511 Vaclavikova, M., Malachova, A., Veprikova, Z., Dzuman, Z., Zachariasova, M., Hajslova, J., 2013.
512 ‘Emerging’ mycotoxins in cereals processing chains: Changes of enniatins during beer and bread
513 making. *Food Chem* 136, 750–757. <https://doi.org/10.1016/j.foodchem.2012.08.031>
- 514 Vejdovsky, K., Warth, B., Sulyok, M., Marko, D., 2016. Non-synergistic cytotoxic effects of Fusarium
515 and Alternaria toxin combinations in Caco-2 cells. *Toxicol Lett* 241, 1–8.
516 <https://doi.org/10.1016/j.toxlet.2015.10.024>
- 517 Wang, M., Zhang, Z., Ruan, P., Zhang, G., Xiao, C., Wang, Y., Gao, Y., 2022. Emodin-induced
518 hepatotoxicity is enhanced by 3-methylcholanthrene through activating aryl hydrocarbon receptor
519 and inducing CYP1A1 in vitro and in vivo. *Chem Biol Interact* 365, 110089.
520 <https://doi.org/10.1016/j.cbi.2022.110089>
- 521 Wu, X.F., Xu, R., Ouyang, Z.J., Qian, C., Shen, Y., Wu, X.D., Gu, Y.H., Xu, Q., Sun, Y., 2013.
522 Beauvericin Ameliorates Experimental Colitis by Inhibiting Activated T Cells via Downregulation
523 of the PI3K/Akt Signaling Pathway. *PLoS One* 8. <https://doi.org/10.1371/journal.pone.0083013>
- 524 Yoo, S., Kim, M.-Y., Cho, J.Y., 2017. Beauvericin, a Cyclic Peptide, Inhibits Inflammatory Responses
525 in Macrophages by Inhibiting the NF- κ B Pathway. *Korean Journal of Physiology and*
526 *Pharmacology* 21, 449–456. <https://doi.org/10.4196/kjpp.2017.21.4.449>
- 527 Zelko, I.N., Mariani, T.J., Folz, R.J., 2002. Superoxide dismutase multigene family: a comparison of the
528 CuZn-SOD (SOD1), Mn-SOD (SOD2), and EC-SOD (SOD3) gene structures, evolution, and
529 expression. *Free Radic Biol Med* 33, 337–349. [https://doi.org/10.1016/S0891-5849\(02\)00905-X](https://doi.org/10.1016/S0891-5849(02)00905-X)
- 530 Zhou, L., Hu, X., Han, C., Niu, X., Han, L., Yu, H., Pan, G., Fu, Z., 2023. Comprehensive investigation
531 on the metabolism of emodin both in vivo and in vitro. *J Pharm Biomed Anal* 223, 115122.
532 <https://doi.org/10.1016/j.jpba.2022.115122>
- 533 Zou, X., Ratti, B.A., O’Brien, J.G., Lautenschlager, S.O., Gius, D.R., Bonini, M.G., Zhu, Y., 2017.
534 Manganese superoxide dismutase (SOD2): is there a center in the universe of mitochondrial redox
535 signaling? *J Bioenerg Biomembr* 49, 325–333. <https://doi.org/10.1007/s10863-017-9718-8>
- 536 Zouaoui, N., Mallebrera, B., Berrada, H., Abid-Essefi, S., Bacha, H., Ruiz, M.J., 2016. Cytotoxic Effects
537 Induced by Patulin, Sterigmatocystin and Beauvericin on CHO-K1 Cells. *Food and Chemical*
538 *Toxicology* 89, 92–103. <https://doi.org/10.1016/j.fct.2016.01.010>
- 539

540 9 CONSIDERAÇÕES FINAIS

541 No geral, os resultados desse estudo forneceram novos *insights* sobre
542 o impacto negativo da ingestão de micotoxinas emergentes sozinhas ou associadas
543 com DON no desempenho, saúde intestinal e parâmetros imunológicos em suínos.
544 Mostrando que essas micotoxinas causaram alterações histológicas em fígado,
545 intestino delgado e linfonodos dos suínos. Também impactaram negativamente na
546 microbiota fecal, com diminuição da diversidade, indicando uma piora na saúde
547 intestinal, podendo afetar também a imunidade desses animais.

548 Além disso, os resultados encontrados forneceram dados adicionais
549 sobre os efeitos tóxicos do DON e outras micotoxinas emergentes, principalmente
550 BEA e ENNs no fígado, evidenciando que explantes de fígado cortados com precisão
551 (PCLS) são uma ferramenta relevante para avaliar a toxicologia de contaminantes
552 alimentares como as micotoxinas.

553 O modelo *ex vivo* de PCLS demonstrou ser uma alternativa melhor ao
554 modelo *in vitro*, pois no modelo de explantes há conservação da estrutura 3D, bem
555 como interações célula-célula e célula-matriz que não ocorrem no cultivo celular.
556 Também é um bom substituto ao modelo *in vivo*, já que mantém características
557 próximas ao *in vivo* e menos animais são utilizados na experimentação.

558 Além das vantagens fornecidas pelo modelo *ex vivo*, mais estudos
559 devem ser realizados para avaliar se uma exposição longa (superior a quatro horas)
560 às micotoxinas emergentes também podem causar alterações morfológicas e
561 transcricionais significativas tardias em explantes de fígado cortados com precisão.

APÊNDICES

APÊNDICE A

Tabela complementar ao artigo B “Deoxynivalenol induces apoptosis and inflammation in the liver: Analysis using precision-cut liver slices”

Table S1. Effects of DON exposure (10 μ M) on hepatic biomarkers in PCLS supernatant (mean \pm SEM).

Hepatic biomarkers	Control	DON
Alkaline phosphatase (U/L)	4.393 \pm 1.599	3.687 \pm 1.892
Alanine transaminase (U/L)	6.333 \pm 4.885	6.500 \pm 2.811
Aspartate aminotransferase (U/L)	260.8 \pm 153.6	278.2 \pm 99.23
Lactate dehydrogenase (U/L)	83.02 \pm 40.27	100.3 \pm 47.71
Total proteins (g/L)	5.707 \pm 0.573	6.311 \pm 0.452

APÊNDICE B

Tabela complementar ao artigo C “Emerging mycotoxins induce ex vivo and in vitro hepatotoxicity in pigs precision-cut liver slices and HepG2 cells”

Table S1: Effects of emerging mycotoxins exposure (10 μ M) on liver enzymes and protein content in PCLS supernatant (mean \pm SEM).

Liver biochemicals	ALP (U/L)	ALT (U/L)	AST (U/L)	LDH (U/L)	TP (g/L)
Control	4.39 \pm 1.31a	6.33 \pm 4.46a	260.83 \pm 140.19a	83.02 \pm 36.76a	5.71 \pm 0.52a
BEA	3.70 \pm 1.18a	6.17 \pm 2.54a	238.00 \pm 71.16a	84.48 \pm 32.87a	6.28 \pm 0.55a
ENN A1	3.00 \pm 1.63a	6.33 \pm 3.77a	238.00 \pm 100.34a	83.02 \pm 43.89a	5.88 \pm 0.83a
ENN B	3.67 \pm 1.77a	6.17 \pm 2.61a	259.67 \pm 92.58a	94.10 \pm 39.19a	6.31 \pm 0.66a
ENN B1	3.65 \pm 1.17a	6.33 \pm 2.92a	242.17 \pm 91.80a	81.28 \pm 36.67a	6.21 \pm 0.56a
AFN	4.06 \pm 2.02a	8.00 \pm 3.37a	249.00 \pm 22.83a	104.88 \pm 33.38a	5.81 \pm 0.69a
API	3.18 \pm 1.24a	5.33 \pm 3.09a	221.33 \pm 122.22a	90.07 \pm 48.27a	5.90 \pm 0.99a